

**A COMBINED PROCESS OF COUNTER-CURRENT
EXTRACTION AND REACTIVE DISTILLATION FOR
RECOVERY AND PURIFICATION OF LACTIC ACID**



**A Thesis Submitted in Partial Fulfillment of the Requirements for
the Degree of Doctor of Philosophy in Chemical Engineering**

Suranaree University of Technology

Academic Year 2019

กระบวนการร่วมของการสกัดแบบสารไหลสวนทางและการกลั่นแบบมี
ปฏิกิริยาเพื่อการกู้คืนและทำบริสุทธิ์กรดแลกติก



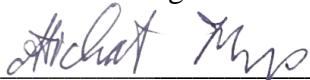
นางสาวคณิณี ช่างษ์

วิทยานิพนธ์นี้เป็นส่วนหนึ่งของการศึกษาตามหลักสูตรปริญญาวิศวกรรมศาสตรดุษฎีบัณฑิต
สาขาวิชาวิศวกรรมเคมี
มหาวิทยาลัยเทคโนโลยีสุรนารี
ปีการศึกษา 2562

**A COMBINED PROCESS OF COUNTER-CURRENT
EXTRACTION AND REACTIVE DISTILLATION FOR
RECOVERY AND PURIFICATION OF LACTIC ACID**

Suranaree University of Technology has approved this thesis submitted in partial fulfillment of the requirements for the Degree of Doctor of Philosophy.

Thesis Examining Committee



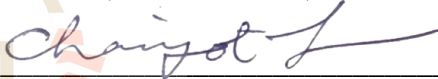
(Assoc. Prof. Dr. Atichat Wongkoblap)

Chairperson



(Asst. Prof. Dr. Panarat Rattanaphanee)

Member (Thesis Advisor)



(Prof. Dr. Chaiyot Tangsathitkulchai)

Member



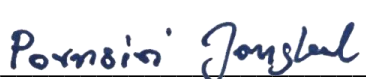
(Prof. Dr. Adrian E. Flood)

Member



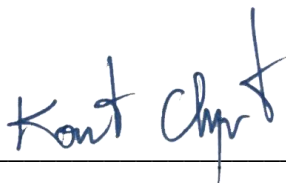
(Assoc. Prof. Dr. Apichat Boontawan)

Member



(Assoc. Prof. Dr. Pornsiri Jongkol)

Dean of Institute of Engineering



(Assoc. Prof. Flt. Lt. Dr. Kontorn Chamniprasart)

Vice Rector for Academic Affairs
and Internationalization

คณิงนิจ ชาวงษ์ : กระบวนการร่วมของการสกัดแบบสารไหลสวนทางและการกลั่นแบบมี
ปฏิกิริยาเพื่อการกู้คืนและทำบริสุทธิ์กรดแลกติก (A COMBINED PROCESS OF
COUNTER-CURRENT EXTRACTION AND REACTIVE DISTILLATION FOR
RECOVERY AND PURIFICATION OF LACTIC ACID) อาจารย์ที่ปรึกษา :
ผู้ช่วยศาสตราจารย์ ดร.พนารัตน์ รัตนพานิ, 213 หน้า.

วิทยานิพนธ์ฉบับนี้มีวัตถุประสงค์เพื่อศึกษากระบวนการร่วมของการสกัดแบบสารไหล
สวนทางและการกลั่นแบบมีปฏิกิริยาเพื่อการกู้คืนและทำบริสุทธิ์กรดแลกติกจากน้ำหมัก โดย
การศึกษาในวิทยานิพนธ์ฉบับนี้แบ่งออกเป็น 4 ส่วน ส่วนแรกเป็นการศึกษาการสกัดกรดแลก
ติกด้วย 1-บิวทานอลโดยใช้คอลัมน์สกัดของเหลว-ของเหลว ชนิดบรรจุแบบสารไหลสวนทางที่
อุณหภูมิห้อง ขนาดเส้นผ่านศูนย์กลาง Sauter (d_{32}) ถูกนำมาใช้ในการประเมินขนาดหยดที่เกิดขึ้นใน
ระบบการสกัดรวมทั้งมีการศึกษาสมการสหสัมพันธ์ของค่าขนาดเส้นผ่านศูนย์กลาง Sauter โดยผล
การศึกษาพบว่า ค่า d_{32} ลดลงเมื่อเพิ่มอัตราการไหลของเฟสกระจาย (Q_d) และลดขนาดเส้นผ่าน
ศูนย์กลางของหัวฉีด (D_N) ส่งผลให้สัมประสิทธิ์การถ่ายเทมวลของเฟสกระจายมีค่าเพิ่มขึ้น ส่วนการ
เพิ่มอัตราการไหลของเฟสต่อเนื่อง (Q_c) นั้นทำให้หยดมีขนาดใหญ่ขึ้นเนื่องมาจากการเชื่อมกันของ
หยด เป็นผลให้สัมประสิทธิ์การถ่ายเทมวลของเฟสกระจายมีค่าลดลง

การศึกษาวิจัยส่วนที่สองเป็นการสังเคราะห์อะลูมิเนียมแอลจินेटและใช้เป็นตัวเร่งปฏิกิริยา
ของแข็งในปฏิกิริยาเอสเทอร์ฟิเคชันของกรดแลกติกด้วย 1-บิวทานอล และศึกษาคุณลักษณะของ
ตัวเร่งปฏิกิริยาที่เตรียมขึ้น โดยพบว่าอะลูมิเนียมแอลจินेटมีความเป็นผลึกต่ำ พื้นผิวขุ่นและมีตำแหน่ง
ที่ว่างไวกรดสูงสำหรับปฏิกิริยาเอสเทอร์ฟิเคชัน อย่างไรก็ตามพบว่าตัวเร่งปฏิกิริยานี้มีความเสถียร
ต่ออุณหภูมิต่ำ มีการศึกษาประสิทธิภาพในการเร่งปฏิกิริยาของตัวเร่งปฏิกิริยาที่เตรียมขึ้นต่อการทำ
ปฏิกิริยาเอสเทอร์ฟิเคชันของกรดแลกติกและพบว่าตัวเร่งปฏิกิริยามีประสิทธิภาพในการเร่ง
ปฏิกิริยาสูงกว่าตัวเร่งปฏิกิริยาที่ใช้ในเชิงพาณิชย์คือแอมเบอร์ลิสต์-15 โดยเปรียบเทียบที่สภาวะการ
ทำปฏิกิริยาเดียวกัน นอกจากนี้ยังพบว่าแบบจำลอง Langmuir-Hinshelwood สามารถอธิบาย
จลนพลศาสตร์ของปฏิกิริยานี้ได้ดีด้วยค่าส่วนเบี่ยงเบนสัมพัทธ์เฉลี่ย (Mean relative deviation,
MRD) ต่ำ

วิทยานิพนธ์ส่วนที่สามเป็นการศึกษาการทำปฏิกิริยาเอสเทอร์ฟิเคชันของกรดแลกติกด้วย
1-บิวทานอลโดยใช้อะลูมิเนียมแอลจินेटเป็นตัวเร่งปฏิกิริยา และปฏิกิริยาไฮโดรไลซิสของนอร์มอล-
บิวทิลแลกเตตกลับเป็นกรดแลกติกโดยใช้แอมเบอร์ลิสต์-15 เป็นตัวเร่งปฏิกิริยา ในคอลัมน์กลั่น
แบบมีปฏิกิริยาแบบกึ่งกะ การทดลองพบว่าค่าการเปลี่ยนแปลง (Conversion) ของกรดแลกติกและ

ผลได้ (Yield) ของนอร์มอล-บิวทิลแลกเตดของปฏิกิริยาเอสเทอร์ฟิเคชัน มีค่าเพิ่มขึ้นตามการเพิ่มขึ้นของอัตราส่วนรีฟลักซ์แต่ปริมาณตัวเร่งปฏิกิริยาไม่มีผลอย่างมีนัยสำคัญต่อค่าทั้งสองนี้ ในขณะที่การเพิ่มอัตราการไหลของสารป้อนส่งผลให้ค่าการเปลี่ยนแปลงและผลได้ลดลง ส่วนการทำปฏิกิริยาไฮโดรไลซิสของนอร์มอล-บิวทิลแลกเตดนั้น ผลการทดลองพบว่าค่าการเปลี่ยนแปลงและผลได้เพิ่มขึ้นตามการเพิ่มปริมาณตัวเร่งปฏิกิริยาขณะที่อัตราการไหลของสารป้อนและอัตราส่วนรีฟลักซ์มีผลต่อค่าทั้งสองเช่นเดียวกับปฏิกิริยาเอสเทอร์ฟิเคชัน นอกจากนี้ยังพบว่าความบริสุทธิ์ของผลิตภัณฑ์กรดแลกติกลดลงเมื่อเพิ่มความดัน เพิ่มอัตราการไหลของสารป้อนและเพิ่มอัตราส่วนรีฟลักซ์

วิทยานิพนธ์ส่วนสุดท้ายเป็นการใช้ผลการทดลองจากการดำเนินงานทั้งสามส่วนในการสร้างแบบจำลองและการประเมินทางเศรษฐศาสตร์ของกระบวนการร่วมของการสกัดแบบสารไหลสวนทางและการกลั่นแบบมีปฏิกิริยาโดยใช้ซอฟต์แวร์ Aspen HYSYS V10 และ Aspen Process Economic Analyzer โดยศึกษาและเปรียบเทียบประสิทธิภาพของการดำเนินงานกระบวนการ 2 แบบ คือแบบที่ไม่มีการกู้คืน (No-recovery) 1-บิวทานอล (กระบวนการ A) และแบบที่มีการกู้คืน (Recovery) 1-บิวทานอล (กระบวนการ B) กลับมาใช้ใหม่ในกระบวนการที่กำลังการผลิต 10,000 ตันต่อปีของกรดแลกติกบริสุทธิ์ 99.99 เปอร์เซ็นต์โดยมวล ผลการศึกษาพบว่าการกู้คืนกรดแลกติกทั้งหมดที่ได้จากกระบวนการ A และ B เท่ากับ 91.19 และ 96.57% โดยมีต้นทุนการผลิตอยู่ที่ 1.67 และ 0.90 ดอลลาร์สหรัฐต่อกิโลกรัมของกรดแลกติก ตามลำดับ

สาขาวิชา วิศวกรรมเคมี
ปีการศึกษา 2562

ลายมือชื่อนักศึกษา ดิเรก
ลายมือชื่ออาจารย์ที่ปรึกษา [ลายมือ]

KANUNGNIT CHAWONG : A COMBINED PROCESS OF COUNTER-CURRENT EXTRACTION AND REACTIVE DISTILLATION FOR RECOVERY AND PURIFICATION OF LACTIC ACID. THESIS ADVISOR : ASST. PROF. PANARAT RATTANAPHANEE, Ph.D., 213 PP.

LACTIC ACID/EXTRACTION/1-BUTANOL/ESTERIFICATION/HYDROLYSIS/
REACTIVE DISTILLATION

This thesis aims to study a combined process of counter-current extraction and reactive distillation for recovery and purification of lactic acid from fermentation broth. Research work in the thesis is divided into four parts. The first part is the study of extraction of lactic acid with 1-butanol at room temperature using counter-current packed liquid-liquid extraction column. Sauter mean drop diameter (d_{32}) was used to evaluate the mean drop size in the extraction and correlation of d_{32} was investigated. The results showed that d_{32} decreased with increasing dispersed phase flow rate (Q_d) and decreasing nozzle diameter (D_N), resulting in increasing dispersed phase mass transfer coefficient. An increase in continuous phase flow rate (Q_c) affected increasing drop size, due to the coalescence of drops, resulting in reducing dispersed phase mass transfer coefficient.

The second part is the synthesis and use of aluminum alginate as a solid catalyst for esterification of lactic acid with 1-butanol. Characteristics of the prepared catalyst were studied. It was found that aluminum alginate has low crystallinity, wrinkle surface and likely create strong Lewis acid sites for esterification. However, it was found that the prepared catalyst was of low thermal stability. Catalytic activity of aluminum alginate in esterification of lactic acid was investigated and found to be higher than the

commercial catalyst, Amberlyst-15, under the same reaction conditions. In addition, it was observed that Langmuir-Hinshelwood model was able to describe the kinetic model of this reaction with small value of mean relative deviation (MRD).

The third part of this thesis studied esterification of lactic acid with 1-butanol using aluminum alginate and hydrolysis of *n*-butyl lactate into lactic acid using Amberlyst-15 as solid catalyst in a semi-batch reactive distillation column. The results showed that lactic acid conversion and yield of *n*-butyl lactate of esterification increased with increasing reflux ratio. Catalyst loading did not have significant effect on value of both parameters while increasing the feed flow rate affects decreasing conversion and yield. For the hydrolysis of *n*-butyl lactate, the conversion and yield were found to increased with increasing catalyst loading while effect of feed flow rate and reflux ratio was similar to that in esterification. In addition, it was found that the purity of lactic acid decreased with increasing pressure, feed flow rate and reflux ratio.

In the final part, experimental data from the previous part were use to design the combined counter-current extraction and reactive distillation. The process was simulated and economically evaluated using Aspen HYSYS V10 and Aspen Process Economic Analyzer. Efficiency of two process operations with no-recovery (Process A) and recovery (Precess B) of 1-butanol was studied and compared at annual capacity of 10,000 tons/year with purity of 99.99%w/w lactic acid. The results showed that the overall recovery of lactic acid obtained from Process A and B equals to 91.19 and 96.57% with production cost at 1.67 and 0.90 USD/kg of lactic acid, respectively.

School of Chemical Engineering

Academic Year 2019

Student's Signature

Kanungnit

Advisor's Signature

[Signature]

ACKNOWLEDGEMENTS

I would like to express my sincere thanks and gratitude to Asst. Prof. Dr. Panarat Rattanaphanee, my graduate advisor for her guidance and support throughout this work. Her guiding light, motivation, and patience was the most important source of my accomplishment and prepare me well for both professional and personal development for the future.

I also would like to thank my thesis committee; Assoc. Prof. Dr. Atichat Wongkoblap, Prof. Dr. Chaiyot Tangsathitkulchai, Prof. Dr. Adrian E. Flood and Assoc. Prof. Dr. Apichat Boontawan for their valuable time to serve as my committee member, and for their unconditional help and advice on the conduction of this work. I would like to thank all of lecturers at School of Chemical Engineering, Suranaree University of Technology, who led me to the world of Chemical Engineering.

I am thankful to Mr. Saran Dokmajkun for helping me with the laboratory facilities and for the valuable recommendations. Special thanks to Mrs. Amporn Ladnongkhun for her skillful secretarial work. I also thank the graduate students in the School of Chemical Engineering for their encouragement and keeping me sane during difficult times.

Finally, I would also like to express my deep sense of gratitude to my parents for their support and encouragement me throughout the course of this study at Suranaree University of Technology.

Kanungnit Chawong

TABLE OF CONTENTS

	Page
ABSTRACT (THAI)	I
ABSTRACT (ENGLISH)	III
ACKNOWLEDGEMENTS	V
TABLE OF CONTENTS	VI
LIST OF TABLES	XIV
LIST OF FIGURES	XVI
SYMBOLS AND ABBREVIATIONS	XXIII
CHAPTER	
I INTRODUCTION	1
1.1 Background and Significance of the Problem	1
1.2 Research Objectives	4
1.3 Scope and Limitation of the Research	5
1.4 Outputs of the Research	6
1.5 References	6
II EXTRACTION OF LACTIC ACID WITH	
1-BUTANOL USING COUNTER-CURRENT	
PACKED LIQUID-LIQUID EXTRACTION COLUMN	9
2.1 Abstract	9
2.2 Introduction	10

TABLE OF CONTENTS (Continued)

	Page
2.3 Theory	12
2.3.1 Packed Liquid-Liquid Extraction Column	12
2.3.2 Drop Behavior	13
2.3.3 Dispersed Phase Mass Transfer Coefficient	14
2.3.3.1 Stagnant Drops	14
2.3.3.2 Circulating Drops	15
2.3.3.3 Oscillating Drops	15
2.3.4 Sauter Mean Drop Diameter	18
2.3.5 Dispersed Phase Sherwood Number	21
2.4 Experimental Procedures	24
2.4.1 Chemicals	24
2.4.2 Experimental Apparatus	24
2.4.3 Procedure	24
2.4.4 Methods of Analysis	26
2.4.4.1 Gas Chromatography Analysis of Lactic Acid	26
2.4.4.2 Drops Analysis	26
2.4.4.3 Density, Viscosity and Interfacial Tension Analysis	26
2.5 Results and Discussion	27
2.5.1 Effect of Operating Parameters on Drop Size	27

TABLE OF CONTENTS (Continued)

	Page
2.5.2 Effect of Operating Parameters on Dispersed Phase Mass Transfer Coefficient and Extraction Efficiency	33
2.5.3 Correlation of Sauter Mean Drop Diameter	36
2.5.4 Correlation of Dispersed Phase Sherwood Number	39
2.5.4.1 Correlating Dispersed Phase Sherwood Number Based on Molecular Diffusivity.....	39
2.5.4.2 Correlating Dispersed Phase Sherwood Number Based on Effective Diffusivity	41
2.6 Conclusion	44
2.7 References.....	45
III SYNTHESIS ALUMINUM ALGINATE AS A SOLID CATALYST FOR ESTERIFICATION OF LACTIC ACID WITH 1-BUTANOL.....	48
3.1 Abstract.....	48
3.2 Introduction.....	50
3.3 Theory	52
3.3.1 Esterification Reaction.....	52
3.3.2 Kinetic Model for Esterification Reaction.....	53
3.3.3 Thermodynamic Model	56
3.3.3.1 Vapor-Liquid Equilibrium	56

TABLE OF CONTENTS (Continued)

	Page
3.3.3.2 Universal functional activity coefficient (UNIFAC) model	57
3.4 Experimental Procedures	61
3.4.1 Chemicals.....	61
3.4.2 Catalyst Preparation	61
3.4.3 Catalyst Characterizations	62
3.4.3.1 Surface Morphology	62
3.4.3.2 Crystallinity	62
3.4.3.3 Functional Group	62
3.4.3.4 Acidity.....	62
3.4.3.5 Thermal Degradation	63
3.4.4 Catalytic Activity in Esterification of Lactic Acid with 1-Butanol.....	63
3.5 Results and Discussion	64
3.5.1 Characterizations of ALA Catalyst	64
3.5.1.1 Surface Morphology	65
3.5.1.2 Crystallinity.....	67
3.5.1.3 Functional Groups	68
3.5.1.4 Acidity.....	70
3.5.1.5 Thermal Degradation	71

TABLE OF CONTENTS (Continued)

	Page
3.5.2 Catalytic Activity in Esterification of Lactic Acid with 1-Butanol.....	72
5.3.2.1 Catalyst Performance	72
5.3.2.2 Effect of Catalyst Loading	74
5.3.2.3 Effect of Initial 1-Butanol to Lactic acid Molar Ratio	75
5.3.2.4 Effect of Reaction Temperature	76
3.5.3 Kinetic Models	77
3.6 Conclusion	81
3.7 References.....	82
IV ESTERIFICATION OF LACTIC ACID AND HYDROLYSIS OF N-BUTYL LACTATE BY REACTIVE DISTILLATION	86
4.1 Abstract.....	86
4.2 Introduction.....	87
4.3 Theory	89
4.3.1 Reactive Distillation.....	89
4.3.2 Advantage of Reactive Distillation.....	92
4.3.3 Limiting of Reactive Distillation	93
4.4 Experimental Procedures	97
4.4.1 Chemicals.....	97

TABLE OF CONTENTS (Continued)

	Page
4.4.2	Reactive Distillation Apparatus 97
4.4.3	Esterification and Hydrolysis in Reactive Distillation Column..... 98
4.5	Results and Discussion 100
4.5.1	Esterification in Reactive Distillation Column 100
4.5.1.1	Effect of Reflux Ratio 104
4.5.1.2	Effect of Catalyst Loading 105
4.5.1.3	Effect of Feed Flow Rate 106
4.5.2	Hydrolysis in Reactive Distillation Column 108
4.5.2.1	Effect of Operating Pressure 111
4.5.2.2	Effect of Reflux Ratio 113
4.5.2.3	Effect of Catalyst Loading 114
4.5.2.4	Effect of Feed Flow Rate 115
4.6	Conclusion 117
4.7	References..... 118
V	TECHNO-ECONOMIC ANALYSIS OF A COMBINED EXTRACTION AND REACTIVE DISTILLATION FOR LACTIC ACID PRODUCTION 120
5.1	Abstract 120
5.2	Introduction..... 121
5.3	Theory 124

TABLE OF CONTENTS (Continued)

	Page
5.3.1 Capital Cost.....	124
5.3.2 Fixed-Capital Investment.....	124
5.3.3 Working Capital.....	125
5.3.4 Purchase Equipment Cost	126
5.3.5 Operating Cost	126
5.3.6 Raw Material Cost	127
5.3.7 Utilities Cost	128
5.3.8 Production Cost	128
5.4 Process Simulation Description	129
5.4.1 Phase Equilibrium and Kinetic Modeling	130
5.4.2 Fermentation Broth and Cell Removal	132
5.4.3 Extraction	133
5.4.4 Esterification and Hydrolysis.....	133
5.4.5 Purification Unit.....	133
5.4.6 Economic Analysis	134
5.5 Results and Discussion	137
5.5.1 Process Analysis	137
5.5.2 Economic Evaluation	145
5.6 Conclusion	150
5.7 References.....	151
VI CONCLUSIONS AND RECOMMENDATIONS.....	154

TABLE OF CONTENTS (Continued)

	Page
6.1 Conclusions.....	154
6.2 Recommendations.....	156
APPENDICES	
APPENDIX A PROPERTIES AND EXAMPLE OF COMPONENT ANALYSIS OF LACTIC ACID, 1-BUTANOL AND N-BUTYL LACTATE	158
APPENDIX B LIQUID-LIQUID EQUILIBRIUM BY UNIFAC AND CALCULATION OF REACTION RATE CONSTANT	167
APPENDIX C PRICE OF RAW MATERIALS AND CALCULATION OF FERMENTATION BROTH COST	177
APPENDIX D LIST OF PUBLICATIONS	181
BIOGRAPHY	213

LIST OF TABLES

Table	Page
2.1 Results of extraction of lactic acid with 1-butanol in packed liquid-liquid extraction column.....	35
2.2 Correlation's constants of Sauter mean drop diameter correlation for packed liquid-liquid extraction column	36
2.3 Correlation's constants of dispersed phase Sherwood number correlation based on D_M and D_{eff}	39
3.1 UNIFAC energy interaction parameters	60
3.2 EDS analysis of ALA catalyst	65
3.3 The main vibrational modes for sodium alginate and aluminum alginate.....	68
3.4 Kinetic parameters for esterification of lactic acid with 1-butanol using ALA catalyst	78
4.1 Boiler point of pure components under atmospheric pressure.....	100
4.2 Experimental data for esterification of lactic acid using Aluminum alginate as a solid catalyst in reactive distillation column	103
4.3 Experimental data for hydrolysis of <i>n</i> -butyl lactate using Amberlyst-15 as a solid catalyst in reactive distillation column	110
5.1 Example of variable and fixed operating cost (Anderson, 2019)	127
5.2 The compositions of fermentation broth	132
5.3 MRS Culture media compositions from Himedia	134
5.4 Raw materials for production of 5 L fermentation broth.....	135

LIST OF TABLES (Continued)

Table	Page
5.5	Calculation of investment cost, including installation and instrumentation 135
5.6	Calculation of operating cost 136
5.7	Comparison of efficiency in each unit operation of both processes 138
5.8	Process simulation data for Process A 141
5.9	Process simulation data for Process B 142
5.10	Flowsheet design results of Process A 143
5.11	Flowsheet design results of Process A 144
5.12	Total capital investment calculation of each process 146
5.13	Operating cost calculation of each process 147
5.14	Economic analysis of conventional lactic acid downstream recovery process compared to proposed process in this work 149
A.1	Chemical and physical properties 159
A.2	Calculated mole of the components in feed, deistillated and residue product 165
C.1	Calculated mole of the components in feed, deistillated and residue product 178
C.2	Himedia MRS culture media cost 179
C.3	Calculated cost of fermentation broth 179
C.4	Calculated cost of aluminum alginate catalyst 180

LIST OF FIGURES

Figure	Page
2.1	Packed liquid-liquid extraction column 12
2.2	Hydrodynamic regions of drop (Bertakis, 2013) 14
2.3	Schematic diagram of packed liquid-liquid extraction column 25
2.4	The Sauter mean drop diameter versus dispersed phase flow rate with different nozzle diameters and continuous phase flow rate 27
2.5	Number of drops at different Q_d using D_N of 1 mm for Q_c of 40 ml/min (a) and 50 ml/min (b) 28
2.6	Number of drops at different Q_d using D_N of 5 mm for Q_c of 40 ml/min (a) and 50 ml/min (b) 29
2.7	Drop size distribution using D_N of 1 mm at $Q_d = 30$ ml/min (red), 50 ml/min (blue) and 70 ml/min (green) for $Q_c = 40$ ml/min (a) and 50 ml/min (b), respectively 30
2.8	Drop size distribution using D_N of 5 mm at $Q_d = 30$ ml/min (red), 50 ml/min (blue) and 70 ml/min (green) for $Q_c = 40$ ml/min (a) and 50 ml/min (b), respectively 31
2.9	Effect of dispersed phase flow rate on dispersed phase mass transfer coefficient 33
2.10	Comparison of experimental d_{32} with calculated values for packed liquid-liquid extraction column in this work 37

LIST OF FIGURES (Continued)

Figure	Page
2.11 Residual plot for the calculated d_{32} from Sauter mean drop diameter correlation	38
2.12 Comparison of experimental and calculated Sh_d based on D_M	40
2.13 Comparison of experimental and calculated Sh_d based on D_{eff}	42
2.14 Residual plot for the calculated Sh_d from Sherwood number correlation based on D_M (*) and D_{eff} (◇)	43
3.1 Esterification of carboxylic acid with alcohol	52
3.2 Esterification between lactic acid and 1-butanol	54
3.3 Aluminum alginate complex (a) and aluminum alginate (ALA) (b)	64
3.4 Cross-linking of sodium alginate with aluminum ions	65
3.5 FESEM images of sodium alginate with magnification 1000× (a), magnification 35000× (b) and ALA catalyst with magnification 50× (c) and magnification 35000× (d)	66
3.6 XRD patterns of sodium alginate and ALA catalyst	67
3.7 FTIR spectrums of sodium alginate (a) and ALA catalyst (b)	69
3.8 TPD-NH ₃ profile of ALA catalyst	71
3.9 TGA-DSC curve of ALA catalyst	72

LIST OF FIGURES (Continued)

Figure	Page
3.10 Conversion of lactic acid in esterification using 1% w/v of catalyst loading and M =5:1 at 65°C (▲), 85°C (●) for ALA catalyst and 65°C (△), 85°C (○) for Ameberlyst-15 (Rattanaphanee, 2010). Solid lines indicate the calculation values from LH model	73
3.11 Effect of catalyst loading on conversion of lactic acid at reaction temperature of 75°C and M=5:1 using 0.25%w/v (●); 0.5%w/v (◆) and 1%w/v (▲) of catalyst loading. Solid lines indicate the calculation values from LH model	74
3.12 Effect of catalyst loading on conversion of lactic acid in a presence of 1% w/v of catalyst loading at the reaction temperature of 75°C; M=1:1 (◆), M=3:1 (●) and M=5:1 (▲). Solid lines indicate the calculation values from LH model	75
3.13 Effect of reaction temperature on conversion of lactic acid in a presence of 1% w/v of catalyst loading and M=5:1 at the reaction temperature of 55°C (□), 65°C (●), 75°C (▲) and 85°C (◆). Solid lines indicate the calculation values from LH model	76
3.14 Arrhenius plot of PH (●), ER (○) and LH (▼) models for ALA catalyzed esterification of lactic acid with 1-butanol.....	79
3.15 Van't Hoff plot of ALA catalyzed esterification of lactic acid with 1-butanol	80

LIST OF FIGURES (Continued)

Figure	Page
4.1	The reactive distillation configuration 91
4.2	Counter-current vapor-liquid contacting in trayed column (Baur, 2000). 94
4.3	Counter-current vapor-liquid contacting in packed column (Baur, 2000). 94
4.4	Catalyst particles enveloped in wire gauze packings and placed inside RD column: spherical baskets (a), cylindrical container for catalyst particles (b), wire gauze envelopes(c), horizontally disposed gutters (d), horizontally disposed wire gauze tubes (e), sandwich in cubical collection (e) and sandwich in a round collection (h) 95
4.5	Schematic diagram of laboratory reactive distillation column 98
4.6	Effect of reflux ratio on conversion of lactic acid (—●—) and yield of <i>n</i> -butyl lactate (···○···) in distillate product for esterification of lactic acid in reactive distillation column at pressure of 255 mbar, T_{reboiler} of 90°C, feed flow rate of 1 ml/min and 1.5 g of catalyst loading. 104
4.7	Effect of catalyst loading on conversion of lactic acid (—●—) and yield of <i>n</i> -butyl lactate (···○···) in distillate product for esterification of lactic acid in reactive distillation column at pressure of 255 mbar, T_{reboiler} of 90°C, feed flow rate of 1 ml/min with reflux ratio of 1. 105

LIST OF FIGURES (Continued)

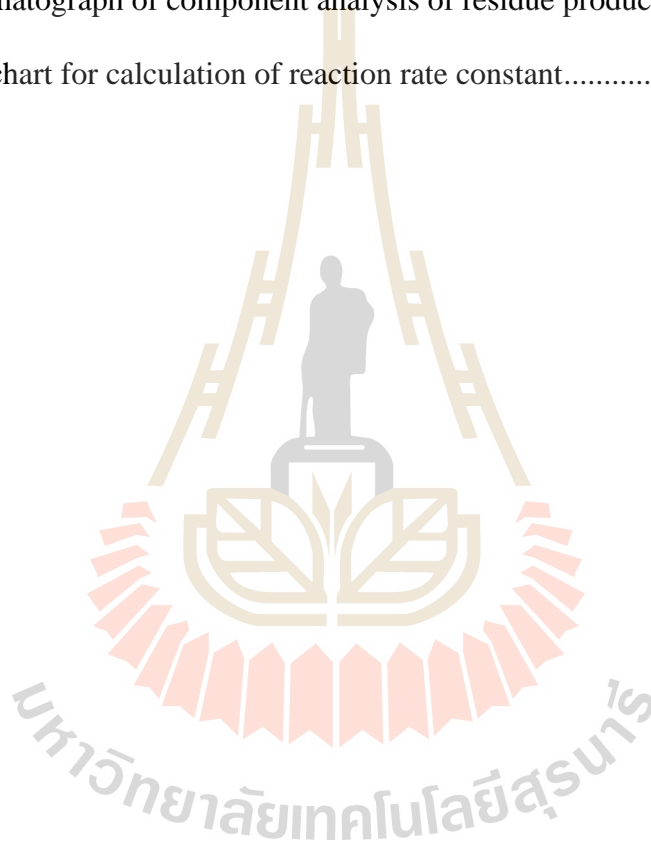
Figure	Page
4.8 Effect of feed flow rate on conversion of lactic acid (—●—) and yield of <i>n</i> -butyl lactate (···○··) in distillate product for esterification of lactic acid in reactive distillation column at pressure of 255 mbar, T_{reboiler} of 90°C, reflux ratio of 1 with 1.5 g of catalyst loading.....	106
4.9 Example of distillate (a) and residue (b) product	107
4.10 Fresh (a) and used (b) aluminum alginate catalyst.	107
4.11 Residue lactic acid product obtained from hydrolysis at pressure of 319 mbar, T_{reboiler} of 90°C, feed flow rate of 1 ml/min, reflux ratio of 0.5 and 4.3 g of catalyst loading.....	111
4.12 Effect of operating pressure on conversion of <i>n</i> -butyl lactate (—●—), yield (···○··) and purity (—▼—) of lactic acid in residue product for hydrolysis of <i>n</i> -butyl lactate in reactive distillation column at T_{reboiler} of 90°C with reflux ratio of 0.5 and feed flow rate of 1 ml/min using 3 g of catalyst loading.....	112
4.13 Effect of reflux ratio on conversion of <i>n</i> -butyl lactate (—●—), yield (···○··) and purity (—▼—) of lactic acid in residue product for hydrolysis of <i>n</i> -butyl lactate in reactive distillation column at T_{reboiler} of 90°C under pressure of 319 mbar with feed flow rate of 1 ml/min using 4.3 g of catalyst loading	114

LIST OF FIGURES (Continued)

Figure	Page
4.14 Effect of catalyst loading on conversion of <i>n</i> -butyl lactate (—●—), yield (···○···) and purity (—▼—) of lactic acid in residue product for hydrolysis of <i>n</i> -butyl lactate in reactive distillation column at T_{reboiler} of 90°C under pressure of 319 mbar with reflux ratio of 1 and feed flow rate of 1 ml/min	115
4.15 Effect of feed flow rate on conversion of <i>n</i> -butyl lactate (—●—), yield (···○···) and purity (—▼—) of lactic acid in residue product for hydrolysis of <i>n</i> -butyl lactate in reactive distillation column at T_{reboiler} of 90°C under pressure of 445 mbar with reflux ratio of 0.5 using 4.3 g of catalyst loading	116
5.1 Scheme of proposed process for recovery and purification of lactic acid.	129
5.2 Process flowsheet for recovery and purification of lactic acid from fermentation broth with Process A.	139
5.3 Process flowsheet for recovery and purification of lactic acid from fermentation broth with Process B.....	139
5.4 Comparison of operating cost for recovery lactic acid using a combined extraction and reactive distillation via different process	149
A.1 Calibration standard curve of lactic acid	159
A.2 Calibration standard curve of <i>n</i> -butyl lactate.....	160
A.3 Calibration standard curve of 1-butanol	160

LIST OF FIGURES (Continued)

Figure	Page
A.4 Chromatograph of component analysis of feed solution	162
A.5 Chromatograph of component analysis of distilled product	163
A.6 Chromatograph of component analysis of residue product	165
B.1 Flowchart for calculation of reaction rate constant.....	168



SYMBOLS AND ABBREVIATIONS

a_i	=	Activity of component i
a_{mn}	=	Energy interaction parameters of functional group m and n
A	=	Cross-section area of column (m^2)
A_o	=	Pre-exponential factor ($\text{mol} \cdot \text{g}^{-1} \cdot \text{min}^{-1}$)
%AARD	=	The average absolute relative deviation
ALA	=	Aluminum-alginate
C_o	=	Initial concentration of solute in disperse phase ($\text{kg} \cdot \text{m}^{-3}$)
C	=	Solute concentration in dispersed phase ($\text{kg} \cdot \text{m}^{-3}$)
C^*	=	Equilibrium concentration of solute in dispersed phase ($\text{kg} \cdot \text{m}^{-3}$)
C_F	=	Initial concentration of solute in feed
C_E	=	Concentration of solute in extract product
d	=	Drop diameter (m)
d_{32}	=	Sauter mean drop diameter (m)
d_i	=	Mean diameter within a narrow size range i .
d_l	=	Length of major axis
d_s	=	Length of minor axis
D_M	=	Molecular diffusivity ($\text{m}^2 \cdot \text{s}^{-1}$)
D_N	=	Nozzle diameter (m)
D_{eff}	=	Effective diffusivity ($\text{m}^2 \cdot \text{s}^{-1}$)
E	=	Degree of extraction
E_A	=	Activation energy ($\text{kJ} \cdot \text{mol}^{-1}$)

SYMBOLS AND ABBREVIATIONS (Continued)

ER	=	Eley-Rideal model
E_{oN}	=	Nozzle Eotvos number
E_{oD}	=	d_{32} Eotvos number
FCI	=	Fixed-capital investment
g	=	Acceleration due to gravity ($\text{m}\cdot\text{s}^{-1}$)
g^E	=	Partial excess Gibbs energy
ΔH°	=	Enthalpy ($\text{kJ}\cdot\text{mol}^{-1}$)
k	=	Reaction rate constant ($\text{mole}\cdot\text{g}^{-1}\cdot\text{min}^{-1}$)
K_d	=	Dispersed phase mass transfer coefficient ($\text{m}\cdot\text{s}^{-1}$)
K_e	=	Equilibrium constant of the reaction.
K_i	=	Adsorption constant of adsorbed component i .
LH	=	Langmuir-Hinshelwood model
m	=	Total number of components. The parameters
M	=	Molecular weight
MRD	=	Mean relative deviation
n_i	=	Number of drops
n	=	Initial mole
N	=	Number of experiments
NaOH	=	Sodium hydroxide
P	=	Pressure
P^*	=	Vapor pressure
PH	=	Pseudo-homogeneous model

SYMBOLS AND ABBREVIATIONS (Continued)

q	=	surface area parameter
Q	=	Volumetric flow rate ($\text{m}^3 \cdot \text{s}^{-1}$)
$-r$	=	Reaction rate ($\text{mol} \cdot \text{g}_{\text{cat}}^{-1} \cdot \text{min}^{-1}$)
r	=	volume parameter
R	=	Universal gas constant ($\text{J} \cdot \text{mol}^{-1} \cdot \text{K}^{-1}$)
Re	=	Reynolds number
SSR	=	Sum of squared residuals
ΔS°	=	Entropy ($\text{J} \cdot \text{mol}^{-1} \cdot \text{K}^{-1}$)
t	=	Time (s)
T	=	Temperature (K) is viscosity
TCI	=	Total capital investment
U_t	=	Terminal velocity ($\text{m} \cdot \text{s}^{-1}$)
U_{slip}	=	Slip velocity ($\text{m} \cdot \text{s}^{-1}$)
U_c	=	Superficial velocity of continuous phase ($\text{m} \cdot \text{s}^{-1}$)
U_d	=	Superficial velocity of continuous and dispersed phase ($\text{m} \cdot \text{s}^{-1}$)
U_N	=	Nozzle velocity ($\text{m} \cdot \text{s}^{-1}$)
USD	=	United State Dollar
UNIFAC	=	Universal functional activity coefficient model
V	=	Volume (m^3)
V_S	=	Molar volume of solute ($\text{cm}^3 \cdot \text{mol}^{-1}$)
w	=	Amount of catalyst (g)

SYMBOLS AND ABBREVIATIONS (Continued)

We	=	Weber number
WC	=	Working capital
x	=	Mole fraction
X_m	=	Mole fraction of group m in the mixture
X	=	Conversion
Y	=	Yield
z	=	Coordination number which is set equal to 10
Greek Symbols		
κ	=	Ratio of dispersed phase viscosity to continuous phase viscosity
μ	=	Viscosity (Pa·s)
ϕ	=	Holdup
ρ	=	Density ($\text{kg}\cdot\text{m}^{-3}$)
σ	=	Interfacial tension ($\text{N}\cdot\text{m}^{-1}$)
$\Delta\rho$	=	Density difference between phases ($\Delta\rho = \rho_c - \rho_d$) ($\text{kg}\cdot\text{m}^{-3}$)
φ	=	Association factor
μ_m	=	Viscosity of mixture (Pa·s)
ε	=	Packing porosity
$\nu_k^{(i)}$	=	Number of functional group of type k in molecule i .
Γ_k	=	Activity coefficient of group k .
$\Gamma_k^{(i)}$	=	Activity coefficient of group k in pure component i .

SYMBOLS AND ABBREVIATIONS (Continued)

γ	=	Activity coefficient
ϕ	=	Surface fraction
θ	=	Volume fractions
Θ_m	=	Area fraction of group m
λ_i	=	Constant value of Eq. (2.2), $i = 1,2,3,\dots$
B_i	=	Constant value of Eq. (2.2), $i = 1,2,3,\dots$

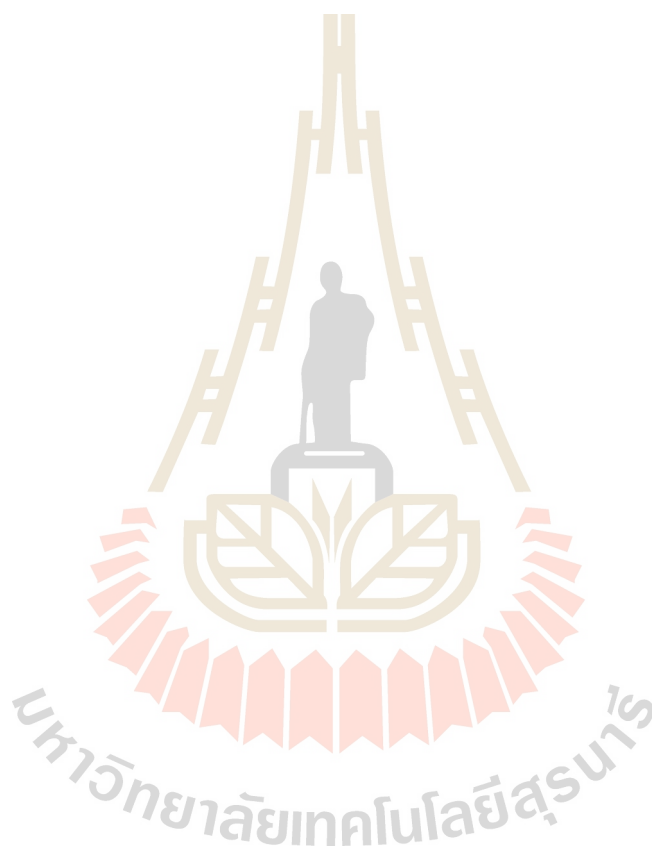
Subscripts

BuLA	=	n -Butyl lactate
BuOH	=	Butanol
c	=	Continuous phase
cat	=	Catalyst
$calc$	=	Calculated
d	=	Dispersed phase
exp	=	Experimental
f	=	Forward reaction
i	=	Component i
j	=	Component j
k	=	Functional group in the molecule i
LA	=	Lactic acid
r	=	Backward reaction
W	=	Water

SYMBOLS AND ABBREVIATIONS (Continued)**Superscripts**

C = Combinatorial

R = Residual term



CHAPTER I

INTRODUCTION

1.1 Background and Significance of the Problem

Lactic acid is an important chemical, which is used in many application fields. There are two isomers of lactic acid that are presented in nature as L(+) and D(-) forms. Lactic acid has been extensively used in food, cosmetic, pharmaceutical, and chemical industries. It can be produced by either chemical synthetic or microbial fermentation. The latter can produce, depending on the microorganism strain nearly enantiomerically pure L(+) lactic acid, which is the preferred feedstock for polylactic acid biodegradable polymer (PLA) (Bishai et al., 2015). The demand of L(+) lactic acid has been dramatically increased due to the PLA production. To obtain high quality PLA, using L(+) lactic acid with high purity is very important. At the end of the fermentation process, lactic acid exists in complex medium of fermentation broth. Thus, the purification of lactic acid from the aqueous fermentation broth remains a problem considering its purity, recovery and cost of purification.

Different downstream processing methods like precipitation with calcium hydroxide, crystallization, electrodialysis have been reviewed recently for purification of lactic acid. Most of these separation technologies shown either have low selectivity or low recovery yield. Precipitation of lactic acid in form of calcium lactate is undesirable and also environmental unfriendly due to consumption of lime and sulfuric acid and the production of calcium sulfate sludge as solid waste in large quantity

(Kertes and King, 1986). Crystallization demonstrated high selectivity, yet, its low recovery of major liquor restrained its application for large-scale purposes (Caboche et al., 2001). Electrodialysis has been used as a technique for the isolation and purification of lactic acid from fermentation media (Vonkaveesuk et al., 1994). Since other anions also go with lactic acid and other broth components end up in the product stream by diffusion, further processing is needed to remove these impurities. The cost of building an electrodialysis unit for large-scale operation is not economically feasible (Evangelista and Nikolov, 1996).

Purification of lactic acid by distillation becomes difficult due to its low volatility, solubility in water, and its polymerizing tendency at a higher temperature. To overcome these limitations, reactive distillation (RD) has been proposed as a promising technique for the recovery of lactic acid with high purity and high yield (Kumar et al., 2006a). The lactic acid is esterified by reacting it with alcohol, yielding corresponding lactate ester. The lactate ester is purified by distillation and then hydrolyzed to obtain pure lactic acid. This process has become an attractive alternative to conventional processes. The advantages of this process are simplification or elimination of the separation system leading to saving in the equipment cost. In addition, it can be improved conversion by separation of products and recycle of reactants, which drives equilibrium and enhance forward reaction as well as improved selectivity of desired products (Kumar et al., 2006b). Reactive distillation employing esterification of lactic acid with methanol and butanol, followed by hydrolysis of the separated lactate ester is an effective technique for separation and purification of lactic acid from aqueous solution. Kumar and Mahajani (2007) studied reactive distillation employing esterification of lactic acid with methanol, ethanol, or 1-butanol using Amberlyst-15 as

a catalyst, followed by hydrolysis for separation and purification of lactic acid. 1-butanol was reported to be a promising competitor to methanol and ethanol for the purpose of lactic acid recovery from the aqueous solutions. In addition, Su et al. (2013) designed and optimized the process for the continuous recovery of lactic acid from fermentation broth by reactive distillation using different esterifying alcohols. They reported that the methanol and butanol processes are the most economically attractive, while the ethanol and isopropanol process are more expensive because it is required to break the alcohol-water azeotrope. Using butanol as esterifying alcohol has additional advantage as it can prevent lactic acid polymerization during the reaction and it is preferred for short payback periods, while methanol process is preferred long payback periods.

Achieving decent rate and extent of reaction is crucial in successful operation of the reactive distillation process, and catalyst activity is the key for this achievement. Esterification of lactic acid can be catalyzed by liquid acid catalyst but it is not preferred because of long reaction time, corrosiveness and difficulty in catalyst separation from reaction medium (Wang et al., 2006). Solid acid catalyst including cation exchange resins (Delgado et al., 2007; Yixin et al., 2009) and metal oxide (Li et al., 2011) has gained more popularity than liquid catalyst as they are less corrosive and easier to be separated from the reaction medium, regenerated and reused. However, this type of catalyst is difficult to prepare, resulting in high production cost. Thus, development of cheap and easy-to-prepare catalyst is still in need to reduce processing cost. Zhang et al. (2013) studied the esterification of oleic acid with alcohols using a new solid acid catalyst prepared from sodium alginate and aluminum chloride. The aluminum alginate catalyst showed high catalytic activity for esterification of oleic acid. It can be applied

to the esterification reaction of fatty acids with various carbon chain lengths and was observed that the conversion increased with the lower carbon chain of fatty acid. Besides, this solid catalyst can be prepared easily at room temperature and was observed to have high activity for esterification reaction. It is, therefore, very attractive to be applied for esterification of lactic acid.

Although reactive distillation has been proposed as a promising technique for purification of lactic acid from its aqueous solution, the other broth components may have an effect on the process. Therefore, the recovery of lactic acid from fermentation broth before reactive distillation is also an important step. Extraction is a promising alternative to conventional methods for recovery of lactic acid from fermentation broth. The method provides high selectivity and enhances recovery by utilizing extractants. The extraction of lactic acid from aqueous solution using 1-butanol was explored in batch extraction (Chawong and Rattanaphanee, 2011). It was reported that butanol can be used as an environmentally friendly solvent to recover lactic acid with significant efficiency. After extraction, the organic phase obtained from this process was rich with 1-butanol and lactic acid, which can be used as the feedstock in reactive distillation. Thus, the combined counter-current extraction and reactive distillation process for recovery and purification of lactic acid is interesting.

1.2 Research Objectives

The aims of this research are the development of an improved process for recovery and purification of lactic acid by combined counter-current extraction and reactive distillation process. The technical feasibility of lactic acid extraction in a continuous mode is investigated by using laboratory scale of a packed liquid-liquid

extraction column. Sauter mean drop diameter in extraction column is determined. Correlation of mean drop size and dispersed phase Sherwood number are investigated. Purification of lactic acid using feedstock obtained from extraction is evaluated by reactive distillation. Kinetic behavior for esterification of lactic acid with 1-butanol using aluminum alginate as a solid catalyst is investigated in batch reactor. The reactive distillation of esterification and hydrolysis reaction are investigated using semi-batch reactive distillation column, which is aluminum alginate and Amberlyst-15 are used to catalyze the esterification and hydrolysis, respectively. In addition, the process simulation and economic is evaluated using Aspen HYSYS V10.

1.3 Scope and limitation of the research

1.3.1 To study counter-current liquid-liquid extraction for separation of lactic acid from synthetic lactic acid aqueous solution and fermentation broth in packed liquid-liquid extraction column at room temperature. The variables to be studied include nozzle diameter, continuous and dispersed phase flow rate.

1.3.2 To correlate Sauter mean drop diameter with operating variables and fluid physical properties to predict the drop size in the liquid-liquid extraction column and improve correlation of dispersed phase Sherwood number based on molecular diffusivity and effective diffusivity.

1.3.3 To characterize and investigate catalytic activity of aluminum alginate catalyst, as well as kinetic behavior of aluminum alginate, catalyzed esterification of lactic acid.

1.3.4 To study esterification and hydrolysis in semi-batch reactive distillation column using aluminum alginate and Amberlyst-15 as a solid catalyst.

1.3.5 To evaluate process simulation and economic of a combined counter-current extraction and reactive distillation for recovery and purification of lactic acid from fermentation broth.

1.4 Output of the research

1.4.1 Extraction efficiency, mass transfer coefficient and effect of operating variables such as nozzle diameter, continuous and dispersed phase flow rate on the extraction of lactic acid using 1-butanol as an extracting solvent in packed liquid-liquid extraction column.

1.4.2 An improve empirical correlation for estimation of Sauter mean drop diameter as well as a correlation of dispersed phase Sherwood number in terms of operating variables and fluid physical properties.

1.4.3 Characteristic data of aluminum alginate catalyst and kinetic model for esterification of lactic acid with 1-butanol using aluminum alginate catalyst.

1.4.4 Conversion and yield of lactic acid from the reactive distillation process.

1.4.5 Process design and production cost of lactic acid

1.5 References

Bishai, M., De, S., Adhikari, B., and Banerjee, R. 2015. A platform technology of recovery of lactic acid from a fermentation broth of novel substrate *Zizyphus oenophlia*. **3 Biotech** 5 (4):455-463.

Caboche, J.-j., Fouache, C., Choque, J.-c., Duflot, P., and Dubois, E. 2001. Process for the separation and purification of lactic acid from a fermentation medium.

- Chawong, K., and Rattanaphanee, P. 2011. n-Butanol as an Extractant for Lactic Acid Recovery. **World Academic of Science Engineering Technology** 56:1437-1440.
- Delgado, P., Sanz, M. T., and Beltrán, S. 2007. Kinetic study for esterification of lactic acid with ethanol and hydrolysis of ethyl lactate using an ion-exchange resin catalyst. **Chemical Engineering Journal** 126 (2-3):111-118.
- Evangelista, R. L., and Nikolov, Z. L. 1996. Recovery and purification of lactic acid from fermentation broth by adsorption. **Applied Biochemistry and Biotechnology** 57 (1):471.
- Kertes, A. S., and King, C. J. 1986. Extraction chemistry of fermentation product carboxylic acids. **Biotechnology and Bioengineering** 28 (2):269-282.
- Kumar, R., and Mahajani, S. M. 2007. Esterification of Lactic Acid with n-Butanol by Reactive Distillation. **Industrial & Engineering Chemistry** 46:6873-6882.
- Kumar, R., Mahajani, S. M., Nanavati, H., and Noronha, S. B. 2006a. Recovery of lactic acid by batch reactive distillation. **Journal of Chemical Technology & Biotechnology** 81 (7):1141-1150.
- Kumar, R., Nanavati, H., Noronha, S. B., and Mahajani, S. M. 2006b. A continuous process for the recovery of lactic acid by reactive distillation. **Journal of Chemical Technology & Biotechnology** 81 (11):1767-1777.
- Li, K.-T., Wang, C.-K., Wang, I., and Wang, C.-M. 2011. Esterification of lactic acid over TiO₂-ZrO₂ catalysts. **Applied Catalysis A: General** 392 (1-2):180-183.
- Su, C.-Y., Yu, C.-C., Chien, I. L., and Ward, J. D. 2013. Plant-Wide Economic Comparison of Lactic Acid Recovery Processes by Reactive Distillation with

Different Alcohols. **Industrial & Engineering Chemistry Research** 52 (32):11070-11083.

Vonktaveesuk, P., Tonokawa, M., and Ishizaki, A. 1994. Stimulation of the rate of l-lactate fermentation using *Lactococcus lactis* IO-1 by periodic electro dialysis. **Journal of Fermentation and Bioengineering** 77 (5):508-512.

Wang, Y., Ou, S., Liu, P., Xue, F., and Tang, S. 2006. Comparison of two different processes to synthesize biodiesel by waste cooking oil. **Journal of Molecular Catalysis A: Chemical** 252 (1):107-112.

Yixin, Q., Shaojun, P., Shui, W., Zhiqiang, Z., and Jidong, W. 2009. Kinetic Study of Esterification of Lactic Acid with Isobutanol and n-Butanol Catalyzed by Ion-exchange Resins. **Chinese Journal of Chemical Engineering** 17 (5):773-780.

Zhang, Q., Li, H., Qin, W., Liu, X., Zhang, Y., Wei, X., and Yang, S. 2013. Solid acid used as highly efficient catalyst for esterification of free fatty acids with alcohols. **China Petroleum Processing and Petrochemical Technology** 15:19-24.

CHAPTER II

EXTRACTION OF LACTIC ACID WITH 1-BUTANOL USING COUNTER-CURRENT PACKED LIQUID- LIQUID EXTRACTION COLUMN

2.1 Abstract

The experimental extraction of lactic acid with 1-butanol in counter-current packed liquid-liquid extraction column was studied. Sauter mean drop diameter, drop size distribution and dispersed phase mass transfer coefficient were investigated at different operating parameters, including nozzle diameter, continuous and dispersed phase flow rate. The Sauter mean drop diameter was found to decrease with increasing the dispersed phase flow rate and decreasing nozzle diameter, which is an influence on increasing dispersed phase mass transfer coefficient. By increasing the continuous phase flow rate, the Sauter mean drop diameter increased due to coalescence of drops. Maximum efficiency in extraction of lactic acid from fermentation broth achieved at 72.53% when using a nozzle diameter of 1 mm with the continuous and dispersed phase flow rate of 40 and 70 ml/min, respectively. Additionally, correlation of Sauter mean drop diameter and dispersed phase Sherwood number were studied. The Sauter mean drop diameter correlation was in a good agreement with experimental values. The modified Sherwood number correlation by effective diffusivity can improve the correlation with higher accuracy for prediction of experimental values.

2.2 Introduction

Packed liquid-liquid extraction column is one of classical extraction column for separation methods. It often used in many industries such as chemical, petroleum, mining and food industries. In liquid-liquid extraction method, solute transferred between two immiscible or slightly miscible liquid phases in column. One liquid dispersed as droplets in other. The liquid is dispersed as droplets namely dispersed phase and the bulk surrounding liquid is called continuous phase.

Normally, efficiency of liquid-liquid extraction is dependent on turbulence of system and interfacial area available for mass transfer. For packed liquid-liquid extraction column, the presence of packing in the column increases local velocities, retards recirculation, reduce back mixing of the continuous phase, and improves distribution and hold up of the dispersed phase. As a result, mass transfer would be further improved. One important parameter is the dispersed phase droplets behavior because of its effect on mass transfer coefficient. The overall mass transfer coefficient is one of most parameters required to design and scaleup of extraction column. Therefore, the knowledge of mean drop size and drop size distribution are important key parameters in study and design of liquid-liquid extraction column. Nowadays, there are several researchers who studied drop size distribution and predicted correlation of mean drop size for packed liquid-liquid extraction column.

GhaffariTooran et al. (2009) predicted correlation for overall Sherwood number in packed liquid-liquid extraction column using the standard system of water/acetic acid/toluene. Thorough consideration of dispersed and continuous phase flow rate influencing parameters, they presented the correlation of Sherwood number in term of dimensionless parameters which has an acceptable average error of about 15.8%.

Salimi-Khorshidi et al. (2013) investigated effect of holdup on Sauter mean drop diameter and on dispersed phase mass transfer coefficient in spray and packed liquid-liquid extraction column of water/acetic acid/toluene system. The results were reported that the dispersed and continuous phase flow rate affected on holdup, mean drop size and dispersed phase mass transfer coefficient. The dispersed phase mass transfer coefficient for the packed column was higher than spray column with smaller mean drop size. Furthermore, the presence of packing improved the performance of extraction approximately 25.6%. Additionally, empirical correlation of Sauter mean drop diameter and Sherwood number were in a good agreement with experimental data.

However, the works existed in previous literature considered behavior of mass transfer coefficient and Sherwood number along molecular diffusivity by neglecting the effects of internal circulations of drops. This neglecting can cause a considerable error in determining the mass transfer inside the drop (Ayyaswamy et al., 1990). An enhancement factor is used to define the correct diffusivity as effective diffusivity for presenting the effect of internal circulation. Azizi et al. (2014) reported the correlation of Sherwood number based on effective diffusivity in structured packed column. The results showed that replacing the molecular diffusivity with effective diffusivity through enhancement factor can modify the mass transfer coefficient and correct their estimation.

Based on previous literature information, this work aims to study packed liquid-liquid extraction column in extraction of lactic acid with 1-butanol. Effect of operating parameters on drop size and dispersed phase mass transfer coefficient were investigated. The correlation of Sauter mean drop diameter was estimated and effective diffusivity was investigated through Sherwood number correlation.

2.3 Theory

2.3.1 Packed Liquid-Liquid Extraction Column

Liquid-liquid extraction is one of important separation method which is used to recover or remove wanted substance from a solution. Different kinds of liquid-liquid contactors are used in the industrial, which are classified according to the mixing type of two liquid phases. Packed liquid-liquid extraction column is widely employed in industrial practice. The flow of liquids in column is driven by difference densities of two liquid phases and contact either with suitable packing material. For counter-current extraction, two liquid phases are fed in the opposite direction of another side column. Lighter liquid is fed at the bottom of the column and distributed as small drops, which is call dispersed phase. The drops rise and flow through the heavier liquid, which flows down as a continuous phase. The heavier liquid leaves at the bottom and the lighter liquid leaves at the top of column.

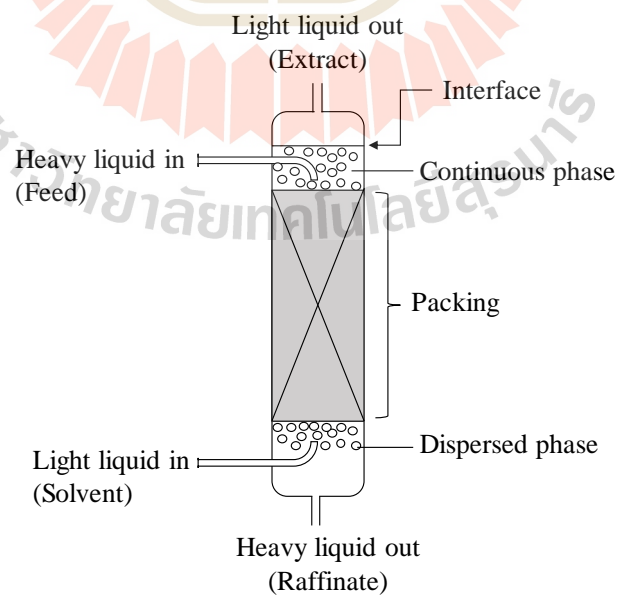


Figure 2.1 Packed liquid-liquid extraction column

Mass transfer between phases is continuous and the composition of phases changes through the column. There is no equilibrium between phases because it is the difference from equilibrium which is the driving force for mass transfer. The mass transfer is the most efficient when the phases are in good contact with each other and this happens in the region, in which the drops are formed. That is why the drops are usually reformed at frequent intervals throughout the column. Dispersed phase depends on the characteristics of the liquids and operation parameters. The dispersed phase should have a higher viscosity than the continuous phase since a low viscosity of continuous phase makes possible a higher phase throughput. The dispersed phase should also have higher flow rate to obtain a maximum mass transfer area. A low interfacial tension between liquid phases is also an important factor for the dispersed phase. The low interfacial tension makes the dispersion possible easily. In any case, the choice of the dispersed phase cannot only base on theoretical considerations. Theories are good aid to experiments which are made, for example, in a pilot column with a real material system.

2.3.2 Drop Behavior

Relationship between the drop behavior with its diameter when rising or falling in a continuous phase can be distinguished in four regions as shown in Figure 2.2. The small diameter drops behave like rigid spheres (I). The shear force at the interface increases with increasing drop diameter and circulation inside the drop is induced which leads to an increased velocity as compared to a rigid drop (II). As the diameter of the drop increases further, the drop starts to visibly lose its spherical shape (III). Simultaneously, the drop starts to oscillate. Finally, the behavior of deformed drops is reached where drops move to wobble through a continuous phase (IV).

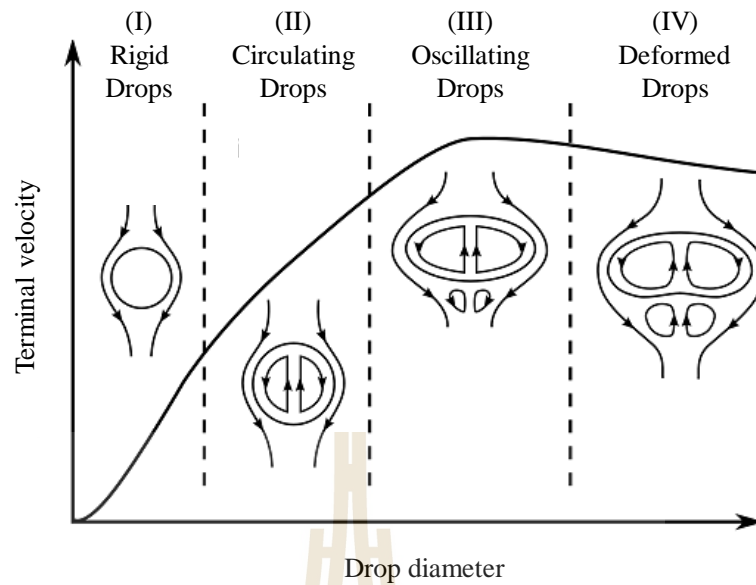


Figure 2.2 Hydrodynamic regions of drop (Bertakis, 2013)

2.3.3 Dispersed Phase Mass Transfer Coefficient

The mass transfer coefficient of the dispersed or continuous phase is one of the fundamental and essential parameters in the extraction column design. Several equations have been presented in past studies for calculation of the mass transfer coefficient of dispersed phase. However, results have usually been considered in the light of three regions of mass transfer inside drops. The three regions commonly considered for determination of mass transfer rate of solute in a drop are stagnant, circulation and oscillating drops.

2.3.3.1 Stagnant Drops

Newman et al. (1932) presented an equation for unsteady-state mass transfer inside a spherical drop based on molecular diffusion (D_M) and neglecting the continuous phase resistance. This equation is used for very small drops that are assumed to be stagnant. The Reynolds number for such drops is usually less than 10.

$$K_d = -\left(\frac{d}{6t}\right) \ln \left[\frac{6}{\pi^2} \sum_i \frac{1}{i^2} \exp\left(\frac{-4D_M \pi^2 i^2 t}{d^2}\right) \right] \quad (2.1)$$

2.3.3.2 Circulating Drops

Kronig and Brink (1951) presented a model based on circulating drops, which are due to the relative motion of the drop and continuous phase. They assumed that these circulations are laminar and the continuous phase resistance is negligible.

$$K_d = -\left(\frac{d}{6t}\right) \ln \left[\frac{3}{8} \sum_i B_i^2 \exp\left(\frac{-64\lambda_i D_M t}{d^2}\right) \right] \quad (2.2)$$

This equation is used for a Reynolds number range of 10 to 200. The constant values of λ_i and B_i were reported by Elzinga and Banchemo (1959).

2.3.3.3 Oscillating Drops

Handlos and Baron (1957) proposed a model for drops with high internal circulation. They considered that in a high Reynolds number ($Re > 200$), drops were completely agitated or oscillated. By assuming eddy diffusion between internal toroidal streamlines and neglecting the continuous phase resistance, they presented the equation below,

$$K_d = -\left(\frac{d}{6t}\right) \ln \left[2 \sum_i B_i^2 \exp\left(\frac{-\lambda_i U_i t}{128(1+\kappa)d^2}\right) \right] \quad (2.3)$$

where U_i is the terminal velocity. d is drop diameter and t is contact time. κ is the ratio of dispersed phase viscosity to continuous phase viscosity;

$$\kappa = \frac{\mu_d}{\mu_c} \quad (2.4)$$

μ_c and μ_d are the viscosity of continuous and dispersed phases, respectively.

Other investigators have replaced the molecular diffusivity (D_M) with effective diffusivity (D_{eff}) which is defined to be the product of an enhancement factor (\mathfrak{R}) to molecular diffusivity in order to show the effect of internal circulation (Amanabadi et al., 2009). Inspired by this fact, Calderbank and Korchinski (1956) have modified the equation of (Kronig and Brink, 1951) replacing D_M with $\mathfrak{R}D_M$,

$$K_d = -\left(\frac{d}{6t}\right) \ln \left[1 - \left(1 - \exp\left(\frac{-4\pi^2 \mathfrak{R}D_M t}{d^2}\right) \right)^{\frac{1}{2}} \right] \quad (2.5)$$

where D_M is molecular diffusivity, which can be calculated by a modified correlation of Wilke and Chang (1955), given by:

$$D_M = 7.4 \times 10^{-5} \frac{(\varphi M)^{1/2} T}{\mu_m V_S^{0.6}} \quad (2.6)$$

where φ is association factor, M is molecular weight, T is temperature, μ_m is viscosity of mixture and V_S is molar volume of solute at normal boiling temperature. The enhancement factor can be calculated following the correlation of Rahbar et al. (2011).

$$\mathfrak{R} = 0.0272(1 + h^{-1}) \text{Re}^{1.258} \quad (2.7)$$

Reynolds number (Re) is calculated considering the physical properties of the continuous phase and slip velocity of drops.

$$\text{Re} = \frac{\rho_c U_{\text{slip}} d_{32}}{\mu_c} \quad (2.8)$$

where ρ_c and μ_c are density and viscosity of continuous phase, d_{32} is Sauter mean drop diameter. U_{slip} is slip velocity between two phases through the column. Since the dispersed and continuous phases flow counter-current through the column, the slip velocity between the phases is obtained as follows:

$$U_{\text{slip}} = \frac{Q_d}{\varepsilon A \phi} + \frac{Q_c}{(1-\phi)} \quad (2.9)$$

where Q_c and Q_d are flow rate of continuous and dispersed phases, respectively. A is a cross-section area of column. ε is packing porosity and ϕ is holdup. To measure holdup, the volume of each phase was measured. To determine reliable results, the height of each phase in the column was maintained constant. The holdup was calculated using equation:

$$\phi = \frac{V_d}{V_c + V_d} \quad (2.10)$$

where V_c and V_d are the volumes of the continuous phase and dispersed phase, respectively.

Experimental dispersed phase mass transfer coefficients (K_d) can be calculated from experimental measurements by considering the mass balance equation for a single drop:

$$K_d = -\frac{d_{32}}{6t} \ln(1-E) \quad (2.11)$$

$$E = \frac{C_0 - C}{C_0 - C^*} \quad (2.12)$$

where d_{32} is Sauter mean drop diameter and t is contact time. C_0 is initial concentration of solute in the dispersed phase. C and C^* are concentration of solute in output and in equilibrium of disperse phase, respectively.

2.3.4 Sauter Mean Drop Diameter

The mass transfer rate is strongly affected by drop size and hydrodynamics of the two phases. The most commonly used representative diameter which used to study the mean drop size in the liquid-liquid extraction columns is Sauter mean diameters (Panahinia et al., 2017). The Sauter mean diameter (d_{32}) is calculated at the experimental conditions by following equation:

$$d_{32} = \frac{\sum_{i=0}^n n_i d_i^3}{\sum_{i=0}^n n_i d_i^2} \quad (2.13)$$

Moving drops could be spherical, elliptical or in other similar forms. For non-spherical drops, the equivalent diameter was expressed as follows:

$$d_i = (d_1^2 d_s)^{1/3} \quad (2.14)$$

where n_i is the number of drops of mean diameter d_i within a narrow size range i . d_1 and d_s are length of major and minor axis, respectively.

A great deal of experimental effort has been expended principally for the purpose of evaluating column performance for design and scale-up. Knowledge of the drop size is of fundamental importance in the design of the liquid-liquid extraction columns. The drop size affects the dispersed phase holdup, the residence time of the dispersed phase, and the allowable throughputs. Furthermore, it determines the interfacial area available for mass transfer and influences both the continuous and dispersed-phase mass transfer coefficients, together with the holdup (Soltanali et al., 2009). Therefore, it is important to be able to correlate the drop size as a function of operating conditions, two-phase flow rates, and physical properties of the liquid-liquid system (Yuan et al., 2012). Salimi-Khorshidi et al. (2013) studied the drop size and dispersed phase mass transfer and proposed correlation of Sauter mean drop diameter in packed liquid-liquid extraction column. To correlate d_{32} , the authors carried out a statistical analysis, which is d_{32} as a function;

$$d_{32} = f(\sigma, U_c, U_d, U_N, \rho_c, \rho_d, \Delta\rho, \mu_c, \mu_d, D_N, \phi, g) \quad (2.15)$$

where σ is interfacial tension.

ρ_c and ρ_d are density of continuous and disperse phase.

$\Delta\rho$ is density difference between phases ($\Delta\rho = \rho_c - \rho_d$).

μ_c and μ_d are viscosity of continuous and disperse phase.

U_c and U_d are superficial velocity of continuous and disperse phase.

U_N is nozzle velocity.

D_N is nozzle diameter.

g is acceleration due to gravity.

By using a dimensionless analysis, Eq. (2.15) can be rearranged as the following equation:

$$\frac{d_{32}}{D_N} = f \left(\text{Re}_d, We, E_{oN}, \frac{\Delta\rho}{\rho_c}, \frac{\Delta\rho}{\rho_d}, \frac{\mu_d}{\mu_c}, \phi \right) \quad (2.16)$$

where We is dimensionless Weber number and E_{oN} is Nozzle Eotvos number. We and E_{oN} can be determined by the following equations:

$$We = \frac{\rho_d U_N^2 D_N}{\sigma} \quad (2.17)$$

$$E_{oN} = \frac{\rho_d g D_N^2}{\sigma} \quad (2.18)$$

Eq. (2.16) can be rewritten in the form of the following equation:

$$\frac{d_{32}}{D_N} = m \phi^a \text{Re}_d^b We^c E_{oN}^d \left(\frac{\Delta\rho}{\rho_c} \right)^e \left(\frac{\Delta\rho}{\rho_d} \right)^f \left(\frac{\mu_d}{\mu_c} \right)^h \quad (2.19)$$

where m , a , b , c , d , e , f , and h are constants of the correlation. However, the authors considered the constants d , e , f , and h are to be zero because they found that cause some errors in the correlation's results. Therefore, the authors modified the dependence

function of the holdup to a power function of linear form of holdup. Eq. (2.19) may be rewritten as the following equation:

$$\frac{d_{32}}{D_N} = m(1 + a\phi)^n \text{Re}_d^b \text{We}^c \quad (2.20)$$

Correlation's constants were calculated using least squares method. The average absolute relative deviation (%AARD) was calculated from the following equation:

$$\%AARD = \frac{1}{N} \sum_{i=1}^n \left| \frac{(d_{32})_{\text{exp}} - (d_{32})_{\text{cal}}}{(d_{32})_{\text{exp}}} \right| \times 100 \quad (2.21)$$

where N is the number of experiments, $(d_{32})_{\text{exp}}$ is the measured data and $(d_{32})_{\text{cal}}$ is the calculated data.

2.3.5 Dispersed Phase Sherwood Number

Sherwood number is a dimensionless number that represents the ratio of convective mass transfer to the rate of diffusive mass transport and is used in the analysis of mass transfer systems such as liquid-liquid extraction. The Sherwood number is directly dependent on mass transfer coefficient, which it proposed the dimensionless group that influences on mass transfer. With regards to the dispersed phase mass transfer coefficient, experimental dispersed phase Sherwood number (Sh_d) is calculated as follows:

$$Sh_d = \frac{K_d d_{32}}{D_M} \quad (2.22)$$

in which, K_d is dispersed phase mass transfer coefficient and d_{32} is Sauter mean drop diameter.

Design of an extraction column for a given separation method needs reliable correlations for prediction of mass transfer coefficients, which is generally calculated through correlations involving the Sherwood number. In a similar way to d_{32} , dispersed phase Sherwood number is proposed to all dimensionless groups that affect the mass transfer by Salimi-Khorshidi et al. (2013). The equation is written in form of Eq. (2.23):

$$Sh_d = f \left(Re_d, We, E_{oD}, \frac{\Delta\rho}{\rho_c}, \frac{\Delta\rho}{\rho_d}, \frac{\mu_d}{\mu_c}, \phi \right) \quad (2.23)$$

where E_{oD} is d_{32} Eotvos number. It can be calculated using Eq. (2.24):

$$E_{oD} = \frac{\rho_d g d_{32}^2}{\sigma} \quad (2.24)$$

Eq. (2.23) can be rewritten in the following form:

$$Sh_d = m\phi^a Re_d^b E_{oD}^c We^d \left(\frac{\Delta\rho}{\rho_c} \right)^e \left(\frac{\Delta\rho}{\rho_d} \right)^f \left(\frac{\mu_d}{\mu_c} \right)^h \quad (2.25)$$

where $m, a, b, c, d, e, f,$ and h are constants. Similar to d_{32} , the value of constants $e, f,$ and h should be equal to 0. In addition, the dependence function of the Eotvos number and the holdup can be changed to a power function with the linear form of holdup to achieve a less error. Subsequently, Eq. (2.25) can be rewritten in the form of Eq. (2.26):

$$Sh_d = m(1 + a\phi)^n Eo_d^b Re_d^c We^d \quad (2.26)$$

The constants were determined by minimizing the differences between the experimental and calculated Sh_d using average absolute relative deviation same with minimizing of d_{32} . In this work, Sauter mean drop diameter and dispersed phase Sherwood number for extraction of lactic acid using 1-butanol in packed liquid-liquid extraction column were correlated using the equation proposed and comprehensively described by (Salimi-Khorshidi et al., 2013).



2.4 Experimental Procedures

2.4.1 Chemicals

Lactic acid with a concentration of 88 % wt and RPE reagent grade of 1-butanol with 99.9%wt purity were purchased from Acros. Fermentation broth was obtained from Bioprocessing pilot plant, Cassava research center of Suranaree University of Technology. Deionized water was used in every experiment.

2.4.2 Experimental Apparatus

The packed liquid-liquid extraction column consists of a glass tube with 25 mm internal diameter, 300 mm height, and with a chamber at top and bottom of the column. The liquids were pumped into the column using peristaltic pumps. Nozzle with diameters of 1 and 5 mm were used to produce drops that fed into the column. The column was randomly packed with $6 \times 6 \times 1$ mm borosilicate glass Raschig ring and porosity factor was about 0.74 for the packed column. The apparatus was performed at room temperature. A schematic diagram of the experiment was shown in Figure 2.2.

2.4.3 Procedure

The experiments were performed using synthesis lactic acid solution and fermentation as liquid feed. The lactic acid solution was prepared by diluting with deionized water at 0.1 M of lactic acid. The experiments were studied at room temperature and atmospheric pressure. The lactic acid solution as a continuous phase and 1-butanol (extracting solvent) as a dispersed phase were fed at a top and bottom of column, respectively. The continuous phase and the dispersed phase were delivered downward and upward, respectively using peristaltic pumps. Volumetric flow rates of both phases were varied at desired values. In this study, different values of volumetric flow rates of the continuous and dispersed phase and nozzle diameters were used to

desired range of drop size for studying the effect of drop size on mass transfer. The experiments were implemented for full factorial experimental design with two different volumetric flow rates of the continuous phase, three different volumetric flow rates of the dispersed phase and two different nozzle diameters. The number of observation points was 12 experiment totally.

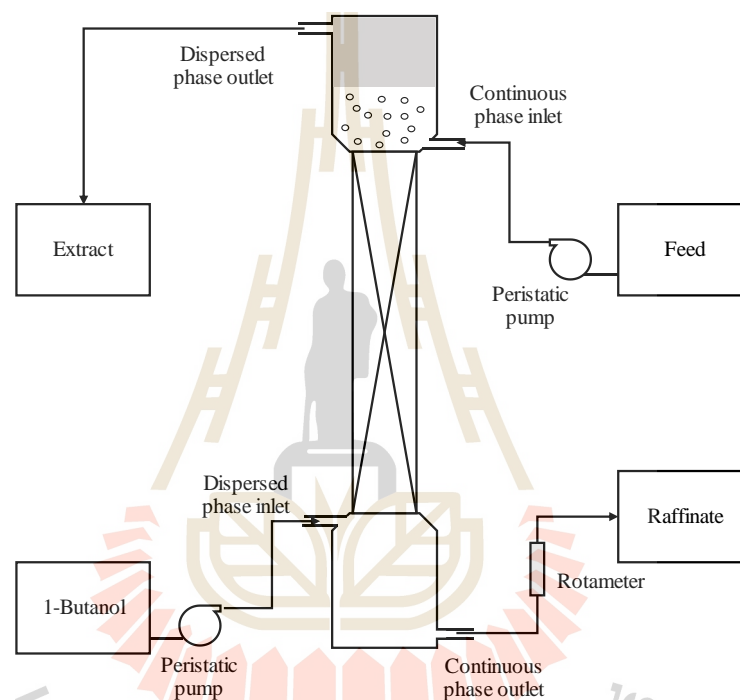


Figure 2.3 Schematic diagram of packed liquid-liquid extraction column

Before each run, the column was slowly filled with the continuous phase up to the level of the interface in chamber. Next, the continuous phase valve was closed, and the dispersed phase was introduced. Then, the continuous phase valve was reopened allowing this phase to enter to the column. The dispersed and continuous phases exited at the top and bottom of column, which it is denoted as extract and raffinate product, respectively. The continuous phase outlet was set at the proper flow

rate to keep the interface level stable. Samples of both products phased were collected at different time intervals for analyzing the concentration of lactic acid. The experiment used four tanks to store the feed, solvent, raffinate, and extract streams.

2.4.4 Methods of Analysis

2.4.4.1 Gas Chromatography Analysis of Lactic Acid

Quantities of lactic acid were analyzed by a Shimadzu GC-14B equipped with flame ionization detector (FID) using helium (99.999 % purity) as the carrier gas. A DB-WAX with 30m x 0.53mm x 0.5m capillary column is used to separate the sample. The samples are diluted with deionized water before analysis. The oven is operated at variable-programmed temperature. Initially, the temperature of the oven is held at 50°C for 3 minutes before increased to 230°C at a rate of 10°C/min and held for 4 minutes. Temperature of injector and detector are at 250°C.

2.4.4.2 Drops Analysis

A photographic technique was used to determine Sauter mean drop diameter. The drops were photographed using a Fuji XA-2 digital camera, followed by analysis with Fiji ImageJ software. At least 300 drops were analyzed for each determination. The Sauter mean drop diameter was calculated from Eq. (2.13).

2.4.4.3 Density, Viscosity and Interfacial Tension Analysis

Densities of each phase were determined by weighing with ± 0.0001 g based on 1 ml of samples. Viscosities were evaluated by Brookfield Rheometer-DV3T at a temperature of 30°C. The liquid sample was performed in a cup with cone spindle CPA-52 using a speed of 120 rpm. The viscosities were obtained at 99% torque. Interfacial tensions were measured at 30°C by Force Tensiometer K100 from Scientific Promotion using ring probe.

2.5 Results and Discussion

2.5.1 Effect of Operating Parameters on Drop Size

Extraction of lactic acid with 1-butanol from synthetic lactic acid solution in packed liquid-liquid extraction was studied at room temperature and atmospheric pressure. Main operating parameters including nozzle diameter (D_N), continuous and dispersed phase flow rate (Q_c and Q_d) were investigated the effect on Sauter mean drop diameter (d_{32}) and drop size distribution. In this study, d_{32} has been studied during steady-state time run for a packed liquid-liquid extraction column. The effect of operating parameters on d_{32} showed in Figure 2.4.

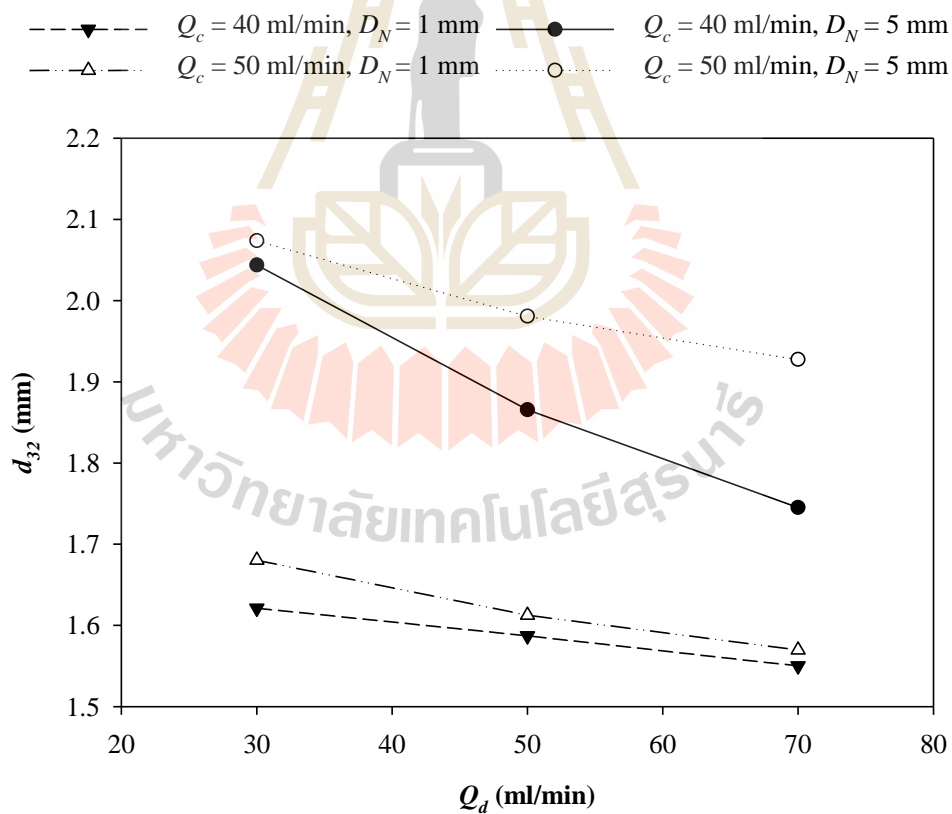


Figure 2.4 The Sauter mean drop diameter versus dispersed phase flow rate with different nozzle diameters and continuous phase flow rate

It was observed that d_{32} decreased with increasing dispersed phase flow rate while increasing continuous phase flow rate influenced in increasing d_{32} . In fact, when the dispersed phase is injected to the drops, the drop's neck is formed, and the volume of drops increases until the size of drops becomes enough to conquer the interfacial force. When the buoyancy force overcomes the interfacial force, the drops begin to rise across the extraction column. The volume of drops formation is the sum of drop's neck and injected dispersed phase. The rising time is proportional to the dispersed phase flow rate. Therefore, increasing of dispersed phase flow rate led to decrease in rising time of drops formation and increased the buoyancy of drops from nozzle. The drops are not enough time for growing as resulting in decreasing d_{32} . In addition, d_{32} is dependent on drop breakage and coalescence due to turbulence of system. Higher dispersed phase flow rate enhances collision of drops with packing and column wall, the drops are breaking into smaller drops as an example shown in Figure 2.5 and 2.6.



Figure 2.5 Number of drops at different Q_d using D_N of 1 mm for Q_c of 40 ml/min (a) and 50 ml/min (b)

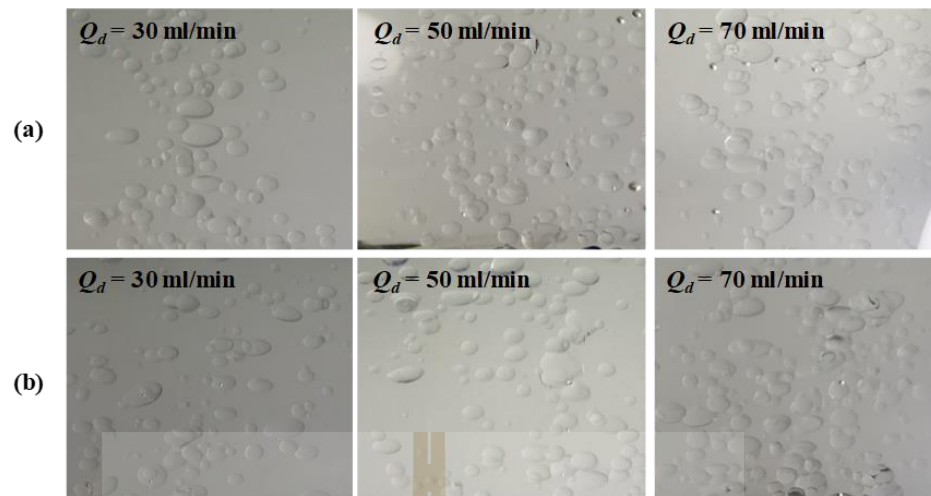


Figure 2.6 Number of drops at different Q_d using D_N of 5 mm for Q_c of 40 ml/min (a) and 50 ml/min (b)

On the other hand, the coalescence will induce rectification of liquid drops into larger ones. By increasing the continuous phase flow rate, the drag force between the drops and the continuous phase increases and consequently slip velocity between phases will decrease, resulting in an increasing residence time of drops. Increasing the residence time of drops enhances the probability for drop coalescence, leading to larger drops. For the effect of nozzle diameter, it can be explained that using a small nozzle diameter produced a small volume of injected dispersed phase as well as volume of drops. So, d_{32} decreased with decreasing nozzle diameter.

Drop size distribution results are presented in Figure 2.7 and 2.8 for nozzle diameter of 1 and 5 mm, respectively. Comparison at the same continuous phase flow rate and nozzle diameter, the drop size distributions clearly shifts toward smaller size and narrow with an increase in the dispersed phase flow rate, evidencing breakage of drops. With different nozzle diameters, drop size distribution found to be shifted to

the larger size with an increase in nozzle diameter and continuous phase flow rate as described above.

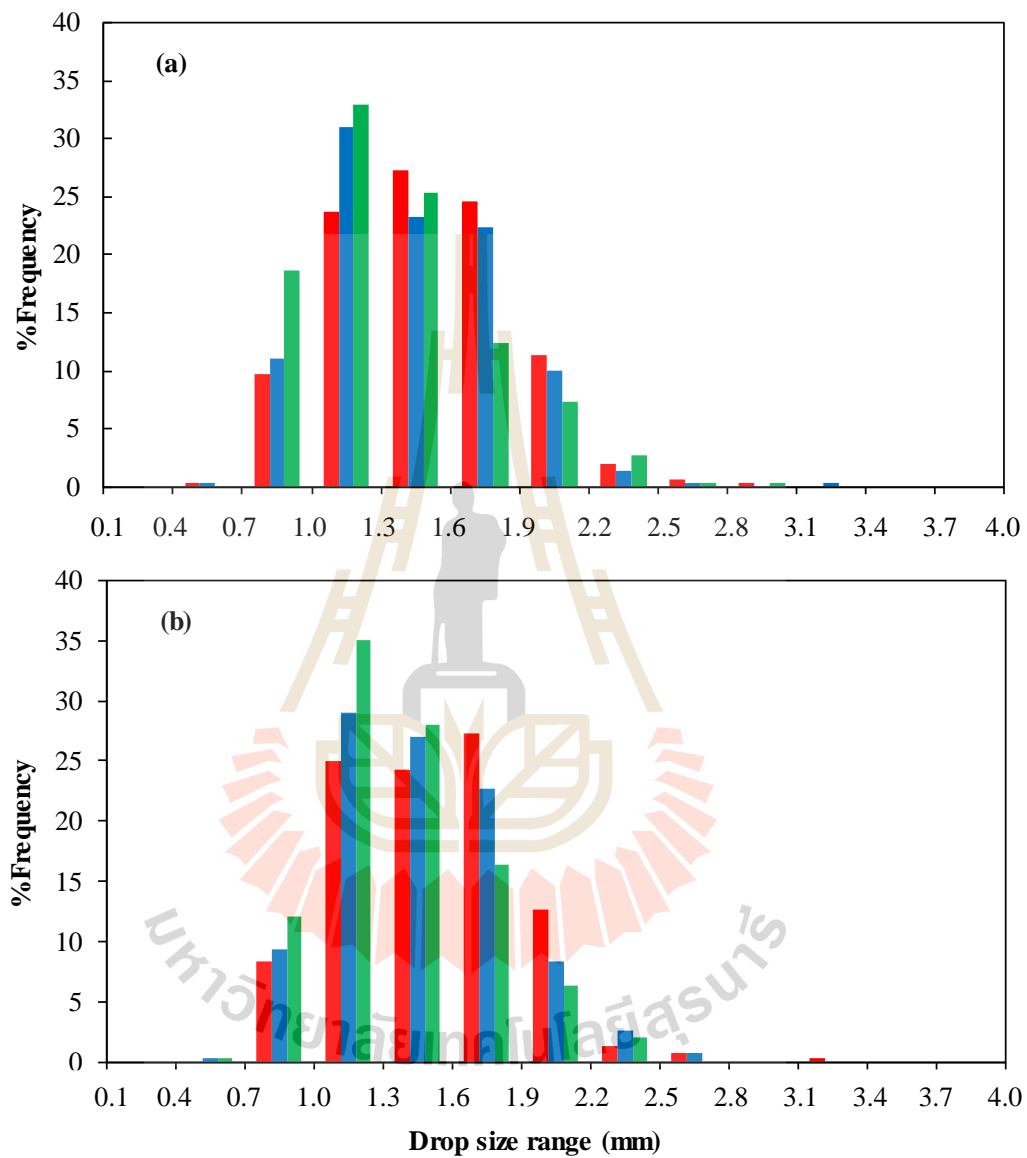


Figure 2.7 Drop size distribution using D_N of 1 mm at $Q_d = 30$ ml/min (red), 50 ml/min (blue) and 70 ml/min (green) for $Q_c = 40$ ml/min (a) and 50 ml/min (b), respectively

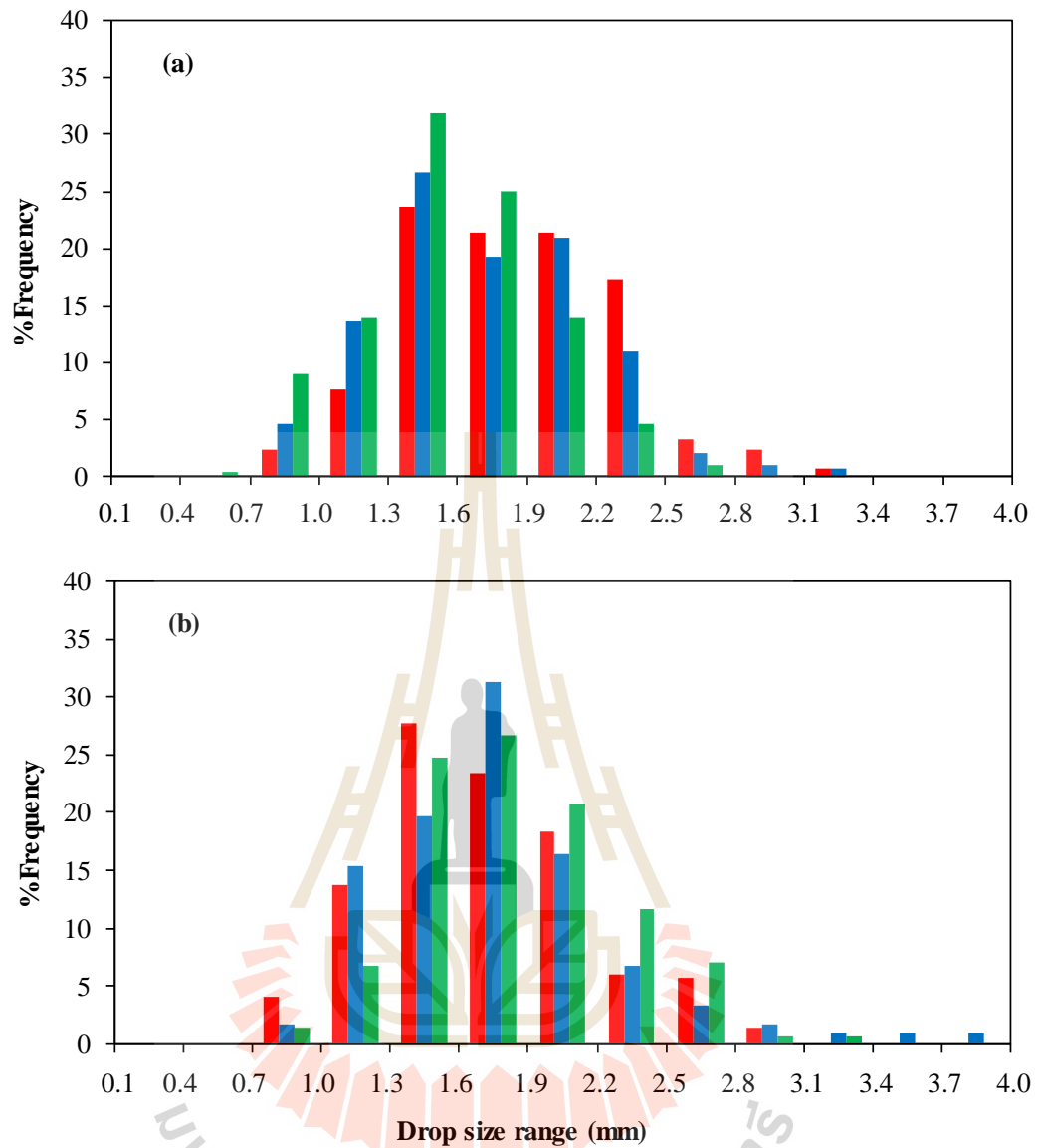


Figure 2.8 Drop size distribution using D_N of 5 mm at $Q_d = 30$ ml/min (red), 50 ml/min (blue) and 70 ml/min (green) for $Q_c = 40$ ml/min (a) and 50 ml/min (b), respectively

In addition, Reynolds number obtained in this work as shown in Table 2.1 was found in the range of $38.28 \leq Re \leq 131.93$, which is the presence of circulating drop according to concept proposed by Kronig and Brink (1951). Similar to criterion is described by Mack (2001), which is used to categorize the drops according to their

diameter in rigid, circulating, or oscillating drops. The categorization is performed according to the following relations:

$$\text{Circulating drops:} \quad \frac{1.83}{Mo^{0.275}} \leq Ar \leq \frac{391}{Mo^{0.275}} \quad (2.27)$$

Archimedes number (Ar) is related to Reynolds number. Morton number (Mo) is a dimensionless number used together with the Eotvos number to characterize the shape of drops moving in the continuous phase.

$$Ar = \frac{d_{32}^3 g \rho_c \Delta \rho}{\mu_c^2} \quad (2.28)$$

$$Mo = \frac{\mu_c^4 g \Delta \rho}{\rho_c^2 \sigma^3} \quad (2.29)$$

From these equations, the drops state can be predicted depending on the drop diameter. The drop diameter with $0.48 \leq d \leq 2.85$ mm according to this criterion should have an internal circulation. In this work, the Morton number and Archimedes number equal to 7.20×10^{-11} and 21111, respectively. It can be seen that Ar is in the range from 1126 to 240604, respectively, and mean drop diameter obtained in this work was found in the range of $1.55 \leq d_{32} \leq 2.07$ mm. It is clearly observed from these results that the drops occurred in this work was circulating drops.

2.5.2 Effect of Operating Parameters on Dispersed Phase Mass Transfer Coefficient and Extraction Efficiency

According to the extraction of lactic acid with 1-butanol, solute was a specific amount of lactic acid. The mass transfer direction is lactic acid from continuous phase to dispersed phase. The main operating parameters that affect mass transfer performance of a packed liquid-liquid extraction column are the nozzle diameter, dispersed phase, and continuous phase flow rate. In this work, dispersed phase mass transfer coefficients (K_d) were calculated from experimental measurements at steady state time run for 120 min using Eq. (2.11).

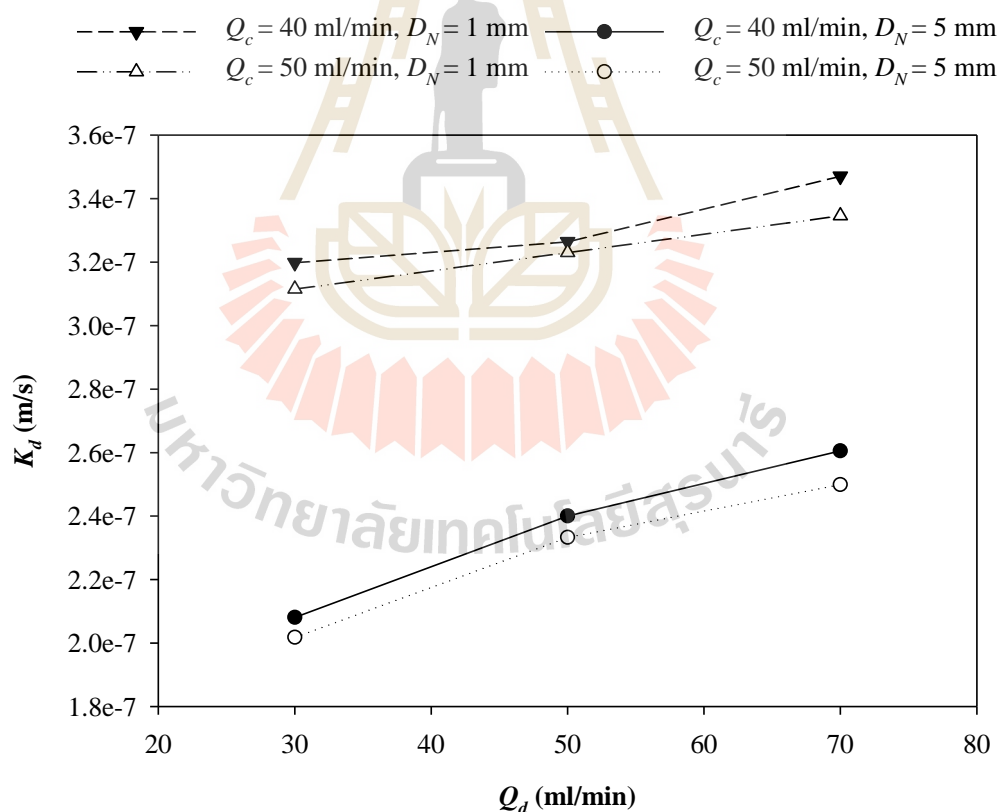


Figure 2.9 Effect of dispersed phase flow rate on dispersed phase mass transfer coefficient

The experimental values of K_d showed in Table 2.1. The effect of operating parameters on K_d showed in Figure 2.9. It was found that the dispersed phase flow rate, continuous phase flow rate, as well as nozzle diameter, are significant effect on K_d , due to d_{32} . The increasing of the dispersed phase flow rate and decreasing of the nozzle diameter enhanced to decreasing drops size with higher number of drops through the column, resulting in increasing interfacial area available for mass transfer. As can be seen, the dispersed phase mass transfer coefficient was slightly decreased by increasing the continuous phase flow rate even an increase in the continuous phase flow rate cause an increase in the drop size. It is therefore expected that the interfacial area is slightly changed when increasing in continuous phase flow rate from 40 to 50 ml/min.

In the extraction of lactic acid with 1-butanol, the efficiency of lactic acid extraction using packed liquid-liquid extraction column were investigated. The extraction efficiency was represented by degree of extraction (% E), which is calculated by Eq. (2.30).

$$\%E = \frac{C_F V_F - C_E V_E}{C_F V_F} \times 100 \quad (2.30)$$

where C_F and C_E , are initial concentration of lactic acid in feed and in extract product. V_F and V_E are the volumes of initial feed and extract product in output, respectively.

As the results in Table 2.1, the extraction efficiencies in extraction of lactic acid from the synthesis solution were found to be the same trends with K_d . High efficiency of lactic acid extraction from synthesis solution was obtained when using nozzle diameter of 1 mm and continuous phase of 40 ml/min with varied dispersed

phase flow rate. So, the extraction of lactic acid from fermentation broth were investigated and compared the extraction efficiency at these conditions.

Table 2.1 Results of extraction of lactic acid with 1-butanol in packed liquid-liquid extraction column

D_N (mm)	Q_c (ml/min)	Q_d (ml/min)	d_{32} (mm)	Re	$K_d \times 10^7$ (m/s)	%E
Fermentation broth (0.18 M of lactic acid)						
1	40	30	-	-	-	60.77
		50	-	-	-	68.61
		70	-	-	-	72.53
Synthesis lactic acid (0.10 M of lactic acid)						
1	40	30	1.62	38.28	3.20	66.08
		50	1.59	55.34	3.26	71.84
		70	1.55	74.07	3.47	75.19
1	50	30	1.68	40.91	3.12	63.46
		50	1.61	60.50	3.23	67.71
		70	1.57	76.28	3.35	70.06
5	40	30	2.04	62.90	2.08	52.89
		50	1.87	102.08	2.29	54.69
		70	1.76	127.34	2.59	56.24
5	50	30	2.07	72.15	2.02	51.26
		50	1.98	113.33	2.33	54.90
		70	1.93	131.93	2.50	55.21

The results were indicated that %E in extraction of lactic acid from synthesis solution was in the range of 66.08 to 75.19%, while in the extraction of lactic acid from fermentation broth was found in the range of 60.77 to 72.53% at increasing dispersed phase flow rate from 30 to 70 ml/min, respectively. It was observed that the

efficiency of lactic acid extraction from fermentation broth was lower than the extraction from synthesis solution about 3 to 8%. It may be due to the impurities in fermentation broth influencing on mass transfer. However, this work was indicated that liquid-liquid extraction can be used to separate lactic acid from fermentation broth with likely good extraction efficiency, even the fermentation broth contains with impurities.

2.5.3 Correlation of Sauter Mean Drop Diameter

A correlation for predicting the Sauter mean drop diameter in packed liquid-liquid extraction column is available in the literature. In this work, Sauter mean drop diameter was correlated using the equation that proposed and comprehensively described by Khorshidi et al. (2013) as shown in Eq. (2.20). Correlation's constants were determined by minimizing the differences between the experimental and calculated d_{32} using average absolute relative deviation (%AARD) as shown in Eq. (2.21).

Table 2.2 Correlation's constants of Sauter mean drop diameter correlation for packed liquid-liquid extraction column

Parameters	Constant values	
	This work	Salimi-Khorshidi et al. (2013)
m	5.13	4.98
a	-1.50	-1.05
b	-0.44	-0.26
c	0.15	0.26
n	1.23	0.64
%AARD	2.56	1.79
R -square (R^2)	0.91	0.84

The correlation's constants obtained in this work are given in Table 2.2 along with the corresponding average absolute relative deviation and coefficient of determination (R^2). According to the result, the proposed correlation for predicting d_{32} in packed liquid-liquid extraction column can be written as;

$$\frac{d_{32}}{D_N} = 5.13(1 - 1.50\phi)^{1.23} \text{Re}_d^{-0.44} \text{We}^{0.15} \quad (2.31)$$

The comparison of experimental d_{32} and calculated values showed in Figure 2.10. As the results in Table 2.2, it was observed that the constant values obtained in this work were the same trend of positive and negative values with the values reported by Salimi-Khorshidi et al. (2013).

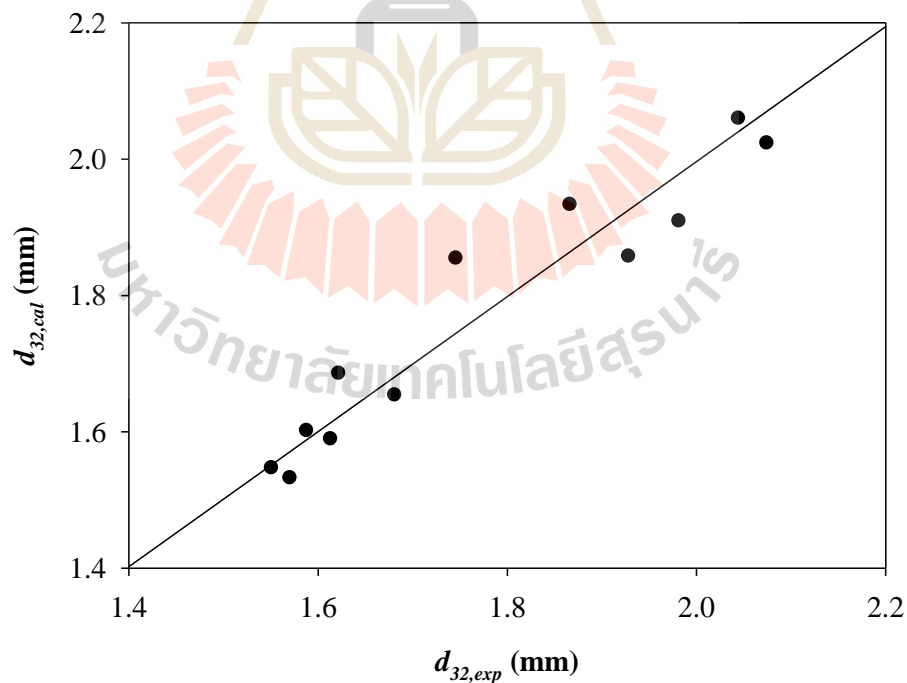


Figure 2.10 Comparison of experimental d_{32} with calculated values for packed liquid-liquid extraction column in this work

Considering the value of R^2 , it was found that the correlation has a good agreement between experimental and calculated values. It means that the correlation of d_{32} with considering the effect of physical properties and operating parameters following the reference equation can be used for the extraction system in this work. A corresponding residual plot is showed in Figure 2.11. It indicated that most of the residual are randomly dispersed around zero axis, which means that the correlation is appropriate for the data.

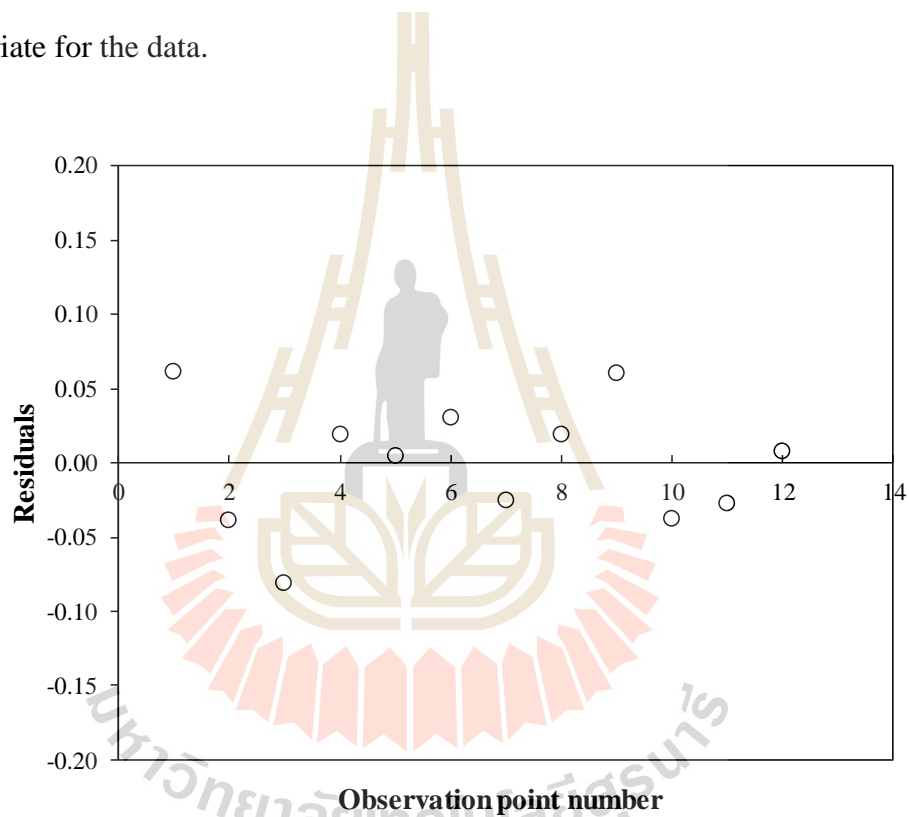


Figure 2.11 Residual plot for the calculated d_{32} from Sauter mean drop diameter correlation

2.5.4 Correlation of Dispersed Phase Sherwood Number

2.5.4.1 Correlating Dispersed Phase Sherwood Number Based on Molecular Diffusivity

This section aims to investigate the correlation of Sherwood number in term of dimensionless groups that present physical properties and operating parameters effect based on molecular diffusivity (D_M). Experimental dispersed phase Sherwood number was calculated using Eq. (2.22). The correlation of Sherwood number proposed by Salimi-Khorshidi et al. (2013) as shown in Eq. (2.26) was used in this work. The correlation's constants were determined by minimizing the difference between the experimental and calculated values using average absolute relative deviation same with minimizing of d_{32} . The obtained constants are showed in Table 2.3 and a comparison of experimental and calculated Sh_d from the correlation based on D_M are presented in Figure 2.12.

Table 2.3 Correlation's constants of dispersed phase Sherwood number correlation based on D_M and D_{eff}

Parameters	Constant values		
	This work		Salimi-Khorshidi et al., (2013) based on D_M
	Based on D_M	Based on D_{eff}	
m	109.99	7.28	102.4
a	-0.94	-0.87	-1.52
b	0.06	-0.78	2.07
c	-0.01	-0.74	-0.36
d	0.04	-0.22	0.25
n	0.71	-3.10	0.71
%AARD	1.92	1.87	4.56
R -square (R^2)	0.92	0.99	0.95

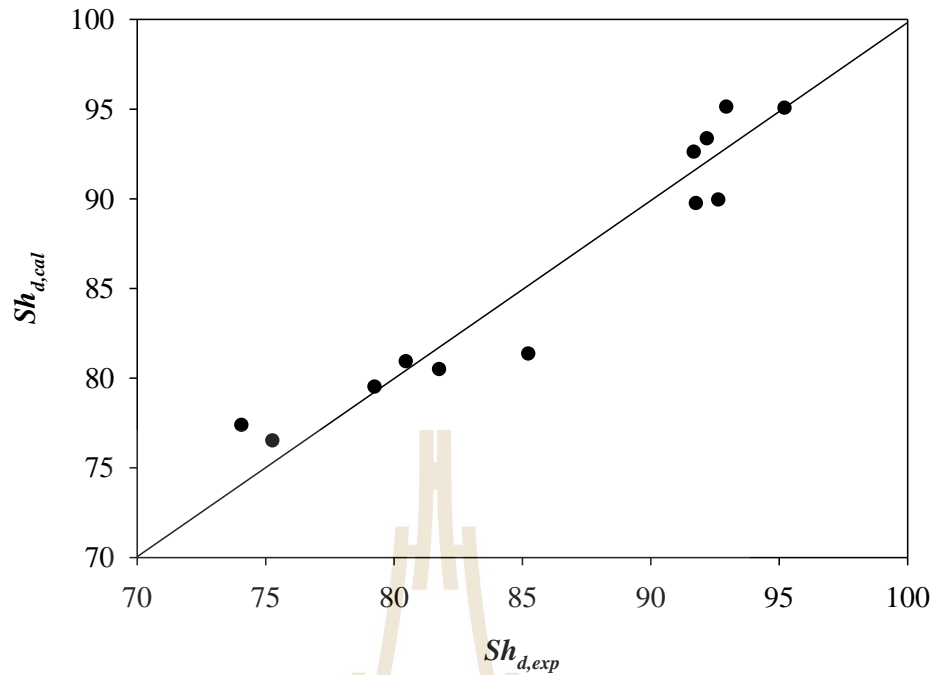


Figure 2.12 Comparison of experimental and calculated Sh_d based on D_M

The obtained correlation of dispersed phase Sherwood number based on D_M in packed liquid-liquid extraction column is;

$$Sh_d = 109.99(1 - 0.94\phi)^{0.71} Eo_d^{0.06} Re_d^{-0.01} We^{0.04} \quad (2.32)$$

As the results in Table 2.3, it was found that the constants obtained in this work were the same trends with Salimi-Khorshidi's values. The value of R^2 showed a good agreement between experimental and calculated Sh_d with the corresponding residual plot of Figure 2.14. It indicates that most residuals are randomly scattered around zero, which means that the correlation is appropriate for the data. Although the obtained correlation in this work seems satisfaction in the predicting of Sh_d , the obtained correlation has R^2 lower than the values that obtained from reference. It may be because drop size in this work was not rigid drops, which mainly mass transfer is controlled by

molecular diffusivity. So, the dispersed phase Sherwood number was improved by using correct diffusivity as presented in next section.

2.5.3.2 Correlating Dispersed Phase Sherwood Number Based on Effective Diffusivity

The mass transfer is strongly affected by drop size and hydrodynamic of two phases. For spherical rigid drop, no circulation occurs inside the drop and mass transfer mainly depends on molecular diffusion (Huang et al., 2016). According to the result in section 2.5.1, the drop dispersed in packed liquid-liquid extraction column of this work was circulating drops, which is internal circulation facilitate the mass transfer in interphase. Neglecting effect of internal circulation of drops can cause a considerable error in calculating the mass transfer inside the drops as well as Sherwood number. Therefore, the dispersed phased Sherwood number was investigated by considering the effect of internal circulation by replacing the molecular diffusivity with effective diffusivity through enhancement factor. The enhancement factor was introduced by Rahbar et al. (2011) and calculated using Eq. (2.7). Thus, the experimental dispersed phased Sherwood number is obtained as follows:

$$Sh_d = \frac{K_d d_{32}}{D_{eff}} = \frac{K_d d_{32}}{\Re D_M} \quad (2.33)$$

By experimental dispersed phase Sherwood number based on effective diffusivity, new constants in the correlation of Sherwood number were determined and obtained as shown in Table 2.3. The obtained correlation of dispersed phase Sherwood number based on D_{eff} in packed liquid-liquid extraction column is;

$$Sh_d = 7.28(1-0.87\phi)^{-3.10} Eo_d^{-0.78} Re_d^{-0.74} We^{-0.22} \quad (2.33)$$

The comparison of experimental and calculated Sh_d values from correlation based on effective diffusivity showed in Figure 2.13. It indicated that the modified correlation of dispersed phase Sherwood number based on D_{eff} can well predict the Sh_d with %AARD of 1.87% and R^2 of 0.99, which reveals better agreement with experimental results than the previous correlation based on D_M . In other words, effective diffusivity can improve the proposed correlation. The mass transfer in this system is not controlled by molecular diffusivity, but by effective diffusivity.

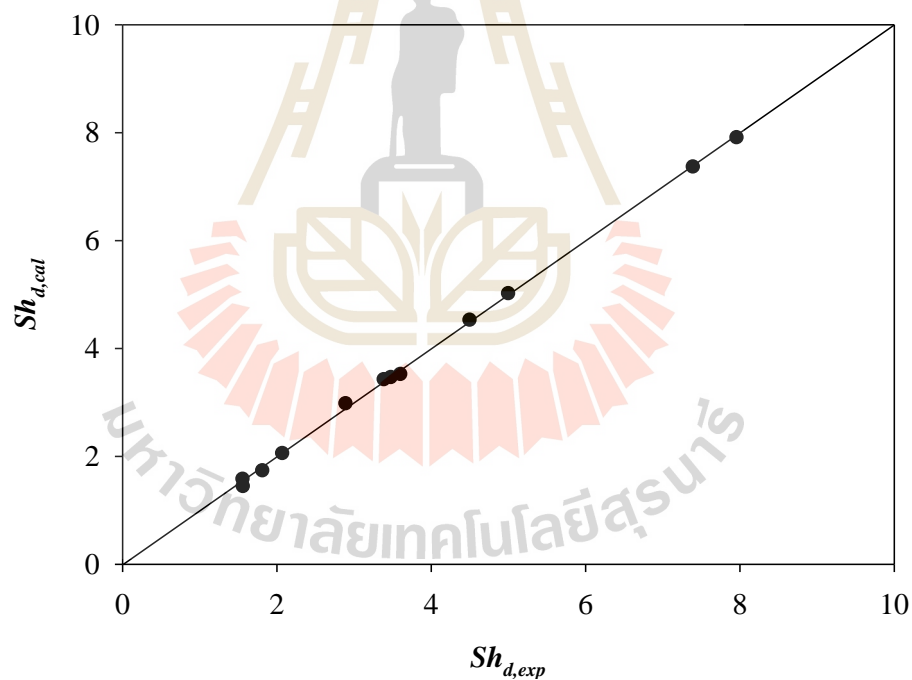


Figure 2.13 Comparison of experimental and calculated Sh_d based on D_{eff}

Corresponding residuals are plotted in Figure 2.14. With a comparative look it is found that random residuals are more concentrated around zero than residuals of correlation based on D_M , which is the correlation appropriate for the

data. In addition, it should be noted that the results from Figure 2.13, the range of Sh_d has been compacted because of using effective diffusivity.

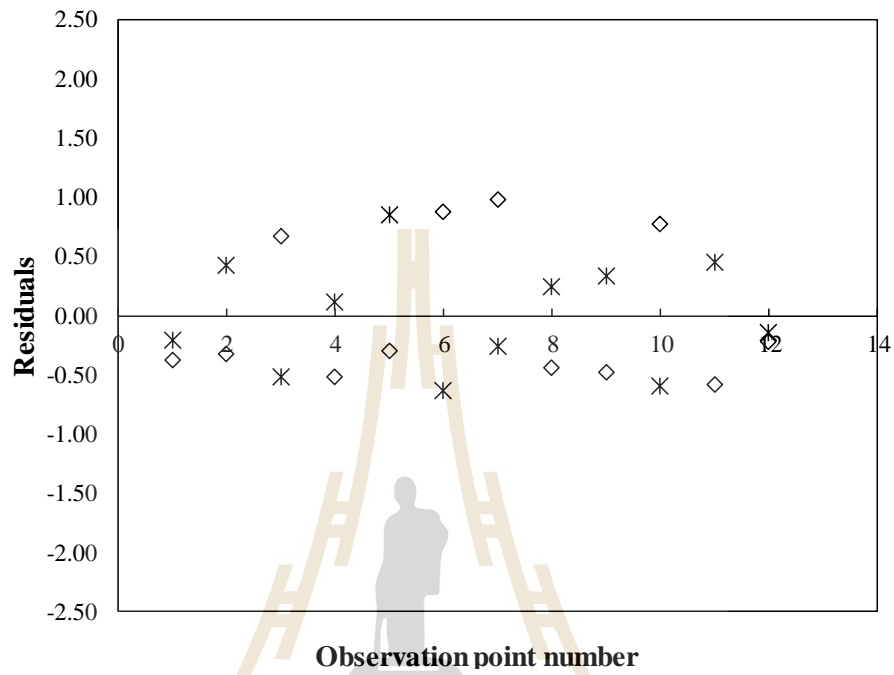


Figure 2.14 Residual plot for the calculated Sh_d from Sherwood number correlation based on D_M (*) and D_{eff} (◇)

มหาวิทยาลัยเทคโนโลยีสุรนารี

2.6 Conclusion

This work presented an experimental extraction of lactic acid with 1-butanol in packed liquid-liquid extraction column. Effect of operating parameters including nozzle diameter, continuous and dispersed phase flow rate on Sauter mean drop diameter, drop size distribution, as well as dispersed phase mass transfer coefficient, were elucidated. It was observed that Sauter mean drop diameter decreased with increasing dispersed phase flow rate and decreasing nozzle diameter, which is an influence on increasing of dispersed phase mass transfer coefficient. While an increased in continuous phase flow rate affected in increasing drop size, due to the coalescence of drops. Maximum efficiency in extraction of lactic acid from synthesis solution and fermentation broth achieved at about 75.19% and 72.53%, respectively when using a nozzle diameter of 1 mm with the continuous and dispersed phase flow rate of 40 and 70 ml/min, respectively.

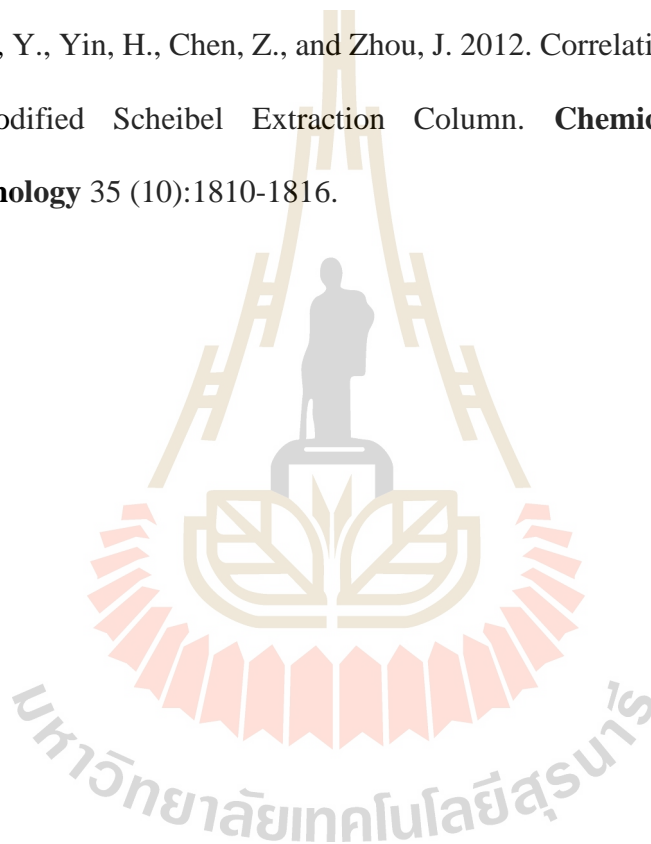
Additionally, the correlation of Sauter mean drop diameter and dispersed phase Sherwood number were studied. The correlation of Sauter mean drop diameter was in a good agreement with experimental data. The dispersed phase Sherwood number correlation was modified through effective diffusivity. It was found that using effective diffusivity instead of molecular diffusivity can improve the dispersed phase Sherwood number correlation significantly with higher accuracy for the prediction of values.

2.7 References

- Amanabadi, M., Bahmanyar, H., Zarkeshan, Z., and Mousavian, M. A. 2009. Prediction of Effective Diffusion Coefficient in Rotating Disc Columns and Application in Design. **Chinese Journal of Chemical Engineering** 17 (3):366-372.
- Ayyaswamy, P. S., Saghal, S. S., and Huang, L. J. 1990. Effect of internal circulation on the transport to a moving drop. **International Communications in Heat and Mass Transfer** 17 (6):689 - 702.
- Azizi, Z., Rezaeimanesh, M., Abolghasemi, H., and Bahmanyar, H. 2014. Effective diffusivity in a structured packed column: Experimental and Sherwood number correlating study. **Chemical Engineering Research and Design** 92 (1):43-53.
- Bertakis, E. 2013. **Interfaces in Fluid-Dynamic Simulations of Single Droplets in Liquid-Liquid Systems**, AVT-Thermal Process Engineering, RWTH Aachen University.
- Calderbank, P. H., and Korchinski, I. J. O. 1956. Circulation in liquid drops: (A heat-transfer study). **Chemical Engineering Science** 6 (2):65-78.
- Elzinga, E. R., and Banchemo, J. T. 1959. Film coefficients for heat transfer to liquid drops. **Chemical engineering progress symposium series** 55 (29):149-161.
- GhaffariTooran, S., Abolghasemi, H., Bahmanyar, H., Esmaili, M., and Safari, A. 2009. A New Correlation for Overall Sherwood Number in Packed Liquid-Liquid Extraction Column. **International Journal of Chemical and Molecular Engineering** 3:344-346.
- Handlos, A. E., and Baron, T. 1957. Mass and heat transfer from drops in liquid-liquid extraction. **AIChE Journal** 3 (1):127-136.

- Huang, Z., Ye, C., Li, L., Zhang, X., and Qiu, T. 2016. Measurement and Correlation of the Mass Transfer Coefficient for a Liquid-Liquid System with High Density Difference. **Brazilian Journal of Chemical Engineering** 33 (4):897-906.
- Kronig, R., and Brink, J. C. 1951. On the theory of extraction from falling droplets. **Applied Scientific Research** 2 (1):142.
- Mack, C. 2001. **Untersuchungen zum Stofftransport von Chrom(III)und Zink(II) bei der Extraktion mittels Bis(2-Ethylhexyl)-Phosphorsäure**, Technischen Universität Darmstadt, Darmstadt.
- Newman, A. B., Science, C. U. f. t. A. o., and Art. 1932. **The Drying of Porous Solids: Diffusion Calculations : Diffusion and Surface Emission Equations**: Cooper Union for the Advancement of Science and Art.
- Panahinia, F., Ghannadi-Maragheh, M., Safdari, J., Amani, P., and Mallah, M.-H. 2017. Experimental investigation concerning the effect of mass transfer direction on mean drop size and holdup in a horizontal pulsed plate extraction column. **RSC Advances** 7 (15):8908-8921.
- Rahbar, A., Azizi, Z., Bahmanyar, H., and Moosavian, M. A. 2011. Prediction of enhancement factor for mass transfer coefficient in regular packed liquid-liquid extraction columns. **The Canadian Journal of Chemical Engineering** 89 (3):508-519.
- Salimi-Khorshidi, A., Abolghasemi, H., Khakpay, A., Kheirjooy, Z., and Esmaili, M. 2013. Spray and packed liquid-liquid extraction columns: drop size and dispersed phase mass transfer. **Asia-Pacific Journal of Chemical Engineering** 8 (6):940-949.

- Soltanali, S., Ziaie-Shirkolaei, Y., Amoabediny, G., Rashedi, H., Sheikhi, A., and Chamanrokh, P. 2009. Hydrodynamics and mass transfer performance of rotating sieved disc contactors used for reversed micellar extraction of protein. **Chemical Engineering Science** 64 (10):2301-2306.
- Wilke, C. R., and Chang, P. 1955. Correlation of diffusion coefficients in dilute solutions. **AIChE Journal** 1 (2):264-270.
- Yuan, S., Shi, Y., Yin, H., Chen, Z., and Zhou, J. 2012. Correlation of the Drop Size in a Modified Scheibel Extraction Column. **Chemical Engineering & Technology** 35 (10):1810-1816.



CHAPTER III

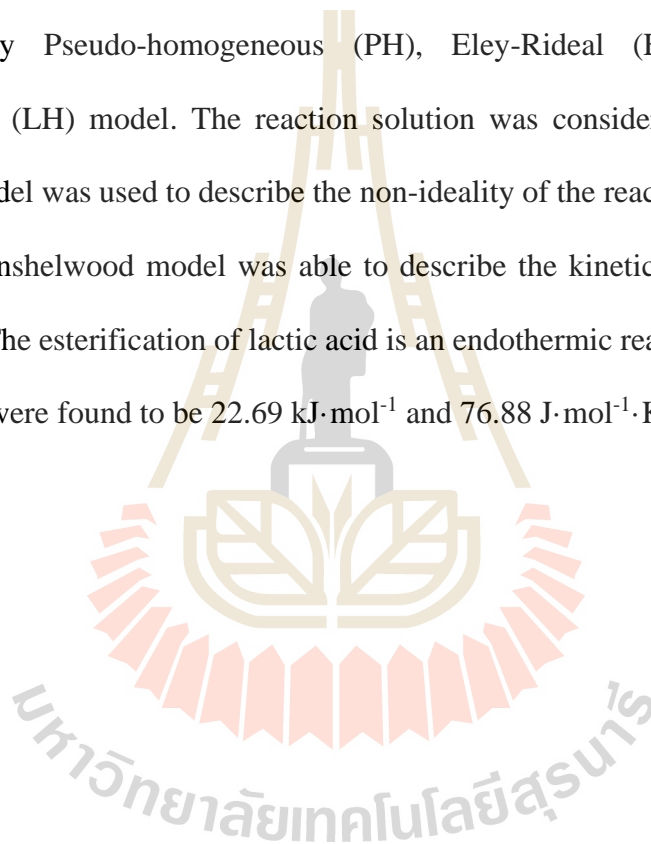
SYNTHESIS ALUMINUM ALGINATE AS A SOLID CATALYST FOR ESTERIFICATION OF LACTIC ACID WITH 1-BUTANOL

3.1 Abstract

Aluminum alginate (ALA) as a solid catalyst for esterification of lactic acid was prepared from aluminum chloride and inexpensive biopolymer sodium alginate. It was synthesized by a sol-gel method using sodium alginate as a gelling agent. Field emission scanning electron microscope (FESEM) with energy dispersive x-ray spectrometer (EDS), Powder x-ray diffraction (XRD), Temperature-programmed desorption of ammonia (TPD-NH₃) and Fourier transform infrared (FTIR) spectra were performed to explore the surface morphology, crystallinity, acid site, as well as functional groups of the prepared catalyst. Thermal degradation was also studied using simultaneous thermal gravimetric analysis and differential scanning calorimetry analysis (TGA-DSC). Based on the results, the presence of aluminum phases in the alginate has successfully lowered crystallinity with the wrinkled surface of catalyst, which created large Lewis acid sites for esterification system.

The aluminum alginate catalyst was used in the esterification reaction of lactic acid with 1-butanol. Effect of processing parameters such as initial 1-butanol to lactic acid molar ratio, catalyst loading, and reaction temperature were investigated on the conversion of lactic acid. It was found that the initial feed molar ratio, catalyst loading

and reaction temperature influence on reaction rate as well as conversion of lactic acid. The catalytic performance was compared with the system using Amberlyst-15 under the same reaction conditions. It was observed that the aluminum alginate has a higher catalytic activity than Amberlyst-15. A maximum lactic acid conversion of 81.18% was achieved over the aluminum alginate after 6 h at 85°C with initial 1-butanol to lactic acid molar ratio of 5:1 and 1% w/v of catalyst loading. Experimental kinetic data were correlated by Pseudo-homogeneous (PH), Eley-Rideal (ER) and Langmuir-Hinshelwood (LH) model. The reaction solution was considered as non-ideal, and UNIFAC model was used to describe the non-ideality of the reaction components. The Langmuir-Hinshelwood model was able to describe the kinetic of this reaction with small error. The esterification of lactic acid is an endothermic reaction, which enthalpy and entropy were found to be 22.69 kJ·mol⁻¹ and 76.88 J·mol⁻¹·K⁻¹.



3.2 Introduction

One of the most promising alternatives for recovery lactic acid is a direct conversion of lactic acid to esters by esterification process. Esterification of lactic acid present in diluted solutions is considered a viable recovery and separation alternative from complex mixtures produced during fermentation. This process has shown remarkable advantages to purify lactic acid applications by reducing processing costs and could provide esters as intermediate products for the synthesis of other chemicals from lactic acid. Accordingly, many researchers have conducted experiments to determine the esterification reaction of lactic acid with various alcohols, including methanol (Kumar et al., 2006), ethanol (Pereira et al., 2008), isopropyl alcohol and butanol (Yixin et al., 2009). However these researches are not aware of any that have compared the cost of processes using different alcohols in order to determine which is preferable from an economic. Su et al. (2013) developed and optimized to minimize cost for the recovery lactic acid from fermentation broth by esterification and hydrolysis with different alcohols. It was observed that methanol and butanol were the most attractive alcohols for using in esterification of lactic acid. The results suggest that the butanol process is preferred for short payback. Therefore, 1-butanol is the interesting alcohol for esterification of lactic acid in this work. With proper choice of catalyst, satisfactory reaction can be achieved.

Currently, the esterification of lactic acid with alcohols is achieved commercially using liquid acid catalysts such as sulfuric, hydrochloride, phosphoric acids or p-toluene sulfonic acid Li et al. (2011). However, liquid acid catalysts are not preferred because of the long reaction time and difficult catalyst separation due to their corrosive nature. Therefore, extensive research had been done over the years to find the

most suitable solid catalyst. Cation-exchanged resins have been used to catalyze the reaction of lactic acid with n-butanol to n-butyl lactate (Kumar and Mahajani, 2007). Kinetic parameters like activation energy and the rate constants are estimated using the pseudo-homogeneous model. Li et al. (2011) presented the esterification of lactic acid with n-butanol over $\text{TiO}_2\text{-ZrO}_2$ catalysts. Though $\text{TiO}_2\text{-ZrO}_2$ catalysts were very active for catalyzing the reaction with a maximum product yield of 94.2%. However, the maximum equilibrium yield of lactic acid was limited by using high reaction temperature ($>100^\circ\text{C}$). In addition, these catalysts were prepared at a high temperature of 550°C , which is more difficult in preparation, resulting in high production cost.

Thus, the development of solid catalyst with cheap and easily reusable characteristics has become a gap in recent research. Zhang et al. (2013) studied the esterification of oleic acid with alcohols using a new heterogeneous acid catalyst prepared from inexpensive sodium alginate and aluminum chloride. The obtained solid catalyst was denoted as aluminum alginate catalyst. The aluminum alginate catalyst showed high catalytic activity for esterification of oleic acid, as well as it can be applied to the esterification of other fatty acids with various carbon chain length.

Based on previous literature information, this work aims to prepare aluminum alginate catalysts from inexpensive and nontoxic sodium alginate. Characteristics of the prepared catalyst were studied, which was further used for the esterification reaction of lactic acid with 1-butanol. Three kinetic models including Pseudo-homogeneous, Langmuir-Hinshelwood, and the Eley-Rideal were used to correlate the experimental data with non-ideal assumption.

3.3 Theory

3.3.1 Esterification Reaction

Esterification can be defined as the transformation of carboxylic acids or their derivatives into esters, and esterification is an important class of reactions in reactive distillation, which the kinetics have been investigated. Synthesis of ester compounds by the treatment of carboxylic acids with alcohol is a reversible reaction, wherein water is a byproduct as shown in Figure 3.1.

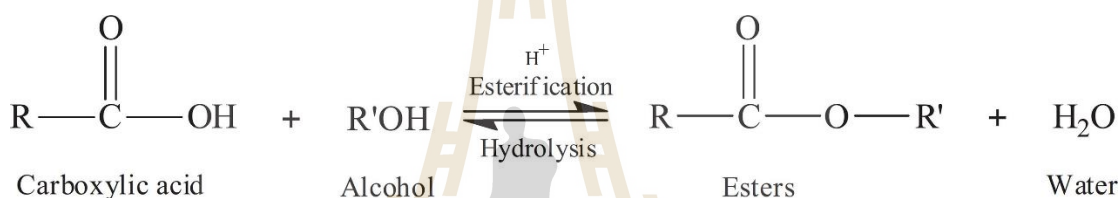


Figure 3.1 Esterification of carboxylic acid with alcohol

Esterification is a slow equilibrium-limited reaction. The equilibrium must be shifted toward the product side by excess use of one of the reactants or continuous removal of one of the products, especially water, by azeotropic distillation. The reaction can proceed with or without a catalyst. However, the uncatalyzed esterification reaction is extremely slow, since its rate depends on the catalysis by the carboxylic acid itself. Therefore, esterification has been performed with external acid catalyst as homogeneous or heterogeneous catalyst, which acts as a proton donor to the carboxylic acid. Homogeneous catalysts such as sulfuric acid, hydrochloric acid, hydrogen iodide, phosphoric acid, p-toluenesulfonic acid, and mixtures of acids are efficient homogeneous catalysts generally used for acid-catalyzed esterification. The homogeneous acid-catalyzed esterification of carboxylic acids has been reported to give

higher conversion than the heterogeneous acid-catalyzed esterification system. However, the conventional acid homogeneous catalyzed esterification suffers from problems with their miscibility with the reaction medium leading to equipment corrosion, expensive separation procedures, long reaction times and discharge of acidic wastes (Troupe and DiMilla, 1957; Il Choi et al., 1996; Benedict et al., 2003).

Esterification is usually carried out in a batch or continuous reactor depending on the scale of operation. It can also be carried out in the vapor phase by heating a mixture of acid, alcohol, and catalyst to the desired temperature. The rate of ester formation depends on the type of carboxylic acid and alcohol reacted. Primary alcohols react faster than secondary alcohols, while the secondary alcohols react faster than tertiary alcohols. Within each series, the reaction rate decreases with increasing molecular mass of carboxylic acid.

3.3.2 Kinetic Model for Esterification Reaction

Kinetics study is essential in the analysis of a reaction system used in an industrial process. The goal of kinetic analysis is to find a model that describes the rate of reaction as a function of system variables that define the chemical process. Chemical kinetics are studied to gain fundamental insight into reaction mechanisms, and to aid reactor design for process development. The reaction has been described with many models depending on the characteristics of the reactants and the catalyst. Esterification reaction catalyzed by solid catalyst can be described using different kinetic models based on homogeneous and heterogeneous approaches. Several researches studied Pseudo-homogeneous (PH), Eley-Rideal (ER) and Langmuir-Hinshelwood (LH) model. The esterification of lactic acid (LA) with 1-butanol to form the *n*-butyl lactate and water is showed in Figure 3.2.

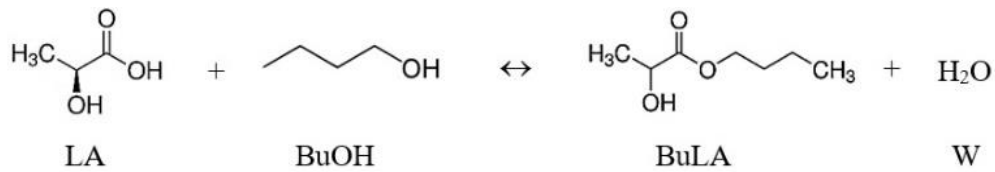


Figure 3.2 Esterification between lactic acid and 1-butanol

The PH model does not take into account the adsorption effect of the species in the reactant medium. It has been successfully used in high polar reaction media (Sanz et al., 2002). To consider non-ideal solution of the liquid phase, the rate law is expressed in terms of activity (a_i) of reaction component instead of the component concentration. In this work, activity coefficient of each liquid phase component was determined by UNIFAC model as described in section 3.3.3. Therefore, the kinetic equations of PH model for esterification of lactic acid can be written as:

$$-r_{LA} = \frac{n_{LA_0}}{w_{cat}} \frac{dX_{LA}}{dt} = k \left(a_{LA} a_{BuOH} - \frac{a_{BuLA} a_W}{K_e} \right) \quad (3.1)$$

The LH and ER models include adsorption effects of species in the reaction. The basic mechanism of LH is assumed that all reactants are adsorbed on the catalyst surface before chemical reaction occurs. Therefore, the kinetic equation of LH model is written as:

$$-r'_{LA} = \frac{n_{LA_0}}{w_{cat}} \frac{dx_{LA}}{dt} = \frac{k \left(a_{LA} a_{BuOH} - \frac{a_{BuLA} a_W}{K_e} \right)}{\left(1 + K_{LA} a_{LA} + K_{BuOH} a_{BuOH} + K_{BuLA} a_{BuLA} + K_W a_W \right)^2} \quad (3.2)$$

The ER mechanism is assumed that one of the reactants is adsorbed onto catalyst surface by considering in high polar species. The reaction takes place between adsorbed reactant and another reactant in bulk solution. The esterification of lactic acid with 1-butanol, the adsorption of lactic acid and water is considered to be strong polar than 1-butanol and *n*-butyl lactate. Hence, the kinetic equation becomes;

$$-r_{LA}' = \frac{n_{LA_0}}{w_{cat}} \frac{dX_{LA}}{dt} = \frac{k \left(a_{LA} a_{BuOH} - \frac{a_{BuLA} a_W}{K_e} \right)}{(1 + K_{LA} a_{LA} + K_W a_W)} \quad (3.3)$$

where $-r_{LA}$ and k are reaction rate and reaction rate constant, respectively. n_{LA_0} is an initial mole of lactic acid and X is conversion. K_e is equilibrium constant of the reaction. K_i is the adsorption constant of adsorbed component i . w is amount of catalyst. Subscripts LA , $BuOH$, $BuLA$, W and cat represent lactic acid, 1-butanol, *n*-butyl lactate, water, and catalyst, respectively. The reaction rate constant is expressed using Arrhenius equation:

$$k = A_o \exp\left(-\frac{E_A}{RT}\right) \quad (3.4)$$

where T is the absolute temperature and R is the universal gas constant. A_o is the pre-exponential factor and E_A is the activation energy, Equilibrium constant of the reaction was calculated from the equilibrium activity of the reaction components,

$$K_e = \left(\frac{a_{BuLA} a_W}{a_{LA} a_{BuOH}} \right)_{eq} = \left(\frac{x_{BuLA} x_W}{x_{LA} x_{BuOH}} \right)_{eq} \left(\frac{\gamma_{BuLA} \gamma_W}{\gamma_{LA} \gamma_{BuOH}} \right) \quad (3.5)$$

where x and γ are the mole fraction and activity coefficient of the component, respectively. The kinetic parameters of the models were obtained by minimizing the sum of squared residuals between the experimental (X_{exp}) and calculated (X_{cal}) conversion of lactic acid as shown in Eq. (3.6) through the nonlinear least square method.

$$SSR = \sum_{i=1}^n (X_{exp} - X_{cal})^2 \quad (3.6)$$

The quality of the fit was estimated by the mean relative deviation of lactic acid conversion as shown in Eq. (3.7) where N is total number of samples.

$$MRD = \frac{1}{N} \sum_{i=1}^n \left| \frac{X_{cal} - X_{exp}}{X_{cal}} \right| \times 100 \quad (3.7)$$

3.3.3 Thermodynamic Model

3.3.3.1 Vapor-Liquid Equilibrium

Vapor-Liquid equilibrium (VLE) is the state of coexistence of liquid and vapor phase. Overall vapor-liquid equilibrium (VLE) relationship for the mixture systems can be described as the following equation:

$$y_i P = x_i \gamma_i P_i^* \quad (3.8)$$

Eq. (3.8) also can be called modified Raoult's Law, and the liquid activity coefficient can be estimated from activity coefficient models that related to the system (Luyben and Chien, 2010). x_i and y_i are mole fraction of component i in liquid and vapor phase,

respectively. γ_i is the activity coefficient of component i . P^* is liquid vapor pressure of component i at system temperature and P is total system pressure.

3.3.3.2 Universal functional activity coefficient (UNIFAC) model

The UNIFAC model was developed by (Abrams and Prausnitz, 1975). They provided the method for estimation activity coefficients depends on the concept that a liquid mixture may be considered a solution of the structural units from which the molecules are formed rather than a solution of the molecules themselves. A molecule is divided into functional groups and molecule-molecule interactions are considered. The UNIFAC model comprised of two additive parts, a combinatorial part to describe the dominant entropic distribution and molecular size as well as shape differences and the residual part to account for intermolecular forces that are responsible for the enthalpy of mixing.

$$\frac{g^E}{RT} = \left(\frac{g^E}{RT}\right)^C + \left(\frac{g^E}{RT}\right)^R \quad (3.9)$$

From the fundamental excess-property relation:

$$\ln \gamma_i = \frac{g^E}{RT} \quad (3.10)$$

Therefore, Eq. (3.9) became to

$$\ln \gamma_i = \ln \gamma_i^C + \ln \gamma_i^R \quad (3.11)$$

where g^E is partial excess Gibbs energy. Superscript C and R refer to combinatorial and residual, respectively. For multi-component system, the combinatorial and residual parts can be written as:

$$\ln \gamma_i^C = \ln \frac{\phi_i}{x_i} + \frac{z}{2} q_i x_i \ln \frac{\theta_i}{\phi_i} + l_i - \frac{\phi_i}{x_i} \sum_{j=1}^m x_j l_j \quad (3.12)$$

$$\ln \gamma_i^R = \sum_{k=1}^m v_k^{(i)} (\ln \Gamma_k - \ln \Gamma_k^{(i)}) \quad (3.13)$$

$$l_i = \frac{z}{2} (r_i - q_i) - (r_i - 1) \quad (3.14)$$

where z is the coordination number which is set equal to 10. m is the total number of components. The parameters ϕ and θ are the surface and volume fractions, respectively. it depends on the volume and surface area parameters r_i and q_i :

$$\phi_i = \frac{x_i r_i}{\sum_{i=1}^m x_i r_i} \quad (3.15)$$

$$\theta_i = \frac{x_i q_i}{\sum_{i=1}^m x_i q_i} \quad (3.16)$$

The parameter r_i and q_i are calculated as the sum of group volume and area parameters, R_k and Q_k , given as:

$$r_i = \sum_k v_k^{(i)} R_k \quad (3.17)$$

$$q_i = \sum_k v_k^{(i)} Q_k \quad (3.18)$$

where $v_k^{(i)}$ is the number of functional group of type k in molecule i .

Γ_k is the activity coefficient of group k .

$\Gamma_k^{(i)}$ is the activity coefficient of group k in pure component i .

Subscript i is identifies component in the system.

Subscript j is identifies component in the system.

Subscript k is functional group in the molecule i .

The group residual activity coefficient, Γ_k , can be expressed in term of following equation:

$$\ln \Gamma_k = Q_k \left[1 - \ln \left(\sum_m \Theta_m \Psi_{mk} \right) - \sum_m \left(\frac{\Theta_m \Psi_{km}}{\sum_n \Theta_n \Psi_{nm}} \right) \right] \quad (3.19)$$

where Θ_m is the area fraction of group m which is calculated by

$$\Theta_m = \frac{Q_m X_m}{\sum_n Q_n X_n} \quad (3.20)$$

X_m is the mole fraction of group m in the mixture, which is given by

$$\Psi_m = \exp \left(-\frac{a_{mn}}{T} \right) \quad (3.21)$$

where a_{mn} is energy interaction parameters of functional group m and n , which is units as degree of Kelvin and $a_{mn} \neq a_{nm}$. In Table 3.1, the value energy interaction parameters are given for each functional group.

The UNIFAC method is applicable to a wide range of nonelectrolyte system. The group-interaction parameters thus obtained can calculate activity coefficients in a large number of binary and multicomponent mixtures with reasonably good accuracy. However, poor results are obtained for systems with very different size of compounds, as well as systems containing polymers because the absence of the free-volume term in the combinatorial term has a marked impact on the accuracy of results (Lohmann et al., 2001). For esterification of lactic acid with 1-butanol in this work, the system contains water, 1-butanol, lactic acid and *n*-butyl lactate. The UNIFAC model is used to calculate the activity coefficient in the liquid phase using MATLAB as detailed in Appendix B.

Table 3.1 UNIFAC energy interaction parameters

j/i	CH ₃	CH ₂	CH	OH	H ₂ O	COOH	COO
CH ₃	0	0	0	986.5	1318	663.5	387.1
CH ₂	0	0	0	986.5	1318	663.5	387.1
CH	0	0	0	986.5	1318	663.5	387.1
OH	156.4	156.4	156.4	0	353.5	199	190.3
H ₂ O	300	300	300	-229.1	0	-14.09	-197.5
COOH	315.3	315.3	315.3	-151	-66.17	0	-337
COO	529	529	529	88.63	284.4	1170	0

www.aim.env.uea.ac.uk/aim/info/UNIFACgroups.html

3.4 Experimental Procedures

3.4.1 Chemicals

Lactic acid with a concentration of 88 %wt and RPE grade of 1-butanol with 99.9% purity were purchased from Acros. Aluminum chloride (AlCl_3) anhydrous with 98.5% extra pure and sodium alginate were purchased from Acros. Deionized water was used in every experiment.

3.4.2 Catalyst Preparation

Aluminum (III)-alginate was synthesized using the procedure described by Zhang et al. (2013) with slight modification. Approximately, 2 g of sodium alginate was added to 100 mL of deionized water, and the mixture was stirred until a clear viscous solution to form gel was obtained. Aluminum cation solution with a concentration of 0.1 M was prepared by anhydrous aluminum chloride and deionized water. The aluminum cation solution was added dropwise into the alginate gel viscous solution under continuous stirring for 250 rpm at room temperature. The resulting solution system was stirred vigorously for 2 h to form the aluminum alginate complex. After that, the prepared aluminum alginate granules were filtered and washed with 100 ml of deionized water at room temperature. It was then evaporated remained liquid using a rotary evaporator at 105°C under pressure of 300 mbar for 1.5 h. Finally, the aluminum alginate granules were dried again in an oven at 60 °C for 3 h. The solid catalyst was crushed and sieved to the size range between 1.00-1.70 mm. It was denoted as ALA catalyst. The dried ALA catalyst was kept in vials and sealed with paraffin films until future usage.

3.4.3 Catalyst Characterizations

3.4.3.1 Surface Morphology

Field Emission Scanning Electron Microscope (FESEM) with Energy Dispersive X-ray Spectrometer (EDS) was performed by Carl Zeiss Ariga to study the surface morphology and elemental analysis using voltage of 5 kV at magnifications of 50× and 35000×.

3.4.3.2 Crystallinity

Powder X-ray diffraction (XRD) from Bruker D2-PHASER was used to determine crystallinity, employing Cu-K α radiation wavelength (λ) = 1.5406Å) with tube voltage and current of 30 kV and 10 mA, respectively. XRD patterns were recorded over goniometric (2θ) ranges from 20–70° with an increment step of 0.02° and a scanning speed of 0.04° per second.

3.4.3.3 Functional Group

Fourier transform infrared (FTIR) spectra were recorded by a Bruker T27/Hyp2000 spectrometer to analyze the functional groups. The scanning was in the range of 400–4000 cm⁻¹ and the resolution was 1 cm⁻¹.

3.4.3.4 Acidity

Temperature-programmed desorption of ammonia (TPD-NH₃) was used to determine acidity, which is performed by a BELCAT-Chemisorption analyzer from BEL, Japan. The sample was kept under helium at 100°C for 60 min and then was saturated with NH₃ at the flow rate of 50 mL/min for 30 min. Subsequently, the sample was flushed with helium for 15 min after which the TPD analysis was started with temperature ramp of 10°C/min up to 900°C.

3.4.3.5 Thermal Degradation

Simultaneous thermal analysis and different scanning calorimetry analysis (TGA-DSC) was used to investigate thermal degradation. The TGA-DSC analyzer was carried out with Toledo TGA/DSC from METTLER in an air flow rate of 50 mL/min. The TGA analyzer was heated at a heating rate of 10°C/min from 35 to 900°C.

3.4.4 Catalytic Activity in Esterification of Lactic Acid with 1-Butanol

Catalytic activity in the esterification of lactic acid with 1-butanol was carried out in a 100 mL glass vessel equipped with a thermometer and a magnetic stirrer. The reaction temperature was maintained by an electric heating thermostatic oil bath. Initially, desired amount of lactic acid was added into the reactor and heated to desired temperature. Once the desired temperature was attained, catalyst was added into the reactor. After that, a known amount of 1-butanol was added to the reactor and the time was considered as the initial reaction time. Liquid samples of 0.01 mL were carefully pipetted out the reactor at different time intervals and analyzed the concentration of lactic acid by titration with 0.01 M NaOH solution.

3.5 Results and Discussion

3.5.1 Characterizations of ALA Catalyst

In this study, when aluminum chloride solution was dropped into the sodium alginate gel, Na^+ ions from alginate chains are exchanged with Al^{3+} ions, which is aluminum alginate complex forming gelatin like white small granules (Cheryl-Low et al., 2015) as shown in Figure 3.3 (a).

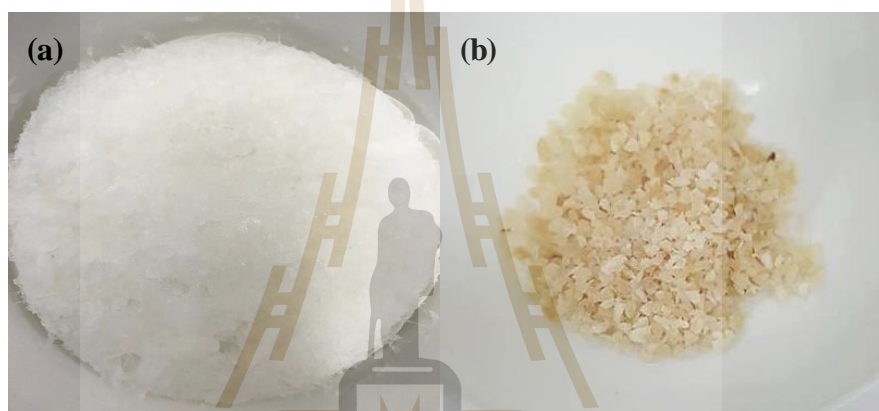


Figure 3.3 Aluminum alginate complex (a) and aluminum alginate (ALA) (b)

The formation of aluminum alginate granules was due to ionic cross-linking process between aluminum(III) cations with binary co-polymeric network (alginate), thus lead to occurrence of three-dimensional network as shown in Figure 3.4. Furthermore, sodium chloride formed during aluminum alginate formation was washed out with deionized water. After drying, the aluminum alginate (ALA) catalyst was obtained as shown in Figure. 3.2 (b).

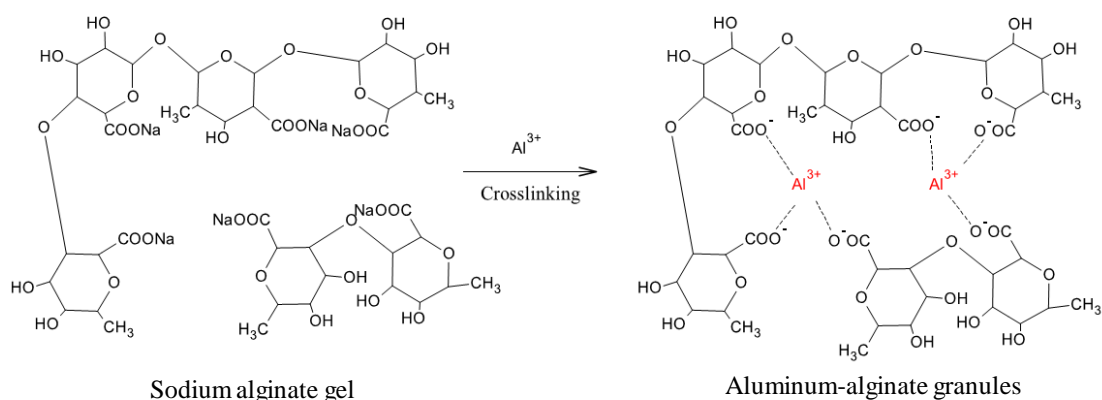


Figure 3.4 Cross-linking of sodium alginate with aluminum ions

3.5.1.1 Surface Morphology

FESEM-EDS analysis was conducted to study the surface morphology and compositions of sodium alginate and ALA catalyst as shown in Figure 3.5. It was observed that the surface of ALA catalyst appeared to be rough and wrinkled surface than sodium alginate. The FESEM images showed significant changes of catalyst surface after addition of Al³⁺ ions into alginate. This means that the ALA catalyst obtained in this work created a larger surface of active sites, which is may enhance to increase catalytic activity in esterification.

Table 3.2 EDS analysis of ALA catalyst

Elements	%Weight			
	1	2	3	Avg.
C	26.91	20.95	20.87	22.91
O	34.57	40.58	40.26	38.47
Na	n/a	n/a	n/a	n/a
Al	38.53	38.46	38.87	38.62
Cl	n/a	n/a	n/a	n/a

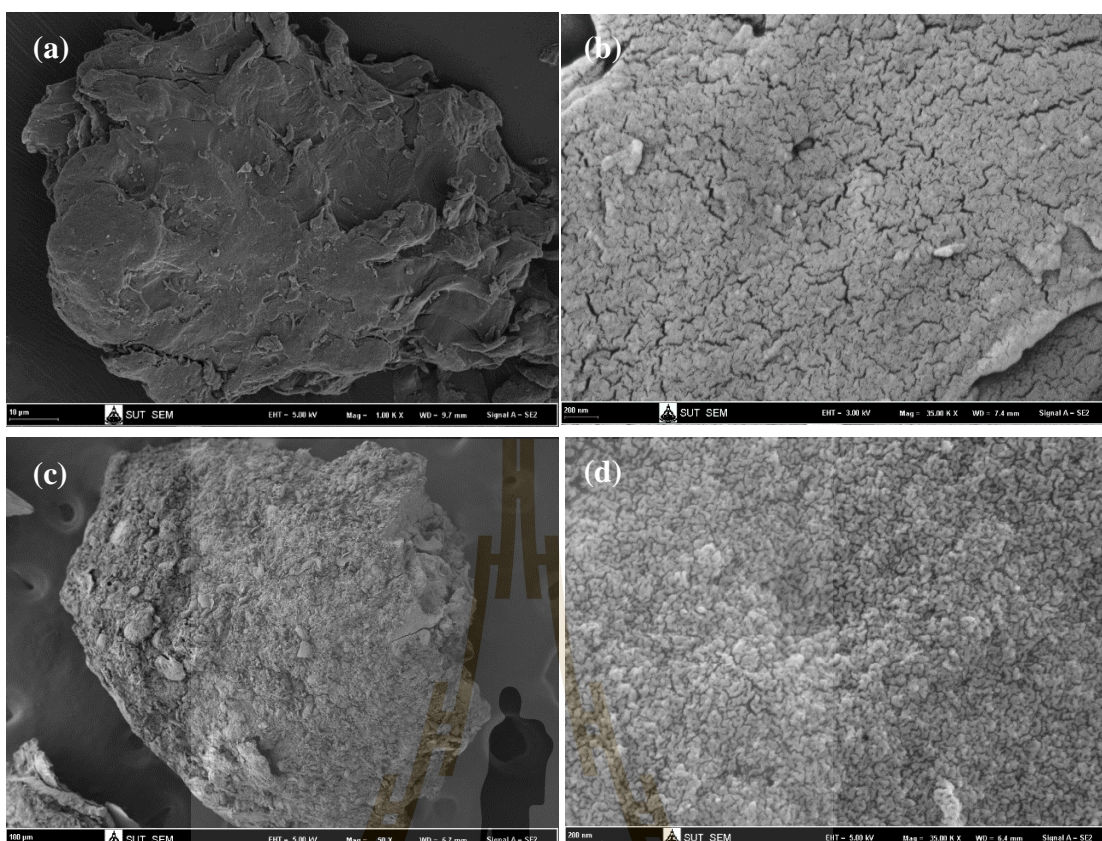


Figure 3.5 FESEM images of sodium alginate with magnification $1000\times$ (a), magnification $35000\times$ (b) and ALA catalyst with magnification $50\times$ (c) and magnification $35000\times$ (d)

The EDS analysis of the ALA catalyst was performed by randomly three areas on the catalyst surface to evaluate average percent weight of compositions. The surface compositions of catalyst presented in Table 3.2. It was found that the ALA catalyst showed C, O, Al elements, which is C and O refer to elements in aluminum alginate crosslink and Al refers to the active site. It can be seen that Na and Cl elements do not occur in the ALA catalyst. This means that the catalyst may be successfully completed preparation of aluminum alginate complex.

3.5.1.2 Crystallinity

The crystallinity of sodium alginate and ALA catalyst were analyzed by XRD analysis as the XRD patterns shown in Figure 3.6. Two diffraction peaks with 2θ values of 22° and 39° were observed for sodium alginate due to the reflection from polyguluronate, polymannuronate and the other from amorphous halo (Parani et al., 2012). The observed peaks of sodium alginate showed the semi-crystalline nature and broad amorphous nature with crystallite size of 8.72 nm, which is less value crystallite phase as well as more amorphous phase. In the case of ALA catalyst, the XRD patterns showed the presence of four diffraction peaks at 2θ values of approximately 31° , 45° , 56° and 66° . The intensity peak exhibits strong peak, due to the Al^{3+} that have been exchanged the Na^+ from sodium alginate. These peaks are similar to pure diaspore ($\beta\text{-AlOOH}$) as reported by Zhang et al. (2013) with crystallite size of 77.56 nm.

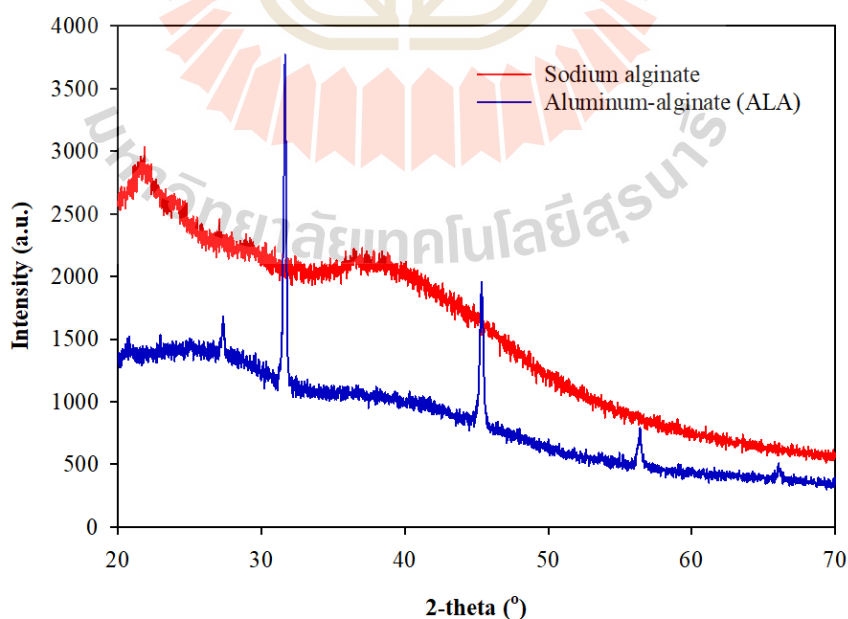


Figure 3.6 XRD patterns of sodium alginate and ALA catalyst

3.5.1.3 Functional Groups

The binding of aluminum (III) to alginate molecules were confirmed by FTIR analysis. Aluminum (III) forms metal carboxylate bonds with alginate molecules during ion-exchange interaction. The Al^{3+} ions in aluminum chloride solution are exchanged with Na^+ ions from the sodium alginate solution. The Al^{3+} ions form bonds with the carboxylate groups of alginate molecules. The Cl^- ions will form bonds with Na^+ ions and are then washed off with deionized water. Table 3.3 lists the functional groups identified in FTIR analysis of sodium alginate and ALA catalyst granules found in this work and compared to functional groups of sodium alginate molecule reported in previous studies (Boey et al., 2012). The FTIR spectrums of sodium alginate and aluminum alginate catalyst obtained in this work are presented in Figure 3.7.

Table 3.3 The main vibrational modes for sodium alginate and aluminum alginate

Vibration	Sodium alginate (Boey et al., 2012)	Sodium alginate (this work)	Aluminum alginate
$\nu(OH)$	3450	3294	3350
$\nu(CH)$ -anomer	2933	2910	2925
$\nu(COO^-)_{sym}$	-	-	1735
$\nu(COO)_{sym}$	1618	1593	1612
$\nu(COO)_{asym}$	1419	1404	1418
$\delta(CCH) + \nu(COH)$	1319	1305	1317
$\nu(CO) + \nu(CCC)$	1095	1087	1088
$\nu(CO) + \delta(CCO) + \delta(CC)$	1026	1032	1032
Mannuronic acid residue	903	883	878
Guluronic acid residues	813	813	810

Sodium alginate showed the absorption bands of hydroxyl, ether and carboxylic functional groups. For sodium alginate in this work, the ($-OH$) group exhibit broadband

at 3294 cm^{-1} . The aliphatic ($-\text{CH}$) was observed broadband at 2910 cm^{-1} and asymmetrical carboxylate groups ($-\text{COO}$) were assigned to the presence at 1593 and 1404 cm^{-1} , similar to the broadbands that found in reference (Boey et al., 2012).

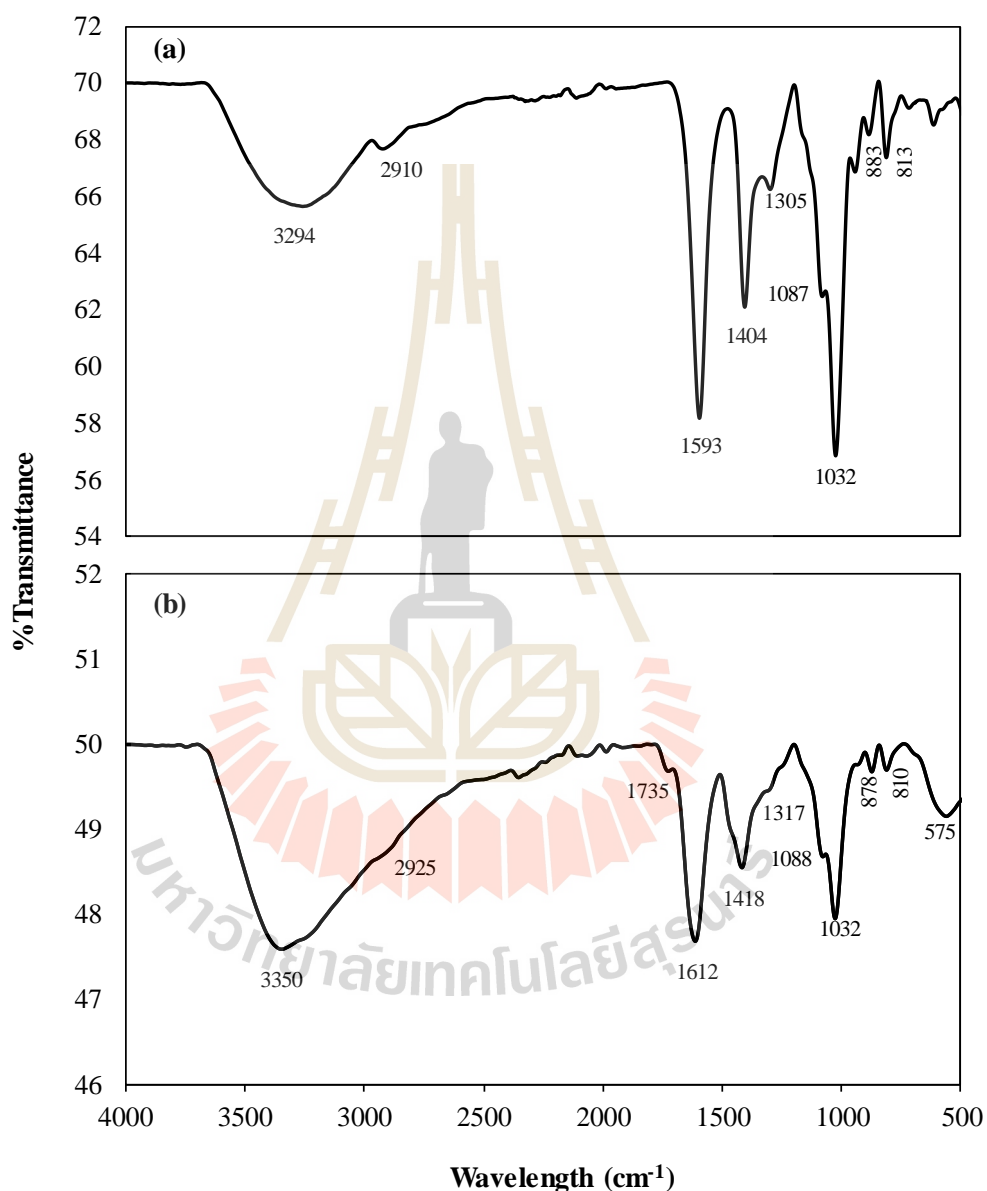


Figure 3.7 FTIR spectrums of sodium alginate (a) and ALA catalyst (b)

The $\text{C}=\text{O}$ of alcoholic and ether groups produces broadband around 1087 cm^{-1} for sodium alginate and 1088 cm^{-1} for the aluminum alginate catalyst.

The broadband at 1032 cm^{-1} is attributed to saccharide structure stretching of sodium alginate (Parani et al., 2012). All above of peaks in sodium alginate were observed in ALA catalyst with the peaks were slight shifted larger broadband. An obvious peak around 1735 cm^{-1} was found only in the aluminum alginate catalyst corresponds to C=O of free carboxylate anion, but this band was not observed in the spectrum of sodium alginate. This might be due to the binding capacity of sodium alginate with Al^{3+} ions. The large broadbands around 500 cm^{-1} are attributed to the stretching vibrations of metal-oxygen bond in metal oxide as reported by Wu et al. (2010).

3.5.1.4 Acidity

In esterification, the type of Lewis acidity which would enhance the catalytic activity for the reaction. The acid site of ALA catalyst was determined via TPD- NH_3 analysis in the temperature range from 100 to 900°C . Amount of ammonia desorbed by the catalyst is represented in Figure 3.8. According to literature, the desorption peaks at different temperature indicate the presence of weak, intermediate and strong acid site. The desorption peaks obtained in the range of $50\text{-}250^\circ\text{C}$ are assigned for weak acid sites, $250\text{-}350^\circ\text{C}$ for moderately strong acid sites. For the temperature at higher than 350°C , desorption peaks represented very strong acid site (Minchitha et al., 2016). As the TPD- NH_3 profile in Figure 3.8, it was found that ALA catalyst contained intense peaks in the range of $136\text{-}240^\circ\text{C}$ and $307\text{-}793^\circ\text{C}$, which is equivalent to 50.65 and $294.62\text{ }\mu\text{mol/g}$ of weak and strong acid sites, respectively. This result indicated that ALA catalyst acted high existence of strong acid site as Lewis acid for esterification reaction.

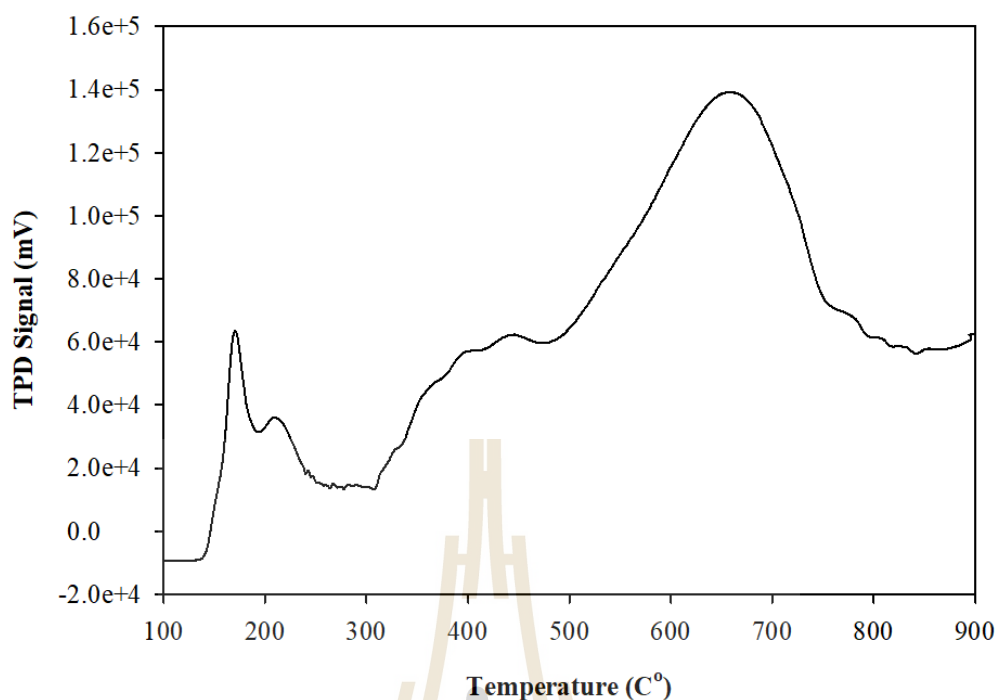


Figure 3.8 TPD-NH₃ profile of ALA catalyst

3.5.1.5 Thermal Degradation

The thermal degradation of ALA catalyst was investigated by TGA-DSC analysis, which the results represented in Figure 3.9. The onset thermal decomposition temperature (T_{onset}) is the point where material starts disintegrating and is the measure of thermal stability of that material. It is defined as the temperature at which 5% weight loss occurs. From TGA-DSC curve, the T_{onset} of ALA catalyst is about 78°C. And then, the faster thermal degradation rate of ALA catalyst takes place with the future increase of temperature. Major thermal degradation of ALA catalyst can be divided into three main stages. The first stage is found in the range of temperature between 35 to 145°C. During the first stage, about 13.3% of total weight is degraded, which is corresponded to the intensive evolution of small molecules (Liu et al., 2015). The second stage in the range of 145 to 383°C, total weight loss about 59.1% is rapidly

degradation due to the preliminary degradation of alginate. Then, its future thermally degraded more slowly to give the more stable intermediate fragments at a slower rate of thermal degradation in the last stage at 383 to 638°C. The amount of char residues at 900°C is obtained about 20.9%.

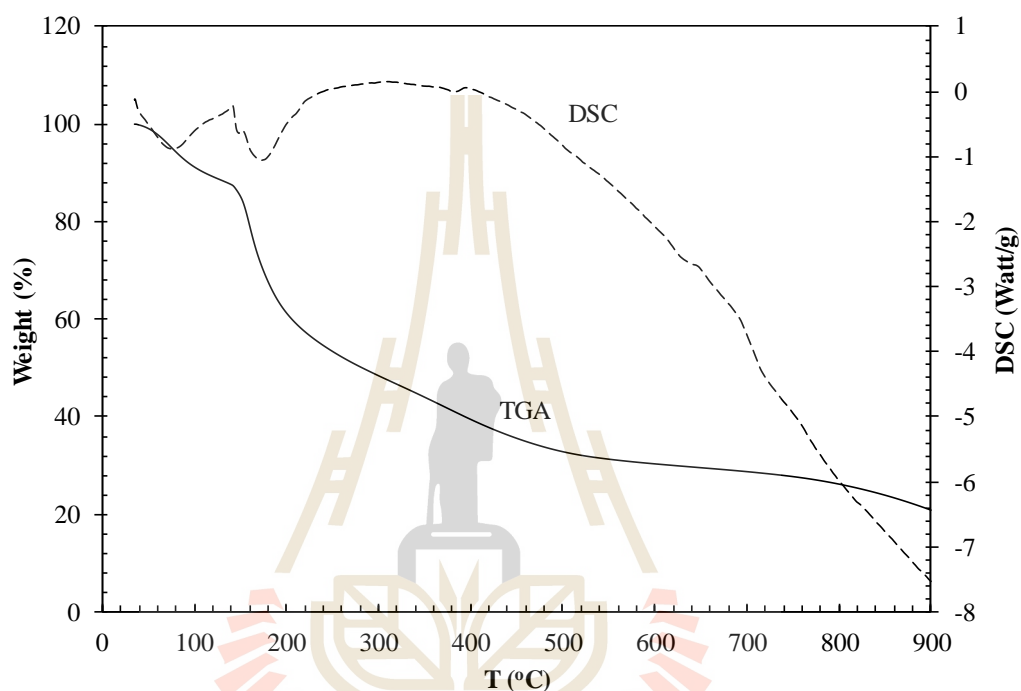


Figure 3.9 TGA-DSC curve of ALA catalyst

3.5.2 Catalytic Activity in Esterification of Lactic Acid with 1-Butanol

3.5.2.1 Catalyst Performance

The performance of catalyst is very important for a reaction system since it is directly related to economical application of the process. In this study, the ALA catalytic activity was first tested by comparison with the previously published results using cationic exchange resin Amberlyst-15 (Rattanaphanee, 2010). The activity of both catalyst on esterification of lactic acid with 1-butanol was compared in the

reaction temperature of 65°C and 85°C with initial 1-butanol to lactic acid molar ratio (M) of 5:1 (M=5:1), catalyst loading of 1% w/v and a reaction time of 6 h. The result presented in Figure 3.10 indicated that the ALA is higher reaction rate than Amberlyst-15 with the conversion of 74.39% and 81.18% at 65°C and 85°C, respectively. While Amberlyst-15 catalyst system was observed that the conversion of 53.19% and 75.17% at 65°C and 85°C, respectively.

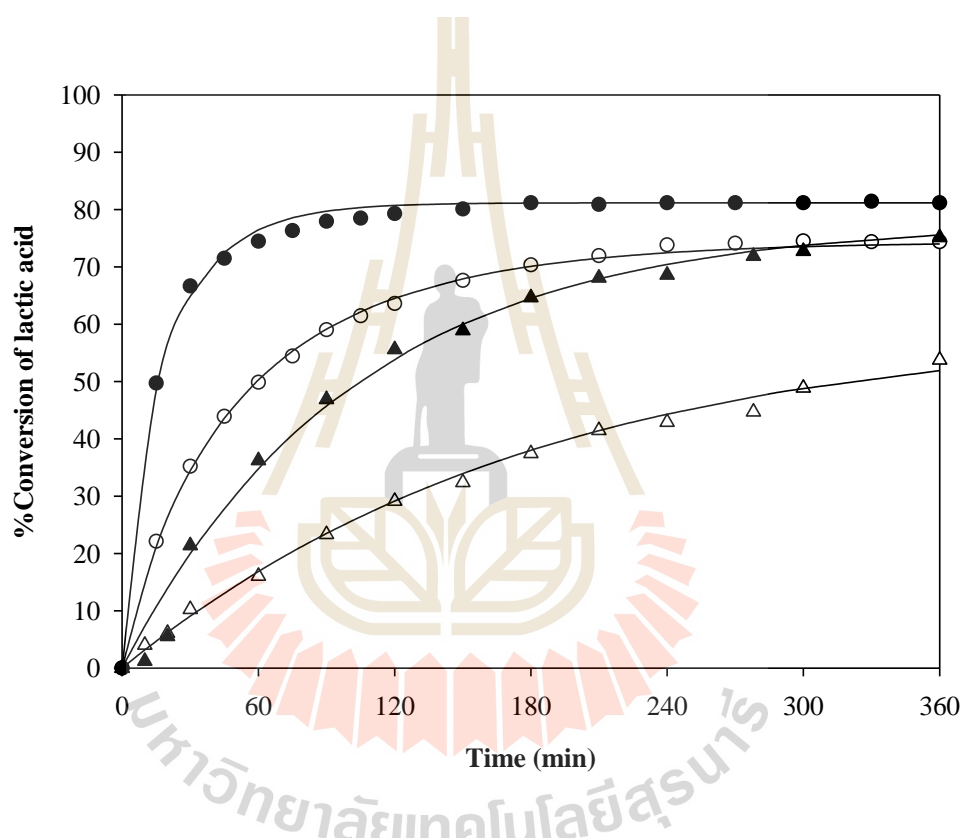


Figure 3.10 Conversion of lactic acid in esterification using 1% w/v of catalyst loading and M =5:1 at 65°C (▲), 85°C (●) for ALA catalyst and 65°C (△), 85°C (○) for Ameberlyst-15 (Rattanaphanee, 2010). Solid lines indicate the calculation values from LH model

3.5.2.2 Effect of Catalyst Loading

Effect of catalyst loading on conversion of lactic acid with 1-butanol was tested. The amount of catalyst was varied in the range of 0.25 to 1% w/v while keeping the constant initial 1-butanol to lactic acid molar ratio of 5:1 and the reaction temperature of 75°C for 6 h. The results obtained in Figure 3.11 indicated that with increase in catalyst loading enhanced in an increasing rate of reaction, as well as conversion of lactic acid because of an increase in number of active sites. Higher loading of catalyst results in reduction of the time required to reach the reaction equilibrium. In addition, it can be seen that equilibrium conversion does not significantly change by various catalyst loading.

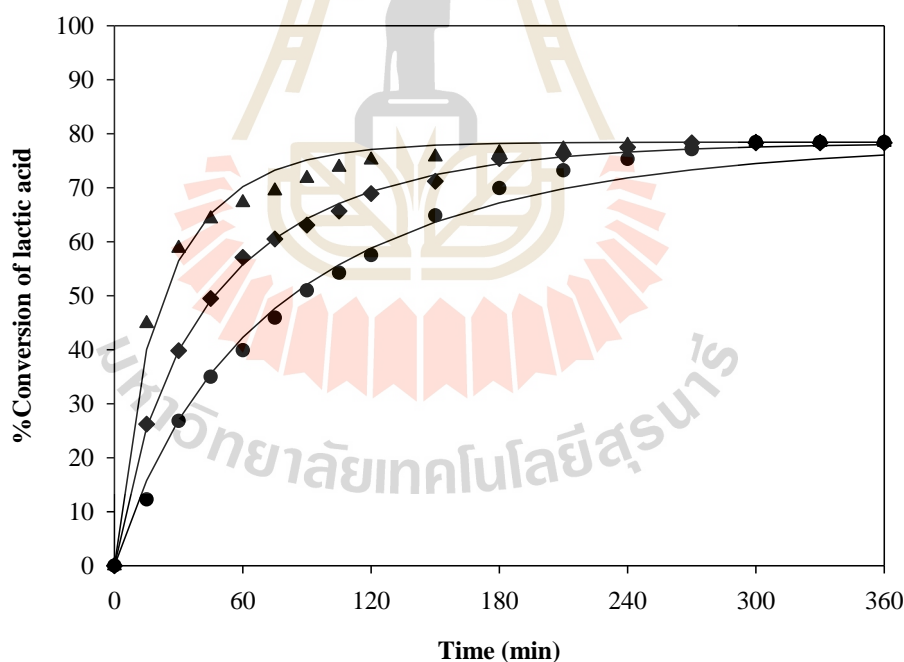


Figure 3.11 Effect of catalyst loading on conversion of lactic acid at reaction temperature of 75°C and M=5:1 using 0.25% w/v (●); 0.5% w/v (◆) and 1% w/v (▲) of catalyst loading. Solid lines indicate the calculation values from LH model

3.5.2.3 Effect of Initial 1-Butanol to Lactic acid Molar Ratio

The esterification of lactic acid with 1-butanol is equilibrium limited reversible reaction and the reaction equilibrium controls the amount of 1-butyl lactate formed. Using an excess quantity of 1-butanol drives the equilibrium towards the formation of 1-butyl lactate and enhances the forward reaction. The effect of initial 1-butanol to lactic acid molar ratio in the range of 1:1 to 5:1 was investigated in a presence of 1%w/v of catalyst loading for 6 h at the reaction temperature of 75°C. It was observed that the conversion of lactic acid increased with the increasing amount of 1-butanol as shown in Figure 3.12.

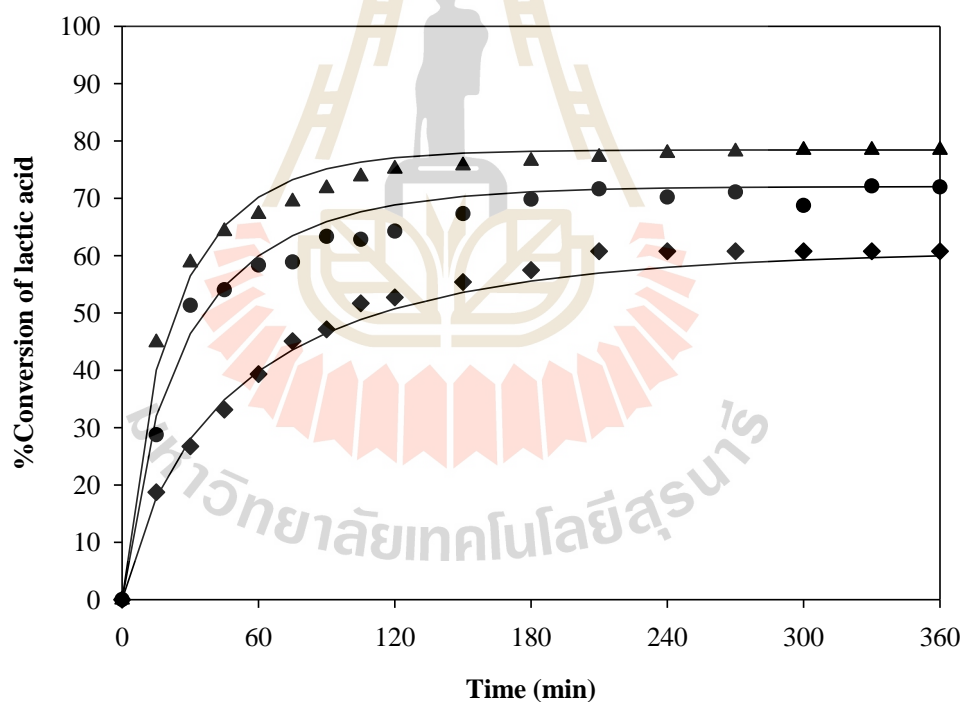


Figure 3.12 Effect of initial 1-butanol to lactic acid molar ratio on conversion of lactic acid in a presence of 1%w/v of catalyst loading at the reaction temperature of 75°C; M=1:1 (◆), M=3:1 (●) and M=5:1 (▲). Solid lines indicate the calculation values from LH model

3.5.2.4 Effect of Reaction Temperature

In this work, the reaction temperature was studied in the range of 55 to 85°C. The reaction was carried out with 1-butanol to lactic acid molar ratio of 5:1 in a presence of 1% w/v catalyst loading and the reaction time of 6 h. Figure 3.13 shows the effect of reaction temperature on the conversion of lactic acid using ALA catalyst. Since the esterification of carboxylic acid with alcohol is an endothermic reaction, the conversion is increased with the reaction temperature (Bart et al., 1994). It can be seen that reaction temperature is a significant effect on the rate of *n*-butyl lactate production and the reaction rate increased sharply with increasing reaction temperature.

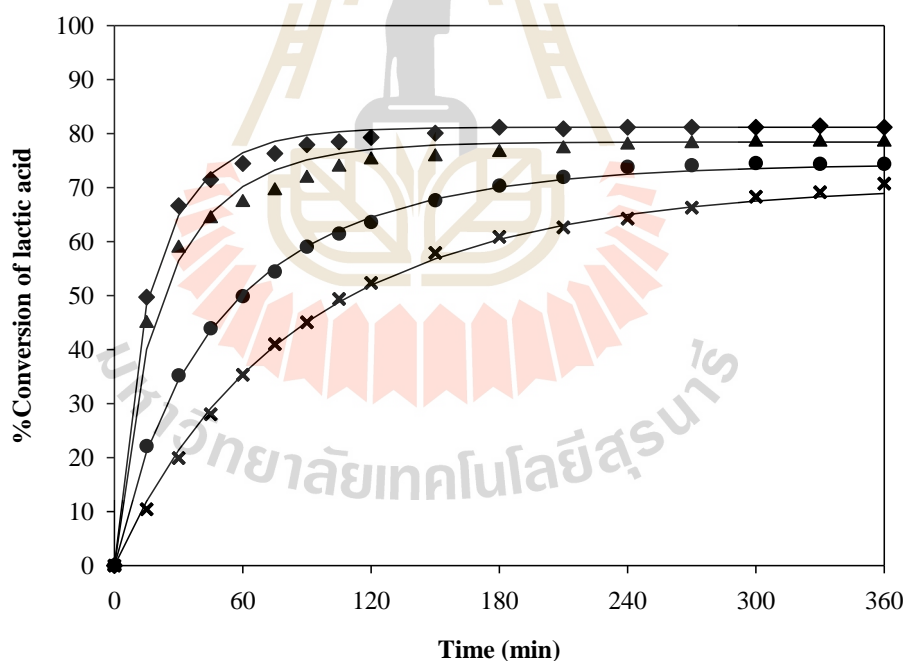


Figure 3.13 Effect of reaction temperature on conversion of lactic acid in a presence of 1% w/v of catalyst loading and M=5:1 at the reaction temperature of 55°C (x), 65°C (●), 75°C (▲) and 85°C (◆). Solid lines indicate the calculation values from LH model

In addition, it was observed that the conversion line obtained at 85°C were closed to the values at 75°C. It might be because the instability of this catalyst occurred during the temperature higher than 78°C, in the presence of catalyst degradation as described in section 3.5.1.5.

3.5.3 Kinetic Models

The kinetic data of ALA catalyzed the esterification of lactic acid with 1-butanol were correlated by PH, ER and LH model with non-ideal assumption as the kinetic equations shown in Eq. (3.1), (3.2) and (3.3), respectively. Reaction rate constant (k), equilibrium constant (K_e) and adsorption constants (K_i) were calculated and showed in Table 3.4. The k and K_e were increased with increasing reaction temperature. Due to the non-ideality of the liquid phase, it is difficult to recognize one model from the others based on the values of SSR and R^2 , since the differences between these values for different models are very small. Therefore, the quality of fitting data between experimental and calculated conversions were also estimated by the mean relative deviation (MRD) of lactic acid conversion. By comparison of MRD values, it can be seen that LH is noticeably more accurate than ER and PH model, respectively.

The reaction rate constant was correlated with temperature by Arrhenius's equation as shown in Eq. (3.4). Taking the natural logarithm of this equation gives;

$$\ln k = \ln A_o - \frac{E_A}{RT} \quad (3.22)$$

A plot of $\ln k$ versus $1/T$ gives a straight line as shown in Figure 3.14. The pre-exponential factor and activation energy are showed in Table 3.4.

Table 3.4 Kinetic parameters for esterification of lactic acid with 1-butanol using ALA catalyst

Model	Temp (°C)	55	65	75	85	75	75	75	75	75	E_A (kJ mol ⁻¹)	A_0 (mol g ⁻¹ min ⁻¹)
	M	5	5	5	5	5	5	5	1	3		
	%Catalyst loading (%w/v)	1	1	1	1	0.25	0.5	1	1	1		
	Ke	1.3998	1.7477	2.2812	2.7771	2.2532	2.2602	2.2812	2.2036	2.5707		
PH model	k (mol·g ⁻¹ ·min ⁻¹)	0.0093	0.0165	0.0410	0.0563	0.0451	0.0397	0.0410	0.0343	0.0379	61.80	6.35×10^7
	SSR	0.0008	0.0044	0.0169	0.0058	0.0042	0.0074	0.0169	0.0022	0.0333		
	MRD	1.5107	3.2257	3.9370	1.9250	3.2951	3.5935	3.9370	2.6283	6.7817		
	R^2	0.9989	0.9940	0.9722	0.9911	0.9956	0.9903	0.9722	0.9957	0.9581		
ER model	k (mol·g ⁻¹ ·min ⁻¹)	0.0403	0.0662	0.1695	0.2193	0.1858	0.1589	0.1695	0.1799	0.1851	58.96	9.59×10^7
	K_{LA}	3.5521	2.3095	1.1569	1.1387	1.5090	1.5285	1.1569	1.4812	2.4972		
	K_w	7.9465	7.2925	7.9212	7.0812	7.8435	7.4102	7.9212	6.8197	7.6113		
	SSR	0.0012	0.0013	0.0100	0.0031	0.0085	0.0024	0.0100	0.0027	0.0243		
	MRD	2.1270	1.6924	3.0526	1.4459	4.2530	1.9192	3.0526	2.7246	5.7052		
R^2	0.9985	0.9982	0.9836	0.9953	0.9911	0.9969	0.9836	0.9948	0.9684			
LH model	k (mol·g ⁻¹ ·min ⁻¹)	0.1889	0.3194	0.7391	1.0241	0.7433	0.7241	0.7391	0.7822	0.7943	57.84	3.00×10^8
	K_{BuOH}	0.6829	0.5340	0.5722	0.4338	0.3816	0.3263	0.5722	0.1532	0.5087		
	K_{LA}	4.2603	3.5790	2.8586	3.3011	3.4612	2.2698	2.8586	1.2748	1.4926		
	K_{BuLA}	0.4390	0.5264	0.4707	0.4416	0.3461	0.4579	0.4707	0.2308	0.6443		
	K_w	6.6665	6.7395	6.3989	6.4257	6.2291	7.1265	6.3989	6.0930	6.4592		
	SSR	0.0024	0.0009	0.0084	0.0025	0.0104	0.0011	0.0084	0.0058	0.0172		
	MRD	2.2541	1.2418	2.7965	1.2840	4.6437	1.1479	2.7965	3.6384	4.7050		
R^2	0.9983	0.9988	0.9863	0.9962	0.9892	0.9985	0.9863	0.9885	0.9758			

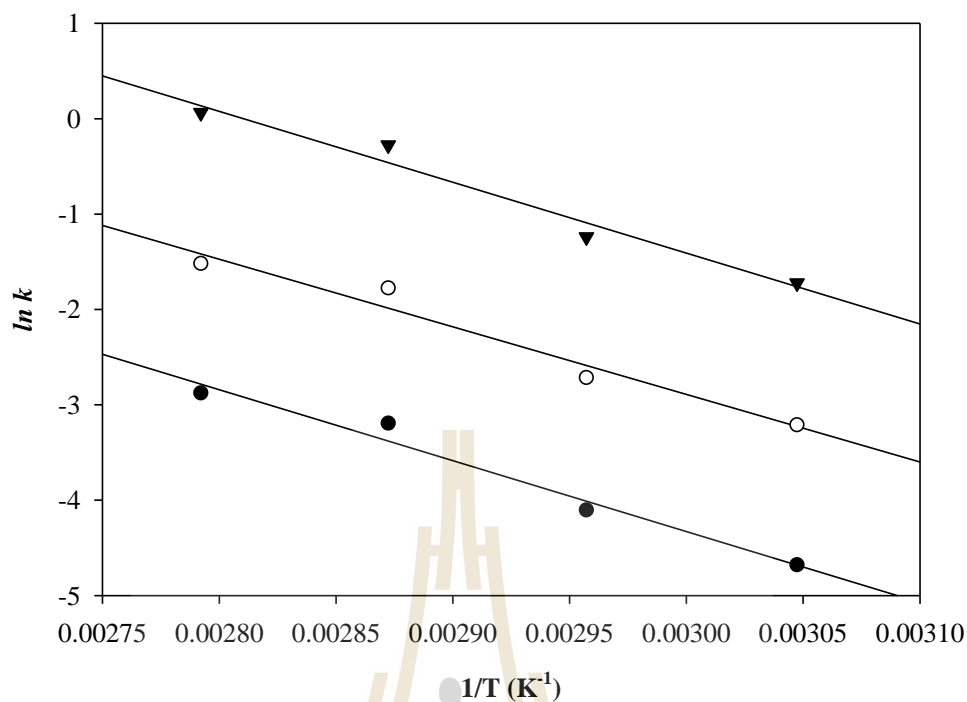


Figure 3.14 Arrhenius plot of PH (●), ER (○) and LH (▼) models for ALA catalyzed esterification of lactic acid with 1-butanol

The equilibrium constants obtained at different reaction temperatures were used to calculate reaction enthalpy (ΔH°) and reaction entropy (ΔS°) for forwards reaction using Van't Hoff equation. The equation is written as;

$$\ln K_e = \frac{-\Delta H^\circ}{RT} + \frac{\Delta S^\circ}{R} \quad (3.23)$$

where ΔH° is enthalpy ($\text{kJ}\cdot\text{mol}^{-1}$) and ΔS° is entropy ($\text{J}\cdot\text{mol}^{-1}\cdot\text{K}^{-1}$) of reaction.

The plot of $\ln K_e$ versus $1/T$ gives the straight line as shown in Figure 3.15. The calculated enthalpy and entropy equal to $22.69 \text{ kJ}\cdot\text{mol}^{-1}$ and $76.88 \text{ J}\cdot\text{mol}^{-1}\cdot\text{K}^{-1}$, respectively. It was found that the ΔH° obtained in this study are positive values, which

suggest that the esterification of lactic acid is an endothermic reaction similar to reported by Bankole (2011) and Toor et al. (2011).

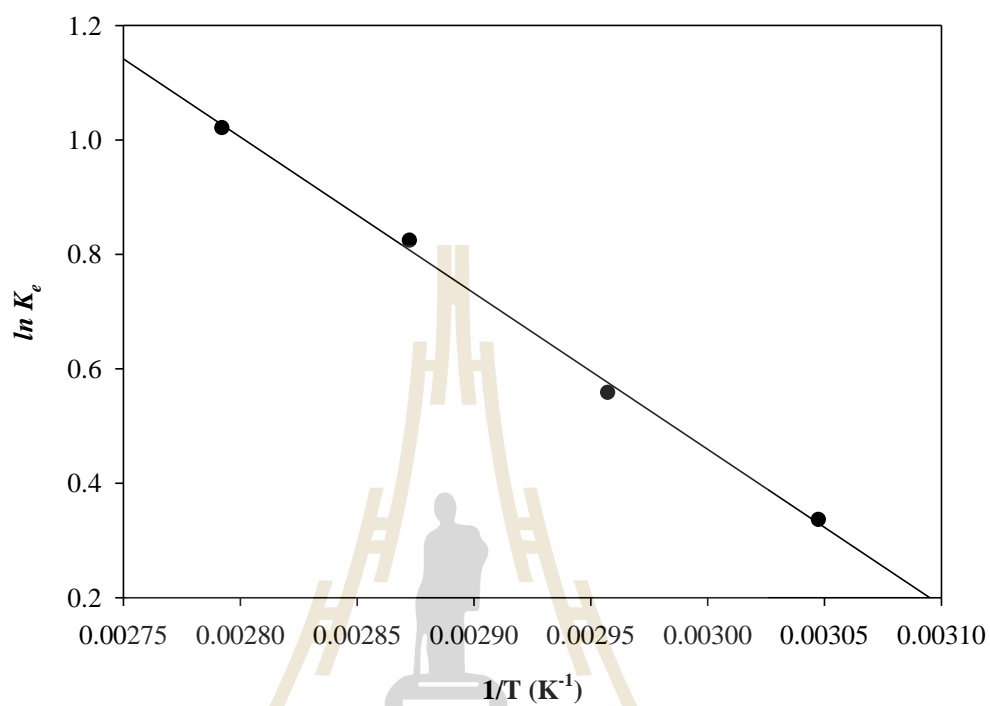


Figure 3.15 Van't Hoff plot of ALA catalyzed esterification of lactic acid with 1-butanol

มหาวิทยาลัยเทคโนโลยีสุรนารี

3.6 Conclusion

The esterification of lactic acid with 1-butanol was successfully carried out over aluminum alginate (ALA) as an acid solid catalyst. The characteristics of the prepared catalyst were investigated. It was observed that the aluminum alginate catalyst created rough surface, in which the presence of cross-linking structure with substantial amount of acidity active sites has led to high esterification activity under mild reaction conditions. The effect of catalyst loading, initial 1-butanol to lactic acid molar ratio and reaction temperature on reaction rate and conversion of lactic acid were investigated. The reaction rate was found to increase with increasing reaction temperature, initial 1-butanol to lactic acid molar ratio and catalyst loading. A maximum lactic acid conversion of 81.18% was achieved over the aluminum alginate after 6 h at 85°C with initial 1-butanol to lactic acid molar ratio of 5:1 and 1% w/v of catalyst loading. The aluminum alginate also showed good catalytic performance for the esterification of lactic acid with 1-butanol. The Langmuir-Hinshelwood model with non-ideal assumption was able to describe the kinetic of this reaction with small error. The esterification of lactic acid is an endothermic reaction, which enthalpy and entropy were found to be 22.69 kJ·mol⁻¹ and 76.88 J·mol⁻¹·K⁻¹.

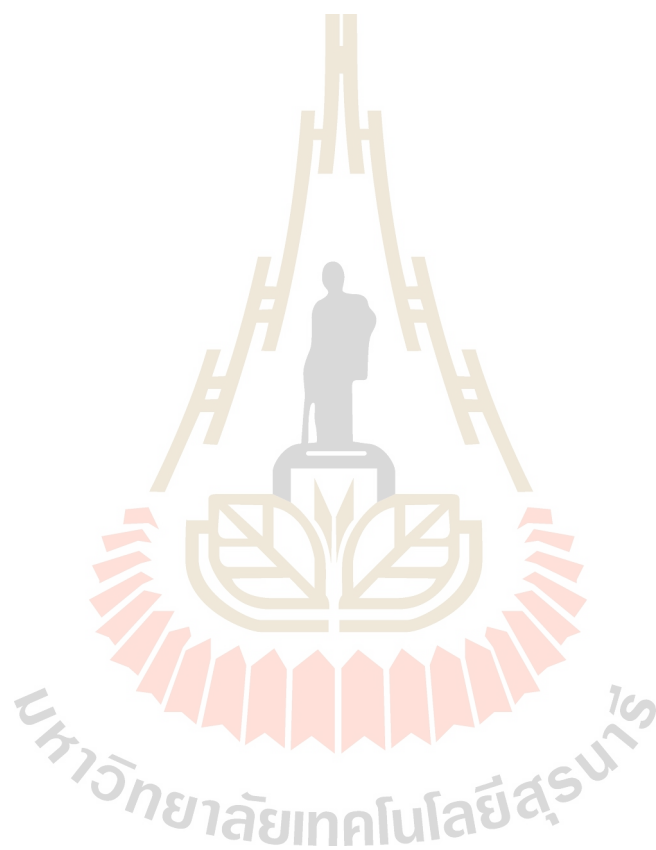
3.7 References

- Abrams, D. S., and Prausnitz, J. M. 1975. Statistical thermodynamics of liquid mixtures: A new expression for the excess Gibbs energy of partly or completely miscible systems. **AIChE Journal** 21 (1):116-128.
- Bankole, K. S. 2011. **Uncatalyzed esterification of biomass-derived carboxylic acids**, University of Iowa.
- Bart, H. J., Reidetschlager, J., Schatka, K., and Lehmann, A. 1994. Kinetics of esterification of levulinic acid with n-butanol by homogeneous catalysis. **Industrial & Engineering Chemistry Research** 33 (1):21-25.
- Benedict, D. J., Parulekar, S. J., and Tsai, S. P. 2003. Esterification of lactic acid and ethanol with/without pervaporation. **Ind. Eng. Chem. Res.** 42:2282.
- Boey, P.-L., Ganesan, S., Maniam, G. P., Khairuddean, M., and Lee, S.-E. 2012. A new heterogeneous acid catalyst system for esterification of free fatty acids into methyl esters. **Applied Catalysis A: General** 433-434:12-17.
- Cheryl-Low, Y. L., Theam, K. L., and Lee, H. V. 2015. Alginate-derived solid acid catalyst for esterification of low-cost palm fatty acid distillate. **Energy Conversion and Management** 106:932-940.
- Il Choi, J., Hong, W. H., and Chang, H. N. 1996. Reaction kinetics of lactic acid with methanol catalyzed by acid resins. **International Journal of Chemical Kinetics** 28 (1):37-41.
- Kumar, R., and Mahajani, S. M. 2007. Esterification of Lactic Acid with n-Butanol by Reactive Distillation. **Industrial & Engineering Chemistry** 46:6873-6882.

- Kumar, R., Nanavati, H., Noronha, S. B., and Mahajani, S. M. 2006. A continuous process for the recovery of lactic acid by reactive distillation. **Journal of Chemical Technology & Biotechnology** 81 (11):1767-1777.
- Li, K.-T., Wang, C.-K., Wang, I., and Wang, C.-M. 2011. Esterification of lactic acid over TiO₂-ZrO₂ catalysts. **Applied Catalysis A: General** 392 (1-2):180-183.
- Liu, Y., Li, Z., Wang, J., Zhu, P., Zhao, J., Zhang, C., Guo, Y., and Jin, X. 2015. Thermal degradation and pyrolysis behavior of aluminum alginate investigated by TG-FTIR-MS and Py-GC-MS. **Polymer Degradation and Stability** 118:59-68.
- Lohmann, J., Joh, R., and Gmehling, J. 2001. From UNIFAC to Modified UNIFAC (Dortmund). **Industrial & Engineering Chemistry Research** 40 (3):957-964.
- Luyben, W. L., and Chien, I. L. 2010. Design and control of distillation systems for separating azeotropes.
- Minchitha, K. U., Nagaraju, H., Nagaraju, N., and Hanumanthaiha, K. 2016. Catalytic Activity Studies of Modified Alumina in the Esterification of Benzyl Alcohol with Different Aliphatic Acids. **Journal of scientific and industrial research** 75:244-252.
- Parani, S., Eswaran, D. P., Marimuthu, A., Baddireddi Subhadra, L., and Kannaiyan, P. 2012. One Pot Synthesis and Characterization of Alginate Stabilized Semiconductor Nanoparticles. **Bulletin- Korean Chemical Society** 33:3218 - 3224.
- Pereira, C. S. M., Pinho, S. P., Silva, V. M. T. M., and Rodrigues, A. E. 2008. Thermodynamic Equilibrium and Reaction Kinetics for the Esterification of

- Lactic Acid with Ethanol Catalyzed by Acid Ion-Exchange Resin. **Industrial & Engineering Chemistry Research** 47 (5):1453-1463.
- Rattanaphanee, P. 2010. Factorial design of experiments for comparative study of lactic acid esterification with ethanol and n-butanol. Paper read at **2010 International Conference on Chemistry and Chemical Engineering**, 1-3 Aug. 2010.
- Sanz, M. T., Murga, R., Beltran, S., Cabezas, J. L., and Coca, J. 2002. Autocatalyzed and ion-exchange-resin-catalyzed esterification kinetics of lactic acid with methanol. **Ind. Eng. Chem. Res.** 41:512.
- Su, C.-Y., Yu, C.-C., Chien, I. L., and Ward, J. D. 2013. Plant-Wide Economic Comparison of Lactic Acid Recovery Processes by Reactive Distillation with Different Alcohols. **Industrial & Engineering Chemistry Research** 52 (32):11070-11083.
- Toor, A. P., Sharma, M., Thakur, S., and Wanchoo, R. K. 2011. Ion-exchange Resin Catalyzed Esterification of Lactic Acid with Isopropanol: a Kinetic Study. **Bulletin of Chemical Reaction Engineering & Catalysis; 2011: BCREC Volume 6 Issue 1 Year 2011 (SCOPUS Indexed)**.
- Troupe, R. A., and DiMilla, E. 1957. Kinetics of the Ethyl Alcohol—Lactic Acid Reaction. **Industrial & Engineering Chemistry** 49 (5):847-855.
- Wu, D., Zhao, J., Zhang, L., Wu, Q., and Yang, Y. 2010. Lanthanum adsorption using iron oxide loaded calcium alginate beads. **Hydrometallurgy** 101 (1-2):76-83.
- Yixin, Q., Shaojun, P., Shui, W., Zhiqiang, Z., and Jidong, W. 2009. Kinetic Study of Esterification of Lactic Acid with Isobutanol and n-Butanol Catalyzed by Ion-exchange Resins. **Chinese Journal of Chemical Engineering** 17 (5):773-780.

Zhang, Q., Li, H., Qin, W., Liu, X., Zhang, Y., Wei, X., and Yang, S. 2013. Solid acid used as highly efficient catalyst for esterification of free fatty acids with alcohols. **China Petroleum Processing and Petrochemical Technology** 15:19-24.



CHAPTER IV

ESTERIFICATION OF LACTIC ACID AND HYDROLYSIS OF N-BUTYL LACTATE IN REACTIVE DISTILLATION

4.1 Abstract

Reactive distillation is one of the most well-established integrative separation and purification of lactic acid. Esterification of lactic acid with 1-butanol followed by hydrolysis of *n*-butyl lactate is an effective technique for this propose. In this work, the esterification and hydrolysis were catalyzed by aluminum alginate and Amberlyst-15, respectively. The effect of operating parameters such as reflux ratio, catalyst loading, feed flow rate and operating pressure were investigated on conversion, yield, and purity. The catalyst loading does not significantly affect conversion and yield for esterification, while an increase in catalyst loading intensive effect in hydrolysis. The conversion and yield seem to decrease with increasing feed flow rate while it was found to be increased when using high reflux ratio. In addition, it was observed that the flooding easily occurred in hydrolysis due to high amount of water was evaporated under study conditions, which is an effect on purity of lactic acid. In this work, the maximum yield of *n*-butyl lactate obtained from esterification is 87.44% and yield of lactic acid obtained from hydrolysis is 33.98% with maximum purity of lactic acid achieved at 98.53% under study condition.

4.2 Introduction

Reactive distillation is an excellent process intensification which combines reaction and separation into one unit. To enhance the equilibrium conversion of the reaction, either one of the reactants must be used in excess or one of the products must be removed continuously from the reaction mixture. The latter can be achieved through separation of water by simultaneous distillation. The reactive distillation has considerable attention process for recovery and purification of lactic acid via esterification and hydrolysis. Esterification of lactic acid with alcohol to form the ester and then hydrolyzing the ester back to lactic acid. The lactic acid is reacted with an alcohol to form a lower boiling ester which can be separated from heavy impurities and the ester is hydrolyzed to recover pure lactic acid. Purification of lactic acid by reactive distillation was investigated by several researchers with different alcohols (Seo et al., 1999; Kumar et al., 2006a; Kumar et al., 2006b; Su et al., 2013; Komesu et al., 2015).

Kumar and Mahajani (2007) investigated the reactive distillation of lactic acid with n-butanol using batch and continuous reactive distillations. The reaction was performed in the presence of Amberlyst-15. Experimental results of continuous reactive distillation are compared with the simulation results observed using the Aspen plus process simulator. 92% conversion of lactic acid was observed in batch distillation and near to quantitative conversion in continuous mode. The reactive distillation helps simultaneous separation of water and enhances the equilibrium conversion and n-butanol is a promising solvent for the purpose of lactic acid recovery from the aqueous solutions.

Su et al. (2013) designed the continuous recovery of lactic acid from fermentation broth by reactive distillation. The solid catalyst used in this work was

acidic ion-exchange resin as Amberlyst-15 (Rohm and Hass). They reported that the process configuration, total process cost, and payback period have been found to varied with the type of esterifying alcohols. The results indicated that methanol and butanol were the most economically attractive. The advantage of methanol is inexpensive. It does not form an azeotrope with water and forms the lowest-boiling ester, while butanol induces a liquid-liquid separated phase that can be exploited to reduce separation costs. In addition, using butanol as esterifying alcohol has an advantage as it can prevent lactic acid polymerization during the reaction.

As the processes mentioned above, esterification of lactic acid with 1-butanol was studied in a reactive distillation column using aluminum alginate as a solid catalyst. The extracted product containing lactic acid in rich 1-butanol phase obtained from the extraction process in Chapter II was used as a single feed for esterification step. *n*-butyl lactate thus formed in reactive distillation be hydrolyzed further to obtain relatively lactic acid using Amberlyst-15 as a solid catalyst. The effect of operating variables such as catalyst loading, reflux ratio operating pressure, as well as feed flow rate on conversion and yield and purity were studied.

4.3 Theory

4.3.1 Reactive Distillation

Reactive distillation (RD) is the combination of reaction and separation in a single vessel which has a specific advantage over the conventional sequential approach of reaction followed by distillation technique (Hiwale et al., 2004). Apart from functioning as a reactor and distillation, reactive distillation column can be an efficient separator to enhance the recovery rate and further purification of chemicals. The suitability of reactive distillation for a reaction depends on various factors such as volatilities of reactants and products, reaction and distillation temperatures, etc. and hence, the use of reactive distillation for every reaction may not be feasible.

When designed correctly, reactive distillation columns can overcome equilibrium limitations by removing the product out of the reaction zone and in turn forcing the reaction to complete conversion. Moderately exothermic reactions are considered ideal to be carried out in reactive distillation columns because the heat of reaction can be used to heat the column and thus drive separation. In this case, the device makes ideal use of the energy produced in the reaction lowering environmental costs. At the same time reactive distillation can bypass distillation boundaries such as azeotropes by reaction.

Distillation boundaries appear because vapor and liquid have the same composition. This makes any composition change by distillation impossible. The equality of concentration in vapor and liquid phase does not limit concentration changes due to reaction. As first reactive distillation systems have reached maturity leading to largescale commercial production. The focus of basic engineering research into these systems has shifted. Due to the high amount of integration, column parameters are more

strongly linked reducing the degrees of freedom for design. Special problems arise with scale-up and a general scale-up method is still not available. The degree of complexity of designing reactive distillation columns increases further if phase splitting into two liquid phases can occur within the system. Strong interaction of operating parameters can also lead to much interesting. Finally, first ideas are being forwarded to couple several reactive distillation columns to achieve reactive separation effects. Reactive distillation allows a chemical reaction and multistage distillation to take place simultaneously in a column. The combined unit operation, especially suits for chemical reactions where reaction equilibrium limits the conversion in a conventional reactor to a low-to-moderate level.

By continuously separating products from reactants while the reaction is carried out, the reaction can proceed to much higher level of conversion. Since this demonstration of its ability to render cost effectiveness and compactness to some chemical plants, reactive distillation has been explored as a potentially important process for several reactions. Along with esterification and etherification, other reactions such as acetalization, hydrogenation, alkylation, and hydration have been explored. The objectives of existing and potential applications of reactive distillation are to: surpass equilibrium limitation, achieve high selectivity towards a desired product, achieve energy integration, perform difficult separations. The reactive distillation can be looked upon as an efficient separator for the recovery or purification of chemicals. The reversible reactions can be exploited for this purpose. For reversible reaction, esterification and hydrolysis are suitable to be used in the reactive distillation column (Mahajan et al., 2008). To considering the reversible esterification, reaction scheme is showed in Eq. (4.1):



where the boiling points of the components followed the sequence A, C, D and B. The alternative reactive distillation configuration is shown in Figure 4.1.

The reactive distillation column consists of a reactive section in the middle with nonreactive rectifying and stripping sections at the top and bottom. The task of the rectifying section is to recover reactant B from the product stream C. In the stripping section, the reactant A is stripped from the product stream D. In the reactive section the products are separated in situ, driving the equilibrium to the right and preventing any undesired side reactions between the reactants A (or B) with the product C (or D).

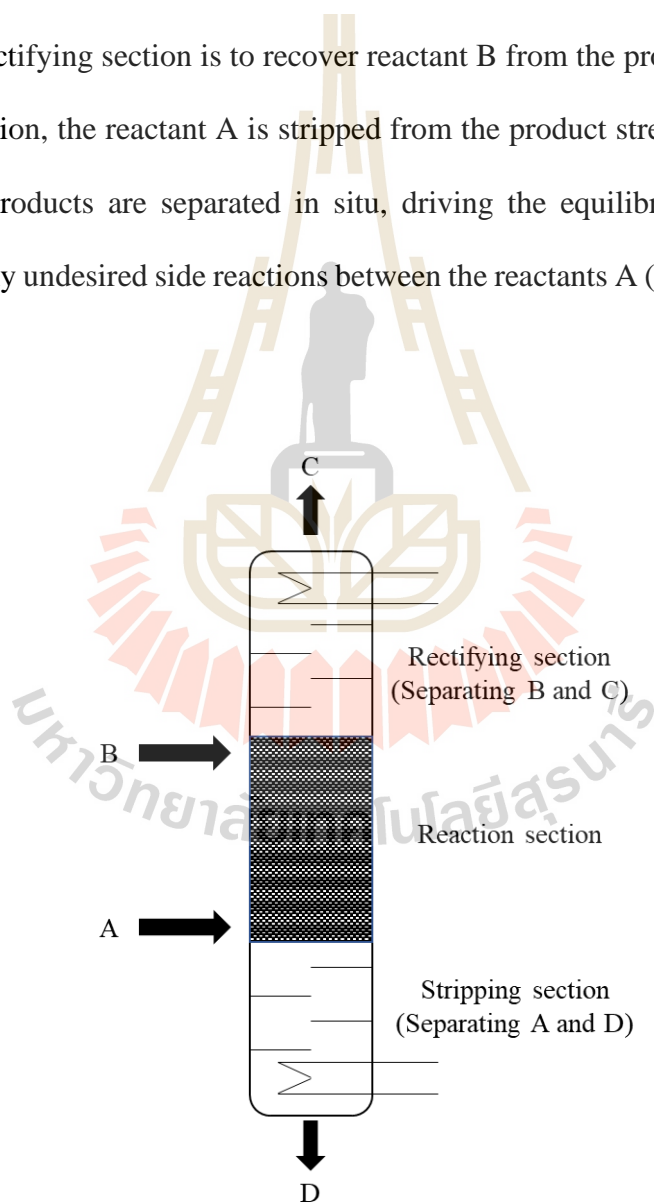


Figure 4.1 The reactive distillation configuration

4.3.2 Advantage of Reactive Distillation

The advantages of reactive distillation can be summarized as follows:

- (a) Simplification system by using separation and reaction in the same device lead to significant capital savings.
- (b) If the reaction is exothermic, the heat released from the reaction can be used for vaporization of liquid, leading to savings of energy costs by the reduction of reboiler duties.
- (c) The maximum temperature in the reaction zone is limited to the boiling point of the reaction mixture, so that the danger of hot spot formation on the catalyst is reduced significantly. A simple and reliable temperature control can be achieved.
- (d) Product selectivity can be improved due to a fast removal of reactants or products from the reaction zone. By this, low concentration of one of the reactants can lead to reduction of the rates of side reactions and hence improved selectivity for the desired products.
- (e) If the reaction zone in the reactive distillation column is placed above the feed point, poisoning of the catalyst can be avoided. This leads to longer catalyst lifetime compared to conventional systems.
- (f) Reactive distillation column can improve conversion of reactant approaching 100 % (Taylor and Krishna, 2000).
- (g) Significantly reduced catalyst requirement for the same degree of conversion.

- (h) Avoidance of azeotropes, reactive distillation is particularly advantageous when the reactor product is a mixture of species that can form several azeotropes with each other. Its conditions can allow the azeotropes to be “reacted away” in a single vessel.
- (i) Reactive distillation process can reduce by-product formation.

4.3.3 Limiting of Reactive Distillation

Against the above-mentioned advantages of RD, there are several constraints and foreseen difficulties (Kulprathipanja, 2002) as:

- (a) Volatility constraints. The reagents and products must have suitable volatility to maintain high concentrations of reactants and low concentrations of products in the reaction zone.
- (b) Residence time requirement. If the residence time for the reaction is long, a large column size and large tray hold-ups will be needed, and it may be more economic to use a reactor-separator arrangement.
- (c) Scale up to large flows. It is difficult to design reactive distillation processes for very large flow rates because of liquid distribution problems in packed reactive distillation columns.
- (d) Process conditions mismatch. In some processes the optimum conditions of temperature and pressure for distillation may be far from optimal for reaction.

The reactive distillation can be performed either homogeneous or heterogeneous processes. For homogeneous reactive distillation processes, counter-current vapor-liquid contacting, with sufficient degree of staging in the vapor and liquid

phases, can be achieved in a multi-tray column as shown in Figure 4.2 or a column with random or structured packings as shown in Figure 4.3.

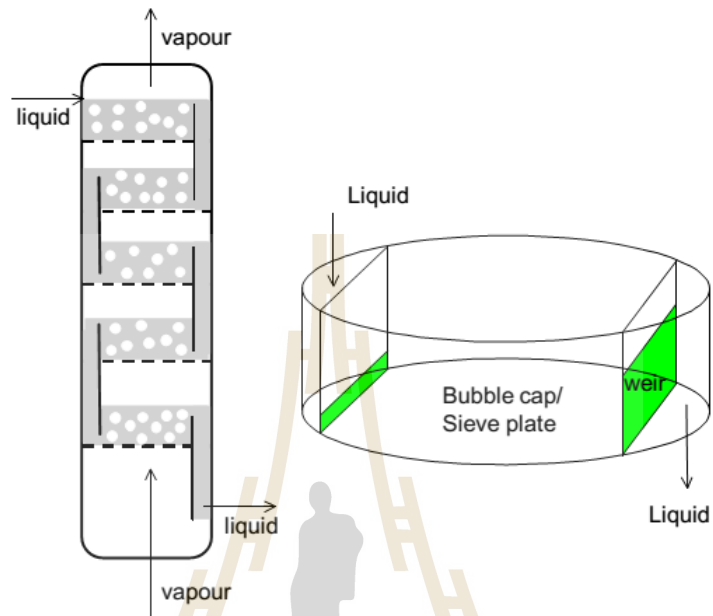


Figure 4.2 Counter-current vapor-liquid contacting in trayed column (Baur, 2000)

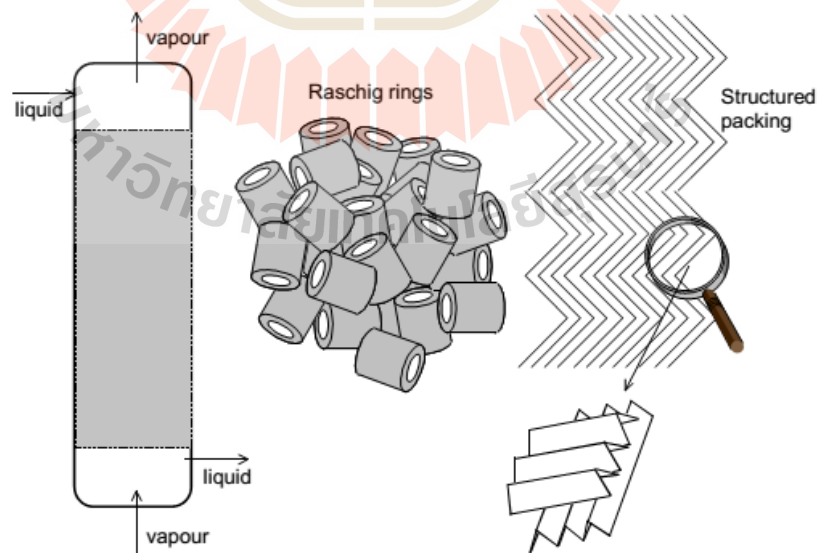


Figure 4.3 Counter-current vapor-liquid contacting in packed column (Baur, 2000)

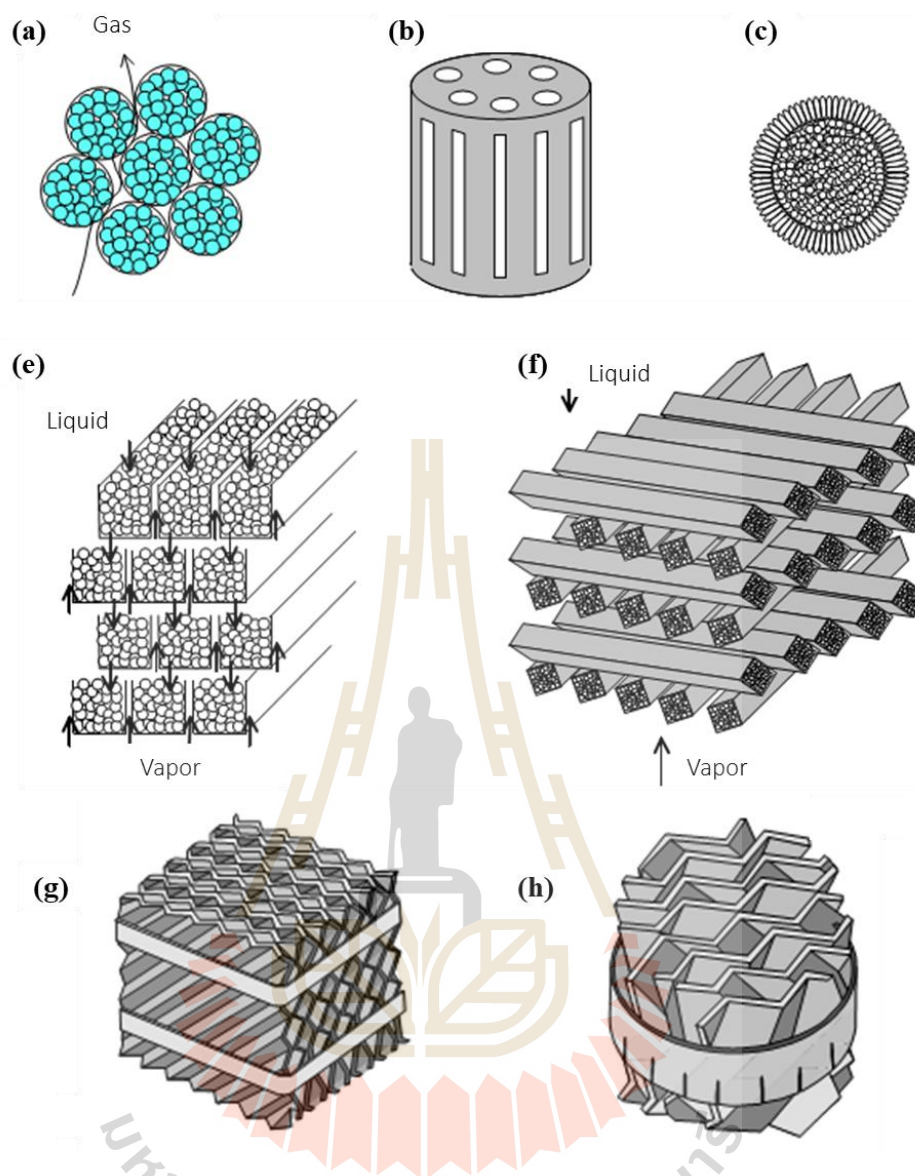
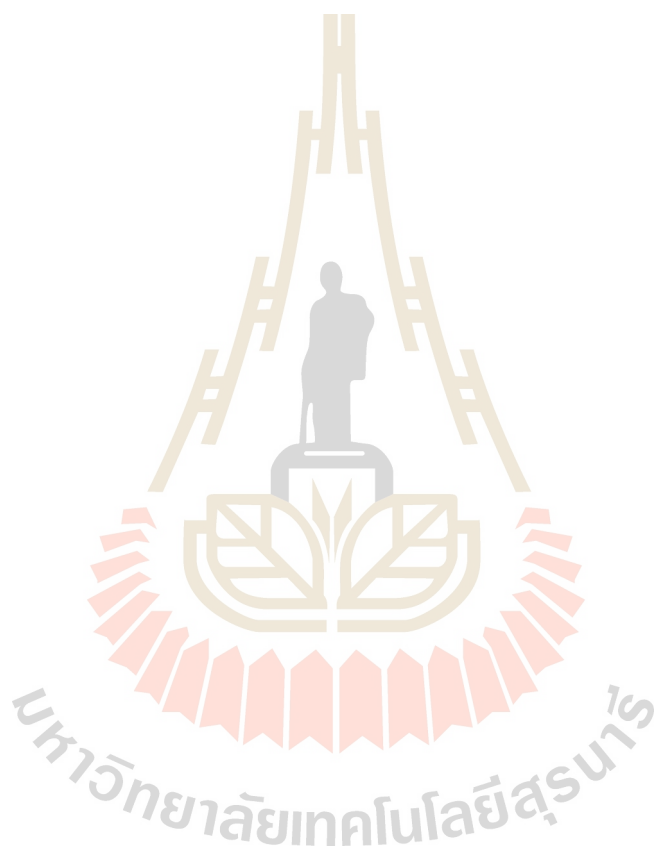


Figure 4.4 Catalyst particles enveloped in wire gauze packings and placed inside RD column: spherical baskets (a), cylindrical container for catalyst particles (b), wire gauze envelopes(c), horizontally disposed gutters (d), horizontally disposed wire gauze tubes (e), sandwich in cubical collection (e) and sandwich in a round collection (h)

For heterogeneous reactive distillation processes, the catalyst particle sizes used in such operations are usually in the range of 1 to 3 mm. Larger particle sizes

lead to intra-particle diffusion limitations. To overcome the limitations of flooding the catalyst particles have to be enveloped within wire gauze envelopes. Most commonly the catalyst envelopes are packed inside the column. Almost every conceivable shape of these catalyst envelopes has been patented; some basic shapes are shown in Figure 4.4.



4.4 Experimental Procedures

4.4.1 Chemicals

Extracted product obtained from the extraction of lactic acid with 1-butanol using packed liquid-liquid extraction in Chapter II was used as a feed solution in this work. Aluminum alginate was prepared and obtained from Chapter III. Amberlyst-15 purchased from Sigma Aldrich, was dried in oven at 60°C for 3 h before used. *n*-Butyl lactate with 99% purity were purchased from Acros. Deionized water was used in every experiment.

4.4.2 Reactive Distillation Apparatus

A single stage reactive distillation column in laboratory scale is setup by following Komesu et al. (2015) with slight modification as shown in Figure 4.5. Total height of glass column is 300 mm and inner diameter is 24 mm. The top of column connected with a condenser, and the bottom is equipped with a round bottom flask using Gerhardt KI heating mantle as heating source. Catalyst is filled in cylindrical stainless gauze envelopes container and located at a middle of column, which is upper and lower of catalyst packing are rectifying and stripping section, respectively. Thermocouple provided in the middle of column for measuring temperature. Peristaltic pumps are used to supply the feed and reflux stream. The operating pressure is controlled by Buchi vacuum pump with vacuum controller. Thermostat heating bath is used to controlled temperature of oil jacket along the column.

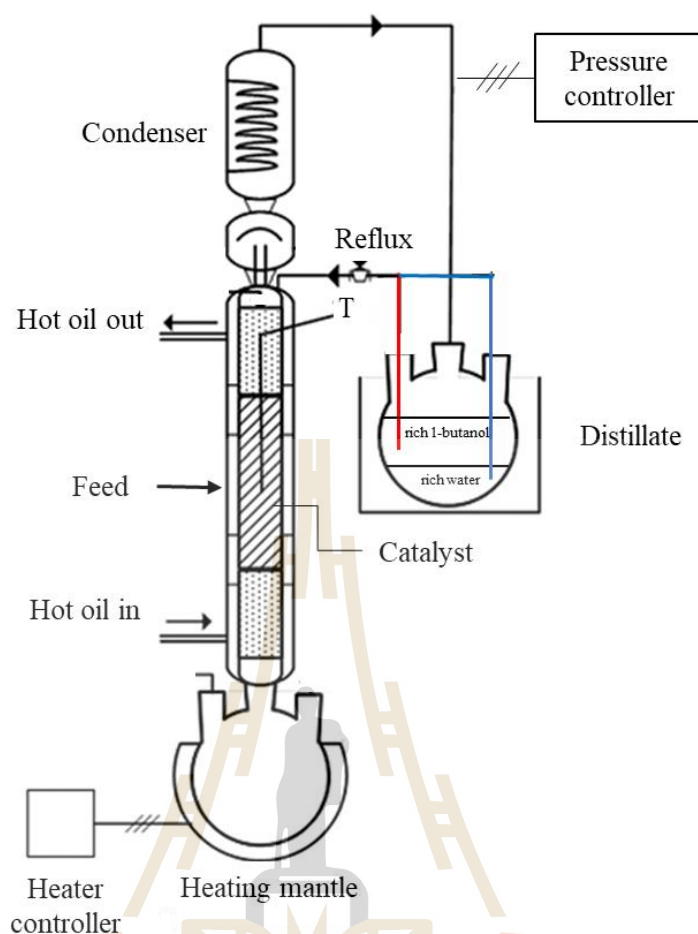


Figure 4.5 Schematic diagram of laboratory reactive distillation column

4.4.3 Esterification and Hydrolysis in Reactive Distillation Column

Esterification and hydrolysis reaction were performed in semi-batch mode of reactive distillation. For esterification process, approximately about 300 g of the extract phase obtained from experimental in extraction part was used as single feed solution, which lactic acid can also react reversibly with 1-butanol to produce butyl lactate and water. The reaction was catalyzed by aluminum alginate as a solid catalyst. Desired amount of aluminum alginate catalyst is randomly filled in packing element and located into the middle of column. Before starting the experiment, temperature of condenser was set at 15°C and the column has hot oil jacket for thermal isolation at

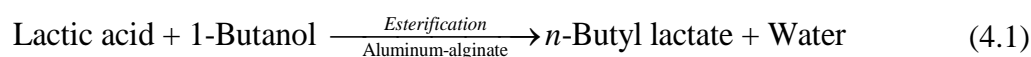
70°C. The heating mantle was set at constant temperature of 90°C. Initial pressure was started at 637 mbar and the feed solution was fed to the reaction zone at middle of column by peristaltic pump with desired feed flow rate at room temperature. After that, the pressure was reduced from 637 to 255 mbar with pressure rate of 10 mbar/min, which is final pressure based on reported by (Sun et al., 2006) with slight modification. The obtained distillate stream separated into two phases, which light phase is unreacted 1-butanol and heavy phase is rich water phase. At steady-state pressure, temperature at bottom and middle of column were recorded. Only the unreacted butanol phase was returned into the column using peristaltic pump by adjusting its reflux value. In each run, the experiment ran until out of feedstock. The samples of distillate and residue were collected and weighed with an accuracy of ± 0.1 g error. The compositions of feed, distillate and residue have analyzed the compositions of 1-butanol, *n*-butyl lactate, and lactic acid by GC with the same method as described in Chapter II. Material balance was verified to ensure mass in equaled mass out of the reactive distillation column.

For hydrolysis process, the experiment was carried out in the same apparatus with esterification. The feed was prepared by mixing of *n*-butyl lactate and deionized water at the same concentration of *n*-butyl lactate containing in distillate product obtained from esterification process. The reaction was catalyzed by Amberlyst-15. Final pressure was set at desired value. In this process, the distillate stream separated into two phases, which lower phase is unreacted water and it was returned into the column at desired reflux ratio value. After done, the compositions of distillate and residue were further analyzed as described before and material balance was verified to ensure mass in equaled mass out of the reactive distillation column.

4.5 Results and Discussion

4.5.1 Esterification in Reactive Distillation Column

For Esterification of lactic acid using reactive distillation in this work, the reaction is involved;



The volatilities of reactants and products play an important role in the design of a reactive distillation process. The order of volatilities of reactants and products involved in this experiment is as follows: water > 1-butanol > *n*-butyl lactate > lactic acid, as shown in Table 4.1.

Table 4.1 Boiler point of pure components under atmospheric pressure (Su et al., 2013)

Component	Normal boiling point (°C)
Water	100.02
1-Butanol	117.75
<i>n</i> -Butyl lactate	186.69
Lactic acid	232.14

As in Table 4.1, lactic acid is almost non-volatile under atmospheric pressure. In this work, concentration of lactic acid in feed solution is about 10.5% by weight with initial molar ratio of 1-butanol to lactic acid is 10:1. Therefore, formation of dimer or oligomer of lactic acid by self-esterification could be ignored because lactic acid feed solution of low concentration (20 % by weight) was used (Troupe and DiMilla, 1957; Asthana et al., 2006). In addition, the temperature at the bottom of column (T_{reboiler}) was fixed approximately about 90°C to prevent lactic acid oligomerization (Asthana et al., 2006).

For a reactive distillation column involving reactions with high thermal effect, operating pressure affects significantly reactant conversion and reaction heat load, giving rise to strong influences on process intensification between the reaction operation and the separation operation involved. It is therefore imperative to designate deliberately operating pressure during process synthesis and design. For esterification in this work, the experiment was designed to collect *n*-butyl lactate in distillate product by using operating pressure at 255 mbar based on the pressure condition reported by Sun et al. (2006). Water, 1-butanol and *n*-butyl lactate could be spit from reboiler to top of column. Distillate product separated to two phases, which is unreacted 1-butanol phase was returned into the reaction zone again for driving forward reaction of esterification. Unreacted lactic acid was collected at the bottom. This design has advantage when the feed solution contains with heavy impurities such as using fermentation broth because it can be separated heavy impurities from ester product and removed at the bottom of reactive distillation column.

The effect of catalyst loading, feed flow rate and reflux ratio were studied on process performance. Experimental data of esterification in producing of *n*-butyl lactate is showed in Table 4.2 and comparison of variables represented in Figure 4.6-4.8 for effect of reflux ratio, catalyst loading and feed flow rate, respectively. Performance of esterification step was determined in terms of conversion of lactic acid and yield of *n*-butyl as follows:

$$\% X_{LA} = \frac{\text{Mole of LA in feed} - \text{Mole of unreacted LA in outing}}{\text{Mole of LA in feed}} \times 100 \quad (4.2)$$

$$\%Y_{BuLA} = \frac{\text{Actual mass of BuLA in distillate product}}{\text{Theoretical mass of BuLA in esterification}} \times 100 \quad (4.3)$$

where X and Y refers to conversion and yield. Subscript of LA and $BuLA$ are lactic acid and n -butyl lactate, respectively. The conversion of lactic acid represented to reacted lactic acid into n -butyl lactate, which is in both distillate and residue product. While the yield of n -butyl lactate refers to n -butyl lactate in distillate product only. As the experimental data at constant pressure of 255 mbar and T_{reboiler} of 90°C, it was found that the conversion of lactic acid was slightly more than yield of n -butyl lactate for all run. It means that the operation under T_{reboiler} and pressure in this work can obtained more n -butyl lactate in distilled product as expected design. From literature, Sun et al. (2006) studied the esterification of lactic acid with 1-butanol in batch reactive distillation column at approximately the same pressure used in this work. The esterification is performed in batch reactor and after the reaction complete already, n -butyl lactate was also collected at bottom and was then separated from bottom by decreasing pressure to 27 mbar. In contrast, the results obtained in this work can separate n -butyl lactate during the reaction to the top of column. It might be because the esterification this work was performed in semi-batch reactive distillation using short column, resulting in short rectifying and stripping zone, which n -butyl lactate might be pushed up to the top of column under study operating conditions.

Table 4.2 Experimental data for esterification of lactic acid using aluminum alginate as a solid catalyst in reactive distillation column

Parameters	Run-1	Run-2	Run-3	Run-4	Run-5	Run-6	Run-7	Run-8	Run-9	Run-10
T_{Liquid at middle}(°C)	82	82	82	83	83	82	82	83	82	83
Pressure (mbar)	255	255	255	255	255	255	255	255	255	255
Feed flow rate (ml/min)	1.0	0.6	1.0	1.0	1.0	1.0	1.0	1.0	2.0	2.0
Catalyst loading (g)	1.5	1.5	1.5	1.5	1.5	0.75	1.5	3.0	1.5	1.5
Reflux ratio	0	0.16	0.16	0.25	0.53	1.00	1.00	1.00	0.15	1.00
Mass of feed (g)	300.50	300.385	301.20	300.53	300.72	300.91	300.65	300.72	299.89	300.25
Mass fraction of feed										
lactic acid	0.1052	0.1046	0.1027	0.1046	0.1046	0.1046	0.1046	0.1046	0.1046	0.1046
1-butanol	0.8597	0.8625	0.8545	0.8625	0.8625	0.8625	0.8625	0.8625	0.8677	0.8625
<i>n</i> -butyl lactate	0.0004	0.0008	0.0005	0.0008	0.0008	0.0008	0.0008	0.0008	0.0008	0.0008
water	0.0347	0.0322	0.0423	0.0322	0.0322	0.0322	0.0322	0.0322	0.0269	0.0322
Mass of distillate (g)	279.14	273.36	285.43	275.88	279.52	287.77	286.52	281.92	259.14	280.90
Mass fraction of distillate										
lactic acid	0.0181	0.0073	0.0092	0.0113	0.0118	0.0106	0.0065	0.0037	0.0269	0.0043
1-butanol	0.8954	0.8677	0.8490	0.8417	0.8380	0.8247	0.8215	0.8002	0.8826	0.8667
<i>n</i> -butyl lactate	0.0469	0.1064	0.1116	0.1168	0.1285	0.1396	0.1464	0.1583	0.0982	0.1264
water	0.0395	0.0186	0.0302	0.0302	0.0216	0.0250	0.0255	0.0378	0.0285	0.0395
Mass of residue (g)	19.69	16.02	10.27	14.23	12.44	8.10	8.88	6.96	19.10	11.74
Mass fraction of residue										
lactic acid	0.9068	0.5579	0.5649	0.5327	0.4490	0.5173	0.4031	0.3895	0.6420	0.6915
1-butanol	0.0078	0.0029	0.0004	0.0016	0.0007	0.0112	0.0082	0.0045	0.0020	0.0042
<i>n</i> -butyl lactate	0.0049	0.0053	0.0040	0.0031	0.0059	0.0048	0.0047	0.0022	0.0033	0.0114
water	0.0805	0.4339	0.4307	0.4626	0.5444	0.4666	0.5840	0.6038	0.3527	0.2929
%X_{LA}	27.54	59.96	62.49	65.96	71.77	76.95	82.68	88.09	55.55	70.45
%Y_{BuLA}	25.51	54.18	60.94	63.17	70.38	78.67	82.23	87.44	52.93	67.19

4.5.1.1 Effect of Reflux Ratio

According to the esterification of lactic acid with 1-butanol in reactive distillation column, effect of reflux ratio was investigated on the performance of process over the range of 0 to 1 at the same other operating parameters as the results shown in Figure 4.6. It was found that conversion of lactic acid and yield of *n*-butyl lactate increase with increasing reflux ratio. It is due to the increase in reflux ratio that complemented by addition of 1-butanol (reflux of 1-butanol) from the top back to the reaction zone in the column, which can further react with lactic acid. Increasing reflux ratio leads to higher ratio of 1-butanol to lactic acid, hence the excess 1-butanol shifts the reaction to forward, resulting in higher conversion as well as yield.

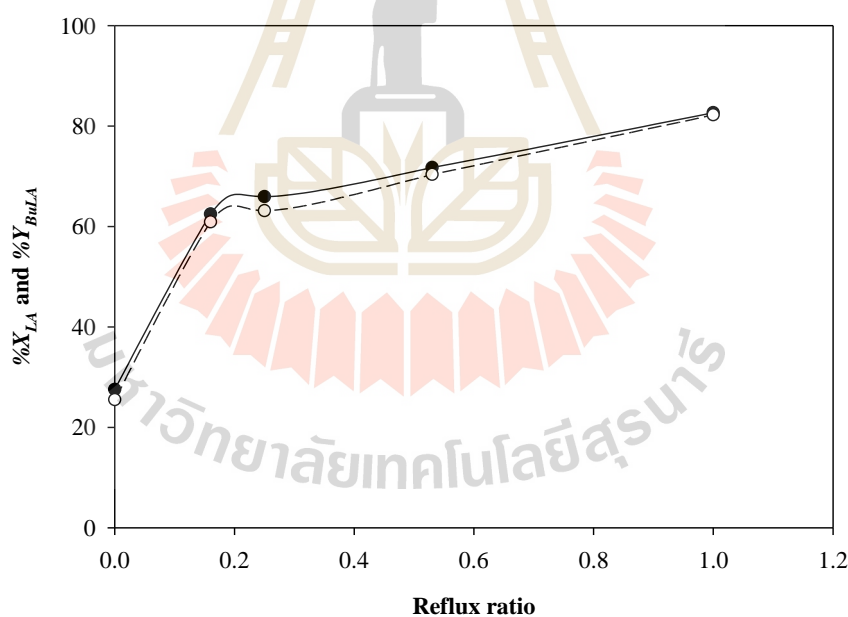


Figure 4.6 Effect of reflux ratio on conversion of lactic acid (—●—) and yield of *n*-butyl lactate (··○··) in distillate product for esterification of lactic acid in reactive distillation column at pressure of 255 mbar, T_{reboiler} of 90°C, feed flow rate of 1 ml/min and 1.5 g of catalyst loading

4.5.1.2 Effect of Catalyst Loading

Aluminum alginate was used to catalyze the esterification of lactic acid in reactive distillation. The amount of catalyst was varied at the same other operating parameters to study the effect of catalyst loading on conversion of lactic acid and yield of *n*-butyl lactate as the results showed in Figure 4.7. It can be seen that over a range of catalyst loading 0.75 to 3 g, both conversion and yield are most insensitive to change in catalyst loading. This indicated that the reaction is reasonably fast, and it is the removal of *n*-butyl lactate from liquid phase as well as the reflux of 1-butanol that determines the overall performance by driving forward reaction. A similar observation was made in previous work (Chapter III) on esterification of lactic acid in batch reactor.

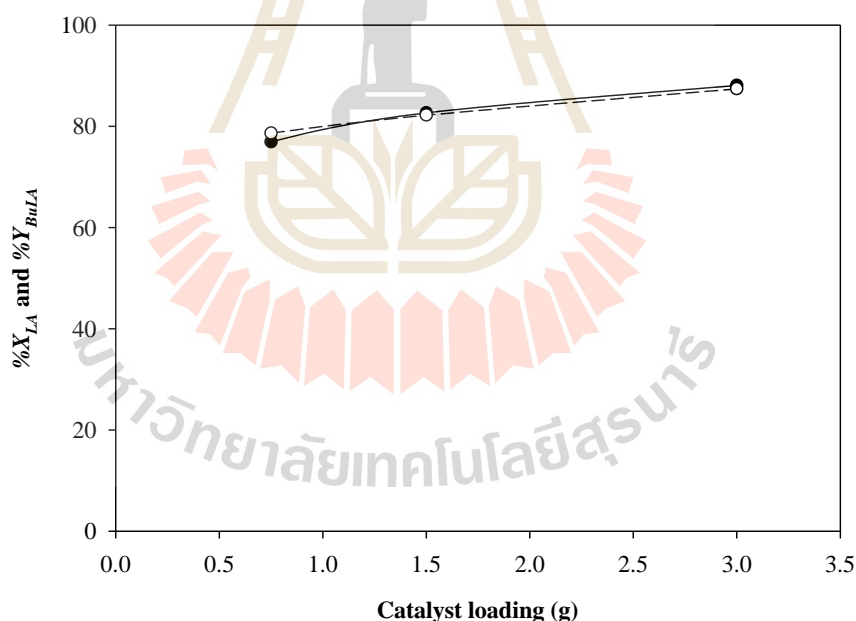


Figure 4.7 Effect of catalyst loading on conversion of lactic acid (—●—) and yield of *n*-butyl lactate (---○---) in distillate product for esterification of lactic acid in reactive distillation column at pressure of 255 mbar, T_{reboiler} of 90°C, feed flow rate of 1 ml/min with reflux ratio of 1

4.5.1.3 Effect of Feed Flow Rate

The effect of feed flow rate was investigated over the range of 0.5 to 2 ml/min at the same other operating parameters. It can be seen the result from Figure 4.8 that the conversion of lactic acid and yield of *n*-butyl lactate increased via increasing feed flow rate from 0.5 to 1 ml/min. Beyond these flow rates, the conversion and yield decreased. It may be because of the rate of evaporation of *n*-butyl lactate removal per mole of lactic acid that comes through the feed decreased, which may be able to backward reaction, resulting in the lower conversion of lactic acid and yield of *n*-butyl lactate.

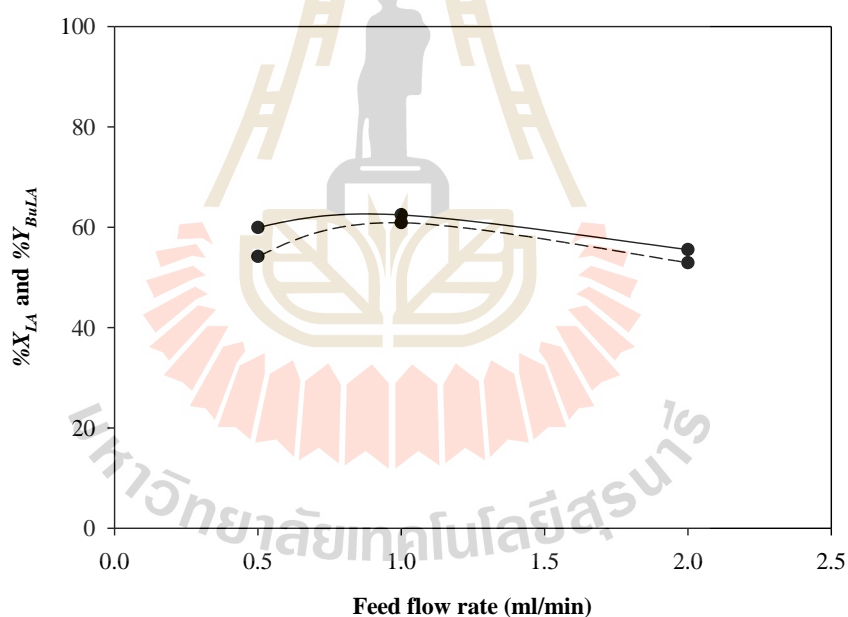


Figure 4.8 Effect of feed flow rate on conversion of lactic acid (—●—) and yield of *n*-butyl lactate (---○---) in distillate product for esterification of lactic acid in reactive distillation column at pressure of 255 mbar, T_{reboiler} of 90°C, reflux ratio of 1 with 1.5 g of catalyst loading

For the esterification of lactic acid in reactive distillation using aluminum alginate as a solid catalyst in this work, the example of distillate product containing *n*-butyl lactate and residue are showed in Figure 4.9. The residue product has brown color, this might be due to color of lactic acid sensitive with temperature. The used aluminum alginate is showed in Figure 4.10. It was observed that the color of catalyst has a little bit changed, including its appearance seem to being welded to pieces, may be due to its gelling property.

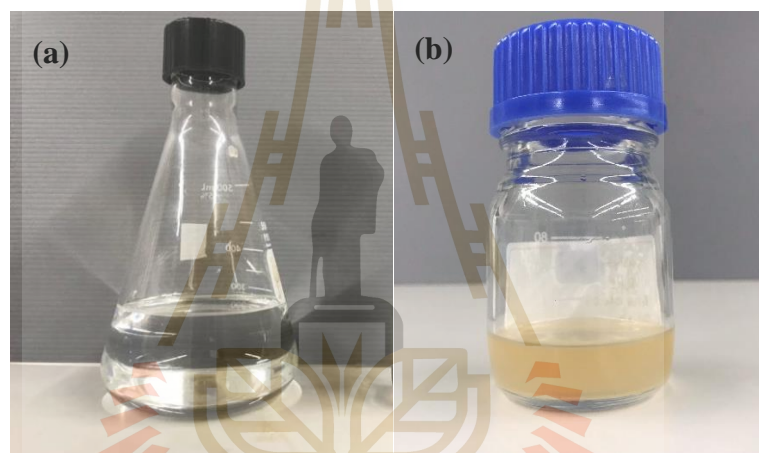


Figure 4.9 Example of distillate (a) and residue (b) product



Figure 4.10 Fresh (a) and used (b) aluminum alginate catalyst

Maximum conversion of lactic acid and yield of *n*-butyl lactate achieved at about 88.09% and 87.44%, respectively under operating pressure of 255 mbar at T_{reboiler} of 90°C using reflux ratio of 1 with feed flow rate of 1 ml/min and 3 g of catalyst loading. It should be noted that the temperature of reaction zone is about 83°C, which is closed to the studied reaction temperature of the same reaction in Chapter II as well as the obtained conversion is similar range.

4.5.2 Hydrolysis in Batch Reactive Distillation Column

Hydrolysis of *n*-butyl lactate using Amberlyst-15 as a solid catalyst was studied in reactive distillation in this work, the reaction is involved;



In hydrolysis process, the feed was prepared by mixing *n*-butyl lactate and deionized water at an equal concentration of *n*-butyl lactate in distillate product of esterification process, which is about 17% by weight. Initial molar ratio of water to *n*-butyl lactate in feed solution is about 40:1. The effect of operating pressure, catalyst loading, feed flow rate and reflux ratio were studied on performance of process using constant T_{reboiler} at 90°C. Performance of hydrolysis was determined in terms of conversion of *n*-butyl lactate and yield of lactic acid as follows;

$$\% X_{\text{BuLA}} = \frac{\text{Mole of BuLA in feed} - \text{Mole of unreacted BuLA in outing}}{\text{Mole of BuLA in feed}} \times 100 \quad (4.5)$$

$$\% Y_{\text{LA}} = \frac{\text{Actual mass of LA in residue product}}{\text{Theoretical mass of LA in hydrolysis}} \times 100 \quad (4.6)$$

In addition, the purity (%*P*) of lactic acid is considered and determined using mass fraction of lactic acid in residue product as;

$$\%P_{LA} = \text{Mass fraction of lactic acid in residue product} \times 100 \quad (4.7)$$

Similar to esterification, the distillate product separated into two phases, unreacted water (heavy phase) was returned into reaction zone for driving forward reaction of hydrolysis and the lactic acid product was collected in the residue product. The experimental data of hydrolysis in producing lactic acid is showed in Table 4.3.

According to the hydrolysis of *n*-butyl lactate using Amberlyst-15 as a solid catalyst, this reaction provided higher activation energy of forward reaction than backward reaction (Dassy et al., 1994). It means that forward reaction is slowly reaction rate than backward reaction. Therefore, reaction time is necessary for this reaction. As the results shown in Table 4.3, conversions of *n*-butyl lactate obtained from semi-batch reactive distillation in this work were found to be in the range of 11.67 to 50.86%, which is seem lower than the value reported by Sun et al. (2006), which is studied hydrolysis of *n*-butyl lactate in batch reactive distillation. Based on studied operating parameters in this work, it might be affected reaction time, which is the reactants have a short time to react in the reaction zone. So, low conversions were obtained. The effect of operating parameters represented and discussed in Figure 4.12-4.15 for effect operating pressure, of reflux ratio, catalyst loading, and feed flow rate, respectively.

Table 4.3 Experimental data for hydrolysis of *n*-butyl lactate using Amberlyst-15 as a solid catalyst in reactive distillation column

Parameters	RUN-1	RUN-2	RUN-3	RUN-4	RUN-5	RUN-6	RUN-7	RUN-8	RUN-9	RUN-10	RUN-11
T_{Liquid at middle}(°C)	83	83	84	84	90	90	90	90	82	83	84
Pressure (mbar)	255	319	319	319	445	445	445	445	319	319	319
Feed flow rate (ml/min)	1.0	1.0	1.0	1.0	1.0	0.5	1.0	2.0	1.0	1.0	1.0
Catalyst (g)	3.00	3.00	4.30	3.00	4.30	4.30	3.00	3.00	4.30	4.30	1.50
Reflux ratio	0.50	0.50	0.50	1.00	0.50	0.50	0.50	0.50	1.00	2.00	1.00
Mass of feed (g)	301.03	301.07	300.64	300.51	301.05	301.73	300.19	300.69	300.42	300.63	300.39
Mass fraction of feed											
lactic acid	0.0000	0.0000	0.0000	0.0000	0.0000	0.0000	0.0000	0.0000	0.0000	0.0000	0.0000
1-butanol	0.0000	0.0000	0.0000	0.0000	0.0000	0.0000	0.0000	0.0000	0.0000	0.0000	0.0000
<i>n</i> -butyl lactate	0.1685	0.1670	0.1671	0.1665	0.1666	0.1696	0.1669	0.1679	0.1666	0.1668	0.1666
water	0.8315	0.8330	0.8329	0.8335	0.8334	0.8304	0.8331	0.8321	0.8334	0.8332	0.8334
Mass of distilled (g)	288.33	285.77	284.78	283.27	244.71	259.86	254.12	273.11	263.30	273.31	279.42
Mass fraction of distillate											
lactic acid	0.0119	0.0160	0.0249	0.0269	0.0038	0.0018	0.0157	0.0224	0.0227	0.0317	0.0069
1-butanol	0.0101	0.0309	0.0278	0.0283	0.0411	0.0400	0.0521	0.0173	0.0396	0.0412	0.0212
<i>n</i> -butyl lactate	0.1554	0.1106	0.1043	0.1181	0.1095	0.0790	0.0720	0.1500	0.1135	0.0971	0.1377
water	0.8226	0.8425	0.8430	0.8266	0.8456	0.8791	0.8602	0.8103	0.8241	0.8301	0.8342
Mass of residue (g)	0.00	9.97	10.68	9.08	49.81	40.72	37.88	17.07	11.48	10.48	6.41
Mass fraction of residue											
lactic acid	0.0000	0.9782	0.9853	0.7478	0.1910	0.3671	0.2979	0.0112	0.8224	0.6220	0.7422
1-butanol	0.0000	0.0051	0.0001	0.0002	0.0193	0.0198	0.0025	0.0033	0.0009	0.0005	0.0004
<i>n</i> -butyl lactate	0.0000	0.0098	0.0006	0.0014	0.0640	0.1136	0.2255	0.0453	0.0064	0.0059	0.0003
water	0.0000	0.0069	0.0139	0.2506	0.7257	0.4995	0.4741	0.9402	0.1703	0.3716	0.2571
%<i>X</i>_{BuLA}	11.67	36.93	40.85	33.14	40.23	50.86	46.45	17.32	40.13	46.97	23.09
%<i>Y</i>_{LA}	0.00	31.46	33.98	22.01	30.78	47.39	36.55	0.61	30.61	21.09	17.11
%<i>P</i>_{LA}	-	97.82	98.53	74.78	19.10	36.71	29.79	1.12	82.24	62.20	74.22

By considering either conversion of *n*-butyl lactate as well as yield and purity of lactic acid under operating condition in this work, the experiment at feed flow rate of 1 ml/min using 4.3 g of catalyst loading with reflux ratio of 0.5 under pressure of 319 mbar seem reasonable in consideration values of 40.85%, 33.98% and 98.53% for conversion, yield and purity, respectively. The residue containing lactic acid obtained from hydrolysis is showed in Figure 4.11.



Figure 4.11 Residue lactic acid product obtained from hydrolysis at pressure of 319 mbar, T_{reboiler} of 90°C, feed flow rate of 1 ml/min, reflux ratio of 0.5 and 4.3 g of catalyst loading.

4.5.2.1 Effect of Operating Pressure

As mentioned in the esterification part, temperature and pressure have strong effect on significantly reaction and separation operation. There are several researchers using operating pressure for hydrolysis in reactive distillation column at atmospheric pressure, which focus to study the conversion of reaction. However, this

work needs to consider the purity of lactic acid so, the operating pressure was studied as the results shown in Figure 4.12.

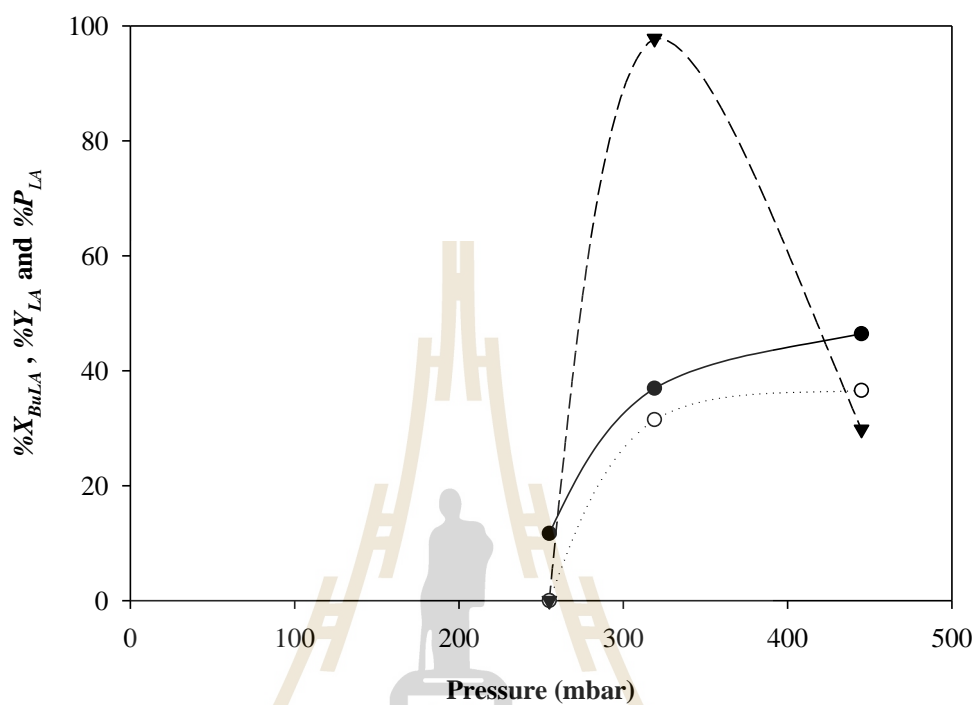


Figure 4.12 Effect of operating pressure on conversion of *n*-butyl lactate (—●—), yield (··○··) and purity (—▼—) of lactic acid in residue product for hydrolysis of *n*-butyl lactate in reactive distillation column at T_{reboiler} of 90°C with reflux ratio of 0.5 and feed flow rate of 1 ml/min using 3 g of catalyst loading

The operating pressure for hydrolysis was varied from 255 to 445 mbar. It was found that when using the pressure at 255 mbar, the conversion of *n*-butyl lactate is very low, as well as purity of lactic acid in residue equal to zero. Due to this reaction, *n*-butyl lactate and water are the reactants, which operating pressure of 255 mbar at T_{reboiler} of 90°C might be enhanced evaporation rate of reactants. So, the

reactants may be evaporated suddenly and may have a short reaction time, resulting in low conversion. In addition, it was observed flooding in rectifying zone during the experiment. Flooding is brought about by excessive vapor flow, causing liquid to be entrained in the vapor up the column. It does not have the residue product at the bottom due to all components evaporated to vapor under this pressure and a small amount of lactic acid occurred in the system may be pushed up to distillate product due to flooding.

When using high operating pressure, the results showed that the conversion and yield increased via operating pressure increased from 319 to 445 mbar while the purity of lactic acid decreased. It can be explained that at these pressures, the reactants have the time to react and 1-butanol can be removed from the reaction zone. Decreasing in concentration of 1-butanol resulted in an increase in conversion as well as yield by driving forward reaction of hydrolysis. However, the purity of lactic acid decreased with increasing pressure to 445 mbar, due to decreasing distillation efficiency.

4.5.2.2 Effect of Reflux Ratio

For the hydrolysis of *n*-butyl lactate in the reactive distillation column, effect of reflux ratio was investigated over the range of 0.5 to 2 at the same other operating parameters as the results shown in Figure 4.13. It was found that the conversion of *n*-butyl lactate increased with increasing reflux ratio while yield and purity of lactic acid in residue decreased. The increase in conversion can be explained the same with the esterification part as it enhanced to increase amount of water returned to the reaction zone, which can future react with *n*-butyl lactate, resulting in shifts forward reaction of hydrolysis. However, when the reflux ratio over 0.5, liquid flooding

occurred during the experiment affected decreased yield and purity due to its reduced separation efficiency.

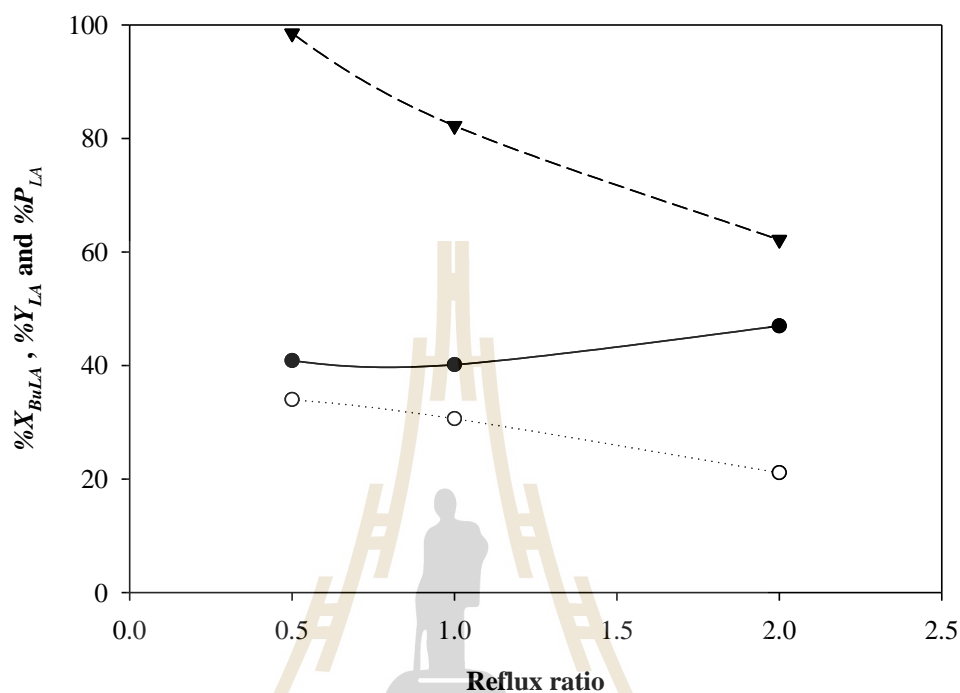


Figure 4.13 Effect of reflux ratio on conversion of *n*-butyl lactate (—●—), yield (···○···) and purity (—▼—) of lactic acid in residue product for hydrolysis of *n*-butyl lactate in reactive distillation column at T_{reboiler} of 90°C under pressure of 319 mbar with feed flow rate of 1 ml/min using 4.3 g of catalyst loading

4.5.2.3 Effect of Catalyst Loading

Amberlyst-15 was used to catalyze the hydrolysis of *n*-butyl lactate in reactive distillation. The effect of catalyst loading was studied in the range of 1.5 to 4.3 g as the results shown in Figure 4.14. An increase in catalyst loading was found to be a significant effect in increasing conversion and yield. As mentioned before,

this reaction is a slow reaction rate so, increasing catalyst loading gives a higher active site to accelerate the rate of the reaction. This work, a further increase in catalyst loading is not recommended, as the height of column is limit for each zone.

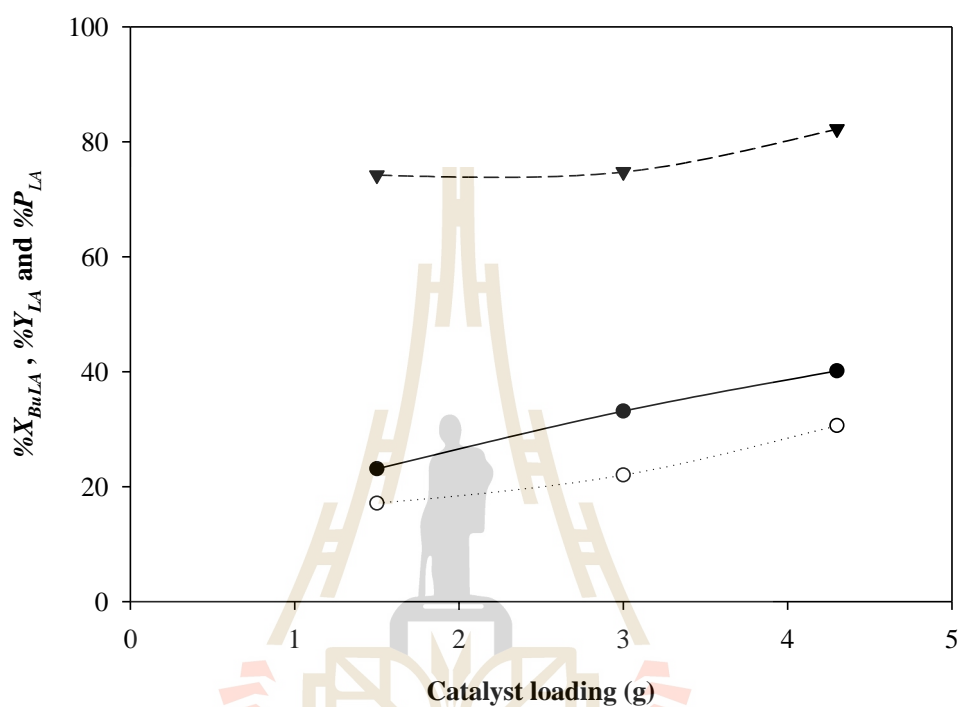


Figure 4.14 Effect of catalyst loading on conversion of *n*-butyl lactate (—●—), yield (⋯○⋯) and purity (—▼—) of lactic acid in residue product for hydrolysis of *n*-butyl lactate in reactive distillation column at T_{reboiler} of 90°C under pressure of 319 mbar with reflux ratio of 1 and feed flow rate of 1 ml/min

4.5.2.4 Effect of Feed Flow Rate

The effect of feed flow rate was investigated in the range of 0.5 to 2 ml/min. The results presented in Figure 4.15. With an increase in feed flow rate, the rate of removal lactic acid per mole of *n*-butyl lactate that comes through the feed

decreases, resulting in shift backward reaction hence a lower conversion of *n*-butyl lactate and yield of lactic acid. In addition, the flooding was observed when increasing the feed flow rate, due to high amount of water vapor, resulting in lower purity.

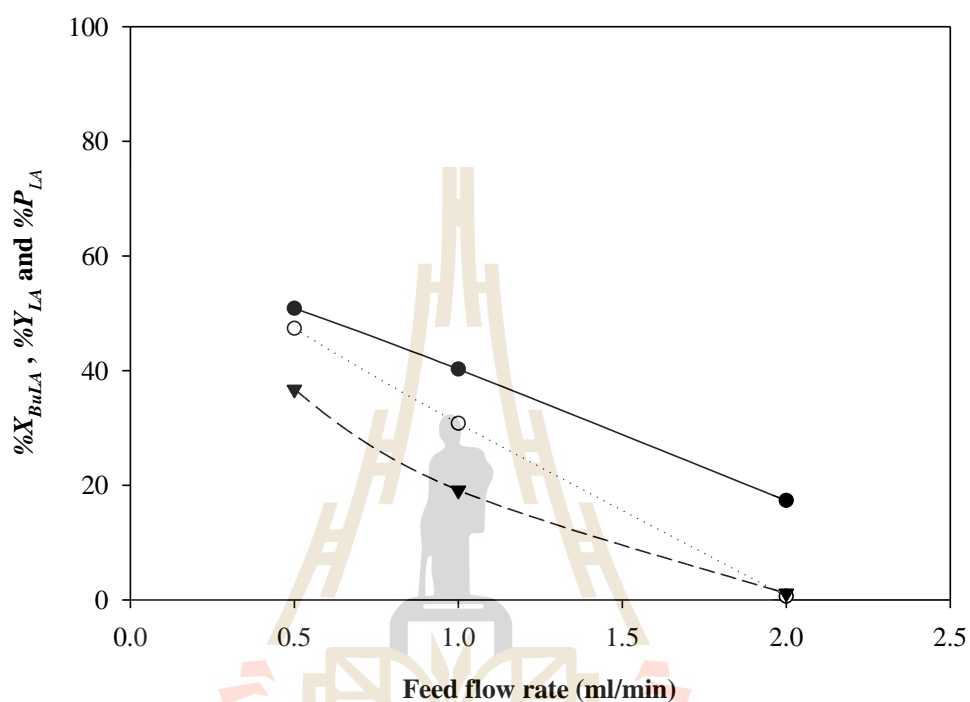


Figure 4.15 Effect of feed flow rate on conversion of *n*-butyl lactate (—●—), yield (···○···) and purity (—▼—) of lactic acid in residue product for hydrolysis of *n*-butyl lactate in reactive distillation column at T_{reboiler} of 90°C under pressure of 445 mbar with reflux ratio of 0.5 using 4.3 g of catalyst loading

4.6 Conclusion

In this work, esterification of lactic acid with 1-butanol followed by hydrolysis of *n*-butyl lactate was studied using a reactive distillation column. The extracted phase obtained from extraction part (Chapter II) was used as a single feed for esterification. Aluminum alginate and Amberlyst-15 were used as a solid catalyst for esterification and hydrolysis, respectively. Effect of operating parameters such as reflux ratio, feed flow rate, catalyst loading, and operating pressure were investigated at constant T_{reboiler} of 90°C. For esterification process under constant operating pressure 255 mbar, The results showed conversion and yield has significant increase with increasing reflux ratio and were insensitive to change in catalyst loading due to reaction is reasonably fast. While increasing the feed flow rate affects conversion and yield decreased. Maximum conversion and yield of *n*-butyl lactate obtained from esterification achieved at 88.09% and 87.44%, respectively under operating pressure of 255 mbar using reflux ratio of 1 with feed flow rate of 1 ml/min and 3 g of catalyst loading.

For hydrolysis process, the effect of reflux ratio and feed flow rate on conversion were the same with esterification. However, conversion and yield were found to be increased via increasing catalyst loading. In addition, purity of lactic acid in residue obtained from hydrolysis was considered. It was found that an increase in pressure, feed flow rate and reflux ratio strongly affected to decrease purity of lactic acid. By consideration of conversion, yield and purity, these values reasonably achieved at 40.85%, 33.98% and 98.53%, respectively under operating pressure of 319 mbar using reflux ratio of 0.5 with feed flow rate of 1 ml/min and 4.3 g of catalyst loading.

4.7 References

- Asthana, N. S., Kolah, A. K., Vu, D. T., Lira, C. T., and Miller, D. J. 2006. A Kinetic Model for the Esterification of Lactic Acid and Its Oligomers. **Industrial & Engineering Chemistry Research** 45:5251-5257.
- Baur, R. 2000. **Modeling Reactive Distillation Dynamics**, Department of Chemical Engineering, Clarkson University.
- Dassy, S., Wiame, H., and Thyron, F. C. 1994. Kinetics of the Liquid Phase Synthesis and Hydrolysis of Butyl Lactate Catalysed by Cation Exchange Resin. **J. Chem. Technol. Biotechnol.** 59:149.
- Hiwale, R. S., Bhate, N. V., Mahajan, Y. S., and Mahajani, S. M. 2004. Industrial Applications of Reactive Distillation: Recent Trends. **International Journal of Chemical Reactor Engineering** 2 (1).
- Komesu, A., Martinez, P. F. M., Lunelli, B. H., Filho, R. M., and Maciel, M. R. W. 2015. Lactic acid purification by reactive distillation system using design of experiments. **Chemical Engineering and Processing: Process Intensification** 95:26-30.
- Kulprathipanja, S. 2002. **Reactive separation processes**. New York, NY: Taylor & Francis.
- Kumar, R., and Mahajani, S. M. 2007. Esterification of Lactic Acid with n-Butanol by Reactive Distillation. **Industrial & Engineering Chemistry** 46:6873-6882.
- Kumar, R., Mahajani, S. M., Nanavati, H., and Noronha, S. B. 2006a. Recovery of lactic acid by batch reactive distillation. **Journal of Chemical Technology & Biotechnology** 81 (7):1141-1150.

- Kumar, R., Nanavati, H., Noronha, S. B., and Mahajani, S. M. 2006b. A continuous process for the recovery of lactic acid by reactive distillation. **Journal of Chemical Technology & Biotechnology** 81 (11):1767-1777.
- Mahajan, Y. S., Shah, A. K., Kamath, R. S., Salve, N. B., and Mahajani, S. M. 2008. Recovery of trifluoroacetic acid from dilute aqueous solutions by reactive distillation. **Separation and Purification Technology** 59 (1):58-66.
- Seo, Y., Hong, W. H., and Hong, T. H. 1999. Effects of operation variables on the recovery of lactic acid in a batch distillation process with chemical reactions. **Korean Journal of Chemical Engineering** 16 (5):556-561.
- Su, C.-Y., Yu, C.-C., Chien, I. L., and Ward, J. D. 2013. Plant-Wide Economic Comparison of Lactic Acid Recovery Processes by Reactive Distillation with Different Alcohols. **Industrial & Engineering Chemistry Research** 52 (32):11070-11083.
- Sun, X., Wang, Q., Zhao, W., Ma, H., and Sakata, K. 2006. Extraction and purification of lactic acid from fermentation broth by esterification and hydrolysis method. **Separation and Purification Technology** 49 (1):43-48.
- Troupe, R. A., and DiMilla, E. 1957. Kinetics of the Ethyl Alcohol—Lactic Acid Reaction. **Industrial & Engineering Chemistry** 49 (5):847-855.

CHAPTER V

TECHNO-ECONOMIC ANALYSIS OF A COMBINED EXTRACTION AND REACTIVE DISTILLATION FOR LACTIC ACID PRODUCTION

5.1 Abstract

Techno-economic analysis of a combined counter-current extraction and reactive distillation for recovery and purification of lactic acid from fermentation broth was performed at an annual capacity of 10,000 tons/year lactic acid product. Process simulation and optimization was performed using Aspen HYSYS V10 by gathering the technical data from laboratory scale. Sizing of unit operations, utilities and equipment costs were acquired from the simulation. The designed process consisted of cell removal, extraction, esterification, and hydrolysis in reactive distillation and purified by distillation. It was found that high process efficiency is obtained when recycling of 1-butanol to use in the process, which maximum overall recovery of lactic acid from the fermentation broth of 96.57% was achieved at purity of 99.99% w/w. The production cost resulted to be 0.90 USD/kg of 99.99% lactic acid. The proposed process reveals that the operating cost could be reduced further by using cheaper fermentation broth cost.

5.2 Introduction

In recent years, biodegradable polylactic acid (PLA) polymer is recent increasing used as a raw material in packaging as well as fiber and foam instead of petrochemical raw materials. The growth of PLA market is the key driver in increasing demand of lactic acid, which is the global lactic acid market is poised to reach USD 8.77 billion by 2025, rising at a CAGR of 18.7% during the forecast period (*Lactic Acid Market Size 2019*). The possibility of manufacturing a biodegradable polylactic acid (PLA) polymer has led to extensive research in recovery of lactic acid produced by fermentation, by different downstream processing routes. However, at industrial scale, recovery and purification of lactic acid from fermentation broth is challenging technology because the broth always contains many impurities including cell, proteins, and unconsumed nutrients.

Comparative assessment of downstream processing options for lactic acid was reported by (Joglekar et al., 2006). The data available and reported in this literature found that expanded bed ion exchange adsorption technology will be highest cost as it involves elution and regeneration of ion exchange. Combined precipitation and reactive distillation with esterification and hydrolysis processes were reported that it is the most economical. However, it generates a large quantity of gypsum, which needs to be disposed of. Among the other processes, using combined adsorption and reactive distillation process has lower investment but higher operating cost. The combined microfiltration and electrodialysis has higher investment and higher product cost, while the combined reactive extraction and reactive distillation has slight high raw material cost, due to the specific reactive solvent in extraction. González et al. (2007) studied economic evaluation of an integrated process for lactic acid production through many

steps; ultrafiltration, ion exchange, reverse osmosis and final concentration by vacuum evaporation. The proposed process was demonstrated to be economically viable. The annual cost resulted to be 1.25 USD/kg for 50% (w/w) lactic acid. (Sikder et al., 2012) proposed production of lactic acid from sugarcane juice using membrane integrated bioreactor with total product cost at 3.15 USD/kg of 89% (w/w). Each process provided the specific function and limited in some specifications such as the purity or yield of lactic acid product, cost spending, energy consumptions as well as remained waste. Therefore, the process design has many unit operations to achieve desired specification of product. Moreover, the combined processes for lactic acid recovery should consider in simple conditions, high performance, suitable cost efficiency, and low environmental impact as well as able to employ in variety lactic acid obtained from different fermentation raw materials.

Liquid-liquid extraction has been one of an alternative technique for lactic acid recovery and has been studied by several researchers. As extraction is not energy-intensive as evaporation or distillation, its advantage is suitability for large capacity processing with low energy consumption. Recently, Chawong et al. (2011) (Chawong and Rattanaphanee, 2011) studied the extraction of lactic acid from aqueous solution using 1-butanol. It was found that using 1-butanol as a single solvent was significantly on extraction efficiency. This result was similar to the counter-current extraction of lactic acid with 1-butanol using packed liquid-liquid extraction obtained in this work as detailed in Chapter II. However, the lactic acid product obtained from the extraction process was found to be low purity. Therefore, the purification of lactic acid after the extraction process is considered as a future problem because lactic acid has a high normal boiling point and affinity for water, and its oligomerization can also occur at

moderate temperatures (Su et al., 2015). These factors make a purification by distillation difficultly. Hence, various purification processes have been investigated.

Reactive distillation has a considerable attention process for purification of lactic acid. This process contains esterification and hydrolysis reactions. The lactic acid is reacted with an alcohol to form a lower boiling ester which can be separated from heavy impurities and the ester is hydrolyzed to recover pure lactic acid. Purification of lactic acid by reactive distillation was investigated by several researchers (Kumar et al., 2006b; Kumar et al., 2006a; Komesu et al., 2015; Su et al., 2013). Su et al. (2013) studied purification of lactic acid by reactive distillation and compared process using different alcohols (methanol, ethanol, propanol, butanol, and pentanol). The results indicated that methanol and butanol were the most economically attractive. The advantage of methanol is inexpensive. It does not form an azeotrope with water and forms the lowest-boiling ester, while butanol induces a liquid-liquid separated phase that can be exploited to reduce separation costs. In addition, using reactive distillation for recovery and purification of lactic acid from extracted product obtained from the extraction process has been proven to be feasible process as described in previous Chapter. Among the processes mentioned above, the extraction and reactive distillation can potentially combine the unit operations to enhance effectiveness in the production of lactic acid. Therefore, this work aims to propose the combination of both processes for recovery and purification of lactic acid and focus is given on the developments of recovery of lactic acid from fermentation broth based on the efficient and economical. The processes were simulated in Aspen HYSYS V10 by gathering the optimized data from laboratory scale and sizing of unit operations, chemicals and utility and estimation of capital and operating costs were acquired from the simulation.

5.3 Theory

5.3.1 Capital Cost

Total capital investment (TCI) of an industrial plant includes purchase of the land, building, offsite, supporting facilities, utilities installation, market research, licensing, and contractor's fee. Total capital investment cost is divided into 2 categories, there are 2 fixed-capital investment (FCI) and working capital (WC). The fixed capital investment is the capital needed to supply the necessary manufacturing and plant facilities. While working capital cost is the capital needed to operate the plant until company gets income (Peters and Timmerhaus, 1991). The equation for calculating Total capital investment (TCI) is:

$$TCI = \text{Fixed - capital investment (FCI)} + \text{Working capital (WC)} \quad (5.1)$$

5.3.2 Fixed-Capital Investment

Fixed capital investment is all cost that is needed to build the plant, office, and its supporting equipment. The fixed capital can be divided into direct cost and indirect cost. The direct cost refers to manufacturing fixed-capital investment, which represents the capital necessary for the installed process equipment with all auxiliaries that are needed for complete process operation. Expenses for piping, instruments, insulation, foundations, and site preparation are typical examples of costs included in the manufacturing fixed-capital investment. The indirect cost refers to nonmanufacturing fixed-capital investment, which is the Fixed capital required for construction overhead and for all plant components that are not directly related to the process operation. These plant components include the land, processing buildings, administrative, and other offices, warehouses, laboratories, transportation, shipping,

and receiving facilities, utility and waste-disposal facilities, shops, and other permanent parts of the plant. The construction overhead cost consists of field-office and supervision expenses, home-office expenses, engineering expenses, miscellaneous construction costs, contractor's fees, and contingencies. In some cases, construction overhead is proportioned between manufacturing and nonmanufacturing fixed-capital investment.

5.3.3 Working Capital

Working capital is the fee paid in the first of the production process before the company earns revenue from product sales. The working capital for an industrial plant consists of the total amount of money invested in

- (1) Raw materials and supplies carried in stock.
- (2) Finished products in stock and semi-finished products in the process of being manufactured.
- (3) Accounts receivable.
- (4) Cash kept on hand for monthly payment of operating expenses, such as salaries, wages, and raw-material purchases.
- (5) Accounts payable.
- (6) Taxes payable

The ratio of working capital to total capital investment varies with different companies, but most chemical plants use an initial working capital amounting to 10 to 20% of the total capital investment cost. This percentage may increase to as much as 50% or more for companies producing products of seasonal demand, because of the large inventories which must be maintained for appreciable periods (Peters and Timmerhaus, 1991).

5.3.4 Purchase Equipment Cost

The cost of purchased equipment is the basis of several predesign methods for estimating capital investment. Sources of equipment prices, methods of adjusting equipment prices for capacity, and methods of estimating auxiliary process equipment are therefore essential to the estimator in making reliable cost estimates. There are many ways to estimate the purchasing cost of equipment. The most accurate method for determining process equipment costs is provided by a current price from suppliers. Another alternative is to use the cost data on previously purchased equipment of the same type. However, for conceptual design, simpler approach to estimate equipment capital cost is necessary.

5.3.5 Operating Cost

Operating cost or manufacturing cost is the cost related to day-to-day operation of an industrial plant. An estimate of the operating costs, cost of producing the product, is needed to judge the viability of a project and to make choices between possible alternative processing schemes. These costs can be estimated from the flowsheet, which gives the raw material and service requirements, and the capital cost estimate (Richardson, 2005). The cost of producing a chemical product will include the items and listed in Table 5.1. They are divided into two groups as;

1. Fixed operating costs: costs that do not vary with production rate. These are the bills that have to be paid whatever the quantity produced.
2. Variable operating costs: costs that are dependent on the amount of product produced.

Table 5.1 Example of variable and fixed operating cost (Anderson, 2009)

Variable operating cost	Fixed operating cost
Raw materials	Capital depreciation
Waste treatment	Operation and supervisory labor
Utilities	Plant maintenance
Operating materials	Supplies
Shipping or packing	Laboratory
	Plant overhead

5.3.6 Raw Material Cost

In the chemical industry, one of the major costs in a production operation is for the raw materials involved in the process. The amount of the raw materials which must be supplied per unit of time or per unit of product can be determined from process material balances. In many cases, certain materials act only as an agent of production and maybe recoverable to some extent. Therefore, the cost should be based on the amount of raw materials actually consumed as determined from the overall material balances. Direct price quotations from prospective suppliers are preferable to published market prices. Moreover, some pricing information is collected by many sources such as ICIS Chemical Business (Chemical Market Reporter) and Chemical Market Associates, Inc (Anderson, 2009). Transportation charges should be included in the raw material costs, and these charges should be based on the form in which the raw materials are to be purchased for use in the final plant. Although bulk shipments are cheaper than smaller-container shipments, they require greater storage facilities and inventory. Consequently, the demands to be met in the final plant should be considered when deciding on the cost of raw materials. The ratio of the cost of raw materials to total plant

cost obviously will vary considerably for different types of plants. In chemical plants, raw-material costs are usually in the range of 10 to 50 percent of the total product cost.

5.3.7 Utilities Cost

There are many types of utilities used in the process such as steam, electricity, process and cooling water, compressed air, natural gas, and fuel oil, varies widely depending on the amount of consumption, plant location, and source. The utility used in the process may be purchased at predetermined rates from an outside source, or the service may be available from self-generated within the company.

Steam requirements include the amount consumed in the manufacturing process plus that necessary for auxiliary needs. An allowance for radiation and line losses must also be made. Electrical power must be supplied for lighting, motors, and various process-equipment demands. As a rough approximation, utility costs for ordinary chemical processes amount to 10 to 20 percent of the total product cost.

5.3.8 Production Cost

The annual production cost can be estimated from the various components of the operating costs which are showed in Table 5.1 while the annual production rate can be obtained from the process flow sheet diagram. The production cost of the process can be estimated from the annual production cost divided by the annual production rate of the desired product as expressed in Eq. 5.2.

$$\text{Production cost (USD / kg)} = \frac{\text{Annual production cost (USD / year)}}{\text{Annual production rate (kg / year)}} \quad (5.2)$$

5.4 Process Simulation Description

Proposed process for recovery and purification of lactic acid from fermentation broth using a combined counter-current extraction and reactive distillation mainly consists cell removal, counter-current extraction, reactive distillation, and purified units as process scheme shown in Figure 5.1.

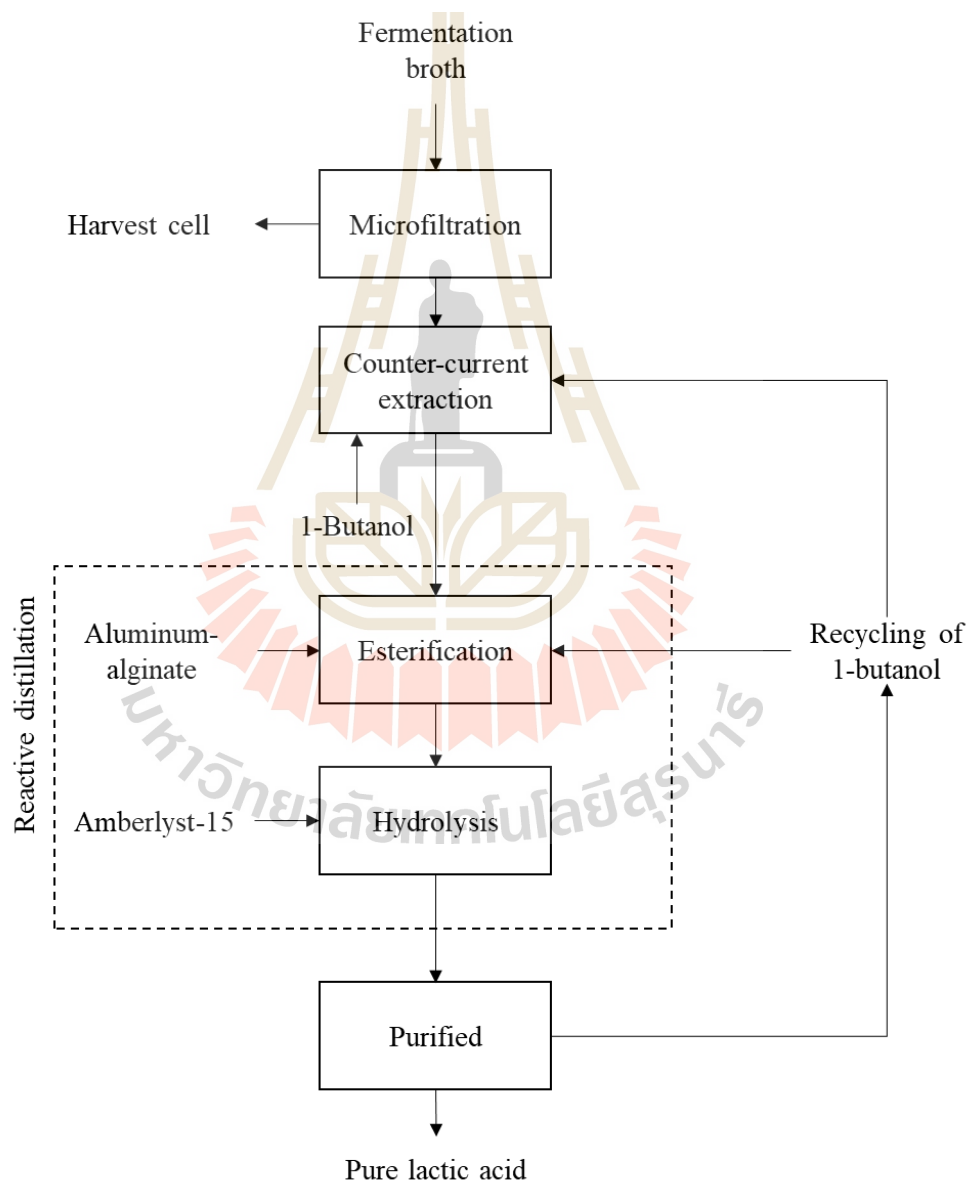


Figure 5.1 Scheme of proposed process for recovery and purification of lactic acid

The operating data of extraction and reactive distillation unit were applied from the previous experimental results performed using laboratory-scale apparatus. The process simulation was evaluated using Aspen HYSYS V10 by gathering the optimized data from laboratory scale.

5.4.1 Phase Equilibrium and Kinetic Modeling

In order to simulation of extraction and reactive distillation process, phase equilibrium and reaction kinetic data are needed. In Chapter III, UNIFAC model was used to determine activity coefficient (a) in liquid phase by considering water, 1-butanol, lactic acid and *n*-butyl lactate system. In this work, fermentation broth contains protein, which is a polymer of amino acid. So, the UNIFAC might be not suitable, due to its limitation for polymer system (Lohmann et al., 2001). To account for nonideal liquid-liquid equilibrium (LLE) and vapor-liquid equilibrium (VLE) in this work, UNIQUAC model is used to calculate activity coefficients in the liquid phase. There is a special form of UNIQUAC for system containing alcohol, where a third surface parameter can increase significantly the accuracy (Dimian, 2003). In addition, the UNIQUAC model uses only binary interaction parameters, which makes the model simpler to use for multicomponent mixtures and enough for accurate simulation. The Aspen built-in association parameters are used to compute binary interaction parameters.

For the reactive distillation process, the reaction rate expressions of esterification and hydrolysis are assumed Pseudo-homogeneous and are expressed in terms of activity as shown in Eq. (5.3)

$$-r_{LA} = \frac{n_{LA_0}}{w_{cat}} \frac{dX_{LA}}{dt} = k_f a_{LA} a_{BuOH} - k_r a_{BuLA} a_W \quad (5.3)$$

in which $-r_{LA}$ is reaction rate ($\text{kgmole}\cdot\text{kg}_{\text{cat}}^{-1}\cdot\text{s}^{-1}$) and w_{cat} is amount of catalyst (kg). k_f and k_r are reaction rate constant ($\text{kgmole}\cdot\text{kg}_{\text{cat}}^{-1}\cdot\text{s}^{-1}$) of forward and backward reaction, respectively. In this study, the kinetic parameters of esterification of lactic acid using aluminum alginate as a solid catalyst was obtained from Chapter III. The reaction rate constant for forward (k_f) and backward (k_r) reaction are expressed using Arrhenius equation (as detailed in Eq. 3.4) with function of reaction temperature as shown in Eq. (5.4) and (5.5), respectively.

$$k_f = 1.06 \times 10^6 \exp\left(-\frac{61799.32}{RT}\right) \quad (5.4)$$

$$k_r = 1.86 \times 10^2 \exp\left(-\frac{39108.04}{RT}\right) \quad (5.5)$$

The kinetic parameters for hydrolysis using Amberlyst-15 as a solid catalyst was obtained from (Kumar and Mahajani, 2007) as k_f and k_r are expressed in Eq. (5.6) and (5.7).

$$k_f = 2.59 \times 10^4 \exp\left(-\frac{53400}{RT}\right) \quad (5.6)$$

$$k_r = 3.80 \times 10^3 \exp\left(-\frac{52240}{RT}\right) \quad (5.7)$$

where R is universal gas constant ($\text{kJ}\cdot\text{kgmole}^{-1}\cdot\text{K}^{-1}$) and T is temperature (K).

5.4.2 Fermentation Broth and Cell Removal

The compositions of fermentation broth using in this work reported by (Boontawan et al., 2019), which is fermented lactic acid from cassava pulp. Summarized compositions of fermentation broth are represented in Table 5.2.

Table 5.2 The compositions of fermentation broth

Components	(Boontawan et al., 2019)	This work
Cell (g/L)	2.75	2.75
Protein (g/L)	2.49	2.49
Glucose (g/L)	8.05	8.05
Na ⁺ (ppm)	34.53	<i>n/a</i>
NH ⁴⁺ (ppm)	159.23	<i>n/a</i>
Mn ²⁺ (ppm)	31.10	<i>n/a</i>
Fe ²⁺ (ppm)	2.42	<i>n/a</i>
SO ₄ ²⁻ (ppm)	454.24	<i>n/a</i>
PO ₄ ³⁻ (ppm)	1909	<i>n/a</i>
Lactic acid (g/L)	136.4	136.4

In this work, Aspen HYSYS V10 cannot use electrolyte package properties due to limiting of purchased license. According to data in Table 5.1, it can be seen that fermentation broth contained with slightly amount of salts ions. There is the research has been reported the extraction of lactic acid from electrolyte system. Chawong et al. (2015) reported that the presence of salts enhanced increasing extraction efficiency of lactic acid and after extraction, the salts ions do not extract from aqueous to 1-butanol phase. So, this work will be assumed negligible salts ions in fermentation broth. Hence, the fermentation broth using in process simulation mainly contained cell, protein, glucose and lactic acid only, which is dextrose and lysine is used as the representative

glucose and protein, respectively in process simulation. The harvest cell was removed from fermentation broth by microfiltration, which some heavier impurities as protein and glucose can also remove with the same unit.

5.4.3 Extraction

In the extraction unit, the fermentation broth was fed to counter-current packed extraction column using 1-butanol as an extracting solvent. The lactic acid was extracted to 1-butanol phase while other heavier impurities were remains in rich aqueous phase. The variables such as temperature, pressure and feed flow rate were preliminary evaluated by gathering the optimized data from laboratory scale as mention in Chapter II. Design variables are feed tray and total tray number.

5.4.4 Esterification and Hydrolysis

In esterification unit, an extract product obtained from extraction unit containing lactic acid and 1-butanol was fed to esterification column. The lactic acid is reacted to *n*-butyl lactate and water, which is more separated from heavier impurities. In hydrolysis unit, the *n*-butyl lactate and water obtained from esterification were mixed and fed to hydrolysis column. The *n*-butyl lactate is hydrolyzed back into lactic acid and 1-butanol. In both units, the variables are pressure, temperature and reflux ratio were preliminary evaluated by gathering the optimized data from laboratory scale. Design variables are feed tray and total tray number.

5.4.5 Purification Unit

In this unit, the lactic acid obtained from reactive distillation was purified by separating 1-butanol to increase purity of lactic acid. 1-butanol was separated from lactic acid product to recycle it back to the extraction and esterification.

The design variables are pressure, temperature, reflux ratio, feed tray and total tray number.

5.4.6 Economic Analysis

The cost evaluation in the production of lactic acid process simulation in this work was investigated by assuming batchwise operation with an annual capacity of 10,000 ton/year lactic acid product. A basis operating time of 330 days per year (7920 h) was used in the evaluation. Cost of fermentation broth was estimated based on the capacity of 5 L. Since the information about composition of culture media was absented, Himedia MRS broth formula was assumed to be the culture media in fermentation as shown in Table 5.3. Amount of raw materials using in production of 5L fermentation broth were assumed based on fermentation of lactic acid by Boontawan et al. (2019) as shown in Table 5.4.

Table 5.3 MRS Culture media compositions from Himedia

Compositions	Amount (g/L)
Proteose peptone	10
HM peptone B	10
Yeast extract	5
Dextrose (Glucose)	20
Polysorbate 80 (Tween 80)	1
Ammonium citrate	2
Sodium acetate	5
Magnesium sulphate	0.1
Manganese sulphate	0.05
Dipotassium Hydrogen phosphate	2
Total	55.15

Table 5.4 Raw materials for production of 5 L fermentation broth

Compositions	Amount
Cassava (kg)	1
MRS Culture media (g)	2.7575
Glucoamylase Enzyme (g)	5
Calcium carbonate (g)	0.25
Water RO (L)	3
Approximately broth (L)	5

Table 5.5 Calculation of investment cost, including installation and instrumentation

Item	Cost
<i>Direct costs</i>	
(1) Equipment	From Aspen HYSYS
(2) Total install equipment	Sum of (1)
(3) Piping	12% of (2)
(4) Electrical	5% of (2)
(5) Instrumentation	6% of (2)
(6) Building	10% of (2)
(7) Land and yard improvement	3% of (2)
(8) Total direct cost	$(2)+(3)+(4)+(5)+(6)+(7)$
<i>Indirect costs</i>	
(9) Engineering and supervisor	12% of (8)
(10) Contractor's fee	4% of (8)
(11) Contingency	8% of (8)
(12) Fixed-capital investment (FCI)	$(8)+(9)+(10)+(11)$
(13) Working capital	12% of (12)
Total capital investment (TCI)	$(12)+(13)$

Table 5.6 Calculation of operating cost

Item	Cost per year
<i>Operating costs</i>	
(1) Raw material	(1)
(2) Catalyst	(2)
(3) Utilities	From Aspen HYSYS
(4) Labor	From Aspen HYSYS
(5) Maintenance	5% of FCI
(6) Operating supplies	2% of FCI
(7) Plant overhead	50% of (4)
<i>Fixed charge</i>	
(8) Depreciation	17% of FCI
(9) Insurance	0.08% of FCI
(10) General and administrative expense	3.5% of sum (1) to (7)
(11) Annual production cost	Sum of (1) to (10)
Production cost (cost/kg)	(11)/annual capacity

The raw material and chemical prices were obtained from quotations from suppliers. The compositions data from Table 5.3 and 5.4 were used to calculate fermentation broth cost, which is approximately equal to 0.0402 USD/L as detail in Appendix C.

In this work, the step for calculation of total capital investment, operating cost, as well as production cost can be summarized in Table 5.5 and 5.6 by following Sikder et al. (2012). The purchased and installation costs for the major equipment and the operating cost including utilities and labor were estimated by Aspen Process Economic Analyzer (APEA), which is the costing engine module in Aspen HYSYS. This module develops estimates based on a “standard basis file” which includes company-standardized, project-standardized, and the geographic cost basis (US Gulf Coast, Europe, Middle East, UK, and Japan) information.

5.5 Results and Discussion

5.5.1 Process Analysis

Based on the experimental data describing the operating conditions, kinetic model and the performance of the proposed unit operations in the previous Chapter, the lactic acid recovery and purification from fermentation broth were estimated by simulation model. By assuming annual production of 10,000 ton/year with purity of 99.99% w/w lactic acid, the simulation predicted the overall process data and its sizing. Two different processes were considered to compare the efficiency as well as economic valuation as non-recovery (Process A) and recovery of 1-butanol stream (Process B). Process flowsheets are showed in Figures 5.2 and 5.3 for operation of Process A and Process B, respectively.

From the process flowsheet, the fermentation broth was fed to microfilter for removing of cell and was then fed to extraction column using 1-butanol as extract solvent. The products obtained from extraction are extracted product at the top and raffinate at the bottom of column. It was found that after extraction, glucose and protein also transfer to extract product. This might be due to it likely dissolved in 1-butanol, while some amount of these components is in raffinate product and it was drained out. The raffinate is more wastewater from the fermentation broth, which maybe has the treatment process in the future.

The extract product mainly consists 1-butanol, water and lactic acid was fed to esterification column and reacted together to *n*-butyl lactate. The optimal result is that *n*-butyl lactate was collected at the bottom of column with impurities and a separate nonreactive column is used to remove the impurities. After removed the impurities, this stream was then mixed with the top product stream and fed to hydrolysis

column for hydrolyzing back to lactic acid. In the hydrolysis column, because 1-butanol and ester have high boiling point. This means that a higher temperature or lower pressure is required in the column for obtained high purity of lactic acid at the bottom. However, high temperature affects oligomerization and color of lactic acid product as well as the low pressure affect reaction activity. So, the optimal design is using a distillation column for purifying lactic acid, as well as recovery of 1-butanol. For recovery of 1-butanol process, it is straightforward to recover high purity 1-butanol about 96% by mole with a single column.

When compared both processes, the recovery of 1-butanol stream can decrease amount of using its fresh stream achieving to 58.54%. This means that can decrease raw material cost. Efficiency of mainly unit operations as extraction, esterification and hydrolysis were compared as shown in Table 5.7. Process simulation data represented in Table 5.8 and 5.9 and flowsheet design result showed in Figures 5.10 and 5.11, for operation of Process A and Process B, respectively.

Table 5.7 Comparison of efficiency in each unit operation of both processes

Parameters	Process	
	Non-recovery (A)	Recovery (B)
Feed fermentation broth (kgmole/h)	510.63	482.10
BuOH feed to extractor (kgmole/h)	150.47	83.58
BuOH : LA molar ratio in extraction	9.79	5.76
BuOH : LA molar ratio in esterification	9.64	10.67
Water : BuLA molar ratio in hydrolysis	13.38	9.43
%Extraction	99.97	97.99
%Conversion of LA (esterification)	92.39	95.11
%Conversion of BuLA (hydrolysis)	99.61	90.20
Purity of lactic acid (% w/w)	99.99	99.99
%Overall recovery of lactic acid	91.19	96.57

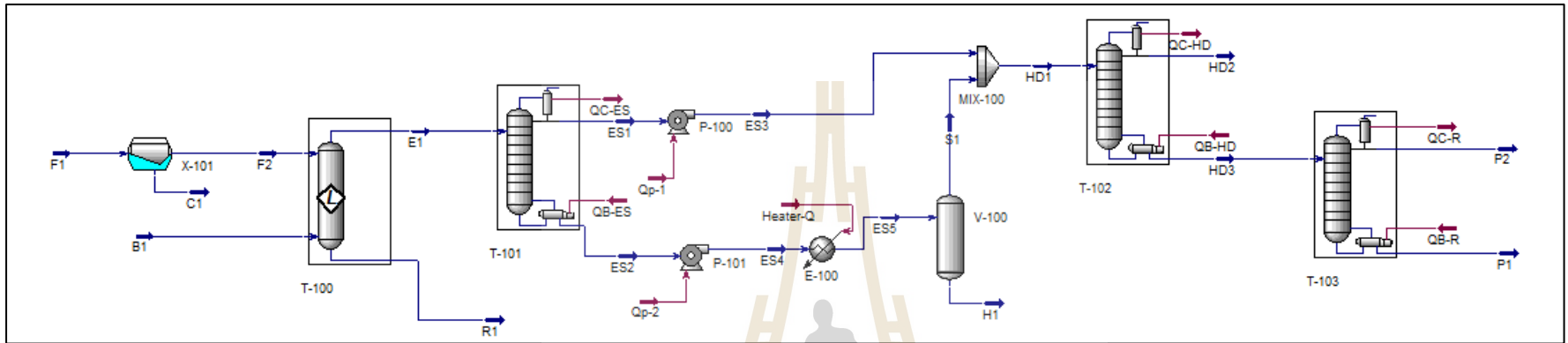


Figure 5.2 Process flowsheet for recovery and purification of lactic acid from fermentation broth with Process A

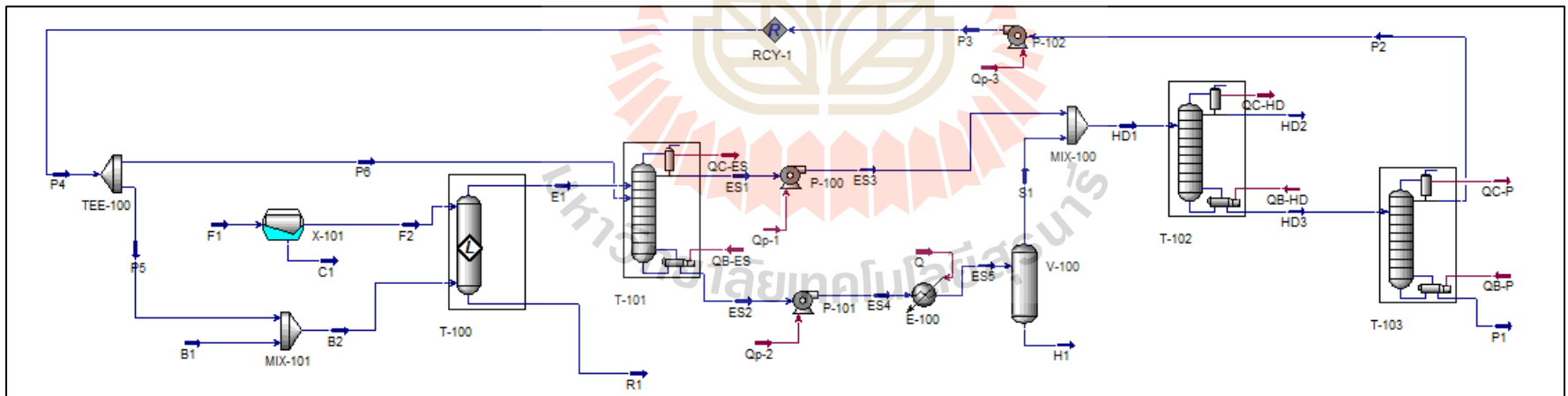


Figure 5.3 Process flowsheet for recovery and purification of lactic acid from fermentation broth with Process B

The optimal results in Table 5.7 showed that Process A needed a higher amount of fermentation broth including initial lactic acid more than Process B, resulting in high amount of 1-butanol required to feed into the extraction column, which is enhanced to increase extraction efficiency at 99.97%. However, it should be noted that high amount of 1-butanol can also affect increasing water transferred from fermentation broth to extracted product due to its partial miscibility. So, it future affects reaction activity in esterification and hydrolysis column. For esterification column, it can be observed that the 1-butanol to lactic acid molar ratio of process A lower than Process B. It is because Process B obtained 1-butanol feed from the extracted product and recovery stream. Hence, higher amount of water and lower 1-butanol to lactic acid molar ratio of Process A might be shift backward reaction in esterification, resulting in lower conversion than Process B.

For hydrolysis column, maximum conversion of Process A achieved to 99.61% while the conversion of 90.20% was obtained in Process B. This might be because Process A has high water to *n*-butyl lactate molar ratio for driving the forward reaction in hydrolysis. In addition, it should be noted that the water which is extracted from fermentation broth reasonable for using in hydrolysis. So, it does not need the water feed from outer source, resulting in economic process. This is one of advantage in a combined extraction and reactive distillation process. As the results in Table 5.7, both processes can obtain purity of lactic acid at 99.99% w/w. However, the overall recovery of lactic acid from fermentation broth of Process B is higher than Process A, which is a maximum to 96.57% of lactic acid recovery.

Table 5.8 Process simulation data for Process A

		B1	F1	C1	F2	E1	R1	ES1	ES2	ES3
Temperature	°C	30.00	30.00	30.00	30.00	30.00	30.01	59.46	85.69	59.46
Pressure	kPa	101.33	101.33	96.33	96.33	96.33	101.33	25.50	25.50	33
Molar Flow	kgmole/h	151.99	510.63	0.92	509.71	338.35	323.35	229.73	108.62	229.73
		Mole fraction								
water		0.0100	0.9666	0.0001	0.9683	0.5143	0.9929	0.8158	0.0076	0.8158
1-butanol		0.9900	0.0000	0.0000	0.0000	0.4380	0.0070	0.1842	0.8439	0.1842
lactic acid		0.0000	0.0301	0.0000	0.0302	0.0454	0.0000	0.0000	0.0107	0.0000
<i>n</i> -butyl lactate		0.0000	0.0000	0.0000	0.0000	0.0000	0.0000	0.0000	0.1307	0.0000
glucose		0.0000	0.0015	0.0000	0.0015	0.0023	1.2E-05	0.0000	0.0070	0.0000
cell		0.0000	0.0018	0.9999	0.0000	0.0000	0.0000	0.0000	0.0000	0.0000
protein		0.0000	5.0e-07	0.0000	5.0e-07	7.5e-07	3.3e-17	0.0000	2.3e-06	0.0000
		ES4	ES5	S1	H1	HD1	HD2	HD3	P2	P1
Temperature	°C	85.69	127.80	127.80	127.80	68.33	64.83	89.19	4.07	91.58
Pressure	kPa	33.00	33.00	33.00	33.00	33.00	32.70	32.70	0.25	0.25
Molar Flow	kgmole/h	108.62	108.62	107.36	1.27	337.09	215.71	121.38	107.36	14.02
		Mole fraction								
water		0.0076	0.0076	0.0076	0.0019	0.5584	0.7975	0.0260	0.0294	0.0000
1-butanol		0.8439	0.8439	0.8524	0.1312	0.3970	0.2025	0.8502	0.9612	0.0000
lactic acid		0.0107	0.0107	0.0089	0.1631	0.0028	0.0000	0.1155	0.0000	0.9999
<i>n</i> -butyl lactate		0.1307	0.1307	0.1311	0.1019	0.0417	0.0000	0.0084	0.0094	0.0000
glucose		0.0070	0.0070	0.0000	0.6017	0.0000	0.0000	0.0000	0.0000	0.0000
cell		0.0000	0.0000	0.0000	0.0000	0.0000	0.0000	0.0000	0.0000	0.0000
protein		2.3e-06	2.3e-06	0.0000	0.0002	0.0000	0.0000	0.0000	0.0000	0.0000

Table 5.9 Process simulation data for Process B

		B1	B2	F1	C1	F2	E1	R1	ES1	ES2	ES3	ES4	ES5
Temperature	°C	30.00	15.17	30.00	30.00	30.00	29.68	21.04	59.44	85.69	59.44	85.69	127.80
Pressure	kPa	101.33	101.33	101.33	96.33	96.33	96.33	101.33	25.50	25.50	33.00	33.00	33.00
Molar Flow	kgmole/h	35.00	85.80	482.15	0.87	481.28	221.52	345.56	168.52	126.10	168.52	126.10	126.10
Mole fraction													
water		0.0100	0.0191	0.9666	0.0001	0.9683	0.5632	0.9924	0.8289	0.0034	0.8289	0.0034	0.0034
1-butanol		0.9900	0.9741	0.0000	0.0000	0.0000	0.3672	0.0065	0.1711	0.8675	0.1711	0.8675	0.8675
lactic acid		0.0000	0.0000	0.0301	0.0000	0.0302	0.0642	0.0008	0.0000	0.0055	0.0000	0.0055	0.0055
<i>n</i> -butyl lactate		0.0000	0.0068	0.0000	0.0000	0.0000	0.0026	0.0000	0.0000	0.1184	0.0000	0.1184	0.1184
glucose		0.0000	0.0000	0.0015	0.0000	0.0015	0.0029	0.0002	0.0000	0.0051	0.0000	0.0051	0.0051
cell		0.0000	0.0000	0.0018	0.9999	0.0000	0.0000	0.0000	0.0000	0.0000	0.0000	0.0000	0.0000
protein		0.0000	0.0000	5.0e-7	0.0000	5.0e-7	1.1e-6	1.4e-14	0.0000	1.9e-6	0.0000	1.9e-6	1.9e-6
		H1	S1	HD1	HD2	HD3	P1	P2	P3	P5	P4	P6	
Temperature	°C	127.80	127.80	73.17	64.83	89.19	91.59	4.61	4.67	4.66	4.66	4.66	
Pressure	kPa	33.00	33.00	33.00	32.70	32.70	0.25	0.25	101.33	101.33	101.33	101.33	
Molar Flow	kgmole/h	0.92	125.18	293.70	154.70	139.00	14.02	124.98	124.98	50.80	123.90	73.10	
Mole fraction													
water		0.0008	0.0035	0.4771	0.7988	0.0227	0.0000	0.0252	0.0252	0.0253	0.0253	0.0253	
1-butanol		0.1324	0.8730	0.4702	0.2012	0.8660	0.0000	0.9631	0.9631	0.9632	0.9632	0.9632	
lactic acid		0.0919	0.0049	0.0021	0.0000	0.1008	0.9999	0.0000	0.0000	0.0000	0.0000	0.0000	
<i>n</i> -butyl lactate		0.0836	0.1187	0.0506	0.0000	0.0105	0.0000	0.0116	0.0116	0.0115	0.0115	0.0115	
glucose		0.6910	0.0000	0.0000	0.0000	0.0000	0.0000	0.0000	0.0000	0.0000	0.0000	0.0000	
cell		0.0000	0.0000	0.0000	0.0000	0.0000	0.0000	0.0000	0.0000	0.0000	0.0000	0.0000	
protein		0.0002	0.0000	0.0000	0.0000	0.0000	0.0000	0.0000	0.0000	0.0000	0.0000	0.0000	

Table 5.10 Flowsheet design results of Process A

	P-100	P-101	X-101	E-100	V-100	T-100	T-101	T-102	T-103
Operation type	Pump	Pump	Filter	Heater	Separator	Extractor	Esterification	Hydrolysis	Distillation
Temperature	-	-	30	127.8	127.8	30.02	79.87	84.69	91.30
Total number of stages	-	-	-	-	-	9	15	15	8
Feed tray	-	-	-	-	-	-	3	5	5
Number of rectifying	-	-	-	-	-	-	2	2	-
Number of reactive	-	-	-	-	-	-	10	12	-
Number of stripping	-	-	-	-	-	-	3	1	-
Reflux ratio	-	-	-	-	-	-	1.66	0.50	0.51
Distillate rate (kgmole/h)	-	-	-	-	-	-	229.73	215.71	107.36
Residue rate (kgmole/h)	-	-	-	-	-	-	108.62	121.38	14.02
Top temperature	-	-	-	-	-	30.00	59.46	64.83	4.07
Bottom temperature	-	-	-	-	-	30.01	85.69	89.19	91.85
Power (kW)	0.021	0.032	-	-	-	-	-	-	-
Duty (kW)	-	-	-	1556.80	-	-	-	-	-
Condenser duty (kW)	-	-	-	-	-	-	-7417.04	-3911.46	-2425.83
Reboiler duty (kW)	-	-	-	-	-	-	9629.92	921.01	1911.81
Column diameter (m)	-	-	-	-	-	1.98	1.83	1.05	1.47
Column height (m)	-	-	-	-	-	12.4968	14.1732	11.2776	8.53
Catalyst (kg)	-	-	-	-	-	-	9245.41	1838.29	-

Table 5.11 Flowsheet design results of Process B

	P-100	P-101	P-102	X-101	E-100	V-100	T-100	T-101	T-102	T-103
Operation type	Pump	Pump	Pump	Filter	Heater	Separator	Extractor	Esterification	Hydrolysis	Distillation
Temperature	-	-	-	30	127.8	127.8	29.68	82.36	85.01	91.32
Total number of stages	-	-	-	-	-	-	9	15	15	8
Feed tray	-	-	-	-	-	-	-	3 and 5	5	5
Number of rectifying	-	-	-	-	-	-	-	2	2	-
Number of reactive	-	-	-	-	-	-	-	10	12	-
Number of stripping	-	-	-	-	-	-	-	3	1	-
Reflux ratio	-	-	-	-	-	-	-	0.5	1.34	0.51
Distillate rate (kgmole/h)	-	-	-	-	-	-	-	168.52	154.70	124.98
Residue rate (kgmole/h)	-	-	-	-	-	-	-	126.10	139.00	14.02
Top temperature	-	-	-	-	-	-	29.68	59.44	64.83	4.61
Bottom temperature	-	-	-	-	-	-	21.04	85.69	89.19	91.59
Power (kW)	0.015	0.037	0.407	-	-	-	-	-	-	-
Duty (kW)	-	-	-	-	1810.89	-	-	-	-	-
Condenser duty (kW)	-	-	-	-	-	-	-	-3063.56	-4367.38	-2821.70
Reboiler duty (kW)	-	-	-	-	-	-	-	5304.24	1075.86	2224.28
Column diameter (m)	-	-	-	-	-	-	1.83	1.44	1.07	1.01
Height	-	-	-	-	-	-	12.50	14.17	11.28	8.53
Catalyst (kg)	-	-	-	-	-	-	-	5690.32	1904.90	-

5.5.2 Economic Evaluation

According to the description in section 5.4.6, the production costs of Processes A and B were estimated. In addition, the production cost of Process B when decreasing annual capacity at 1,000 tons/year of 99.99%w/w lactic acid was investigated. The comparative assessment of total capital investment in each process presented in Table 5.12. When compared process B with different annual capacity, it was observed that the process with low capacity required lower total capital investment than the process with large capacity, due to reduction of installation equipment cost. The comparison between Process A and B, it can be seen that Process A slightly required higher total capital investment than Process B about 3.6% due to installation cost. This is because Process A need suitable diameter of column when using high amount of feed 1-butanol.

The operating cost and production cost of each process were estimated as shown in Table 5.13 and the comparison of operating costs presented in Figure 5.4. For operating cost, it was observed that labor cost obtained in each process are the same values because it depends on number of operators. In each process have the same number of operator due to the similar unit operation in processing steps. In Figure 5.4, labor cost primarily contributed to operating cost for the lower production capacity. While increasing of 1-butanol feed resulted in an increased operating cost of Process A. The reduction of 1-butanol feed by its recovery in Process B lowered operating cost.

The results in Table 5.13 suggested that using a combined process of counter-current extraction and reactive distillation with recycling of 1-butanol (Process B) led to reducing production cost in this study. Minimum cost achieved at 0.90 USD/kg for 99.99%w/w lactic acid. The reduction costs were 67.27% compared to

lower production capacity process and 46.10% compared to the process with non-recovery 1-butanol.

Table 5.12 Total capital investment calculation of each process

Units	Operation type	Cost (USD)		
		10,000 tons/year		1,000 tons/year
		Process A	Process B	Process B
<i>Direct cost</i>				
P-100	Pump	33,500	32,200	28,200
P-101	Pump	33,500	33,600	28,200
V-100	Separator	120,900	130,300	116,900
P-102	pump	-	30,500	28,700
E-100	Heater	66,400	66,400	65,000
X-101	Microfilter	16,900	16,400	12,500
T-101, Esterification column				
	Condenser	58,700	58,700	59,700
	Reboiler	66,400	66,400	65,000
	Main Tower	313,900	269,500	193,300
T-102, Hydrolysis column				
	Condenser	59,000	59,000	59,600
	Reboiler	66,400	66,400	65,000
	Main Tower	197,500	198,500	154,000
T-100, Liquid-liquid extractor				
	Main Tower	291,700	278,000	136,400
T-103, Distillation column				
	Condenser	70,600	70,600	69,300
	Reboiler	66,400	66,400	65,000
	Main Tower	214,000	182,400	176,100
Total installed equipment		1,675,800	1,625,300	1,322,900
Piping		201,096	195,036	158,748
Electrical		83,790	81,265	66,145
Instrumentation		100,548	97,518	79,374
Building		167,580	162,530	132,290
Land and Yard improvements		50,274	48,759	39,687
Total direct cost		2,279,088	2,210,408	1,799,144
<i>Indirect cost</i>				
Engineering and supervision		273,491	265,249	215,897
Contractor's fee		91,164	88,416	71,966
Contingency		182,327	176,833	143,932
Fixed capital investment		2,826,069	2,740,906	2,230,939
Working capital		339,128	328,909	267,713
Total capital investment		3,165,197	3,052,060	2,498,651

Table 5.13 Operating cost calculation of each process

Item	Cost (USD/year)		
	10,000 tons/year		1,000 tons/year
	Process A	Process B	Process B
Operating cost			
1 Raw materials			
Broth	3,242,846	3,061,979	299,063
1-Butanol	8,855,096	2,039,136	283,136
2 Catalyst	410,612	357,141	85,180
3 Utilities	1,832,447	1,444,517	326,479
4 Labor	752,400	752,400	752,400
5 Maintenance	141,303	137,045	111,547
6 Operating supplies	70,652	68,523	55,773
7 Plant overhead	376,200	376,200	376,200
Fixed charges			
8 Depreciation	480,432	465,954	379,260
9 Insurance	2,261	2,193	1,785
10 General and administrative expense	544,656	285,709	79,438
11 Annual production cost	16,708,904	8,990,797	2,750,262
Production cost (USD/kg)	1.67	0.90	2.75

However, it can be seen that the main operating cost of Process B is fermentation broth due to the fermentation unit cost. This cost could be reduced by using alternate cheap raw materials in the fermentation broth or fermentation process.

In addition, Table 5.14 showed the unit cost of lactic acid production per kilogram using conventional lactic acid recovery processes (Joglekar et al., 2006; González et al., 2007; Sikder et al., 2012). The conventional recovery process is usually involved acidification, solid removal, neutralization, precipitation, filtration, extraction, adsorption, distillation, membrane and evaporation. These processes suggested that the number of unit operations and process steps in the downstream process for high-purity lactic acid production usually led to high recovery costs. High consumption of chemicals was also responsible for the high cost. For example, using a large amount of H₂SO₄ for the acidification of calcium lactate broth affected to increase the gypsum and

wastewater during the operation (Pal et al., 2009). In some separation units such as distillation, the feed solution with high inorganic contents is prohibited, and thus, the pretreatment unit prior distillation is required. This results in the additional consumption of chemicals and utilities (Chen et al., 2012). Operations with evaporation and crystallization are considered an energy-intensive process such as high steam consumption and high cooling rate. Using membrane process are considered high cost of membrane and difficult to scale up as well as polarization problem (Komesu et al., 2016). In contrast, a combined counter-current extraction and reactive distillation process was suggested to be an economical route. The Extraction does not have the generation of gypsum and reduction in the risk of thermal decomposition because it generally occurs at room temperature and is thus considered an energy-saving process. The reactive distillation integrated reaction and separation in the same unit, resulting in reducing of equipment cost and low energy consumption. In addition, the 1-butanol solvent and extracted water is continuously used as the reactant in reactive distillation, resulting is low chemical consumption.

As a result, the proposed processes in this study based on a combined extraction and reactive distillation (with recycle of 1-butanol) could provide a low unit cost of lactic acid compared to those in the previous literature and commercial sale price (1.0-1.8 USD/kg) (Zacharof and Lovitt, 2013). Therefore, it can summarize from the simulated data that the proposed process provides a new lactic acid downstream recovery process. The process not only gives a sufficiently high product yield and purity but are also considered economical and environmentally friendly routes due to cost-effectiveness, low chemical consumption, low waste as well as low energy consumption.

Table 5.14 Economic analysis of conventional lactic acid downstream recovery process compared to proposed process in this work

Processes	Purity %w/w	%Overall recovery	Cost (USD/kg)	References
1 Reactive extraction, re-extraction and reactive distillation	100	-	1.59	
2 Precipitation, acidification and reactive distillation	100	-	1.40	Joglekar et al. (2006)
3 Microfiltration, electro dialysis and reactive distillation	100	-	1.74	
4 Ultrafiltration, ion-exchange, and vacuum evaporation	50	59	1.25	González et al. (2007)
5 Membrane integrated bioreaction	95	89	3.15	Sikder et al. (2012)
6 Counter-current extraction and reactive distillation	99.99	96.57	0.90	This work

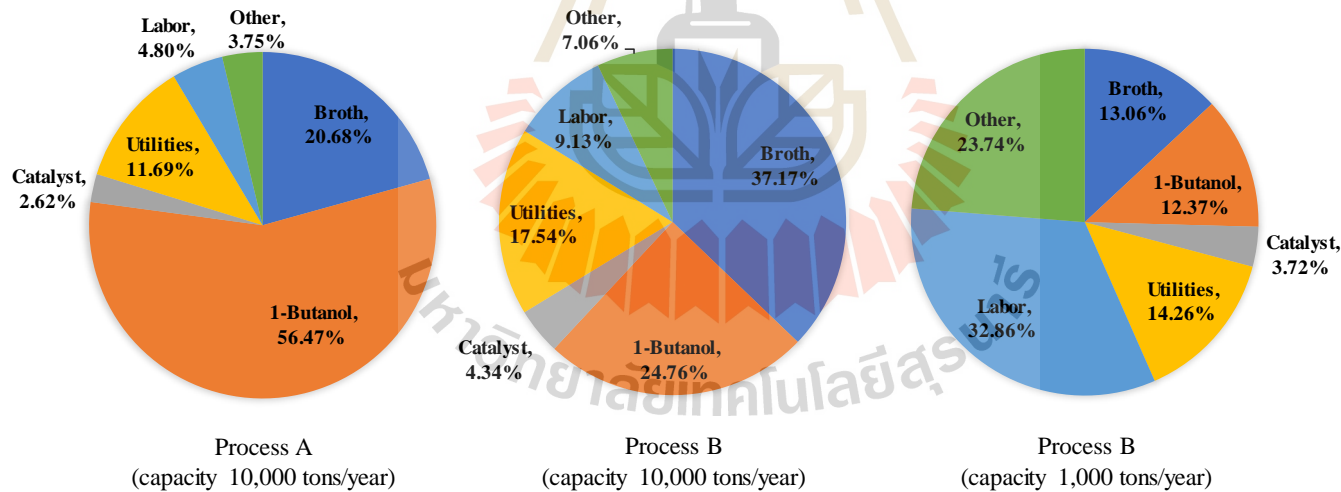


Figure 5.4 Comparison of operating cost for recovery lactic acid using a combined extraction and reactive distillation via different process

5.6 Conclusion

A combined counter-current extraction and reactive distillation for recovery and purification of lactic acid from fermentation broth was proposed. The process design and economic has been evaluated using technical data obtained from laboratory scale in previous work by Aspen HYSYS V10 and Aspen Process Economic Analyzer. The process design consisted of the following steps; cell removal, extraction, esterification and hydrolysis in reactive distillation and purified by distillation. Three different processes as recovery and non-recovery of 1-butanol at the same production capacity and the process with decreasing annual production capacity were compared the production cost. It was found that production cost decreased via increasing annual production capacity and recovery of 1-butanol for using in the process. By using the process with recovery 1-butanol, the proposed process can be recovery lactic acid from fermentation broth achieved to 96.57% with purity of 99.99% w/w. The production cost of lactic acid was evaluated at 0.90 USD/kg.

5.7 References

- Anderson, J. 2009. Determining manufacturing costs. **American Institute of Chemical Engineers**:27-31.
- Boontawan, P., Baimark, Y., and Boontawan, A. 2019. Fermentation and Purification of L-Lactic Acid by Using Biorefinery Concept to Produce a High Molecular Weight Poly(L-Lactide) Polymer. **Journal of Biobased Materials and Bioenergy** 13 (1):43-52.
- Chawong, K., and Rattanaphanee, P. 2011. n-Butanol as an Extractant for Lactic Acid Recovery. **World Academic of Science Engineering Technology** 56:1437-1440.
- Chawong, K., Rayabsri, C., and Rattanaphanee, P. 2015. Extraction of Lactic Acid in Mixed Solvent Electrolyte System Containing Water, 1-Butanol and Ammonium Sulfate. **International Journal of Chemical Reactor Engineering** 13 (2).
- Chen, L., Zeng, A., Dong, H., Li, Q., and Niu, C. 2012. A novel process for recovery and refining of L-lactic acid from fermentation broth. **Bioresour Technol** 112:280-284.
- Dimian, A. 2003. Integrated Design & Simulation of Chemical Processes. **Computers & Chemical Engineering**.
- González, M. I., Álvarez, S., Riera, F., and Álvarez, R. 2007. Economic evaluation of an integrated process for lactic acid production from ultrafiltered whey. **Journal of Food Engineering** 80 (2):553-561.

- Joglekar, H. G., Rahman, I., Babu, S., Kulkarni, B. D., and Joshi, A. 2006. Comparative assessment of downstream processing options for lactic acid. **Separation and Purification Technology** 52 (1):1-17.
- Komesu, A., Martinez, P. F. M., Lunelli, B. H., Filho, R. M., and Maciel, M. R. W. 2015. Lactic acid purification by reactive distillation system using design of experiments. **Chemical Engineering and Processing: Process Intensification** 95:26-30.
- Komesu, A., Wolf Maciel, M. R., Rocha de Oliveira, J. A., da Silva Martins, L. H., and Maciel Filho, R. 2016. Purification of Lactic Acid Produced by Fermentation: Focus on Non-traditional Distillation Processes. **Separation & Purification Reviews** 46 (3):241-254.
- Kumar, R., and Mahajani, S. M. 2007. Esterification of Lactic Acid with n-Butanol by Reactive Distillation. **Industrial & Engineering Chemistry** 46:6873-6882.
- Kumar, R., Mahajani, S. M., Nanavati, H., and Noronha, S. B. 2006a. Recovery of lactic acid by batch reactive distillation. **Journal of Chemical Technology & Biotechnology** 81 (7):1141-1150.
- Kumar, R., Nanavati, H., Noronha, S. B., and Mahajani, S. M. 2006b. A continuous process for the recovery of lactic acid by reactive distillation. **Journal of Chemical Technology & Biotechnology** 81 (11):1767-1777.
- Lactic Acid Market Size* September 2019 [cited. Available from <https://www.grandviewresearch.com/press-release/global-lactic-acid-and-poly-lactic-acid-market>].
- Lohmann, J., Joh, R., and Gmehling, J. 2001. From UNIFAC to Modified UNIFAC (Dortmund). **Industrial & Engineering Chemistry Research** 40 (3):957-964.

- Pal, P., Sikder, J., Roy, S., and Giorno, L. 2009. Process intensification in lactic acid production: A review of membrane based processes. **Chemical Engineering and Processing: Process Intensification** 48 (11):1549-1559.
- Peters, M. S., and Timmerhaus, K. D. 1991. Plant design and economics for chemical engineers. In **McGraw-Hill Chemical Engineering Series**.
- Richardson, C. 2005. **Chemical Engineering Design**. 4th Edition ed. Vol. 6.
- Sikder, J., Roy, M., Dey, P., and Pal, P. 2012. Techno-economic analysis of a membrane-integrated bioreactor system for production of lactic acid from sugarcane juice. **Biochemical Engineering Journal** 63:81-87.
- Su, C.-Y., Yu, C.-C., Chien, I. L., and Ward, J. D. 2013. Plant-Wide Economic Comparison of Lactic Acid Recovery Processes by Reactive Distillation with Different Alcohols. **Industrial & Engineering Chemistry Research** 52 (32):11070-11083.
- Su, C.-Y., Yu, C.-C., Chien, I. L., and Ward, J. D. 2015. Control of Highly Interconnected Reactive Distillation Processes: Purification of Raw Lactic Acid by Esterification and Hydrolysis. In **Industrial & Engineering Chemistry Research**, 6932-6940.
- Zacharof, M.-P., and Lovitt, R. W. 2013. Complex Effluent Streams as a Potential Source of Volatile Fatty Acids. **Waste and Biomass Valorization** 4 (3):557-581.

CHAPTER VI

CONCLUSIONS AND RECOMMENDATIONS

6.1 Conclusions

- For extraction of lactic acid with 1-butanol using packed liquid-liquid extraction column, Sauter mean drop diameter decreased via increased dispersed phase flow rate and decreased nozzle diameter, which is an influence on increasing dispersed phase mass transfer coefficient. While an increase in continuous phase flow rate affected increasing drop size, due to the coalescence of drops, resulting in reducing dispersed phase mass transfer coefficient. Maximum efficiency in the extraction of lactic acid from synthesis solution and fermentation broth achieved at about 75.19% and 72.53%, respectively when using a nozzle diameter of 1 mm with the continuous and dispersed phase flow rate of 40 and 70 ml/min, respectively.
- The correlation of Sauter mean drop diameter was in good agreement with experimental data. Using effective diffusivity instead of molecular diffusivity can improve the dispersed phase Sherwood number correlation significantly with higher accuracy for the prediction.
- The prepared aluminum alginate catalyst was found to be created a rough surface and the presence of acidity active sites led to high esterification activity under mild reaction conditions. The reaction rate was found to increase with increasing reaction temperature, initial 1-butanol to lactic acid molar ratio and catalyst loading. The esterification of lactic acid with 1-butanol was successfully carried out over the

aluminum alginate (ALA) with a maximum lactic acid conversion achieving at 81.18%. This catalyst showed better activity performance than commercial Amberlyst-15. The Langmuir-Hinshelwood model with non-ideal assumption was able to describe the kinetic model of this reaction with small error. The esterification of lactic acid is an endothermic reaction, in which enthalpy and entropy were found to be $22.69 \text{ kJ}\cdot\text{mol}^{-1}$ and $76.88 \text{ J}\cdot\text{mol}^{-1}\cdot\text{K}^{-1}$.

- Esterification of lactic acid with 1-butanol followed by hydrolysis of *n*-butyl lactate was studied using a reactive distillation column. For esterification process, the results showed that conversion and yield have a significant increase with increasing reflux ratio and were insensitive to change in catalyst loading due to fast reaction rate. While increasing the feed flow rate affects conversion and yield decreased. Maximum conversion of lactic acid and yield of *n*-butyl lactate obtained from esterification achieved at 88.09% and 87.44%, respectively under operating pressure of 255 mbar using the reflux ratio of 1 with feed flow rate of 1 ml/min and 3 g of catalyst loading.

For hydrolysis process, the effect of the reflux ratio and feed flow rate are the same with esterification. However, conversion and yield were found to be increased via increasing catalyst loading. The purity of lactic acid was found to be decreased via increase in pressure, feed flow rate and reflux ratio. By consideration of conversion, yield and purity, these values reasonably achieved at 40.85%, 33.98% and 98.53%, respectively under operating pressure of 319 mbar using reflux ratio of 0.5 with feed flow rate of 1 ml/min and 4.3 g of catalyst loading.

- The process design and economic of a combined counter-current extraction and reactive distillation for recovery and purification of lactic acid from fermentation broth has been evaluated by Aspen HYSYS V10 and Aspen Process

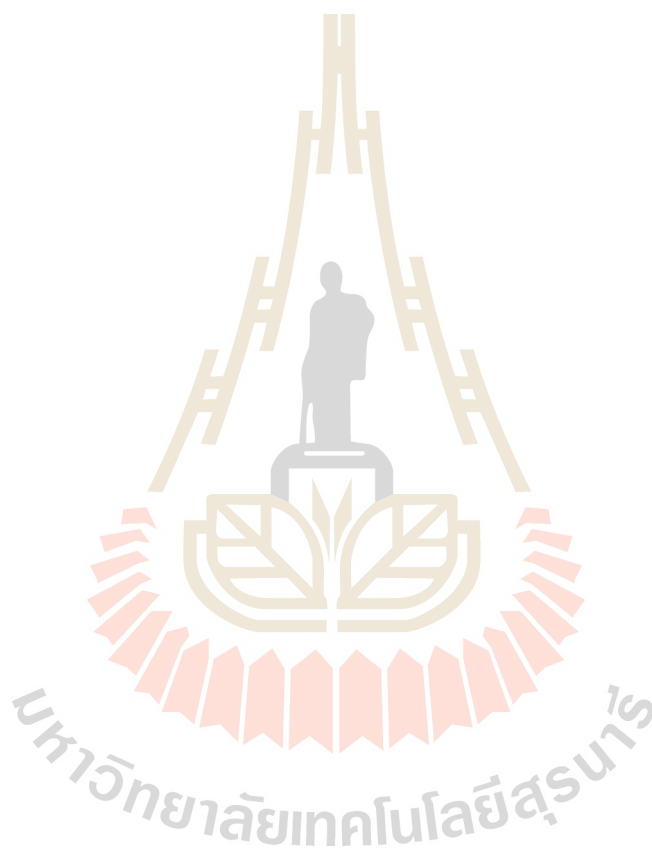
Economic Analyzer. The process design consisted of the following steps; cell removal, extraction, esterification and hydrolysis in reactive distillation and purified by distillation. The results showed that production cost decreased via increasing annual production capacity and recovery of 1-butanol for using in the process. By using the process with recovery 1-butanol, the proposed process can be recovery lactic acid from fermentation broth achieved to 96.57% with a purity of 99.99%w/w. The production cost of lactic acid was evaluated at 0.90 USD/kg

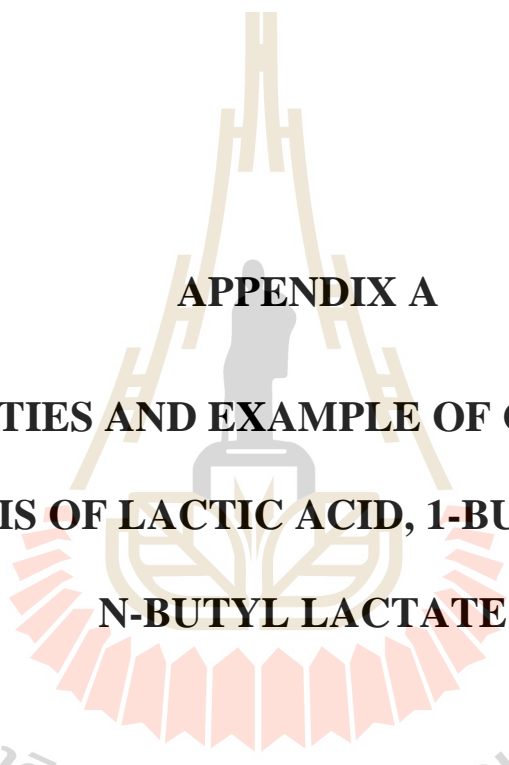
6.2 Recommendations

Some recommendations for future work are summarized as follows:

- In extraction column, diameter of column should be more than diameter of packing about 6 times. However, the experiments in this work were carried out using short column diameter (25mm), while the diameter of packing material is 6 mm, due to the limit of column having in the laboratory and commercial size of raschig ring, which is packing seem large diameter. It maybe has effect on mass transfer in system as well as extraction efficiency. So, the suitable column diameter and packing should be used.
- Due to thermal degradation and gelling property in nature of alginate, the aluminum alginate cannot be used at high temperatures. From observation during the experiment. the catalyst was found to be breakage to small particles and seem scorched at the reaction temperature of 85°C, this might be decreased catalytic activity. So, it should have to study in improving thermal stability and mechanical strength, as well as its uniform shape in the future. Maybe use other compounds to support the catalyst such as boehmite, clay, etc.

- Process simulation in this work was simulated by assuming neglecting of inorganic salts in the fermentation broth because of software license limiting. If possible, it should be extensively used real compositions of fermentation broth.





APPENDIX A
PROPERTIES AND EXAMPLE OF COMPONENT
ANALYSIS OF LACTIC ACID, 1-BUTABOL, AND
N-BUTYL LACTATE

มหาวิทยาลัยเทคโนโลยีสุรนารี

A.1 Properties of Lactic acid, 1-Butanol and *n*-Butyl Lactate

Table A.1 Chemical and physical properties

Properties	Lactic acid	1-butanol	<i>n</i> -butyl lactate
Chemical formula	C ₃ H ₆ O ₃	C ₄ H ₁₀ O	C ₇ H ₁₄ O ₃
Molar mass (g/mol)	90.08	74.12	146.186
Purity	88% w/w	99.9% w/w	99% w/w
Density (g/cm ³)	1.22	0.81	0.98
Melting point (°C)	18	-89.8	-43
Boiling point (°C)	232.14	117.75	186.69
Solubility in water	Miscible	73 g/L @ 25 °C	Slight
Surface Tension (mN/m)	45.5	24.7	29.5

A.2 Calibration Standard Curve of Lactic Acid

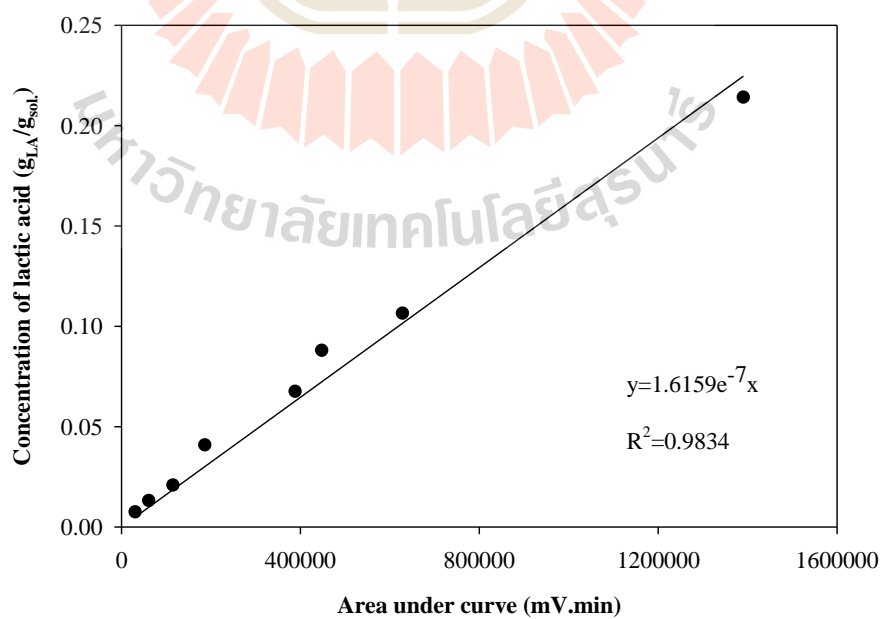


Figure A.1 Calibration standard curve of lactic acid

A.3 Calibration Standard Curve of *n*-Butyl Lactate

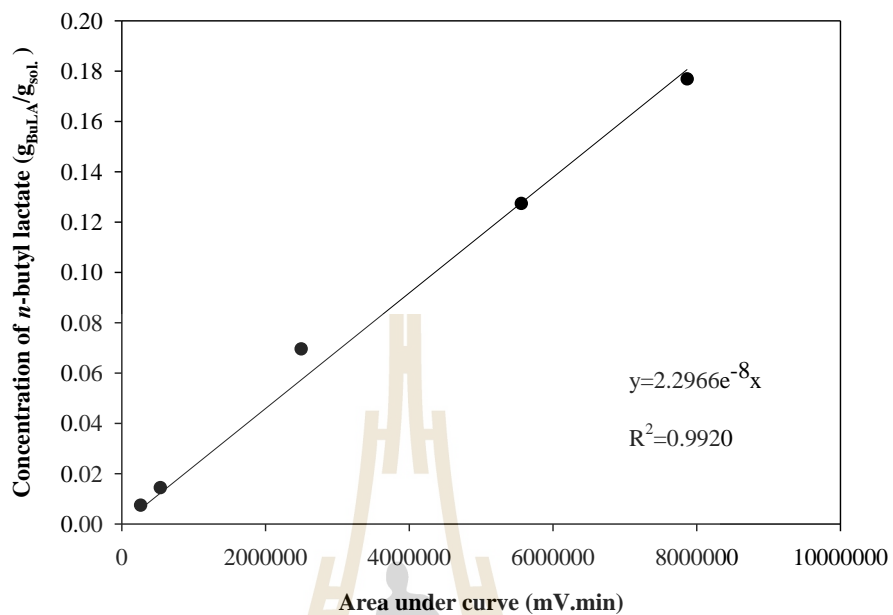


Figure A.2 Calibration standard curve of *n*-butyl lactate

A.4 Calibration Standard Curve of 1-Butanol

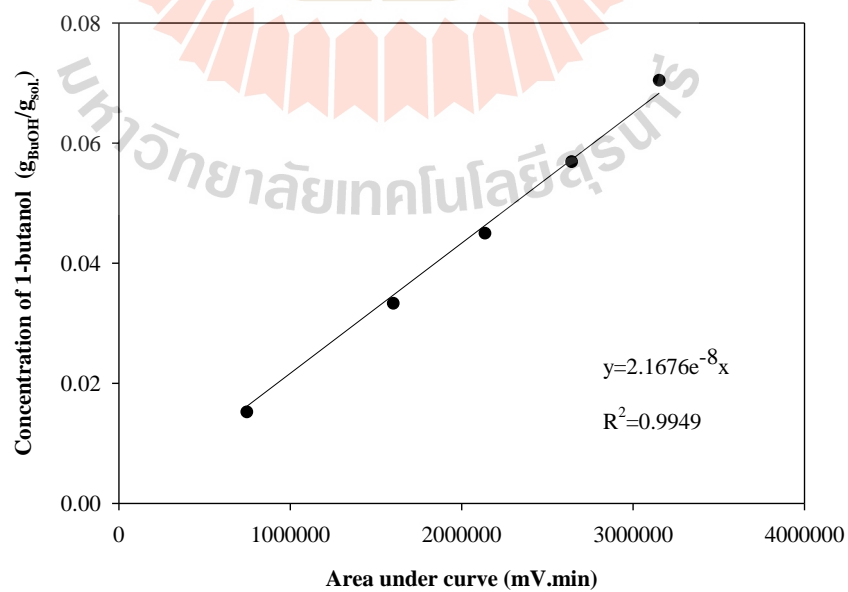


Figure A.3 Calibration standard curve of 1-butanol

A.5 Component Analysis of Lactic Acid, 1-Butanol and *n*-Butyl lactate

Example analysis of components for esterification using reactive distillation is detailed below;

A.5.1 Feed solution analysis

$$\text{Total mass of feed} = 300.3850 \text{ g}$$

The extracted product from extraction was used as the feed solution for esterification, which has a slight amount of *n*-butyl lactate because lactic acid and 1-butanol can autocatalyzed. Feed sample was diluted with DI water:

$$\text{Mass of sample} = 0.1222 \text{ g}$$

$$\text{Mass of DI water} = 0.9677 \text{ g}$$

$$\text{Total mass} = 0.1222 + 0.9677 = 1.0899 \text{ g}$$

From GC-TCD analysis, the chromatogram is showed in Figure A.4. The area under curve of each component will be taken to calculate the quantity from the calibration curve.

The quantity from calibration curve, which is the concentration equal to 0.0958, 0.0001, 0.0115 g/g_{sol} for 1-butanol, *n*-butyl lactate and lactic acid, respectively. Therefore, the amount of each component in feed solution can be calculate as;

$$\therefore \text{1-Butanol} = \frac{0.0958 \text{ g}}{\text{g solution}} \times \frac{1.0899 \text{ g solution}}{0.1222 \text{ g sample}} \times 300.3850 \text{ g} = 256.6606 \text{ g}$$

$$\therefore \textit{n}\text{-Butyl lactate} = \frac{0.0001 \text{ g}}{\text{g solution}} \times \frac{1.0899 \text{ g solution}}{0.1222 \text{ g sample}} \times 300.3850 \text{ g} = 0.2679 \text{ g}$$

$$\therefore \text{Lactic acid} = \frac{0.0115 \text{ g}}{\text{g solution}} \times \frac{1.0899 \text{ g solution}}{0.1222 \text{ g sample}} \times 300.3850 \text{ g} = 30.8100 \text{ g}$$

The water component in feed was determined by mass balance:

$$\text{Water} = (\text{total feed}) - (1\text{-butanol}) - (n\text{-butyl lactate}) - (\text{lactic acid})$$

$$\therefore \text{Water} = 300.3850 - 256.6606 - 0.2679 - 30.8100 = 12.6465 \text{ g}$$

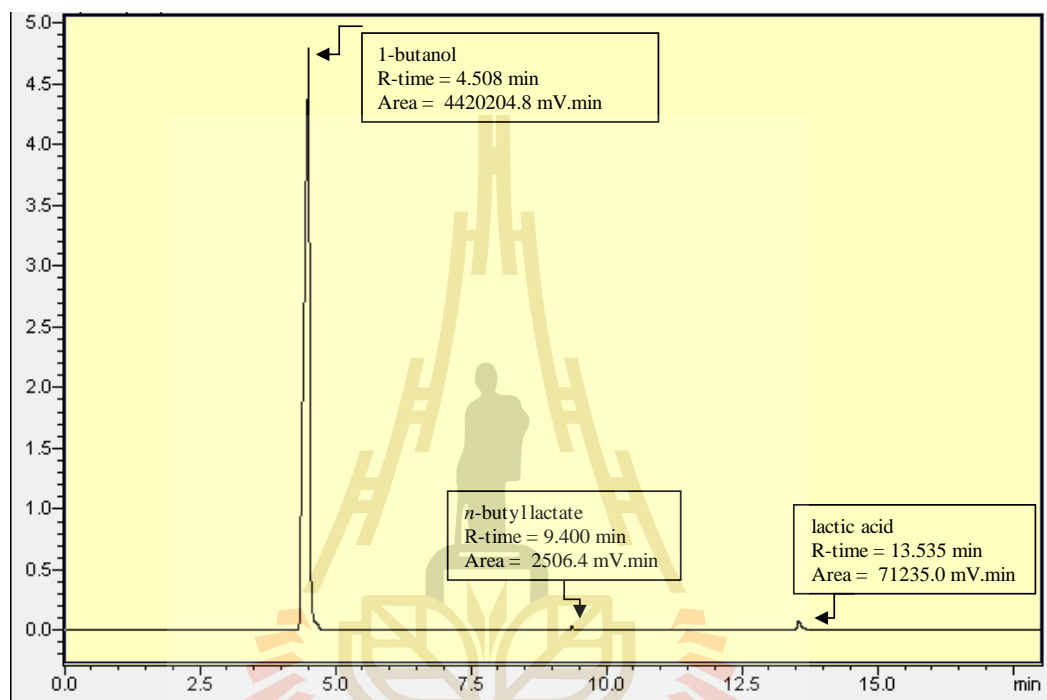


Figure A.4 Chromatogram of component analysis of feed solution

A.5.2 Distillated product analysis

After finished the experiment, weight of distillated product were determined;

$$\text{Total mass of distillated product} = 273.3613 \text{ g}$$

The sample was diluted with DI water:

$$\text{Mass of sample} = 0.0992 \text{ g}$$

$$\text{Mass of DI water} = 0.9086 \text{ g}$$

$$\text{Total mass} = 0.0992 + 0.9086 = 1.0078 \text{ g}$$

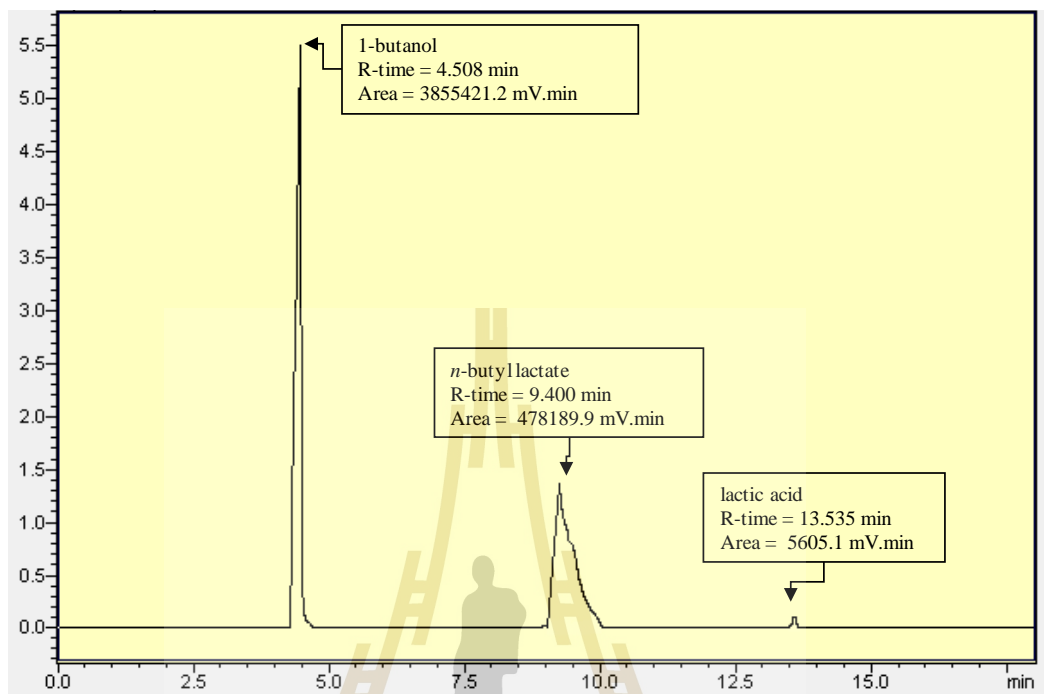


Figure A.5 Chromatograph of component analysis of distilled product

From GC-TCD analysis, the chromatogram is showed in Figure A.5. The quantity from calibration curve, which is the concentration equal to 0.0836, 0.0110, 0.00091 g/g_{sol} for 1-butanol, *n*-butyl lactate and lactic acid, respectively. Therefore, the amount of each component in distilled product can be calculate as;

$$\therefore \text{1-Butanol} = \frac{0.0836 \text{ g}}{\text{g solution}} \times \frac{1.0078 \text{ g solution}}{0.0992 \text{ g sample}} \times 273.3613 \text{ g} = 232.1699 \text{ g}$$

$$\therefore \text{n-Butyl lactate} = \frac{0.0110 \text{ g}}{\text{g solution}} \times \frac{1.0078 \text{ g solution}}{0.0992 \text{ g sample}} \times 273.3613 \text{ g} = 30.5487 \text{ g}$$

$$\therefore \text{Lactic acid} = \frac{0.00091 \text{ g}}{\text{g solution}} \times \frac{1.0078 \text{ g solution}}{0.0992 \text{ g sample}} \times 273.3613 \text{ g} = 2.5272 \text{ g}$$

The water component in feed was determined by mass balance:

$$\text{Water} = (\text{Total feed}) - (1\text{-Butanol}) - (n\text{-Butyl lactate}) - (\text{Lactic acid})$$

$$\therefore \text{Water} = 273.3613 - 232.1669 - 30.5487 - 2.5272 = 8.1185 \text{ g}$$

A.5.3 Residue product analysis

After finished the experiment, weight of residue product were determined;

$$\text{Total weight of residue product} = 16.0237 \text{ g}$$

The sample was diluted with DI water:

$$\text{Weight of sample} = 0.1063 \text{ g}$$

$$\text{Weight of DI water} = 0.9276 \text{ g}$$

$$\text{Total weight} = 0.1063 + 0.9276 = 1.0339 \text{ g}$$

From GC-TCD analysis, the chromatogram is showed in Figure A.6.

The quantity from calibration curve, which is the concentration equal to 3.8622×10^{-5} , 4.1286×10^{-4} , $0.0581 \text{ g/g}_{\text{sol}}$ for 1-butanol, *n*-butyl lactate and lactic acid, respectively.

Therefore, the amount of each component in residue product can be calculate as;

$$\therefore 1\text{-Butanol} = \frac{3.8622 \times 10^{-5} \text{ g}}{\text{g solution}} \times \frac{1.0339 \text{ g solution}}{0.1063 \text{ g sample}} \times 16.0237 \text{ g} = 0.0060 \text{ g}$$

$$\therefore n\text{-Butyl lactate} = \frac{4.1286 \times 10^{-4} \text{ g}}{\text{g solution}} \times \frac{1.0339 \text{ g solution}}{0.1063 \text{ g sample}} \times 16.0237 \text{ g} = 0.0643 \text{ g}$$

$$\therefore \text{Lactic acid} = \frac{0.0581 \text{ g}}{\text{g solution}} \times \frac{1.0339 \text{ g solution}}{0.1063 \text{ g sample}} \times 16.0237 \text{ g} = 9.0549 \text{ g}$$

The water component in feed was determined by mass balance:

$$\text{Water} = (\text{Total feed}) - (1\text{-Butanol}) - (n\text{-Butyl lactate}) - (\text{Lactic acid})$$

$$\therefore \text{Water} = 16.0237 - 0.0060 - 0.0643 - 9.0549 = 6.8985 \text{ g}$$

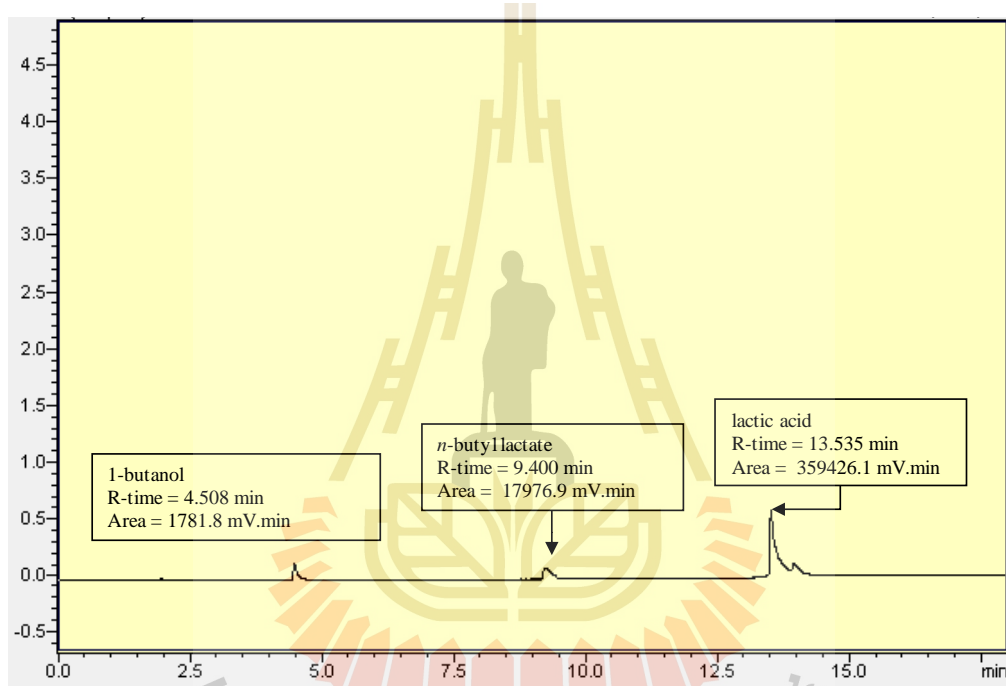


Figure A.6 Chromatograph of component analysis of residue product

Table A.2 Calculated mole of the components in feed, deistilled and residue product

Component	MW (g/gmole)	Mole		
		Feed solution	Distilled product	Residue product
1-butanol	74.12	3.4628	3.1323	0.0001
<i>n</i> -butyl lactate	146.19	0.0018	0.2090	0.0004
lactic acid	90.08	0.3420	0.0281	0.1005
water	18	0.7026	0.4510	0.3833
Total		4.5092	3.8204	0.4843

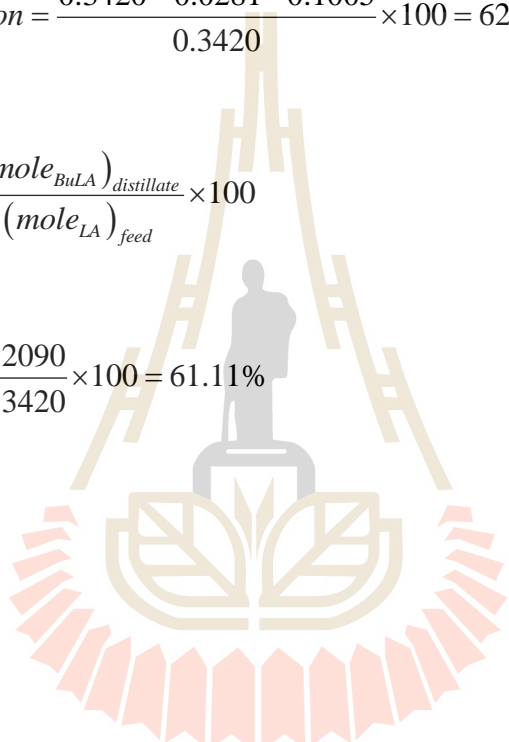
Therefore, mole of each component were calculated as shown in Table A.1 The conversion of lactic acid and yield of n-butyl lactate can be determined as follows;

$$\%Conversion = \frac{(mole_{LA})_{feed} - (mole_{LA})_{distillated} - (mole_{LA})_{residue}}{(mole_{LA})_{feed}} \times 100$$

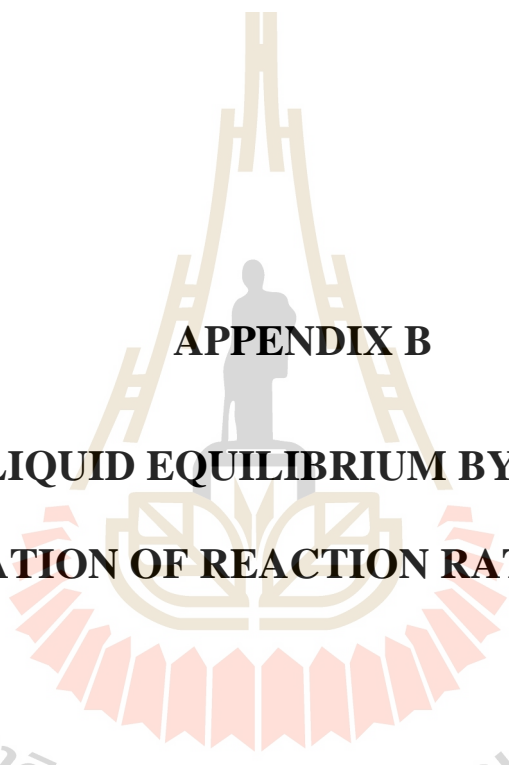
$$\%Conversion = \frac{0.3420 - 0.0281 - 0.1005}{0.3420} \times 100 = 62.40\%$$

$$\%Yield = \frac{(mole_{BuLA})_{distillate}}{(mole_{LA})_{feed}} \times 100$$

$$\%Yield = \frac{0.2090}{0.3420} \times 100 = 61.11\%$$



มหาวิทยาลัยเทคโนโลยีสุรนารี



APPENDIX B

**LIQUID-LIQUID EQUILIBRIUM BY UNIFAC AND
CALCULATION OF REACTION RATE CONSTANT**

มหาวิทยาลัยเทคโนโลยีสุรนารี

MATLAB®(VersionR2017a) with built-in function, ode45 solver, was used to solve the ordinary differential equations. UNIFAC model was used to calculate the liquid phase activity coefficient of lactic acid+1-butanol+n-butyl lactate+water system using functional-group of each component in the solution as shown in Table 3.1.

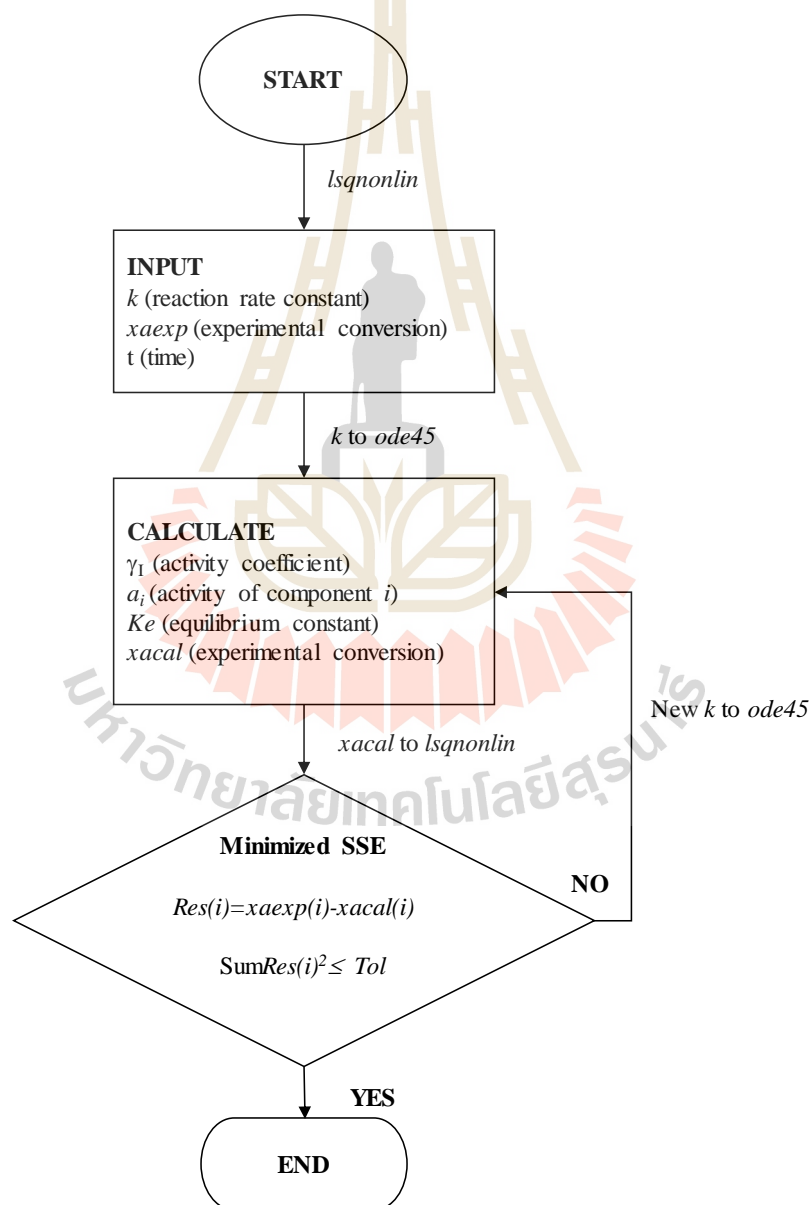


Figure B.1 Flowchart for calculation of reaction rate constant

The ode45 solver was based on explicit 4th-order Runge-Kutta method. The liquid phase activity coefficient and calculated conversion were calculated at initial guess of reaction rate constant. Then, the calculation conversions at any time were sent to nonlinear least-square regression solver, lsqnonlin, to minimize the sum of squared errors between the experimental and the calculated conversion. Both solvers were simultaneously operated. The optimal reaction rate constant was obtained from nonlinear least-square regression. The flowchart of program algorithm was shown in Figure B.1.

B.1 *lsqnonlin* Program

```
function SSE=obfunction(T)
global k %k1 k2 k3 k4
%SSE=obfunction(348.15)
k=kcal(1,1);
%k1=kcal(2,1);
%k2=kcal(3,1);
%k3=kcal(4,1);
%k4=kcal(5,1);
%-----INPUT DATA-----
%Temperature = 55 C
[t,xa]=ode45(@kinetic,[0 15 30 45 60 75 90 105 120 150 180 210 240
270 300 330 360],0);xaexp=[0.0000 0.1042 0.1989 0.2801 0.3532 0.4100
0.4506 0.4939 0.5237 0.5792 0.6089 0.6265 0.6428 0.6631 0.6834 0.6915
0.7077];
%-----
xacal=xa
%-----
H=length(t);
for i=1:H
ob(i)=(xaexp(i)-xacal(i)).^2;
end
SSE=sum(ob);
for i=2:H
MSD(i)=abs((xacal(i)-xaexp(i))./xacal(i));
end
SSMSD=(1/(H-1)).*sum(MSD).*100
plot(t,xaexp,'O',t,xacal,'-'),xlabel('t'),ylabel('xa');
end
```

B.2 UNIFAC Model and *ode45* Program

```

function dxa=kinetic(t,xa)
global k k1 k2 k3 k4
dxa=zeros(1,1);      %Conversion

%*****Data for Effect of temperature*****
T=328.15;           %reaction temperature
xae=0.7077;
m=4.9864;           %molar ratio of BuOH to LA
n=0.6820;           %molar ratio of Water to LA
mc=1.0051;          %amount of catalyst
na0=0.1847;         %Constant for the reaction at 55C
%*****
%VLE calculation by UNIFAC model
%*****
%----The system is Esterification of lactic acid with 1-butanol----
% BuOH(1)+LA(2) <---> BuLA(3) + W(4)
%*****
%Function group
%BuOH    --> 1CH3.3CH2.1OH
%LA      --> 1CH3.1CH.1OH.1COOH
%BuLA    --> 2CH3.3CH2.1CH.1OH.1COO
%W       --> 1H2O
%Set k   --> CH3=1, CH2=2, CH=3, OH=4, H2O=5, COOH=6, COO=7
%*****
%Parameters from "Chemical Engineering Thermodynamics", Y.V.C. Rao,
%Sangam Books, London, 1997.
%-----
%Area parameters of functional group k
Qk=[0.8480 0.5400 0.2280 1.2000 1.4000 1.2240 1.2000];
%Volume parameters of functional group k
Rk=[0.9011 0.6744 0.4469 1.0000 0.9200 1.3013 1.3800];
%-----
%Find volume parameters& area parameters of chemical i(r(i)and q(i))
z=10;           %Coordination number
for i=1:4
    if i==1
        r(i)=Rk(1)+3*Rk(2)+Rk(4);
        q(i)=Qk(1)+3*Qk(2)+Qk(4);
        L(i)=(z/2)*(r(i)-q(i))-(r(i)-1);
    elseif i==2
        r(i)=Rk(1)+Rk(3)+Rk(4)+Rk(6);
        q(i)=Qk(1)+Qk(3)+Qk(4)+Qk(6);
        L(i)=(z/2)*(r(i)-q(i))-(r(i)-1);
    elseif i==3
        r(i)=2*Rk(1)+3*Rk(2)+Rk(3)+Rk(4)+Rk(7);
        q(i)=2*Qk(1)+3*Qk(2)+Qk(3)+Qk(4)+Qk(7);
        L(i)=(z/2)*(r(i)-q(i))-(r(i)-1);
    else
        r(i)=Rk(5);
        q(i)=Qk(5);
        L(i)=(z/2)*(r(i)-q(i))-(r(i)-1);
    end
end
end
%*****
%Interaction parameters a(i,j) data
%www.aim.env.uea.ac.uk/aim/info/UNIFACgroups.html

```

```

%*****
a=[0 0 0 986.5 1318 663.5 387.1;...
  0 0 0 986.5 1318 663.5 387.1;...
  0 0 0 986.5 1318 663.5 387.1;...
  156.4 156.4 156.4 0 353.5 199 190.3;...
  300 300 300 -229.1 0 -14.09 -197.5;...
  315.3 315.3 315.3 -151 -66.17 0 -337;...
  529 529 529 88.63 284.4 1179 0];
%Group interaction parameters f(i,j)
for i=1:7
  for j=1:7
    psi(i,j)=exp(-a(i,j)./T);
  end
end
%*****CALCULATION AT
EQUILIBRIUM*****
%Finding the Combinatorial Part Gamma of UNIFAC at equilibrium
%-----
% lnG_comb = lnPhi/xi+(z/2)qi ln(Theta/Phi)+Li-(Phi/xi)sum(xiLi)
%*****
%Determined mole fraction of component i
%at equilibrium xe(i)xe1=(m-xae)/(1+m+n);
xe1=(m-xae)/(1+m+n);
xe2=(1-xae)/(1+m+n);
xe3=xae/(1+m+n);
xe4=(n+xae)/(1+m+n);
xe=[xe1 xe2 xe3 xe4];
%molecular surface area fr.(theta) and molecular volume fr.(phi)
for i=1:4
  thetae(i)=xe(i).*q(i)./(xe(1).*q(1)+xe(2).*q(2)+xe(3).*q(3)+xe(4).*q(4));
  phie(i)=xe(i).*r(i)./(xe(1).*r(1)+xe(2).*r(2)+xe(3).*r(3)+xe(4).*r(4));
end
  SumxeLe=xe(1).*L(1)+xe(2).*L(2)+xe(3).*L(3)+xe(4).*L(4);
  for i=1:4
    lnG_Comb(i)=(log(phie(i)./xe(i))+(z/2).*q(i).*log(thetae(i)./phie(i))
    ...
      +L(i)-(phie(i)./xe(i)).*SumxeLe);
  end
%*****
%Finding the Residual Part Gamma of UNIFAC at equilibrium
%-----
% lnG_Res=Sigma Vk(i) (lnTk-lnTki)
%-----
%Vk(i)is number of functional group of type k in molecule i
%Tk is activity coefficient of group k
%Tki is activity coefficient of group k in pure component i
%*****
%Mole fraction of group m(k=1-7) in mixture i, X,mi
%Molecular surface area fraction of group m(k=1-7) in mixture i,
Thi,mi
%Set m --> CH3=1, CH2=2, CH=3, OH=4, H2O=5, COOH=6, COO=7

```

```

%*****
*****
%for component 1: BuOH = 1CH3.3CH2.1OH
X11=1/5;
X21=3/5;
X41=1/5;
Thi11=Qk(1).*X11/(Qk(1).*X11+Qk(2).*X21+Qk(4).*X41);
Thi21=Qk(2).*X21/(Qk(1).*X11+Qk(2).*X21+Qk(4).*X41);
Thi41=Qk(4).*X41/(Qk(1).*X11+Qk(2).*X21+Qk(4).*X41);
%for component 2: LA = 1CH3.1CH.1OH.1COOH
Thi12=Qk(1)./(Qk(1)+Qk(3)+Qk(4)+Qk(6));
Thi32=Qk(3)./(Qk(1)+Qk(3)+Qk(4)+Qk(6));
Thi42=Qk(4)./(Qk(1)+Qk(3)+Qk(4)+Qk(6));
Thi62=Qk(6)./(Qk(1)+Qk(3)+Qk(4)+Qk(6));
%for component 3: BuLA = 2CH3.3CH2.1CH.1OH.1COO
X13=2/8;
X23=3/8;
X33=1/8;
X43=1/8;
X73=1/8;
Thi13=Qk(1).*X13./(Qk(1).*X13+Qk(2).*X23+Qk(3).*X33+Qk(4).*X43+Qk(7).*X73);
Thi23=Qk(2).*X23./(Qk(1).*X13+Qk(2).*X23+Qk(3).*X33+Qk(4).*X43+Qk(7).*X73);
Thi33=Qk(3).*X33./(Qk(1).*X13+Qk(2).*X23+Qk(3).*X33+Qk(4).*X43+Qk(7).*X73);
Thi43=Qk(4).*X43./(Qk(1).*X13+Qk(2).*X23+Qk(3).*X33+Qk(4).*X43+Qk(7).*X73);
Thi73=Qk(7).*X73./(Qk(1).*X13+Qk(2).*X23+Qk(3).*X33+Qk(4).*X43+Qk(7).*X73);
%for component 4: W = 1H2O
Thi54=1;
%finding lnGmi
%Set k--> CH3=1, CH2=2, CH=3, OH=4, H2O=5, COOH=6, COO=7
%For component 1: BuOH = 1CH3.3CH2.1OH
S11=Thi11.*psi(1,1)+Thi21.*psi(2,1)+Thi41.*psi(4,1);
S21=Thi11.*psi(1,2)+Thi21.*psi(2,2)+Thi41.*psi(4,2);
S41=Thi11.*psi(1,4)+Thi21.*psi(2,4)+Thi41.*psi(4,4);
Tk11=Qk(1).*(1-
log(Thi11.*psi(1,1)+Thi21.*psi(2,1)+Thi41.*psi(4,1))...
-(Thi11.*psi(1,1)./S11)-(Thi21.*psi(1,2)./S21)-
(Thi41.*psi(1,4)./S41));
Tk21=Qk(2).*(1-
log(Thi11.*psi(1,2)+Thi21.*psi(2,2)+Thi41.*psi(4,2))...
-(Thi11.*psi(2,1)./S11)-(Thi21.*psi(2,2)./S21)-
(Thi41.*psi(2,4)./S41));
Tk41=Qk(4).*(1-
log(Thi11.*psi(1,4)+Thi21.*psi(2,4)+Thi41.*psi(4,4))...
-(Thi11.*psi(4,1)./S11)-(Thi21.*psi(4,2)./S21)-
(Thi41.*psi(4,4)./S41));
%for component 2: LA = 1CH3.1CH.1OH.1COOH
S12=Thi12.*psi(1,1)+Thi32.*psi(3,1)+Thi42.*psi(4,1)+Thi62.*psi(6,1);
S32=Thi12.*psi(1,3)+Thi32.*psi(3,3)+Thi42.*psi(4,3)+Thi62.*psi(6,3);
S42=Thi12.*psi(1,4)+Thi32.*psi(3,4)+Thi42.*psi(4,4)+Thi62.*psi(6,4);
S62=Thi12.*psi(1,6)+Thi32.*psi(3,6)+Thi42.*psi(4,6)+Thi62.*psi(6,6);
Tk12=Qk(1).*(1-log(Thi12.*psi(1,1)+Thi32.*psi(3,1)+Thi42.*psi(4,1)...
+Thi62.*psi(6,1))-(Thi12.*psi(1,1)./S12)-
(Thi32.*psi(1,3)./S32)...

```

```

- (Thi42.*psi(1,4)./S42) - (Thi62.*psi(1,6)./S62));
Tk32=Qk(3).*(1-log(Thi12.*psi(1,3)+Thi32.*psi(3,3)+Thi42.*psi(4,3)...
+Thi62.*psi(6,3)) - (Thi12.*psi(3,1)./S12) -
(Thi32.*psi(3,3)./S32)...
- (Thi42.*psi(3,4)./S42) - (Thi62.*psi(3,6)./S62));
Tk42=Qk(4).*(1-log(Thi12.*psi(1,4)+Thi32.*psi(3,4)+Thi42.*psi(4,4)...
+Thi62.*psi(6,4)) - (Thi12.*psi(4,1)./S12) -
(Thi32.*psi(4,3)./S32)...
- (Thi42.*psi(4,4)./S42) - (Thi62.*psi(4,6)./S62));
Tk62=Qk(6).*(1-log(Thi12.*psi(1,6)+Thi32.*psi(3,6)+Thi42.*psi(4,6)...
+Thi62.*psi(6,6)) - (Thi12.*psi(6,1)./S12) -
(Thi32.*psi(6,3)./S32)...
- (Thi42.*psi(6,4)./S42) - (Thi62.*psi(6,6)./S62));
%for component 3: BuLA= 2CH3.3CH2.1CH.1OH.1COO
S13=Thi13.*psi(1,1)+Thi23.*psi(2,1)+Thi33.*psi(3,1)...
+Thi43.*psi(4,1)+Thi73.*psi(7,1);
S23=Thi13.*psi(1,2)+Thi23.*psi(2,2)+Thi33.*psi(3,2)...
+Thi43.*psi(4,2)+Thi73.*psi(7,2);
S33=Thi13.*psi(1,3)+Thi23.*psi(2,3)+Thi33.*psi(3,3)...
+Thi43.*psi(4,3)+Thi73.*psi(7,3);
S43=Thi13.*psi(1,4)+Thi23.*psi(2,4)+Thi33.*psi(3,4)...
+Thi43.*psi(4,4)+Thi73.*psi(7,4);
S73=Thi13.*psi(1,7)+Thi23.*psi(2,7)+Thi33.*psi(3,7)...
+Thi43.*psi(4,7)+Thi73.*psi(7,7);
Tk13=Qk(1).*(1-log(Thi13.*psi(1,1)+Thi23.*psi(2,1)+Thi33.*psi(3,1)...
+Thi43.*psi(4,1)+Thi73.*psi(7,1))...
- (Thi13.*psi(1,1)./S13) - (Thi23.*psi(1,2)./S23)...
- (Thi33.*psi(1,3)./S33) - (Thi43.*psi(1,4)./S43) -
(Thi73.*psi(1,7)./S73));
Tk23=Qk(2).*(1-log(Thi13.*psi(1,2)+Thi23.*psi(2,2)+Thi33.*psi(3,2)...
+Thi43.*psi(4,2)+Thi73.*psi(7,2))...
- (Thi13.*psi(2,1)./S13) - (Thi23.*psi(2,2)./S23)...
- (Thi33.*psi(2,3)./S33) - (Thi43.*psi(2,4)./S43) -
(Thi73.*psi(2,7)./S73));
Tk33=Qk(3).*(1-log(Thi13.*psi(1,3)+Thi23.*psi(2,3)+Thi33.*psi(3,3)...
+Thi43.*psi(4,3)+Thi73.*psi(7,3))...
- (Thi13.*psi(3,1)./S13) - (Thi23.*psi(3,2)./S23)...
- (Thi33.*psi(3,3)./S33) - (Thi43.*psi(3,4)./S43) -
(Thi73.*psi(3,7)./S73));
Tk43=Qk(4).*(1-log(Thi13.*psi(1,4)+Thi23.*psi(2,4)+Thi33.*psi(3,4)...
+Thi43.*psi(4,4)+Thi73.*psi(7,4))...
- (Thi13.*psi(4,1)./S13) - (Thi23.*psi(4,2)./S23)...
- (Thi33.*psi(4,3)./S33) - (Thi43.*psi(4,4)./S43) -
(Thi73.*psi(4,7)./S73));
Tk73=Qk(7).*(1-log(Thi13.*psi(1,7)+Thi23.*psi(2,7)+Thi33.*psi(3,7)...
+Thi43.*psi(4,7)+Thi73.*psi(7,7))...
- (Thi13.*psi(7,1)./S13) - (Thi23.*psi(7,2)./S23)...
- (Thi33.*psi(7,3)./S33) - (Thi43.*psi(7,4)./S43) -
(Thi73.*psi(7,7)./S73));
%for component 4: W= 1H2O
Tk54=Qk(5).*(1-log(Thi54.*psi(5,5)) -
(Thi54.*psi(5,5)/Thi54.*psi(5,5)));
%*****
%Finding mole fraction of group m
xte=5.*xe(1)+4.*xe(2)+8.*xe(3)+xe(4);
for i=1:7 %i=k
if i==1
Xe(i)=(xe(1)+xe(2)+2*xe(3))./xte;

```

```

elseif i==2
    Xe(i)=(3.*xe(1)+3.*xe(3))./xte;
elseif i==3
    Xe(i)=(xe(2)+xe(3))./xte;
elseif i==4
    Xe(i)=(xe(1)+xe(2)+xe(3))./xte;
elseif i==5
    Xe(i)=xe(4)./xte;
elseif i==6
    Xe(i)=xe(2)./xte;
else
    Xe(i)=xe(3)./xte;
end
end
%Area fraction of group m (k=1:7)
Thie=Qk(1).*Xe(1)+Qk(2).*Xe(2)+Qk(3).*Xe(3)+Qk(4).*Xe(4)...
    +Qk(5).*Xe(5)+Qk(6).*Xe(6)+Qk(7).*Xe(7);
for i=1:7 %i=k
The(i)=Qk(i).*Xe(i)./Thie;
end
for i=1:7
Se(i)=The(1).*psi(1,i)+The(2).*psi(2,i)+The(3).*psi(3,i)...
+The(4).*psi(4,i)+The(5).*psi(5,i)+The(6).*psi(6,i)+The(7).*psi(7,i);
end
for i=1:7
Tke(i)=Qk(i).*(1-
log(The(1).*psi(1,i)+The(2).*psi(2,i)+The(3).*psi(3,i)...
+The(4).*psi(4,i)+The(5).*psi(5,i)+The(6).*psi(6,i)+The(7).*psi(7,i))
...
-(The(1).*psi(i,1)./Se(1))-The(2).*psi(i,2)./Se(2))...
-(The(3).*psi(i,3)./Se(3))-The(4).*psi(i,4)./Se(4))...
-(The(5).*psi(i,5)./Se(5))-The(6).*psi(i,6)./Se(6))...
-(The(7).*psi(i,7)./Se(7)));
end
%Finding lnG_Res
lnG_Res(1)=(Tke(1)-Tk11)+3.*(Tke(2)-Tk21)+(Tke(4)-Tk41);
lnG_Res(2)=(Tke(1)-Tk12)+(Tke(3)-Tk32)+(Tke(4)-Tk42)+(Tke(6)-Tk62);
lnG_Res(3)=2.*(Tke(1)-Tk13)+3.*(Tke(2)-Tk23)+(Tke(3)-Tk33)+(Tke(4)-
Tk43)+(Tke(7)-Tk73);
lnG_Res(4)=(Tke(5)-Tk54);
%-----
%Find activity coefficient and activity at equilibrium
%-----
for i=1:4
gammaEq(i)=exp(lnG_Comb(i)+lnG_Res(i)); %activity coefficient
acte(i)=xe(i).*gammaEq(i); %activity
end
%-----
%Find Equilibrium constant, Ke
%-----
Ke=acte(3).*acte(4)./(acte(1).*acte(2))

%*****END FOR EQUILIBRIUM CALCULATION*****
%*****START FOR ODES*****
%Find mole fraction x(i) as a function of conversion (xa)
x1=(m-xa(1))/(1+m+n);

```

```

x2=(1-xa(1))/(1+m+n);
x3=xa(1)/(1+m+n);
x4=(n+xa(1))/(1+m+n);
x=[x1 x2 x3 x4];
%*****For Combinatorial
Part*****
%Find volume fraction (Phi) and area fraction (Theta) for component i
for i=1:4
phi(i)=x(i).*r(i)./(x(1).*r(1)+x(2).*r(2)+x(3).*r(3)+x(4).*r(4));
theta(i)=x(i).*q(i)./(x(1).*q(1)+x(2).*q(2)+x(3).*q(3)+x(4).*q(4));
end
%Activity coefficient for combinatorial part (ln gammaC)
sumxL=x(1).*L(1)+x(2).*L(2)+x(3).*L(3)+x(4).*L(4);
for i=1:4
    if x(i)==0
        lnG_C(i)=0;
    else
lnG_C(i)=log(phi(i)./x(i))+(z/2).*q(i).*log(theta(i)./phi(i))...
        +L(i)-((phi(i)./x(i)).*sumxL);
    end
end
%*****For Residual Part*****
%mole fraction of group m (k=1-7)
xt=5.*x(1)+4.*x(2)+8.*x(3)+x(4);
for i=1:7 %i=k
    if i==1
        X(i)=(x(1)+x(2)+2.*x(3))./xt;
    elseif i==2
        X(i)=(3.*x(1)+3.*x(3))./xt;
    elseif i==3
        X(i)=(x(2)+x(3))./xt;
    elseif i==4
        X(i)=(x(1)+x(2)+x(3))./xt;
    elseif i==5
        X(i)=x(4)./xt;
    elseif i==6
        X(i)=x(2)./xt;
    else
        X(i)=x(3)./xt;
    end
end
%area fraction of group m (k=1:7)
ThT=Qk(1).*X(1)+Qk(2).*X(2)+Qk(3).*X(3)+Qk(4).*X(4)+Qk(5).*X(5)...
    +Qk(6).*X(6)+Qk(7).*X(7);
for i=1:7 %i=k
    Th(i)=Qk(i).*X(i)./ThT;
end
for i=1:7
    B(i)=Th(1).*psi(1,i)+Th(2).*psi(2,i)+Th(3).*psi(3,i)...
    +Th(4).*psi(4,i)+Th(5).*psi(5,i)+Th(6).*psi(6,i)+Th(7).*psi(7,i);
end
for i=1:7
G(i)=Qk(i).*(1-log(Th(1).*psi(1,i)+Th(2).*psi(2,i)+Th(3).*psi(3,i)...
    +Th(4).*psi(4,i)+Th(5).*psi(5,i)+Th(6).*psi(6,i)+Th(7).*psi(7,i))...
    -Th(1).*psi(i,1)./B(1)-Th(2).*psi(i,2)./B(2)-
    Th(3).*psi(i,3)./psi(3)...

```

```

    -Th(4).*psi(i,4)./B(4)-Th(5).*psi(i,5)./B(5)-
    Th(6).*psi(i,6)./B(6)...
    -Th(7).*psi(i,7)./B(7));
end
%find gammaR
lnG_R(1)=(G(1)-Tk11)+3.*(G(2)-Tk21)+(G(4)-Tk41);
lnG_R(2)=(G(1)-Tk12)+(G(3)-Tk32)+(G(4)-Tk42)+(G(6)-Tk62);
lnG_R(3)=2.*(G(1)-Tk13)+3.*(G(2)-Tk23)+(G(3)-Tk33)+(G(4)-Tk43)+(G(7)-
Tk73);
lnG_R(4)=(G(5)-Tk54);
%-----
%Finding activity coefficient and activity
%-----
for i=1:4
gamma(i)=exp(lnG_C(i)+lnG_R(i)); %activity coefficient
act(i)=x(i).*gamma(i); %activity
end

%-----Kinetic Model-----
%Pseudo-Homogeneous modelH Model
dxa=k.*(mc./na0).*(act(1).*act(2)-(act(3).*act(4)./Ke));
%-----
%k=rate constant
%k1=adsorption constant of 1-butanol(comp1)
%k2=adsorption constant of lactic acid (comp2)
%k3=adsorption constant of butyl lactate (comp3)
%k4=adsorption constant of water (comp4)
%-----
%Eley-Rideal (ER) model with surface reaction is the limitng
%LA ann water adsorption terms
%dxa=k.*(mc./na0).*(act(1).*act(2)-
(act(3).*act(4)./Ke))./(1+k2.*act(2)+k4.*act(4));
%-----
%Langmuir Hinsherwood (ER) model with surface reaction is the limitng
%LH 4 components
dxa=k.*(mc./na0).*(act(1).*act(2)-
(act(3).*act(4)./Ke))./((1+k1.*act(1)+k2.*act(2)+k3.*act(3)+k4.*act(4)
).^2);

end

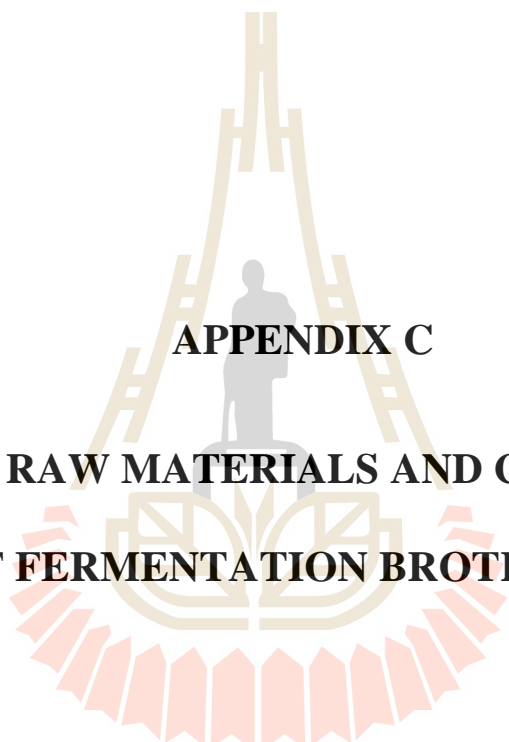
```

B.3 Minimizing Program

```

k0=[0.1]; %initial guess
lb=[];
ub=[];
%-----Using lsqnonlin-----
options = optimset('Display','iter','Tolx',1e-14,'TolFun',1e-16);
[kcal,resnorm,residual,exitflag,output]=lsqnonlin(@obfunction,k0,lb,u
b,options)

```



APPENDIX C

**PRICE OF RAW MATERIALS AND CALCULATION
OF FERMENTATION BROTH COST**

มหาวิทยาลัยเทคโนโลยีสุรนารี

C.1 Price of Chemicals and Raw Materials

Price of chemicals used to be the composition in MRS culture media and raw materials of fermentation broth is listed in Table C.1

Table C.1 Price of chemicals and raw materials

Chemicals and materials	Source	Unit	Price/unit
Proteose peptone	Guangzhou Ikeme Technology	g	0.0556
HM peptone B	Guangdong Huankai Microbial Sci.	g	0.007
Yeast extract	Angel Yeast	g	0.003
Dextrose (Glucose)	Inner Mongolia Dixing Chemical	g	0.0004
Polysorbate 80 (Tween 80)	Itrade Chemical(jiangsu)	g	0.0022
Ammonium citrate	Hangzhou Showland Technology	g	0.001
Sodium acetate	Lanzhou A.T.V. Trading	g	0.0001
Magnesium sulphate	Tianjin Chengyuan Chemical	g	0.0001
Manganese sulphate	Zhengzhou Sino Chemical	g	0.0004
Dipotassium Hydrogen phosphate	Nanjing Jiayi Sunway Chemical	g	0.001
Cassava	North Eastern Tapioca Trade	kg	0.0672
Cellulase Enzyme (Ctec)	Shandong Sukahan Bio-Technology	g	0.001
Water RO	Khunchon Technology	L	0.0319
calcium carbonate	Xiamen Xingyan Chemicals	kg	0.1
Sodium alginate	Haihang Industry (jinan)	g	0.001
Aluminum Chloride anhydrous	Hebi Taihang Technology	g	0.0005
Amberlyst -15	BOSS CHEMICAL INDUSTRY	kg	45
1-Butanol 99%	Beijing Huamaoyuan Fragrance	kg	0.1

C.2 Cost of MRS Culture Media

Himedia MRS culture media was assumed to used in preparation of fermentation broth. The standard ratio of prepared media is 55.15g/L, which is the cost calculated and showed in Table C.2

Table C.2 Himedia MRS culture media cost

Ingredient	Amount (g/L)	Cost (USD)
Proteose peptone	10	0.5556
HM peptone B	10	0.0700
Yeast extract	5	0.0150
Dextrose (Glucose)	20	0.0074
Polysorbate 80 (Tween 80)	1	0.0022
Ammonium citrate	2	0.0020
Sodium acetate	5	0.0005
Magnesium sulphate	0.1	0.0000
Manganese sulphate	0.05	0.0000
Dipotassium Hydrogen phosphate	2	0.0020
Total	55.15	0.6547

C.3 Cost of Fermentation Broth

This work assumed the amount of each raw material used in fermentation broth preparation by following Boontawan et al. (2019). Approximately 5L of fermentation broth will be obtained by using each materials as detailed in Table 5.4 and cost of fermentation broth can be calculated as shown in Table C.3.

Table C.3 Calculated cost of fermentation broth

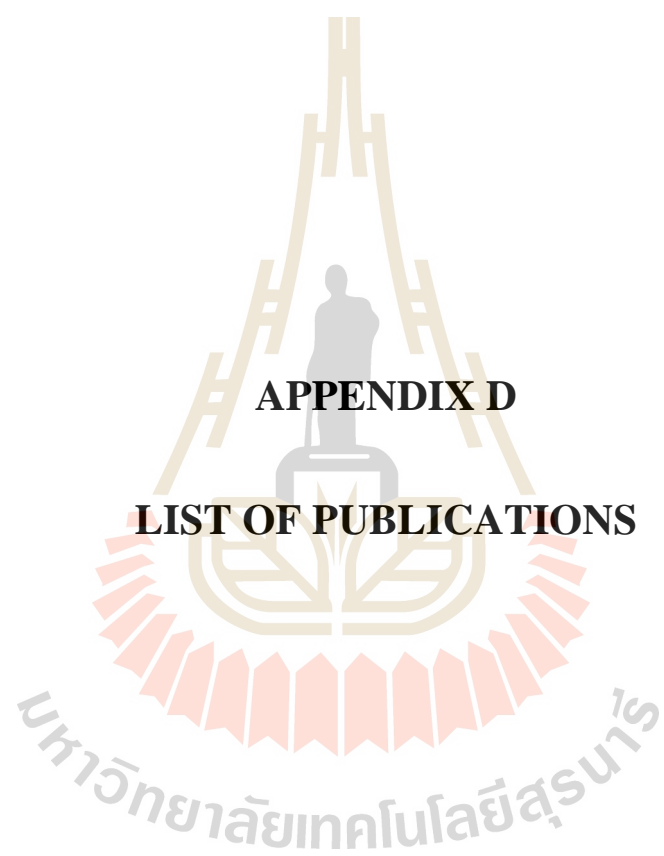
Raw materials	Unit	Price (USD/unit)	Amount	Cost (USD)
Cassava	kg	0.0672	1	0.0672
Cellulase Enzyme (Ctec)	g	0.0010	5	0.0050
Water RO	L	0.0319	3	0.0957
MRS	g	0.0119	2.7575	0.0327
Calcium carbonate	kg	0.1000	0.0025	0.0003
Total cost per 5L				0.2009
Total cost per 1L				0.0402

C.4 Cost of Aluminum Alginate catalyst

According to using aluminum alginate as a solid catalyst in the reactive distillation, so cost of this catalyst was calculated based on raw materials in its preparation as detailed in Chapter III. Based on the preparation, approximately amount 2 g of aluminum alginate catalyst can be obtained and its cost can be calculated as shown in Table C.4

Table C.4 Calculated cost of aluminum alginate catalyst

Raw materials	Unit	Price (USD/unit)	Amount	Cost (USD)
Sodium alginate	g	0.001	2	0.0020
Aluminum chloride	g	0.0005	1.3334	0.0007
Water	L	0.0319	0.1	0.0032
Total cost per 2 g				0.0059
Total cost per 1 kg				2.9284



APPENDIX D

LIST OF PUBLICATIONS

List of Publications

- Chawong, K., Daengpradab, B., and Rattanaphanee, P. (2017). Liquid–Liquid Equilibrium of Water +1-Butanol + Inorganic Salt Systems at 303.15, 313.15 and 323.15 K: Experiments and Correlation. **J Solution Chem.** 46:1077-1091.
- Chawong, K., Poncharee, C., Daengpradab, B., and Rattanaphanee, P. (2017). Kinetic Study of Aluminum – Alginate Catalyzed Esterification of Lactic Acid with 1-Butanol. **AJChE.** 17(1):22-28.
- Chawong, K., Deangpradab, B., Rattanaphanee, P. (2016). Aluminum alginate as a solid catalyst for esterification of lactic acid with 1-butanol. **KKU Engineering Journal.** 43: 236-238.
- Chawong, K., Rayabsri, C., Rattanaphanee, P. (2015). Extraction of lactic acid in mixed solvent electrolyte system containing water, 1-butanol and ammonium sulfate. **Int. J. Chem. React. Eng.** 13(2): 183-188.



Liquid–Liquid Equilibrium of Water + 1-Butanol + Inorganic Salt Systems at 303.15, 313.15 and 323.15 K: Experiments and Correlation

Kanungnit Chawong¹ · Boonpradab Daengpradab¹ · Panarat Rattanaphanee¹

Received: 12 November 2016 / Accepted: 22 March 2017 / Published online: 8 May 2017
© Springer Science+Business Media New York 2017

Abstract Liquid–liquid equilibria (LLE) and tie-line data of systems containing 1-butanol, water and NaCl, Na₂SO₄, NH₄Cl or (NH₄)₂SO₄ were investigated at 303.15, 313.15 and 323.15 K and atmospheric pressure. The salt decreases mutual solubilities of these two solvents leading to a higher degree of phase separation at equilibrium. The effect is more pronounced at high salt concentration. Temperature in the studied range had a minor effect on LLE behavior of these mixtures. Experimental data were correlated using a modified extended UNIQUAC model. Satisfactory agreement between the calculated and measured mass fractions of the components was achieved.

Keywords Liquid–liquid equilibrium · Modified extended UNIQUAC model · Salting out · 1-Butanol

Nomenclature

Symbols

a	Binary interaction parameter
G^E	Excess Gibbs energy
K	Partition coefficient
M	Number of tie lines
N	Number of components
n	Number of ions
q	Surface area parameter
R	Gas constant (J·mol ⁻¹ ·K ⁻¹)
r	Volume parameter
T	Temperature (K)

✉ Panarat Rattanaphanee
panarat@sut.ac.th

¹ School of Chemical Engineering, Institute of Engineering, Suranaree University of Technology, Nakhon Ratchasima, Thailand

- w Mass fraction
 γ Activity coefficient for a component

Subscripts

i, j, k Component i, j, k

Superscripts/subscripts

PDH	Pitzer–Debye–Hückel term
UNIQUAC	UNIQUAC term
Born	Born term
I	Equilibrium aqueous phase
II	Equilibrium organic phase
exp	Experimental value
calc	Calculated value

1 Introduction

Biologically produced butanol has gained interest from its possible application as renewable fuel for internal combustion engines. Butanol has a larger calorific value and lower hygroscopicity than ethanol. Its longer carbon chain also makes it closer to gasoline than ethanol is and it can be used as a 100% bio-butanol fuel [1]. This great potential, consequently, leads to the projection of growing global market of it in the near future [2]. Currently, bio-butanol is produced by the acetone–butanol–ethanol (ABE) fermentation process using a variety of carbohydrate containing materials as feedstock.

One of the core challenges in the commercial production of bio-butanol is, however, how to recover and purify it from the fermentation broth efficiently and economically. Distillation appears to be inefficient for this purpose as it is very energy-intensive and not suitable for separation of the desired solute, which is presented in the highly impure fermentation media at low concentration [3]. Amongst several separation techniques being investigated, solvent extraction appears to be a quite promising approach. Nevertheless, reliable experimental data and accurate thermodynamic models describing the LLE behavior of mixtures of water and 1-butanol are crucial for the successful design of this process. Since several inorganic salts are normally present in the fermentation broth, their effect on the LLE behavior should also be considered.

The influence of inorganic salts or electrolytes on the equilibrium behavior of mixtures containing water and butanol has been frequently investigated [4–12]. Several thermodynamic models have even been specifically developed and examined in predicting the LLE behavior of such systems. The conventional UNIQUAC model contains only two terms: a combinatorial term concerning “shape differences” that represents a deviation from ideality of the system, and a residual term focusing on the interactions between molecules. This model does not take into account the long-range forces resulting from electrostatic interaction between the ionic solutes and the solvents. As a result, it typically gives unsatisfactory agreement in the correlation of systems containing electrolytes.

Sander et al. in 1986 [13] introduced an extended UNIQUAC model, which was derived by adding a Debye–Hückel term to its conventional counterpart. The model, which has been continually adjusted, has demonstrated its potential for describing the phase equilibria and thermal properties of aqueous solutions containing electrolytes and non-electrolytes. Pirahmadi et al. [7] further modified this model to study the LLE behavior of the

1-butanol + water + NaNO_3 system at 298.15 and 308.15 K and the 1-butanol + water + NH_4Cl system at 298.15, 308.15 and 318.15 K [8]. In their work, the modified extended UNIQUAC model, consisting the original UNIQUAC term, a Pitzer–Debye–Hückel term and a Born term, appeared to calculate the LLE of such systems slightly better than the original extended UNIQUAC model. Nonetheless, most of their work and the other work in this area so far concern only systems with monovalent ions such as Na^+ , NH_4^+ , Cl^- , and NO_3^- . Experimentally determined model parameters for systems containing divalent ions are thus scarce, despite reports indicating that divalent ions are more effective in altering the equilibrium composition of the organic–aqueous systems than the monovalent ions [14].

In this study, the effect of NaCl , Na_2SO_4 , NH_4Cl and $(\text{NH}_4)_2\text{SO}_4$ on the LLE of water + 1-butanol mixtures at 303.15, 313.15 and 323.15 K was measured. It was found that both sulfate salts decreased the mutual solubility between water and 1-butanol and induced their phase separation more than did the chloride salts. Experimental data were correlated by a modified extended UNIQUAC model. The tie-line compositions and binary interaction parameters for the systems with sulfate salts were determined.

2 Materials and Method

2.1 Chemicals

1-Butanol, ACS reagent grade with mass fraction purity ≥ 0.995 , was purchased from Acros. Ammonium sulfate ($(\text{NH}_4)_2\text{SO}_4$), sodium sulfate (Na_2SO_4), ammonium chloride (NH_4Cl) and sodium chloride (NaCl) were obtained from Carlo Erba. All the salts were of RPE grade with mass fraction purity ≥ 0.995 . All chemicals were used as received, without further purification. Deionized water was used in every experiment.

2.2 Solubility of Salts in Water and 1-Butanol

In order to verify the accuracy and reproducibility of our experimental procedure, the solubilities of the inorganic salts in water and in 1-butanol were measured first. An excess amount of each salt was dissolved in 75 mL of the corresponding solvent. Some solutions were briefly heated in order to facilitate dissolution of excess salt. The solution was then agitated at the desired temperature for 24 h before being kept still for another 12 h to allow complete solid–liquid phase separation. The temperature precision of the shaking and settling bath was ± 0.10 K. To measure the salt solubility in each solvent, about 25 mL of the clear solution was quickly transferred to another pre-weighed test tube. Solid contents of the solutions were determined gravimetrically after drying.

2.3 Salt Effect on the LLE of the Water + 1-Butanol System

In this study, the LLE data of water + 1-butanol + salt systems were determined by direct analysis of the phase concentrations after the mixtures were fully mixed and settled to allow complete phase separation. Each experiment was started by mixing pre-weighed quantities of the components. The mixtures were then shaken vigorously in a thermostatic shaking bath with ± 0.10 K temperature control precision. Based on our preliminary study to determine the proper time for mixing and complete phase separation, the shaking and

Table 1 Solubility of NaCl, NH₄Cl, Na₂SO₄ and (NH₄)₂SO₄ in water and 1-butanol in the temperature range 303.15–353.15 K under an atmospheric pressure of 98.9 kPa

Temperature (K)	Solubility of salt in water [S , $\text{g}_{\text{salt}} \cdot (100 \text{ g}_{\text{water}})^{-1}$]							
	NaCl		Na ₂ SO ₄		NH ₄ Cl		(NH ₄) ₂ SO ₄	
	This work	Ref. [10]	This work	Ref. [10]	This work	Ref. [10]	This work	Ref. [10]
303.15	36.05	36.03	39.62	40.8	39.95	41.4	78.09	78.0
313.15	36.54	36.60	48.71	48.8	44.73	45.8	80.66	81.0
323.15	36.82	36.67	46.65	46.7	49.89	50.4	83.96	n/a
333.15	37.43	37.06	45.31	45.3	54.84	55.2	87.81	88.0
343.15	37.71	37.8	44.38	n/a	59.78	60.2	90.57	n/a
353.15	38.25	38.4	43.68	43.7	65.02	65.6	94.76	95.3

Temperature (K)	Solubility of salt in 1-butanol [S , $\text{g} \cdot (100 \text{ g} \text{ 1-butanol})^{-1}$]				
	NaCl		Na ₂ SO ₄	NH ₄ Cl	(NH ₄) ₂ SO ₄
	This work	Ref. [16]			
303.15	0.0062	n/a	ND ^a	0.0762	ND
313.15	0.0070	0.0070	ND	0.0904	ND
323.15	0.0077	0.0077	ND	0.0946	ND
333.15	0.0084	n/a	0.0014	0.1069	0.0034
343.15	0.0097	n/a	0.0024	0.1211	0.0063
353.15	0.0111	n/a	0.0038	0.1391	0.0102

Standard deviation of the solubility measurement is $\leq 0.25\%$. Standard uncertainties u are $u(T) = 0.10 \text{ K}$, $u(p) = 0.2 \text{ kPa}$, and $u(S) = 0.01 \text{ g}$ for the solubility in water and $u(S) = 0.0001 \text{ g}$ for the solubility in 1-butanol

^a ND means no salt was detected and it is regarded as the salt being insoluble in 1-butanol at that temperature

settling time were 24 and 12 h, respectively. To measure the phase composition, samples were carefully withdrawn from the upper and the lower phases of the mixtures after equilibration and component analysis was then performed.

Concentrations of 1-butanol were analyzed using a Shimadzu gas chromatography (GC)-14B equipped with a flame ionization detector (FID) using helium of 99.999% purity as the carrier gas. A TR-FFAP capillary column with length \times inside diameter (ID) of 30 m \times 0.53 mm was used. The oven temperature was initially held at 323.15 K for 3 min before being increased to 503.15 K at a rate of 10 K \cdot min⁻¹ and held for 4 min. The temperature of the injector and the detector were 523.15 K. Every sample was diluted with deionized water before analysis. The injection volume was 1 μ L.

Water content in each sample was analyzed using a Chrompack CP-3380 GC (Varian) equipped with a stainless steel column packed with Chromosorb 102 80/100 and a thermal conductivity detector (TCD). The column length \times ID was 2 m \times 0.32 cm. Helium of 99.999% purity was used as the carrier gas with a flow rate of 6.5 mL \cdot min⁻¹. The oven temperature was kept constant at 373.15 K. The injection temperature was 373.15 K, and the detector temperature was 523.15 K. Each sample was diluted with deionized water before analysis. The injection volume was also 1 μ L.

Table 2 Measured liquid–liquid equilibrium data of the water(1) + 1-butanol(2) + NaCl(3) system at 303.15, 313.15 and 323.15 K and an under atmospheric pressure of 98.9 kPa

Temperature (K)	Aqueous phase			Organic phase			K
	%w ₁₁	%w ₂₁	%w ₃₁	%w ₁₂	%w ₂₂	%w ₃₂	
303.15	92.98	7.02	0.00	20.71	79.29	0.00	11.30
	91.84	7.12	1.04	14.68	85.30	0.02	11.98
	91.11	6.18	2.71	13.21	86.75	0.04	14.04
	90.00	4.80	5.20	10.15	89.77	0.08	18.70
	86.93	3.20	9.87	8.51	91.37	0.12	28.67
	80.58	1.69	17.73	6.89	92.95	0.16	55.00
	74.59	1.13	24.28	6.56	93.26	0.18	82.53
313.15	93.23	6.77	0.00	22.47	77.53	0.00	11.45
	92.41	6.46	1.13	14.22	85.76	0.02	13.28
	91.48	5.76	2.75	12.22	87.74	0.04	15.23
	90.04	4.62	5.34	11.97	87.95	0.08	19.04
	86.60	3.42	9.98	8.77	91.10	0.13	26.64
	80.10	1.93	17.97	7.43	92.39	0.18	47.87
	74.30	1.15	24.55	6.41	93.35	0.24	81.17
323.15	93.41	6.53	0.00	23.87	76.13	0.00	11.66
	91.19	7.67	1.13	22.60	77.36	0.04	10.09
	90.62	6.59	2.79	16.76	83.20	0.04	12.63
	89.28	5.43	5.29	14.44	85.49	0.07	15.74
	86.41	3.63	9.96	12.16	87.71	0.13	24.16
	79.98	2.10	17.92	8.06	91.75	0.18	43.69
	74.94	1.07	23.99	7.87	91.91	0.22	85.90

Standard uncertainties u are $u(T) = 0.10$ K, $u(p) = 0.2$ kPa, and $u(w) = 0.01$ g

The last portion of the samples was weighed and dried at 393.15 K for 12 h to completely remove all the liquid. Salt content was determined from the residue mass. Every experiment and analysis was carried out under atmospheric pressure of 98.9 ± 0.2 kPa and was repeated at least 3 times with the target standard deviation $<0.25\%$. The results are reported here as average value obtained from the valid experiments.

3 Results and Discussion

3.1 Solubility of Salts in Water and 1-Butanol

Water and 1-butanol are partially miscible by nature. Data for their mutual solubility have been well documented [15]. In this study, the solubilities of NaCl, Na₂SO₄, NH₄Cl and (NH₄)₂SO₄ in water and in 1-butanol were measured in the temperature range 303.15–353.15 K. The results are presented in Table 1. The quality of the measurements was judged by comparing them with available published data. The solubility of each salt in both solvents was found to increase with increasing temperature. As expected, each salt

Table 3 Measured liquid–liquid equilibrium data of the water(1) + 1-butanol(2) + NH_4Cl (3) system at 303.15, 313.15 and 323.15 K under an atmospheric pressure of 98.9 kPa

Temperature (K)	Aqueous phase			Organic phase			K
	%w ₁₁	%w ₂₁	%w ₃₁	%w ₁₂	%w ₂₂	%w ₃₂	
303.15	92.98	7.02	0.00	20.71	79.29	0.00	11.30
	92.21	6.69	1.10	15.20	84.75	0.05	12.67
	90.68	6.42	2.90	12.71	87.21	0.07	13.58
	89.10	5.63	5.27	11.11	88.72	0.17	15.76
	87.24	4.35	8.40	9.87	89.78	0.35	20.64
	82.29	2.68	15.03	7.72	91.74	0.54	34.23
	73.77	2.53	23.70	6.47	92.80	0.73	36.68
313.15	93.23	6.77	0.00	22.47	77.53	0.00	11.45
	91.88	7.01	1.11	15.30	84.66	0.04	12.08
	91.01	6.31	2.69	12.69	87.21	0.10	13.82
	89.35	5.47	5.19	11.61	88.19	0.20	16.12
	86.25	4.09	9.67	9.29	90.36	0.35	22.09
	79.63	3.04	17.33	8.28	91.13	0.59	29.98
	73.46	2.71	23.83	7.02	92.17	0.80	34.01
323.15	93.47	6.53	0.00	23.87	76.13	0.00	11.66
	90.93	8.15	0.92	11.55	88.43	0.02	10.85
	89.71	7.86	2.43	9.57	90.41	0.02	11.50
	87.90	7.25	4.85	9.03	90.90	0.07	12.54
	84.56	6.10	9.33	8.16	91.60	0.23	15.02
	78.48	4.60	16.91	5.93	93.59	0.47	20.35
	72.51	3.80	23.69	5.25	94.05	0.70	24.75

Standard uncertainties u are $u(T) = 0.10$ K, $u(p) = 0.2$ kPa, and $u(w) = 0.01$ g

dissolved well in water with $(\text{NH}_4)_2\text{SO}_4$ being the most soluble, while the salt solubilities in 1-butanol were comparatively minuscule.

3.2 Salting Effect on LLE of Water + 1-Butanol Mixtures

The presence of dissolved salts in an aqueous–organic mixture is known to either increase or decrease the solubility of the organic solute in the aqueous solution. The positive salting effect, where the solute's solubility increases with salt concentration in the system, is called "salting in". The negative effect, called "salting out", is encountered when the solute's solubility is diminished upon addition of a particular salt and is normally observed when a sufficient amount of kosmotropic salt is added into the solution [17]. The latter effect offers possibilities in partitioning the organic compounds from solution. As a result, it has been applied in many separation processes, examples of which include extractive and azeotropic distillation to produce bio-butanol [18], extraction to recover organic acids [19], and antisolvent or extractive crystallization to prepare carrier particles in drug delivery [20].

Table 4 Measured liquid–liquid equilibrium data of the water(1) + 1-butanol(2) + Na₂SO₄(3) system at 303.15, 313.15 and 323.15 K under an atmospheric pressure of 98.9 kPa

Temperature (K)	Aqueous phase			Organic phase			<i>K</i>
	%w ₁₁	%w ₂₁	%w ₃₁	%w ₁₂	%w ₂₂	%w ₃₂	
303.15	92.98	7.02	0.00	20.71	79.29	0.00	11.30
	92.44	6.38	1.18	12.82	87.17	0.01	13.66
	91.93	5.23	2.84	10.09	89.90	0.01	17.19
	90.81	3.96	5.24	9.89	90.03	0.08	22.74
	87.26	2.29	10.45	8.67	91.27	0.06	39.86
	80.83	0.82	18.36	8.23	91.76	0.02	111.90
	74.49	0.30	25.21	6.45	93.53	0.01	311.77
313.15	93.23	6.77	0.00	22.47	77.53	0.00	11.45
	92.66	6.14	1.20	16.71	83.28	0.01	13.56
	92.09	4.94	2.97	13.44	86.54	0.03	17.51
	91.11	3.41	5.48	10.65	89.33	0.01	26.20
	87.42	2.11	10.47	9.97	90.01	0.02	42.66
	81.20	0.78	18.02	8.47	91.51	0.02	117.32
	75.59	0.28	24.13	7.26	92.71	0.03	331.11
323.15	93.47	6.53	0.00	23.87	76.13	0.00	11.66
	92.85	5.96	1.19	15.16	84.80	0.04	14.23
	91.52	5.55	2.93	14.14	85.85	0.02	15.47
	90.48	3.81	5.71	12.00	88.00	0.01	23.10
	87.02	2.45	10.53	9.72	90.27	0.01	36.85
	80.83	0.93	18.24	8.95	91.04	0.01	97.89
	73.64	0.35	26.01	7.86	92.13	0.01	262.89

Standard uncertainties *u* are $u(T) = 0.10$ K, $u(p) = 0.2$ kPa, and $u(w) = 0.01$ g

The measured LLE data of water + 1-butanol systems containing different inorganic salts at temperature of 303.15, 313.15 and 323.15 K are presented in Tables 2, 3, 4, and 5. In those tables, %w_{*ij*} denotes the mass percent of species *i* in phase *j*. Here, *i* = 1, 2, and 3 refer to water, 1-butanol, and the corresponding salt, respectively, *j* = 1 refers to the aqueous phase, and *j* = 2 refers to the organic phase. The results clearly show that, upon addition of these salts, the aqueous phase became salt rich and 1-butanol appeared to be excluded as its concentration in this phase was decreased. The salting-out effects of NaCl, Na₂SO₄, NH₄Cl and (NH₄)₂SO₄ were observed as the percentage of 1-butanol was found to decrease with increasing concentration of the salts in these systems. In other words, the alcohol is less soluble in aqueous solutions when more salt is added, leading to a higher degree of immiscibility and enlarged heterogeneous region of the mixture in the ternary diagrams. Na₂SO₄ appears to be the most effective studied kosmotropic salt while NH₄Cl is the least effective. It should be noted that the temperature in the studied range had no significant effect on the LLE behavior of these systems.

The salting-out capability was further elucidated using the partition coefficient (*K*), which is defined by Eq. 1, and is an indicator of how 1-butanol is distributed between the organic and the aqueous phases at equilibrium:

Table 5 Measured liquid–liquid equilibrium data of the water(1) + 1-butanol(2) + (NH₄)₂SO₄(3) system at 303.15, 313.15 and 323.15 K under an atmospheric pressure of 98.9 kPa

Temperature (K)	Aqueous phase			Organic phase			<i>K</i>
	%w ₁₁	%w ₂₁	%w ₃₁	%w ₁₂	%w ₂₂	%w ₃₂	
303.15	92.98	7.02	0.00	20.71	79.29	0.00	11.30
	93.93	5.14	0.93	8.24	91.76	0.01	17.85
	93.50	4.31	2.19	7.87	92.12	0.01	21.37
	92.25	3.62	4.13	7.73	92.25	0.02	25.48
	88.66	2.33	9.01	6.34	93.65	0.01	40.19
	83.53	0.94	15.53	5.85	94.14	0.01	100.15
313.15	76.92	0.58	22.50	5.36	94.62	0.01	163.14
	93.23	6.77	0.00	22.47	77.53	0.00	11.45
	92.41	6.35	1.24	14.24	85.76	0.00	13.51
	92.19	5.02	2.79	14.25	85.75	0.01	17.08
	90.09	3.96	5.94	9.18	90.80	0.01	22.93
	86.14	2.76	11.10	9.21	90.78	0.01	32.89
323.15	80.22	1.17	18.61	7.08	92.91	0.01	79.41
	75.55	0.87	23.58	6.17	93.81	0.01	107.83
	93.47	6.53	0.00	23.87	76.13	0.00	11.66
	92.14	6.65	1.21	11.02	88.98	0.00	13.38
	91.39	5.57	3.04	10.27	89.72	0.01	16.11
	90.19	4.23	5.58	9.94	90.05	0.01	21.29
	86.53	2.78	10.70	8.55	91.43	0.02	32.89
	79.96	1.24	18.80	7.56	92.42	0.02	74.53
	74.49	0.35	25.16	6.81	93.17	0.02	266.2

Standard uncertainties *u* are $u(T) = 0.10$ K, $u(p) = 0.2$ kPa, and $u(w) = 0.01$ g

$$K = \frac{\%w_{22}}{\%w_{21}} \quad (1)$$

where %w₂₂ and %w₂₁ are mass percentages of 1-butanol in the aqueous and organic phases, respectively. Values of this parameter are given in Tables 2, 3, 4, and 5. The partition coefficients obtained in the systems containing divalent sulfate salts are significantly higher than the values in the systems with the monovalent chloride salts. The highest partition coefficient was obtained for the system with Na₂SO₄.

3.3 Thermodynamic Modelling

In this work, experimental LLE data for the water + 1-butanol system containing each of the salts were correlated using the modified extended UNIQUAC model proposed and comprehensively described by Pirahmadi et al. [7]. In this model, water and 1-butanol are regarded as solvents, and their activity coefficients are defined by the symmetrical convention. The activity coefficients of cationic and anionic species from dissociation of the salt are defined using the asymmetric convention. The excess Gibbs energy consists of three terms as shown in Eq. 2:

$$\frac{G^E}{RT} = \frac{G^E, \text{UNIQUAC}}{RT} + \frac{G^E, \text{PDH}}{RT} + \frac{G^E, \text{Bom}}{RT} \quad (2)$$

Table 6 Binary interaction parameters of the modified extended UNIQUAC model for water(1) + 1-butanol(2) mixtures containing different inorganic salt

303.15 K		313.15 K		323.15 K		
$a_{12}(\text{K})$	$a_{21}(\text{K})$	$a_{12}(\text{K})$	$a_{21}(\text{K})$	$a_{12}(\text{K})$	$a_{21}(\text{K})$	
water(1) + 1-butanol(2)						
192.60	81.68	215.95	65.56	239.16	48.57	
303.15 K		313.15 K		323.15 K		
ij	$a_{ij}(\text{K})$	$a_{ji}(\text{K})$	$a_{ij}(\text{K})$	$a_{ji}(\text{K})$	$a_{ij}(\text{K})$	$a_{ji}(\text{K})$
water(1) + 1-butanol(2) + $\text{NH}_4^+(3)$ + $\text{Cl}^-(4)$						
13	-1944.03	57.11	-1970.67	114.59	-1997.31	172.07
14	-1876.69	-217.04	-1888.40	-169.38	-1900.11	-121.73
23	7923.90	10293.87	7984.39	10555.06	8044.87	10816.25
24	7573.08	13169.66	7795.54	13505.08	8018.00	13840.50
34	3382.90	966.01	3355.92	1002.43	3328.94	1038.85
% Δw	0.03		0.04		0.19	
303.15 K		313.15 K		323.15 K		
ij	$a_{ij}(\text{K})$	$a_{ji}(\text{K})$	$a_{ij}(\text{K})$	$a_{ji}(\text{K})$	$a_{ij}(\text{K})$	$a_{ji}(\text{K})$
water(1) + 1-butanol(2) + $\text{NH}_4^+(3)$ + $\text{SO}_4^{2-}(4)$						
14	2326.46	-1132.18	3591.84	-1105.07	4390.77	-932.57
24	-1345.59	4418.18	-1476.43	4136.03	-1493.71	3974.09
34	-2110.03	-27.62	-3461.04	-34.10	-3541.37	-40.71
% Δw	1.19		0.99		1.02	
303.15 K		313.15 K		323.15 K		
ij	$a_{ij}(\text{K})$	$a_{ji}(\text{K})$	$a_{ij}(\text{K})$	$a_{ji}(\text{K})$	$a_{ij}(\text{K})$	$a_{ji}(\text{K})$
water(1) + 1-butanol(2) + $\text{Na}^+(3)$ + $\text{Cl}^-(4)$						
13	218.04	57.39	212.32	91.79	206.55	126.19
23	79.23	338.23	69.95	336.15	60.68	334.06
34	-3125.15	-12751.59	-3382.82	-12863.96	-3811.80	-13332.00
% Δw	1.72		1.80		2.22	
303.15 K		313.15 K		323.15 K		
ij	$a_{ij}(\text{K})$	$a_{ji}(\text{K})$	$a_{ij}(\text{K})$	$a_{ji}(\text{K})$	$a_{ij}(\text{K})$	$a_{ji}(\text{K})$
water(1) + 1-butanol(2) + $\text{Na}^+(3)$ + $\text{SO}_4^{2-}(4)$						
34	-2078.04	-9451.72	-3555.29	-7004.81	-3518.31	-6464.51
% Δw	1.30		1.57		2.14	

The first term is the original UNIQUAC term accounting for short-range entropic and energetic effects in the mixture. The second term, the Pitzer–Debye–Hückel (PDH) contribution, is responsible for long-range interaction effects. The last term is the Born term, which is used to describe the energy associated with the transfer of ionic species from an infinite dilution state in the mixed solvent to an infinitively dilute aqueous phase. The activity coefficients of ions (γ_k^*) and solvents (γ_j) can be written as

$$\ln \gamma_k^* = \ln \gamma_k^{\text{UNIQUAC}} + \ln \gamma_k^{\text{PDH}} + \ln \gamma_k^{\text{Born}} \quad (3)$$

$$\ln \gamma_j = \ln \gamma_j^{\text{UNIQUAC}} + \ln \gamma_j^{\text{PDH}} + \ln \gamma_j^{\text{Born}} \quad (4)$$

where k and j refer to the corresponding ion and solvent. An asterisk indicates the activity coefficients of the ions that are defined using the asymmetric convention.

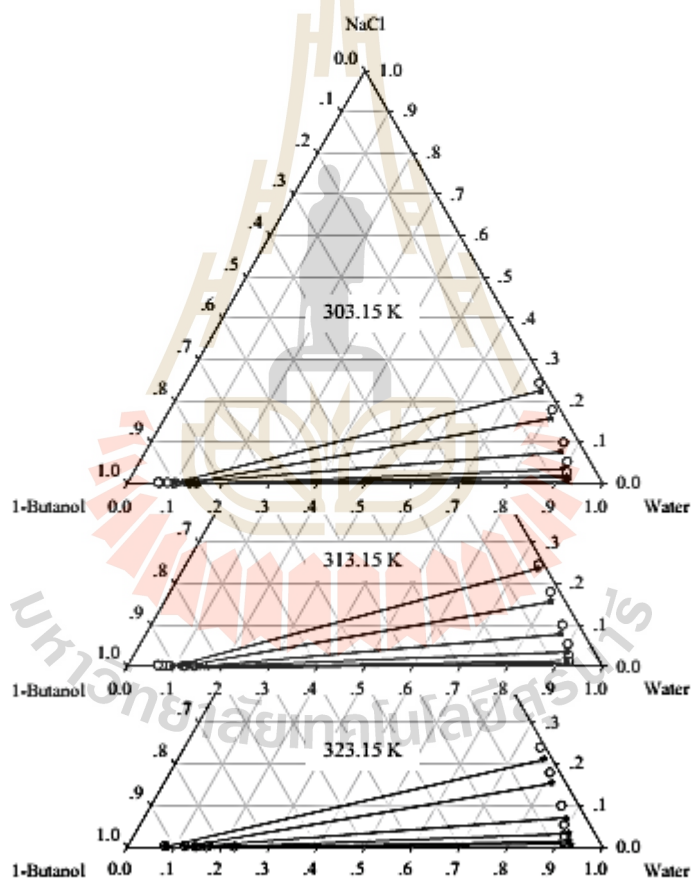


Fig. 1 Experimental (open circle) and calculated (filled star) liquid–liquid equilibrium tie-lines for the water + 1-butanol + NaCl system at 303.15, 313.15, 323.15 K under an atmospheric pressure of 98.9 kPa

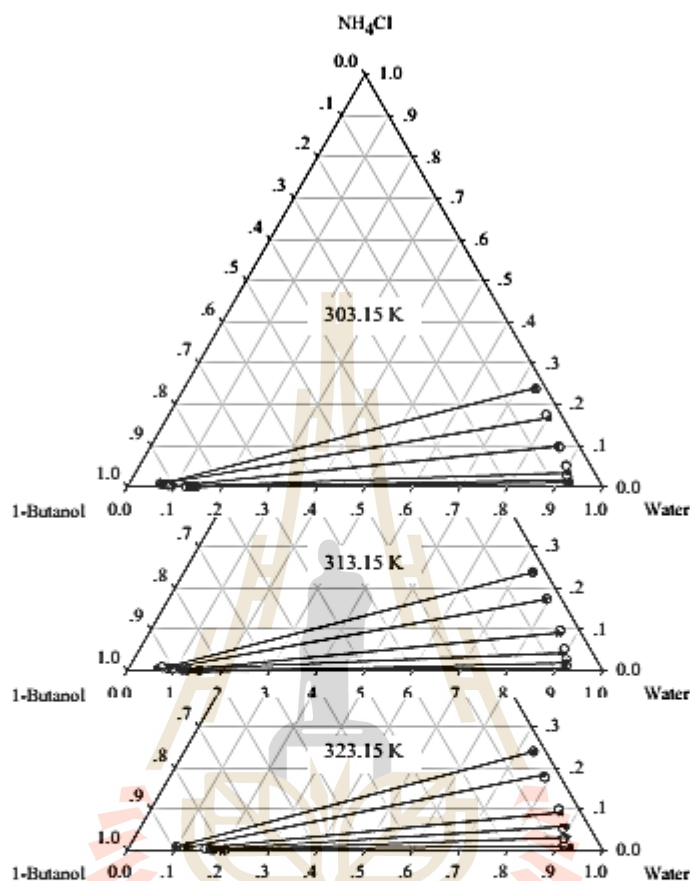


Fig. 2 Experimental (open circle) and calculated (filled star) liquid–liquid equilibrium tie-lines for the water + 1-butanol + NH_4Cl system at 303.15, 313.15, 323.15 K under an atmospheric pressure of 98.9 kPa

Values of volume and surface area parameters (r and q , respectively) for water and 1-butanol, which are needed in the original UNIQUAC term, were taken from Pirahmadi et al. [7, 8]. Values of these parameters for the inorganic salts were derived from Mascus [21] and Wang and Bao [22]. The binary interaction parameters in the original UNIQUAC model for the water + 1-butanol system were adopted from Winkelman et al. [23].

The binary interaction parameters for ion–water, ion–1-butanol and ion–ion interactions for the system containing water, 1-butanol and NH_4Cl at 298.15, 308.15 and 318.15 K were taken from the work of Pirahmadi et al. [8]. In order to obtain values of the model parameters in the temperature range studied in this work, a temperature-dependent polynomial correlation of the form of $a_{ij} = a_{ij}^0 + a_{ij}^1T + a_{ij}^2T^2$ was assumed to extrapolate values of the binary interaction parameters. The extrapolated values were then used in correlating the systems investigated in this study.

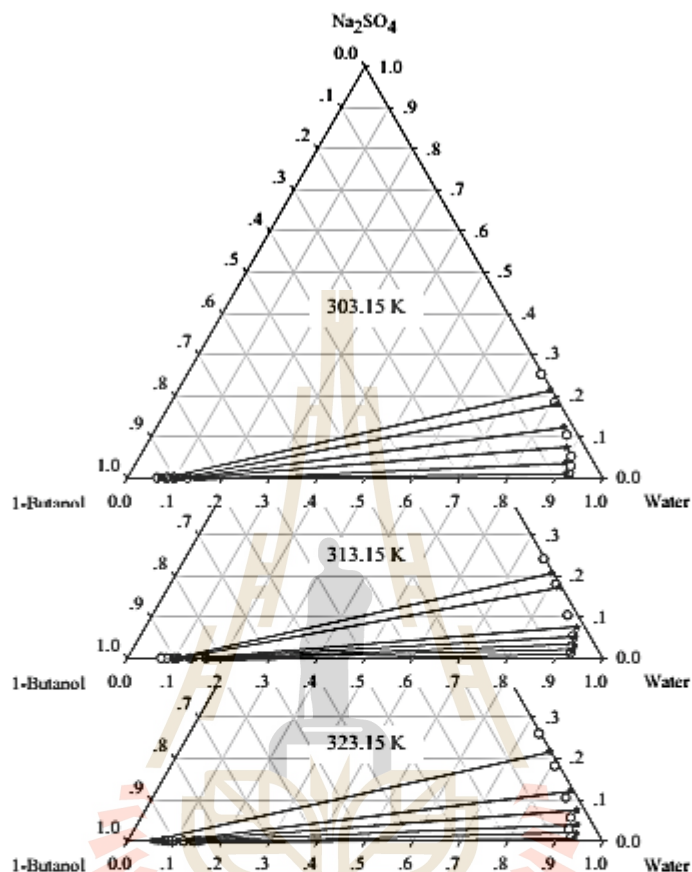


Fig. 3 Experimental (open circle) and calculated (filled star) liquid-liquid equilibrium tie-lines for the water + 1-butanol + Na_2SO_4 system at 303.15, 313.15, 323.15 K under an atmospheric pressure of 98.9 kPa

Since the experimental LLE data for the system containing water, 1-butanol, and $(\text{NH}_4)_2\text{SO}_4$ have not been reported, the binary interaction parameters for water-ion, 1-butanol-ion and ion-ion interactions were estimated using the measured experimental data in this work. Values of all the adjustable interaction parameters were determined by minimizing the differences between the experimental and calculated mass fractions for component i in solvent j using the objective function expressed by Eq. 5:

$$OF = \sum_{j=1}^M \sum_{i=1}^N \left[\left(w_{ij}^{\text{calc}} - w_{ij}^{\text{exp}} \right)_I^2 + \left(w_{ij}^{\text{calc}} - w_{ij}^{\text{exp}} \right)_{II}^2 \right] \quad (5)$$

where M and N are the number of tie-lines and the number of components, w^{calc} and w^{exp} denote the calculated and experimental mass fraction of the concerned components at equilibrium, I represents the aqueous phase and II the organic phase.

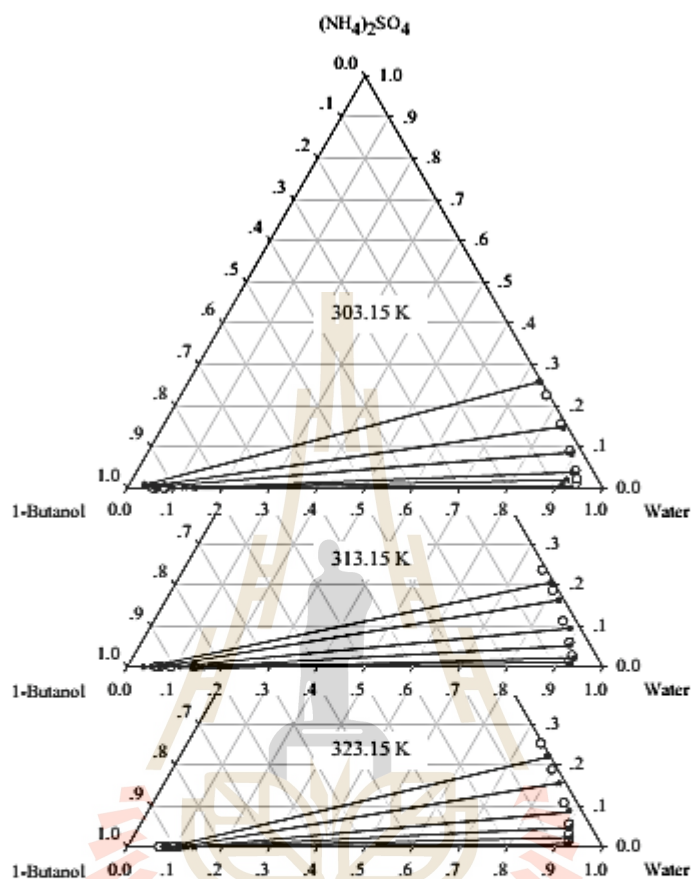


Fig. 4 Experimental (*open circle*) and calculated (*filled star*) liquid–liquid equilibrium tie-lines for the water + 1-butanol + $(\text{NH}_4)_2\text{SO}_4$ system at 303.15, 313.15, 323.15 K under an atmospheric pressure of 98.9 kPa

The number of experimental LLE data points for the systems containing NaCl obtained in this work is quite limited in comparison with the number of adjustable parameters. The binary interaction parameters for this system, consequently, were evaluated by incorporating the additional LLE data for the water + 1-butanol + NaNO_3 system at 298.15 and 308.15 K [7] into the calculation to estimate the parameters associated with Na^+ . All the data sets were used in order to evaluate the temperature dependence of the binary interaction parameters for water– Na^+ and 1-butanol– Na^+ . As in the other systems, the polynomial form of temperature dependence was assumed. The binary cation–anion interaction parameters for the system containing NaCl and Na_2SO_4 were determined using the same procedure.

Quality of the data correlation was judged by agreement between the calculated and experimental mass fractions. Deviations between these two variables were calculated in terms of the root-mean-square absolute deviation as expressed by Eq. 6:

$$\% \Delta w = 100 \left[\frac{\sum_{j=1}^M \sum_{i=1}^N \left[\left(w_{ij}^{\text{calc}} - w_{ij}^{\text{exp}} \right)_I^2 + \left(w_{ij}^{\text{calc}} - w_{ij}^{\text{exp}} \right)_II^2 \right]^{1/2}}{2MN} \right] \quad (6)$$

The binary interaction parameters for every system are given in Table 6 along with the corresponding root-mean-square absolute deviation. Ternary diagrams illustrating the experimental and calculated tie-line data for water + 1-butanol systems containing each salt are shown in Figs. 1, 2, 3, and 4. Excellent agreement of the correlation was accomplished for the system containing NH_4Cl as the average root-mean-square absolute deviations were relatively small. This indicates that the experimental results obtained in this work fit very well with the binary interaction parameters reported by Pirahmadi et al. [8]. Good agreement was achieved for the systems containing $(\text{NH}_4)_2\text{SO}_4$, NaCl and Na_2SO_4 . The binary interaction parameters for every system obtained in this study appear to be temperature-dependent, which has also been previously observed and reported [7, 8, 10].

4 Conclusion

Liquid–liquid equilibrium data for mixed solvent electrolyte systems containing 1-butanol, water and different inorganic salts were measured at temperatures of 303.15, 313.15 and 323.15 K. It was observed that the presence of the salts changed the mutual solubility of these solvents significantly. The salting-out effect was found in every system at every temperature in the studied range, with Na_2SO_4 being the most powerful kosmotrope in this study. The modified extended UNIQUAC model was used to correlate the experimental LLE data. The corresponding optimized UNIQUAC binary interaction parameters were reported. Satisfactory agreement between the experimental and the calculated data was achieved. It was concluded that the modified extended UNIQUAC model is able to successfully correlate the LLE data of the concerned systems.

References

- Hönic, V., Linhart, Z., Táborský, J., Marák, J.: Determination of the phase temperature and the water solubility in the mixtures of gasoline with biobutanol and bioethanol. *Agron. Res.* **13**, 550–557 (2015)
- <http://www.shalegas.international/2014/07/03/global-polyethylene-and-n-butanol-markets-are-set-to-grow-new-report-finds/> (2014). Accessed 15 Aug 2016
- Stoffers, M., Heitmann, S., Lutze, P., Görak, A.: Integrated processing for the separation of biobutanol. Part A: experimental investigation and process modeling. *Green Process. Synth.* **2**, 101–120 (2013)
- Santis, R.D., Marrelli, L., Muscetta, P.N.: Influence of temperature on the liquid–liquid equilibrium of the water–*n*-butyl alcohol–sodium chloride system. *J. Chem. Eng. Data* **21**, 324–327 (1976)
- Xu, W., Min, J.: Liquid–liquid equilibrium for 1-butanol–water–KF and 1-butanol–water– K_2CO_3 systems. *Wuhan Univ. J. Nat. Sci.* **10**(5), 892–896 (2005)

Kinetic Study of Aluminum – Alginate Catalyzed Esterification of Lactic Acid with 1-Butanol

Kanungnit Chawong ¹
Chitkamon Poncharee ¹
Boonpradab Daengpradab ¹
Panarat Rattanaphanee ^{*1}

¹ School of Chemical Engineering, Institute of Engineering, Suranaree University of Technology, Nakhon Ratchasima, Thailand

*e-mail: panarat@sut.ac.th

Aluminum-alginate catalyst prepared from aluminum chloride and inexpensive biopolymer sodium alginate is used in lactic acid esterification with 1-butanol. Effect of initial reactant molar ratio, catalyst loading and reaction temperature on the acid conversion is investigated. Maximum conversion of about 81.2% was achieved after 6 h of reaction at 85°C with initial 1-butanol-to-lactic-acid molar ratio of 5 and catalyst loading of 1%w/v. Experimental kinetic data are correlated by pseudo-homogeneous model using UNIFAC to describe non-ideality of the reaction components. Satisfactory agreement between the experimental and calculated data is achieved. The specific rate and equilibrium constant for this reaction are reported.

Keywords : Esterification, 1-Butanol, Lactic acid, Sodium alginate, Butyl lactate

INTRODUCTION

Lactic acid is a commodity chemical utilized in several application including in food, agricultural, chemical and pharmaceutical industries. It is also used as an important raw material for the manufacture of biodegradable polymers such as polylactic acid and its copolymers, which could be alternative materials to conventional petroleum-based polymers. The acid can be produced by either chemical synthesis or by fermentation. The latter is gaining more attractive because

production of pure optical isomer of lactic acid can be realized by selecting the proper strain of microorganism. Recovery of the acid from fermentation broth, however, presents numerous challenges due to the dilute and complex natures of the broth. Several separation and purification techniques have been investigated to overcome this difficulty. Amongst those, a reactive distillation process employing simultaneous catalyzed esterification of lactic acid and separation of lactate ester, which will later be hydrolyzed back into its acid form, has

Kanungnit Chawong, Chitkamon Poncharee, Boonpradab Daengpradab, and Panarat 23 Rattanaphanee

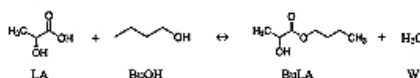
shown remarkable viability in lactic acid purification. Accordingly, many researchers have conducted experiments to investigate catalytic esterification of lactic acid with various alcohols. Su *et al.*, (2013) developed and optimized reactive distillation process to minimize the cost for lactic acid recovery from fermentation broth by esterification and hydrolysis with different alcohols. The results suggest that the process using butanol is economically preferred if short payback period is to be achieved.

Zhang *et al.*,(2013) studied the esterification of oleic acid with alcohols using a new heterogeneous acid catalyst prepared from inexpensive aluminum chloride and biopolymer sodium alginate. The aluminum-alginate catalyst showed high catalytic activity in esterification of oleic acid. It can be applied to the esterification reaction of fatty acids with various carbon chain lengths.

In this work, aluminum-alginate catalyst is used in the esterification of lactic acid with 1-butanol. Effect of reaction variables on conversion of lactic acid are examined. Experimental kinetic data is simulated by pseudo-homogeneous model with non-ideal assumption. Specific rate and rate constant of this reaction are reported.

THEORY AND KINETIC MODELING

Esterification reaction of lactic acid (LA) with 1-butanol (BuOH) to form the butyl lactate (BuLA) and water (W) can be written as:



In order to incorporate the non-ideality of liquid phase components into the reaction kinetics, reaction rate law is expressed in terms of activity of reaction component i (a_i) following a pseudo-homogeneous model as shown in Eq. (1).

$$-r_{LA} = \left(\frac{N_{A0}}{m_{cat}} \right) \frac{dX_{LA}}{dt} = k \left(a_{LA} a_{BuOH} - \frac{a_{BuLA} a_{H_2O}}{K_e} \right) \quad (1)$$

where $-r_{LA}$ is the reaction rate ($\text{mol}\cdot\text{g}^{-1}\cdot\text{min}^{-1}$), N_{A0} is number of moles of lactic acid initially charged into the reactor, m_{cat} is catalyst mass (g), X_{LA} is lactic acid conversion, t is reaction time (min), k is specific rate or rate constant (min^{-1}) and K_e is equilibrium constant. Activity of each reaction component is determined using UNIFAC model.

Both specific rate and rate constant are temperature dependent. The former relates to the activation energy (E_A) of the reaction by Arrhenius equation in Eq. (2).

$$k = A \exp\left(-\frac{E_A}{RT}\right) \quad (2)$$

where A is pre-exponential factor (min^{-1}), T is absolute temperature (K) and R is the gas constant ($\text{J}\cdot\text{mol}^{-1}\cdot\text{K}^{-1}$). The equilibrium constants is calculated from the component activity at equilibrium using Eq. (3).

$$\begin{aligned}
 K_e &= \left(\frac{a_{BuLA} a_{H_2O}}{a_{LA} a_{BuOH}} \right)_{eq.} \\
 &= \left(\frac{x_{BuLA} x_{H_2O}}{x_{LA} x_{BuOH}} \right)_{eq.} \left(\frac{\gamma_{BuLA} \gamma_{H_2O}}{\gamma_{LA} \gamma_{BuOH}} \right)_{eq.}
 \end{aligned} \quad (3)$$

24 Kinetic Study of Aluminum – Alginate Catalyzed Esterification of Lactic Acid with 1-Butanol

where x_i and γ_i are mole fraction and activity coefficient of component i , respectively, at equilibrium.

The kinetic parameters of the models are obtained by minimizing sum of squared residuals (SSR) between the experimental (X_{exp}) and the calculated (X_{cal}) conversion of experiment j as shown in Eq. (4) through the non-least square method.

$$SSR = \sum_{j=1}^M (X_{exp,j} - X_{cal,j})^2 \quad (4)$$

EXPERIMENT

Materials

Lactic acid with concentration of 88 %wt and 1-butanol are purchased from Carlo Erba. Aluminum chloride ($AlCl_3$) powder of 98.5% purity and technical grade sodium alginate are from Acros.

Catalyst Preparation

Aluminum (III)-alginate is synthesized using the procedure described by Qiuyun *et al.*, (2013) with slight modification. Approximately, 2 g of sodium alginate is added to 100 mL of deionized water. The liquid is stirred until a clear viscous solution is achieved. The viscous solution is added stepwise into 100 mL of 0.1 M $AlCl_3$ solution at room temperature. The solution is left to equilibrate for 2 h before it is mixed with 100 ml of deionized water. The liquid is then evaporated out using a rotary evaporator at 105°C and 300 mbar for 1.5 h. Finally, the aluminum-alginate granules are oven-dried at 60°C for 3 h.

This catalyst is denoted as ALA catalyst.

Kinetic Study of Lactic Acid Esterification

A kinetic study of lactic acid esterification with 1-butanol is performed in a 100 mL glass vessel equipped with a thermometer and a magnetic stirrer. The reaction temperature is controlled by a thermostatic oil bath. Weighed amount of lactic acid and the catalyst is firstly charged into the reactor and heated to the desired temperature. Once that is attained, a known amount of preheated 1-butanol at the same temperature is added. This time is considered as a starting point of the reaction. The liquid samples of 0.01 mL are carefully pipetted out from the reactor at different time intervals. The concentration of non-reacted lactic acid is analyzed by titration with the standard 0.01 M NaOH solution. Every experiment is carried out for 6 h.

RESULTS AND DISCUSSIONS

Effect of Catalyst Loading

Effect of catalyst loading on conversion of lactic acid is investigated at 75°C and initial 1-butanol-to-lactic-acid molar ratio of 5:1 with the catalyst loading of 0.25, 0.50 and 1.00 %w/v. The result is shown in **figure 1**. Rate of reaction is found to increase with the catalyst loading but nearly the same equilibrium conversion is achieved in every experiment.

Effect of Initial 1 – Butanol – to – Lactic – Acid Molar Ratio

Esterification is a reversible reaction, and using excess quantity of the alcohol can drive the reaction equilibrium toward

Kanungnit Chawong, Chitkamon Poncharee, Boonpradab Daengpradab, and Panarat 25 Rattanaphanee

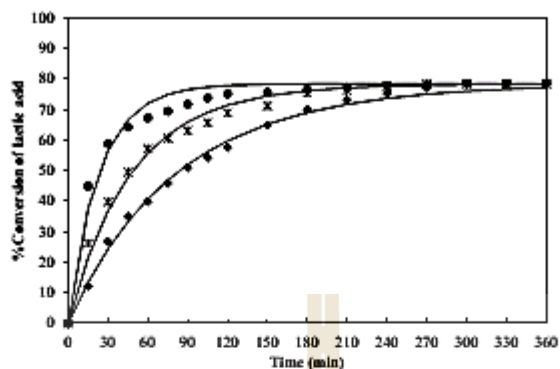


Fig. 1: Effect of catalyst loading on conversion of lactic acid at 75°C and initial 1-butanol-to-lactic-acid molar ratio of 5:1: (◆) 0.25%w/v; (*) 0.5%w/v; (●) 1%w/v. Solid lines indicate the calculation values.

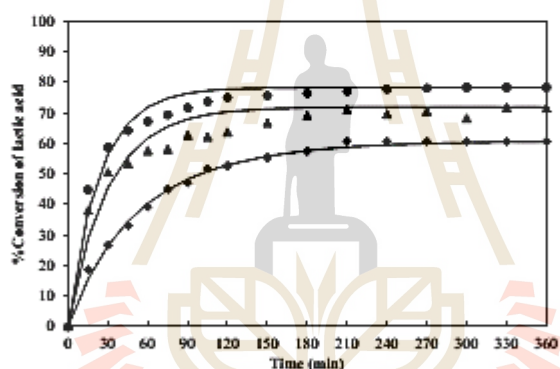


Fig. 2: Effect of initial 1-butanol-to-lactic-acid molar ratio on conversion of lactic acid at 75°C and 1% w/v catalyst loading: (▲) 1:1; (■) 3:1; (●) 5:1. Solid lines indicate the calculation values.

the formation of ester product. In this work, effect of initial 1-butanol-to-lactic-acid molar ratio of 1:1, 3:1 and 5:1 on lactic acid conversion is studied. The reaction is carried out at 75°C using

1%w/v of catalyst loading. As shown in figure 2, lactic acid conversion is increased with increasing reactant molar ratio.

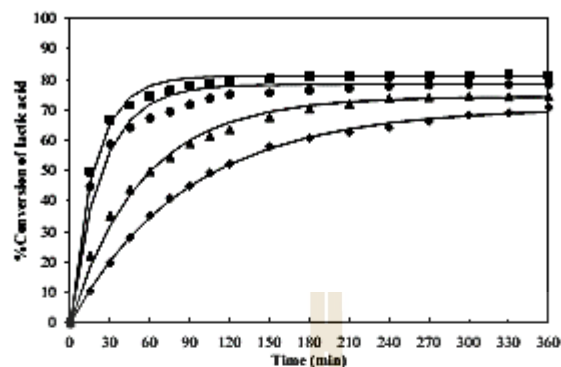


Fig. 3: Effect of reaction temperature on conversion of lactic acid at 1-butanol-to-lactic-acid molar ratio of 5:1 and catalyst loading of 1%w/v: (♦)55°C; (▲)65°C; (■)75°C; (●)85°C. Solid lines indicate the calculation values.

Table 1. Kinetic parameters for esterification of lactic acid with 1-butanol catalyzed by ALA catalyst.

Reaction condition			k	K_e	SSR	R^2
85	5	1	0.0536	2.7771	0.0058	0.9911
75	5	1	0.0410	2.2812	0.0169	0.9722
65	5	1	0.0165	1.7477	0.0044	0.9940
55	5	1	0.0093	1.3998	0.0008	0.9989
75	3	1	0.0379	2.5707	0.0333	0.9581
75	1	1	0.0343	2.2036	0.0022	0.9957
75	1	0.50	0.0397	2.2602	0.0074	0.9903
75	1	0.25	0.0451	2.2532	0.0042	0.9956

Effect of Temperature

Effect of reaction temperature on conversion of lactic acid is studied in the range of 55 to 85°C using 1-butanol-to-lactic-acid molar ratio of 5:1 and catalyst loading of 1 %w/v. The result is in figure 3, which clearly shows substantial increase of the reaction rate with the increase of reaction temperature. Equilibrium conversion of lactic acid is found to be dependent of the reaction temperature as well. This is likely due to the endothermic

nature of esterification reaction, which is confirm from value of the activation energy explicated in the next section.

Kinetic Modeling

The experimental kinetic data of esterification of lactic acid with 1-butanol are correlated by pseudo-homogeneous model with non-ideal assumption in order to determine the specific rate and the equilibrium constant. As shown in Table 1, small value of SSR and value of

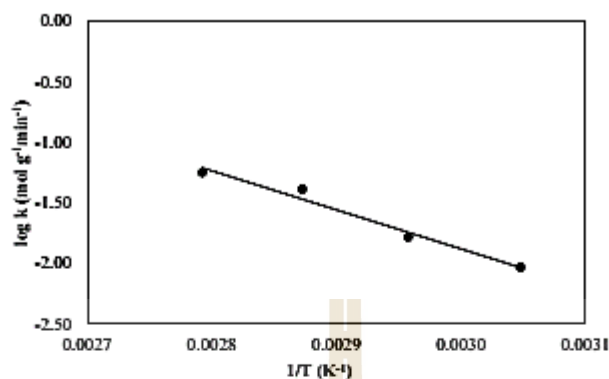


Fig. 4: Arrhenius plot for ALA catalyzed esterification of lactic acid with 1-butanol

coefficient of determination (R^2) closed to unity indicate good agreement between the experimental and the calculated conversion. Slight variation in value of equilibrium constant at 75°C is observed, which may be due to error in component analysis caused by phase separation in water+lactic acid+1-butanol mixtures reported by Chawong *et al.*, (2015). This issue has been mention in the study concerning esterification of fatty acid as well (Hassan and Vinjamur, 2013).

Plotting $\log k$ versus $1/T$ at constant initial 1-butanol to lactic acid molar ratio and catalyst loading gives a straight line as shown in figure 4. Slope and intercept of the plot are used to calculate the pre-exponential factor and the activation energy of this ALA-catalyzed reaction. The values obtained are $3.60 \times 10^8 \text{ min}^{-1}$ for pre-exponential factor and $61.57 \text{ kJ} \cdot \text{mol}^{-1} \cdot \text{K}^{-1}$ for activation energy of the reaction.

CONCLUSION

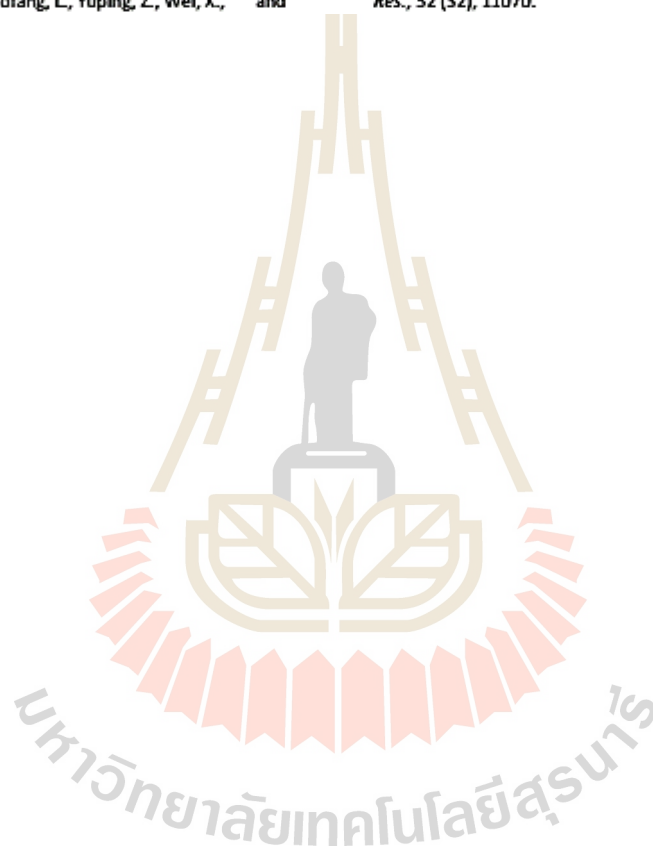
Esterification of lactic acid with 1-butanol catalyzed by aluminium-alginate (ALA) catalyst is studied. Effect of reaction temperature, initial 1-butanol-to-lactic-acid molar ratio, as well as catalyst loading on lactic acid conversion is elucidated. The ALA catalyst appears to be effective for this reaction. The pseudo-homogeneous model with non-ideal assumption is able to describe the reaction kinetic with satisfactory agreement. The pre-exponential factor and activation energy for this reaction are found to be $3.60 \times 10^8 \text{ min}^{-1}$ and $61.57 \text{ kJ} \cdot \text{mol}^{-1} \cdot \text{K}^{-1}$, respectively.

REFERENCES

1. Chawong, K., Rayabsri, C., and Rattanaphanee, P. (2015). Extraction of lactic acid in mixed solvent electrolyte

28 Kinetic Study of Aluminum – Alginate Catalyzed Esterification of Lactic Acid with 1-Butanol

- system containing water, 1-butanol and ammonium sulfate, *Int. J. Chem. React. Eng.*, 13(2): 183.
- Hassan, S. Z., and Vinjamur, M. (2013). Analysis of sensitivity of equilibrium constant to reaction conditions for esterification of fatty Acids with alcohols, *Ind. Eng. Chem. Res.*, 52 (3), 1205.
 - Qiyun, Z., Li, H., Wenting, Q., Xiaofang, L., Yuping, Z., Wei, X., and Song, Y. (2013). Solid acid used as highly efficient catalyst for esterification of free fatty acids with alcohols, *China Pet. Process Pe.*, 15(1), 19.
 - Su, C., Yu, C., Chien, I., Ward, J. D. (2013). Plant-wide economic comparison of lactic acid recovery processes by reactive distillation with different alcohols, *Ind. Eng. Chem. Res.*, 52 (32), 11070.





Aluminum alginate as a solid catalyst for esterification of lactic acid with 1-butanol

Kanungnit Chawong, Boonpradab Daengpradab and Panarat Rattanaphanee*

School of Chemical Engineering, Institute of Engineering, Suranaree University of Technology,
 Nakhon Ratchasima 30000, Thailand.

Received April 2016
 Accepted June 2016

Abstract

Aluminum-alginate (ALA) was used as a solid catalyst for esterification of lactic acid with 1-butanol at different temperature in a range of 55 to 85°C. Conversion of lactic acid was found to increase with increasing reaction temperature with the maximum conversion of 81.18% after 6 h of reaction at 85°C with 1-butanol to lactic acid molar ratio of 5 and 1%w/v of catalyst loading. The result was compared with the system using Amberlyst 15 under the same reaction condition. It was observed that ALA has a higher catalytic activity than Amberlyst 15. Experimental kinetic data were correlated by pseudo-homogeneous model with an assumption of ideal behavior. The kinetics of this reaction could be described using this model with minor errors. The activation energy for ALA-catalyzed esterification of lactic acid with 1-butanol was found to be 61.16 kJ/mol.

Keywords: Esterification, Kinetic study, Lactic acid, 1-Butanol, Sodium alginate

1. Introduction

Lactic acid is an important chemical utilized in many industries. Major challenge in lactic acid production, however, is an extravagance of the acid recovery and purification cost. Reactive distillation comprising of esterification of lactic acid and hydrolysis of the lactate ester has been one of the promising process as it has lower capital cost and is able to produce highly pure lactic acid, which is the key feedstock in the production of biodegradable polymer. The interesting research was reported by Chien et al. [1], where the recovery of lactic acid from fermentation broth by esterification and hydrolysis using different alcohols was compared. The result showed that 1-butanol is the most attractive candidate, as it gives a short payback period for this process. Esterification between lactic acid and 1-butanol has, therefore, become increasingly attractive and extensive researches have been done over the years to find the most suitable solid catalyst for this reaction.

Zhang et al. [2] studied the esterification of oleic acid with alcohols using a new and easily prepared solid acid catalyst obtained from inexpensive sodium alginate and aluminum chloride. The aluminum-alginate catalyst showed high catalytic activity for esterification of oleic acid. In this work, this catalyst is used for the esterification reaction of lactic acid with 1-butanol. The kinetic data is simulated by pseudo-homogeneous model. The rate constant, equilibrium constant as well as the activation energy is also determined.

2. Materials and methods

2.1 Materials

Lactic acid with concentration of 88 %wt and 1-butanol of RPE grade with 99.9% purity were purchased from Carlo Erba. Aluminum chloride (AlCl₃) and sodium alginate were purchased from Acros.

2.2 Catalyst preparation

Aluminum (III)-alginate was synthesized using the procedure described by Zhang et al. [2] with slight modification. Approximately, 2 g of sodium alginate was added to 100 mL of deionized water, and the mixture was stirred until a clear viscous solution was obtained. The viscous solution was added stepwise into 100 mL of 0.1 M AlCl₃ solution at room temperature. The aluminum-alginate complex in the solution was left to equilibrate for 2 h. After that, 100 mL of deionized water was added into the solution. The liquid was then evaporated out using a rotary evaporator at 105°C under pressure of 300 mbar for 1.5 h. Finally, the aluminum-alginate flakes were dried in oven at 60°C for 3 h. This catalyst was denoted as ALA catalyst.

2.3 Characterization of the catalyst

The powder X-ray diffraction (XRD) patterns of the catalyst sample was performed using a Bruker D2 PHASER

*Corresponding author. Tel.: +66 4422 4591
 Email address: panarat@sut.ac.th
 doi: 10.14456/kkuenj.2016.98

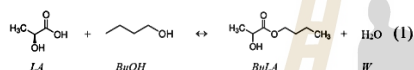
X-ray diffractometer (CuK α radiation, $\lambda = 1.5406 \text{ \AA}$). Patterns were recorded over goniometric (2θ) ranges from $20\text{--}80^\circ$.

2.4 Apparatus and procedure

A kinetic study of esterification of lactic acid with 1-butanol was performed in a 100 mL glass vessel equipped with a thermometer and a magnetic stirrer. The reaction temperature was maintained by an electric heating thermostatic oil bath. Amount of lactic acid and 1-butanol used in this work was 18.91 and 68.45 g, respectively. The lactic acid and 1 g of catalyst were firstly charged into the reactor and heated to the desired temperature. Once the desired temperature was attained, a known amount of preheated 1-butanol at the same temperature was added to the reactor and the time was considered as the initial reaction time. The liquid samples of 0.01 mL were carefully pipetted out from the reactor at different time intervals and the concentration of non-reacted lactic acid was analyzed by titration with 0.01 M NaOH solution.

3. Kinetic model

Esterification reaction of lactic acid (LA) with 1-butanol (BuOH) to form the butyl lactate (BuLA) and water (W) can be written as:



Assume the liquid behaves as an ideal solution, the reaction kinetics can be expressed using a pseudo-homogeneous model as follows:

$$-r_{LA} = \frac{dx_{LA}}{dt} = k \left(C_{LA} C_{BuOH} - \frac{C_{BuLA} C_W}{K_e} \right) \quad (2)$$

$$K_e = \left(\frac{C_{BuLA} C_W}{C_{BuOH} C_{LA}} \right)_{eq} \quad (3)$$

where $-r_{LA}$ is the reaction rate ($\text{mol L}^{-1} \text{min}^{-1}$), C_i is concentration of component i (mol L^{-1}), k is the rate constant ($\text{L mol}^{-1} \text{min}^{-1}$) and K_e is equilibrium constant. The kinetic parameters of the models were obtained by minimizing the sum of squared residuals (SSR) between the experimental (x_{exp}) and calculated (x_{cal}) mole fraction as shown in Eq. (4):

$$SSR = \sum (x_{exp} - x_{cal})^2 \quad (4)$$

The reaction constant is expressed using Arrhenius equation as in Eq. (5).

$$k = A \exp\left(\frac{-E_A}{RT}\right) \quad (5)$$

where A is the pre-exponential factor (min^{-1}), E_A is the activation energy (J mol^{-1}), T is the absolute temperature (K) and R is the gas constant ($\text{J mol}^{-1} \text{K}^{-1}$).

4. Results and discussion

4.1 Characterization of the ALA catalyst

In this study, when aluminum chloride was mixed with sodium alginate, aluminum alginate is formed immediately, as shown in Figure 1(a), indicating gelling property of the alginate. The process of gelation is the simply exchange of Al^{3+} ions for Na^+ ions. The final ALA catalyst granules is shown in Figure 1(b). It was found that the peaks at 2θ angles of approximately 31° , 45° and 56° are similar to the pure diaspore peaks reported by Zhang et al. [2], which matched with the typical aluminum oxyhydroxide particle.

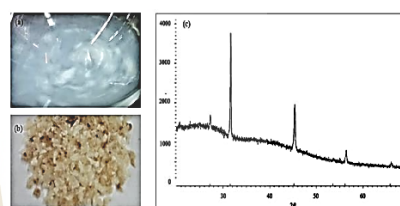


Figure 1 ALA catalyst prepared in this work; (a) ALA gelation, (b) ALA flakes, (c) XRD patterns of ALA catalyst

4.2 Catalyst performance

The performance of catalyst is very important for a reaction system since it is directly related to economical application of the process. In this study, the ALA catalyst activities was firstly tested by comparison with the commercially available catalyst Amberlyst 15. The activity of both catalysts on esterification of lactic acid with 1-butanol was compared in the reactions with temperature of 65°C and 85°C with 1-butanol to lactic acid molar ratio of 5:1 ($M=5$), catalyst loading of 1 %w/v and the reaction time of 6 h. The results presented in Figure 2 indicate that the ALA catalyst had higher activity than Amberlyst 15 with the conversion of 74.39% and 81.18% at the temperature of 65°C and 85°C , respectively, while the conversion when Amberlyst 15 was used was 53.19% at 65°C and was 75.17% at 85°C .

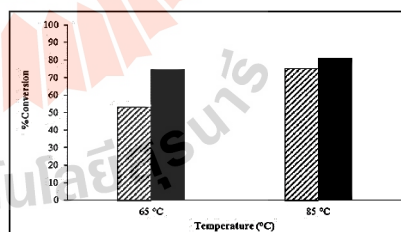


Figure 2 Comparison of conversion for esterification of lactic acid with 1-butanol using (▨) Amberlyst-15 and (■) ALA as reaction catalyst

Table 1 Kinetic parameters for esterification of lactic acid with 1-butanol using ALA and Amberlyst 15 as solid catalysts at different temperatures

Temperature (°C)	Catalyst	k (L mol ⁻¹ min ⁻¹)	K_e	SSR	R^2
55	ALA	0.0699	0.7866	0.0010	0.9987
65		0.1225	0.9765	0.0056	0.9922
75		0.3036	1.2700	0.0186	0.9694
85		0.4142	1.5439	0.0065	0.9900
65	Amberlyst 15	0.0241	0.9763	0.0056	0.9989
85		0.0641	1.5435	0.0151	0.9981

4.3 Effect of temperature

The reaction temperature was studied in the range of 55 to 85°C. The reaction was carried out with 1-butanol to lactic acid molar ratio of 5:1 (M=5), catalyst loading of 1 %w/v and the reaction time of 6 h. Figure 3 shows the effect of temperature on the conversion of lactic acid with ALA and Amberlyst-15 as catalysts. Since the esterification of carboxylic acid with alcohol is an endothermic reaction, the conversion is increased with the reaction temperature [3]. Similar trends were reported in the literature [4]. It can be seen from the result that the effect of temperature on the rate of 1-butyl lactate production is significant. In both catalytic systems, the reaction rate increased sharply with increasing temperature. In addition, it was found that the ALA catalyst gave the maximum conversion of 81.18% at the temperature of 85°C.

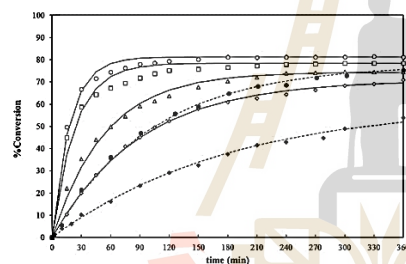


Figure 3 Effect of temperature on the conversion of lactic acid. Reaction temperature; (○) 55°C, (△) 65°C, (□) 75°C, (◇) 85°C for ALA catalyst. (●) 65°C, (■) 85°C for Amberlyst-15. Solid and dash lines indicated the calculated conversion of reaction with ALA and Amberlyst 15, respectively

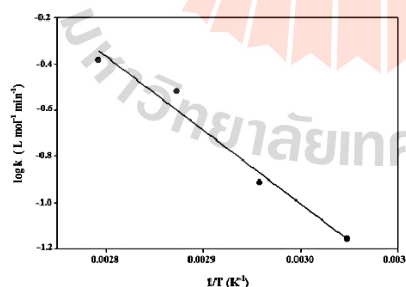


Figure 4 Arrhenius plot for ALA catalyzed esterification of lactic acid with 1-butanol

4.4 Kinetic parameters

The kinetic data of esterification of lactic acid with 1-butanol were correlated with pseudo-homogeneous model. The adjustable kinetic parameters k and K_e obtained by data fitting are shown in Table 1. It was found that both kinetic parameters increase with the reaction temperature, with the value from ALA catalyzed reaction higher than the one catalyzed by Amberlyst-15. It means that the faster reaction can be achieved over ALA catalyst. Increasing of K_e is due to high equilibrium concentration of products.

As shown in Table 1, the coefficient of determination (R^2) indicates good agreement between the experimental and the calculated conversion. It should be noted that the assumption of ideal behavior results in small errors. Taking the natural logarithm of both sides of the Arrhenius equation (Eq.5) gives:

$$\log k = \log A - \frac{E_a}{2.303RT} \quad (6)$$

A plot of $\log k$ versus $1/T$ at constant 1-butanol to lactic acid molar ratio and catalyst loading gives a straight line as shown in Figure 4. The pre-exponential factor and activation energy obtained from this work is found to be $3.7705 \times 10^8 \text{ min}^{-1}$ and 61.16 kJ/mol, respectively.

5. Conclusions

The esterification reaction of lactic acid with 1-butanol was successfully carried out over ALA solid catalyst. The reaction temperatures in the range of 55 to 85°C were investigated. It has been observed that the conversion of lactic acid increased with increasing temperature. ALA catalyst also showed better catalytic performance than Amberlyst 15. The reaction rate constant and equilibrium constant were influenced by the reaction temperature. The pseudo-homogeneous model was able to describe the kinetics of this esterification with small error. The activation energy of lactic acid esterification was found to be 61.16 kJ/mol.

6. References

- [1] Chien YS, Cheng CY, I-Lung C, Jeffrey DW. Plant-Wide economic comparison of lactic acid recovery processes by reactive distillation with different alcohols. *Industrial & Engineering Chemistry Research* 2013;52(33):11070-11083.
- [2] Zhang Q, Li H, Qin W, Liu X, Zhang P, Xue W, Yang S. Solid acid used as highly efficient catalyst for esterification of free fatty acids with alcohols. *China Petroleum Processing and Petrochemical Technology* 2013;15(1):19-24.
- [3] Bart HJ, Reidschlagler J, Schatka K, Lehmann. A kinetics of esterification of levulinic acid with n-butanol by homogeneous catalysis. *Industrial & Engineering Chemistry Research* 1994;33(1):21-25.
- [4] Zhang Y, Ma L, Yang J. Kinetics of esterification of lactic acid with ethanol catalyzed by cation-exchange resins. *Reactive and Functional Polymers* 2004;61(1):101-114.

Kanungnit Chawong, Chanita Rayabsri and Panarat Rattanaphanee*

Extraction of Lactic Acid in Mixed Solvent Electrolyte System Containing Water, 1-Butanol and Ammonium Sulfate

DOI 10.1515/ijcre-2014-0132

Abstract: Extraction of lactic acid from its aqueous solution was carried out at 30.0°C in a mixed solvent electrolyte system containing water, 1-butanol and ammonium sulfate ((NH₄)₂SO₄). The salt appeared to reduce mutual solubility between water and 1-butanol leading to an enlarged two-phase region of the mixture. The effect was more pronounced at high salt concentration. In view of extraction, ternary mixture containing water, 1-butanol and lactic acid, (NH₄)₂SO₄ effectively salted-out 1-butanol and lactic acid leading to a reduced concentration of these two components in the aqueous phase. Distribution coefficient and degree of lactic acid extraction were significantly improved with increasing concentration of the salt. Additionally, (NH₄)₂SO₄ helped lessen the transfer of one solvent into the other, which is the problem normally encountered in extraction when partially miscible solvents are employed. It also advantageously allowed the extraction to be carried out at a high solvent-to-aqueous phase volume ratio, where large recovery of the acid was achieved. Extraction of lactic acid in this mixed solvent electrolyte system could be further improved by operating it in a stage-wise mode rather than a batch one.

Keywords: lactic acid, extraction, liquid-liquid equilibrium, 1-butanol, ammonium sulfate

1 Introduction

Lactic acid is one of important carboxylic acids in chemical industries. It is primarily produced biologically through fermentation of sugary, starchy, or cellulosic materials and is widely used as acidulants and preservatives in food

industry. It also has a potential of becoming an important feedstock for production of biodegradable plastics and other environmental-friendly compounds. The production of these compounds requires lactic acid in a highly purified form. Recovery of this acid from an aqueous fermentation media is, therefore, a crucial step, and, unfortunately, its cost can account for up to 50% of the total cost in fermentation-based lactic acid production process (Wasewar et al. 2002).

Several separation and purification techniques have been proposed for recovery of lactic acid from the fermentation media, and solvent extraction is one of the promising techniques among them. As extraction is not as energy-intensive as evaporation or distillation, its advantage is suitability for large capacity processing with low energy consumption. With proper choice of solvent or extractant, satisfactory selective separation of desired solutes can be achieved.

Common extractants for lactic acid recovery include organic bases or amine such as tri-n-octylamine (TOA), alkyl phosphate esters, such as tributyl phosphate (TBP) and trioctyl phosphine oxide (TOPO), and the extractants that function as ion exchangers such as quaternary ammonium salts like the commercial extractant Aliquat 336 or methyltrialkyl (C₈-C₁₀) ammonium chloride. Despite the high distribution coefficient obtained from the extraction, some of the extractants are expensive and might inherit some toxicity. Specifically, major disadvantages in solvent extraction using amine are high initial investment cost on extractant supply since large amount of the amine is needed. It is also quite difficult to separate lactic acid from the ammonium lactate intermediate and to regenerate the amine solvent after extraction.

Extraction of lactic acid using ionic liquid (ILs) had been suggested. Experiments with phosphonium ILs showed promising results as sufficiently high distribution coefficient of lactic acid was achieved (Marták and Schlosser 2007; Oliveira et al. 2012). Pertraction of lactic acid through supported liquid membranes (SLM) containing phosphonium ILs was also investigated in a spiral channel flat sheet module (Marták et al. 2008). It was found that pertraction worked well for a broad

*Corresponding author: Panarat Rattanaphanee, School of Chemical Engineering, Suranaree University of Technology, Suranaree, Muang, Nakhon Ratchasima, 30000, Thailand, E-mail: panarat@sut.ac.th

Kanungnit Chawong, Chanita Rayabsri: School of Chemical Engineering, Suranaree University of Technology, Suranaree, Muang, Nakhon Ratchasima, 30000, Thailand, E-mail: kanungnit.cha@hotmail.com, chanita1813@yahoo.com

spectrum of organic compounds. Utilization of ILs was also considered as a green process since the toxicity and volatility of this solvent is fairly low. The drawback of this process, however, could be significant for operation in a large scale since the ILs is very expensive compared to other solvents. As a result, recovery of lactic acid by extraction with more economical and environmental friendly solvents is still needed (Stepan et al. 2001).

With an aim to recover lactic acid from its aqueous solution using aliphatic alcohols as extracting solvent, liquid-liquid equilibrium and extraction efficiency of water-lactic acid-alcohols system had been investigated (Sahin et al. 2009; Chawong and Rattanaphanee 2011; Domingues et al. 2013). For the system of water-lactic acid-1-butanol, it was reported that extraction efficiency was significantly increased with decreasing pH of lactic acid solution. This process characteristic would be beneficial for acid extraction at large capacity since volume of the feed solution could be reduced to increase the acid concentration or, in other words, to reduce the solution pH, before it is subjected to the extractor. Disadvantage of lactic acid extraction with 1-butanol is, however, the fact that water and 1-butanol are partially miscible solvents. During the operation, water in the aqueous phase was fractionally transferred into the organic phase, and vice versa, leading to an incorporation of both phases and, in turn, incomplete solvent recovery and complicated lactic acid purification in the subsequent steps (Chawong and Rattanaphanee 2011).

Addition of inorganic salts (or electrolytes) in an aqueous solution can either raise or diminish the solubility of a solute in the solution and influence the distribution characteristic of the solute between the partial miscible phases in the system (Ghalami-Choobar et al. 2011). In the study concerning effect of chloride salts such as NaCl, MgCl₂ or CaCl₂ on extraction to recover lactic acid from its aqueous solution using 1-butanol, it was found that, when the salt concentration was sufficiently high, degree of lactic acid extraction was increased with increasing salt concentration (Chawong and Rattanaphanee 2012).

In this study, effect of ammonium sulfate (NH₄)₂SO₄, on extraction of lactic acid from its aqueous solution with 1-butanol was investigated. Liquid-liquid equilibrium data of water-1-butanol-lactic acid system with and without a presence of this salt were investigated. Efficiency of extraction process was evaluated from the acid distribution coefficient and degree of its extraction.

2 Materials and methods

Lactic acid with concentration of 88 %W and 1-butanol with 99.9% purity were purchased from Acros. Anhydrous (NH₄)₂SO₄ was from Carlo Erba. Deionized water, produced in-house, was used in all the experiments.

Weighed quantity of (NH₄)₂SO₄ was added into 10 ml DI water. Equal volume of 1-butanol was then mixed with the prepared solution in a 125 ml of Erlenmeyer flask. The mixture was agitated in a temperature-controlled shaking bath for 12 h before being transferred to a separatory funnel and was left for complete phase separation in the bath for another 12 h. The samples of top and bottom phases were taken for analysis. Mass fractions of 1-butanol were analyzed by gas chromatograph (GC) equipped with TR-FFAP capillary column and flame ionization detector (FID). Water content was analyzed by GC equipped with thermal conductivity detector (TCD). In both cases, helium was used as a carrier gas. A stainless steel Chromosorb® packed-column was used to separate the components. Lactic acid concentration was determined by HPLC using Hypersil BDS C18-column (Agilent) using 0.005 M sulfuric acid solution as a mobile phase. Detection was at a UV wavelength of 210 nm. Salt contents were lastly analyzed by drying the samples at 120°C for 12 h to completely remove all the liquid.

3 Results and discussion

3.1 Effect of (NH₄)₂SO₄ on LLE of water-1-butanol system

Effect of (NH₄)₂SO₄ on liquid-liquid equilibrium behavior of water-1-butanol mixture at 30.0°C was measured, and the results are given in Table 1. Upon mixing, water and

Table 1: Mass percent of water(1), 1-butanol(2) and (NH₄)₂SO₄(3) system at 30.0°C.

	Water-rich phase			1-Butanol-rich phase		
	%W ₁	%W ₂	%W ₃	%W ₁	%W ₂	%W ₃
92.50	7.50	0	12.95	87.05	0	
93.93	5.14	0.93	8.24	91.76	0.01	
93.50	4.31	2.19	7.87	92.12	0.01	
92.25	3.62	4.13	7.73	92.25	0.02	
88.66	2.33	9.01	6.34	93.65	0.01	
83.53	0.94	15.53	5.85	94.14	0.01	
76.92	0.58	22.50	5.36	94.62	0.01	

1-butanol naturally separate into two phases. The top phase is rich in 1-butanol, and it is normally referred to as organic phase. The bottom phase is called aqueous phase as its main content is water. Due to their partial miscibility, water is fractionally transferred into the organic phase and a portion of 1-butanol is transferred into the aqueous phase. Equilibrium composition of each phase in water-1-butanol mixture without the presence of $(\text{NH}_4)_2\text{SO}_4$ is given in the first row of Table 1. Under the experimental conditions used in this work, equilibrium concentration of 1-butanol in the aqueous phase was 7.5% and that of water in the organic phase was approximately 13% of water. The result showed that the solubility of water in 1-butanol was higher than the solubility of 1-butanol in water, which agreed with the results observed in other work concerning liquid-liquid equilibrium behavior of water-1-butanol system (Pirahmadi et al. 2010, 2012).

When $(\text{NH}_4)_2\text{SO}_4$ was added to the system, mass percent of water in the organic phase decreased from 12.95 to 5.36% and mass percent of 1-butanol in the aqueous phase decreased from 7.50 to 0.94% upon increasing $(\text{NH}_4)_2\text{SO}_4$ concentration. This observation indicated that the mutual solubility between the two

components was reduced as the salt concentration increased. In other words, $(\text{NH}_4)_2\text{SO}_4$ salted out 1-butanol from water, and, as expected, the salt itself preferred to be in the aqueous phase so only trace concentration of it was found in the organic phase.

3.2 Extraction of lactic acid in water-1-butanol- $(\text{NH}_4)_2\text{SO}_4$ system

It has been reported that addition of inorganic salt into aqueous solution of an organic acid can result in either decrease or increase in solubility of the acid in the solution (Tan et al. 1999). If the acid solubility is increased upon the addition of salt, the effect is called "salting in". On the other hand, if its solubility is diminished when the salt is added, the effect is called "salting out". In this study, effect of $(\text{NH}_4)_2\text{SO}_4$ on solubility and distribution of lactic acid in aqueous and organic phase was investigated. The results are depicted as ternary diagrams as shown in Figure 1.

It can be seen in Figure 1(A), which is the system without $(\text{NH}_4)_2\text{SO}_4$, that the tie-lines in the diagram were mostly horizontal indicating the even distribution of the

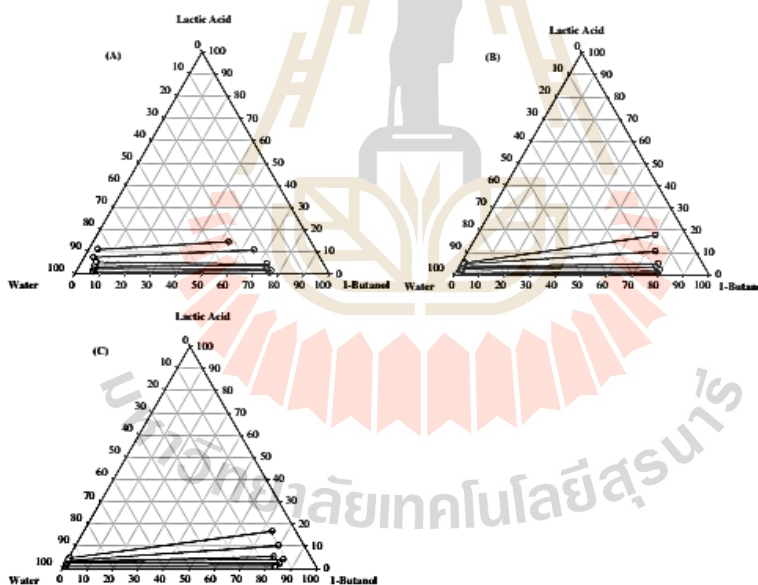


Figure 1: Salt-free basis LLE of water-1-butanol-lactic acid system at (A) 0 g, (B) 2 g, (C) 5 g $(\text{NH}_4)_2\text{SO}_4$.

acid between both phases. In Figure 1(B) and 1(C) where $(\text{NH}_4)_2\text{SO}_4$ was added, the tie-lines became inclined with mass fraction of lactic acid in the organic phase higher than that in the aqueous phase. The inclination suggested that the acid preferred to be in the organic phase under the presence of $(\text{NH}_4)_2\text{SO}_4$. Comparison of the tie-line length in Figure 1(B) and 1(C) visualized the dependency of liquid-liquid equilibrium behavior of this ternary system on mass of $(\text{NH}_4)_2\text{SO}_4$. Similar to the data previously presented in Table 1, mass fraction of water in the organic phase and of 1-butanol in the aqueous phase were reduced with increasing concentration of this salt. The phenomena were evidenced by the longer tie-lines and the larger two-phase region in the ternary diagram when mass of $(\text{NH}_4)_2\text{SO}_4$ was increased from 2 g to 5 g. In addition, it should be noted that the slope of the tie-lines increased with increasing lactic acid concentration in the system, which signified the improved extraction efficiency in system with higher concentration, hence lower solution pH, of lactic acid.

Equilibrium mass fractions of lactic acid in aqueous ($W_{\text{LA, aq}}$) and organic ($W_{\text{LA, org}}$) phase with and without the presence of $(\text{NH}_4)_2\text{SO}_4$ were graphically shown in Figure 2. The ratio of lactic acid mass fraction in the organic phase to that in the aqueous phase was higher in system with higher mass of $(\text{NH}_4)_2\text{SO}_4$, which confirmed that the acid extraction with 1-butanol was promoted when this salt was added to the system.

Efficiency of lactic acid extraction was evaluated from the distribution coefficient (D) and the degree of lactic acid extraction (% E) obtained from the process. The distribution coefficient is defined as the ratio between number of moles of lactic acid in the organic phase to that in the aqueous phase. Partial miscibility

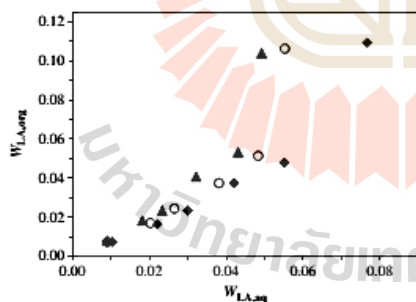


Figure 2: Equilibrium mass fraction of lactic acid in organic and aqueous phase in extraction with 0 g (\blacklozenge), 2 g (\circ) and 5 g (\blacktriangle) $(\text{NH}_4)_2\text{SO}_4$.

between water and 1-butanol led to the unequal volumes of each phase after extraction. As a result, the phase volumes were taken into account when calculating the distribution coefficient of lactic acid in this study as shown in eq. [1]. The degree of lactic acid extraction is expressed as percent of the acid recovered into the organic phase in relative with its initial amount in the aqueous phase and can be calculated as shown in eq. [2].

$$D = \frac{C_{\text{org}} V_{\text{org}}}{C_{\text{aq}} V_{\text{aq}}} \quad (1)$$

$$\%E = \frac{C_0 V_0 - C_{\text{aq}} V_{\text{aq}}}{C_0 V_0} \times 100 \quad (2)$$

The distribution coefficient and degree of lactic acid extraction in system with and without $(\text{NH}_4)_2\text{SO}_4$ are given in Table 2. It was found that these parameters were promoted when more salt was added to the system. The result emphasized the salting out effect of $(\text{NH}_4)_2\text{SO}_4$ in extraction of lactic acid using 1-butanol. It should also be noted that both parameters were also enhanced with increasing lactic acid concentration in the starting aqueous solution. This phenomenon was expected and was similar to the result observed and reported in the previous study (Chawong and Rattanaphanee 2011). As previously mention, this process characteristic implies that process intensification is feasible as volume of the dilute lactic acid solution or the fermentation broth could be reduced to increase the acid concentration, or to reduce the solution pH, prior to the extraction. Reduction in sizes of process equipments and easier handling of process streams will be the major benefits in the actual operation.

Effect of initial volume ratio of 1-butanol to aqueous solution on lactic acid extraction was also investigated in this study. As shown in Table 3, distribution coefficient and degree of lactic acid extraction were increased significantly when higher volume ratios were employed. In

Table 2: Distribution coefficient and degree of lactic acid extraction at 30.0°C in extraction with different mass of $(\text{NH}_4)_2\text{SO}_4$.

Lactic acid concentration (M)	0 g $(\text{NH}_4)_2\text{SO}_4$		2 g $(\text{NH}_4)_2\text{SO}_4$		5 g $(\text{NH}_4)_2\text{SO}_4$	
	D	%E	D	%E	D	%E
0.1	0.77	44.01	0.85	46.16	1.05	47.06
0.3	0.84	48.97	0.96	49.84	1.17	51.23
0.5	0.95	50.05	1.07	51.87	1.22	55.38
0.8	1.08	52.96	1.22	55.93	1.57	61.15
1.0	1.11	56.68	1.30	58.95	1.67	63.29
2.0	2.51	72.25	2.73	75.74	3.12	77.88
3.0	5.16	84.72	6.10	86.41	7.69	89.08

Table 3: Effect of 1-butanol-to-aqueous phase volume ratio on distribution coefficient and degree of lactic acid extraction from 1.0 M solution at 30.0°C.

Initial phase volume (ml)		Equilibrium phase volume (ml)		5 g (NH ₄) ₂ SO ₄	
Aqueous	1-Butanol	Aqueous	1-Butanol	D	%E
10	10	8.78	11.20	1.67	63.29
10	15	8.75	16.45	1.96	66.67
10	20	8.15	21.60	2.52	73.22
10	30	7.20	32.45	4.60	83.35

Initial phase volume (ml)		Equilibrium phase volume (ml)		0 g (NH ₄) ₂ SO ₄	
Aqueous	1-Butanol	Aqueous	1-Butanol	D	%E
10	10	9.0	11.0	1.03	51.01
10	20	6.4	23.1	3.29	77.13
10	30	4.0	35.6	7.87	88.92
10	40	1.3	48.5	30.82	96.97

extraction with the initial phase volume ratio of 1:1, about 62.4% of lactic acid was recovered. The recovery was drastically raised to approximately 83.4% when the ratio of 3:1 was used.

To highlight the effect of (NH₄)₂SO₄ in extraction with high 1-butanol-to-aqueous phase volume ratio, the distribution coefficient and degree of lactic acid extraction in the process without salt obtained from our previous study (Chawong and Rattanaphanee 2011) were also given in Table 3. Equilibrium phase volume in the experiments without salt showed that substantial fraction of aqueous phase was incorporated into the organic phase since its volume was enlarge while the aqueous phase volume was reduced after extraction. This was due to the partial miscibility of the two solvents with the solubility of water

in 1-butanol higher than the solubility of 1-butanol in water as earlier described in Section 3.1. The phase incorporation was more pronounced in the process with higher initial phase volume ratio. Although the distribution coefficient and degree of lactic acid extraction appeared to be of higher values in extraction without salt, it was merely because the bulk aqueous phase containing lactic acid was conveyed into the organic phase. The phase incorporation like this would hamper the extraction. High water content in the organic phase could complicate the purification processes following the extraction and obstruct efficient solvent recovery and recycle making it not feasible to enhance lactic acid recovery by performing the extraction at a high 1-butanol-to-aqueous phase volume ratio.

The presence of (NH₄)₂SO₄ in water-1-butanol-lactic acid system appeared to lessen the problem of organic and aqueous phase incorporation. As shown in Table 3 for extraction with 5 g of (NH₄)₂SO₄, when the initial phase volume ratio was increased from 1:1 to 3:1, volume of the aqueous phase was slightly reduced. It is, therefore, concluded in this study that addition of (NH₄)₂SO₄ advantageously allowed the extraction of lactic acid with 1-butanol to be carried out at a high organic-to-aqueous phase volume ratio, where large recovery of the acid would be achieved.

In an attempt to further improve extraction of lactic acid in mixed solvent electrolyte system containing water, 1-butanol and (NH₄)₂SO₄, successive extraction was performed using three consecutive extraction stages. The concentration of lactic acid in the starting aqueous solution was 1 M, and the quantity of (NH₄)₂SO₄ in the system was 5 g. The result is shown in Table 4. The total lactic acid extraction of 94.92% was achieved in the successive extraction, which was approximately 11.6% higher than that obtained in the single batch process. This result suggested that, in order to achieve higher degree of lactic acid

Table 4: Extraction of lactic acid in single-batch and successive mode.

Single-batch extraction				Successive extraction			
Initial volume (ml)	Extracted lactic acid (mmole)	Stage number		Initial volume (ml)	Extracted lactic acid (mmole)		
Aqueous	1-Butanol			Aqueous	1-Butanol		
10	30	8.335	1	10	10	6.422	
			2	8.5	10	2.474	
			3	7.3	10	0.596	
%E		83.35		%E		94.92	

recovery, the extraction should be operated in the successive mode rather than the batch one.

4 Conclusions

Mixed solvent electrolyte system containing water, 1-butanol and the inorganic salt $(\text{NH}_4)_2\text{SO}_4$ was applied in extraction of lactic acid from its aqueous solution at 30° C. Salting-out effect leading to reduced concentration of 1-butanol and lactic acid in the aqueous phase and increase of their concentration in the organic phase was observed. The presence of $(\text{NH}_4)_2\text{SO}_4$ in this system also appeared to lessen the problem of phase incorporation and facilitate lactic acid at a high organic-to-aqueous phase volume ratio, where high acid recovery was achieved. Further improvement of extraction efficiency was accomplished when the process was carried out in stage-mode rather than the batch one.

Acknowledgments: This work is financially supported by the National Innovation Agency, Ministry of Science and Technology, Thailand. All the research work was performed using the research facilities and infrastructures of Suranaree University of Technology.

Notation

C	molar concentration of lactic acid
D	distribution coefficient
$\%E$	degree of extraction
V	phase volume
W	weight fraction
$\%W$	percent by weight

Subscripts

0	starting solution
1	water
2	1-butanol
3	$(\text{NH}_4)_2\text{SO}_4$
LA	lactic acid
aq	aqueous phase
org	organic phase

References

- Chawong, K., Rattanaphanee, P., 2011. n-butanol as an extractant for lactic acid recovery. *World Academy of Science, Engineering and Technology* 80, 239–242.
- Chawong, K., Rattanaphanee, P., 2012. Effect of chloride salt on extraction of lactic acid with n-butanol. *Engineering Transaction* 15, 66–71.
- Domingues, L., Cussolin, P.A., Lopes da Silva Jr, J., Hadlich de Oliveira, L., AznarM., 2013. Liquid-liquid equilibrium data for ternary systems of water + lactic acid + C4-C7 alcohols at 298.2 K and atmospheric pressure. *Fluid Phase Equilibria* 354, 12–18.
- Ghalami-Chooabar, B., Ghanadzadeh, A., Kousarimehr, S., 2011. Salt effect on the liquid-liquid equilibrium of (water + propionic acid + cyclohexanol) system at $T = (298.2, 303.2, 308.2)$ K. *Chinese Journal of Chemical Engineering* 19, 565–569.
- Marták, J., Schlosser, S., 2007. Extraction of lactic acid by phosphonium ionic liquids. *Separation and Purification Technology* 57, 483–494.
- Marták, J., Schlosser, S., Šilvia Vlíčková, S., 2008. Pertraction of lactic acid through supported liquid membranes containing phosphonium ionic liquid. *Journal of Membrane Science* 318, 298–310.
- Oliveira, F.S., Araújo, F.S., Ferreira, J.M.M., Rebelo, R., Marrucho, L.P.N., Isabel M., 2012. Extraction of l-lactic, l-malic, and succinic acids using phosphonium-based ionic liquids. *Separation and Purification Technology* 85, 137–146.
- Pirahmadi, F., Deghani, M.R., Behzadi, B., Seyedi, S.M., Rabiee, H., 2010. Experimental and theoretical study on liquid-liquid equilibrium of 1-butanol + water + NaNO_3 at 25 and 35°C. *Fluid Phase Equilibria* 299, 122–126.
- Pirahmadi, F., Deghani, M.R., Behzadi, B., 2012. Experimental and theoretical study on liquid-liquid equilibrium of 1-butanol + water + NH_4Cl at 298.15, 308.15 and 318.15 K. *Fluid Phase Equilibria* 325, 1–5.
- Sahin, S., Kirbaslar, I., Bilgin, M., 2009. (Liquid + liquid) equilibria of (water + lactic acid + alcohol) ternary system. *Journal of Chemical Thermodynamics* 41, 97–102.
- Stepan, D.J., Olson, E.S., Shockey, R.E., Stevens, B.G., Gallagher, J.R., 2001. Recovery of lactic acid from American crystal sugar company waste water. Final Topical Report prepared for AAD Document Control, National Energy Technology Laboratory, USA.
- Tan, T.C., Aravinth, S., 1999. Liquid-liquid equilibria of water/ acetic acid/1-butanol system—effect of sodium (potassium) chloride and correlations. *Fluid Phase Equilibria*. 163, 243–257.
- Wasewar, K.L., Heesink, A.B.M., Versteeg, G.F., Pangarkar, V.G., 2002. Reactive extraction of lactic acid using alamine 336 in MIBK: equilibria and kinetics. *Journal of Biotechnology* 97, 59–68.

BIOGRAPHY

Miss Kanungnit Chawong was born on August 20, 1987 in Bangkok, Thailand. She earned her Bachelor and Master's degree in Chemical Engineering from Suranaree University of Technology (SUT). Her senior project in Bachelor degree was extraction of lactic acid from aqueous solution. For her Master's degree, her thesis was in the topic of "Effect of inorganic salts on liquid-liquid equilibrium in extraction of lactic acid using 1-butanol". She then continued her PhD's degree in Chemical Engineering, School of Chemical Engineering at Suranaree University of Technology under the guidance Asst. Prof. Dr. Panarat Rattanapanee. Her expertise includes the field of liquid-liquid extraction and reactive distillation as well as catalyst improving. During her PhD's degree study, she participated in the Cooperative Education Program for six months on 1st March – 31st August 2015 in field of chemical engineering at SCG Chemical Co., Ltd. Her research project during cooperative program was development of high throughput solvent screening for using in separation process in chemical industrial. She presented three oral presentations during her study, the first presentation entitled of "Aluminum alginate as a solid catalyst for esterification of lactic acid with 1-butanol" in the 6th KKU International Engineering conference, Thailand. The second is presenting of "Kinetic study of aluminum alginate catalyzed esterification of lactic acid with 1-butanol" in 23rd Regional Symposium on Chemical Engineering (RSCE2016), Vung Tau, Viet Nam and the last one presented "Characterization and catalytic activity of boehmite-supported aluminum catalyst in esterification of lactic acid with 1-butanol" in 24th RSCE2017, Semarang, Indonesia.